

**Elucidation and functional characterization of the phenylpropanoid
pathway in Hortensia species**

Dissertation

zur Erlangung des
Doktorgrades der Naturwissenschaftlichen (Dr. rer. nat.)
der

Naturwissenschaftlichen Fakultät I
- Biowissenschaften -

der Martin-Luther-Universität
Halle-Wittenberg

vorgelegt

von Herrn **Goutham Padmakumar Sarala**

Gutachter

1. Prof. Dr. Nicolaus von Wirén
2. Prof. Dr. Jörg Degenhardt
3. Prof. Dr. Ghasem Hosseini Salekdeh

Verteidigt in Halle (Saale) am 18.04.2024

To those who embody compassion and empathy,
May this work be a testament to our shared humanity.

Table of contents

1 Summary.....	1
2 Introduction	3
2.1 Phenylpropanoid biosynthesis in plants	3
2.1.1 Effect of drought stress on phenylpropanoid biosynthesis.....	4
2.1.2 Effect of light stress on phenylpropanoid biosynthesis	5
2.2 Coumarins: Structure and Functions.....	6
2.3 Physiology and biochemical profile of <i>H. macrophylla</i>	8
2.3.1 Physiology and growth habits of <i>H. macrophylla</i>	8
2.3.2 Biochemical profile of <i>Hydrangea</i> species	9
2.4 Phyllodulcin.....	10
2.4.1 Health benefits of phyllodulcin	11
2.4.2 Biosynthesis of phyllodulcin in <i>H. macrophylla</i>	12
2.5 Use of phyllodulcin as a natural sweetener.....	14
2.6 Aim of the present work	16
3 Materials and methods.....	18
3.1 Plant material and sample processing	18
3.2 Chemicals	18
3.3 Extraction and concentration of PD and HD.....	19
3.4 Extraction of phenolic compounds	19
3.5 Extraction of coumarins.....	20
3.6 Extraction and quantification of carbohydrates	20
3.7 Extraction and quantification of amino acids	21
3.8 UPLC-MS analysis.....	21
3.9 RNA isolation, sequencing and analysis	22
3.10 Validation of gene expression using qRT-PCR	23

3.11 Gene co-expression analysis	25
3.12 Drought stress experiment	26
3.13 Light stress experiment	26
3.14 β -glucosidase digestion	27
3.15 Statistical analysis.....	27
4 Results	28
4.1 Analysis of metabolites in <i>H. macrophylla</i> via UPLC-MS/MS.....	28
4.2 Screening and selection of <i>H. macrophylla</i> accessions based on phylodulcin (PD) and hydrangenol (HD) content.....	34
4.3 Distribution of PD and HD in different plant organs of <i>H. macrophylla</i>	37
4.4 Variation of PD and HD levels at different developmental stages of <i>H. macrophylla</i>	41
4.5 Variations in phenylpropanoid metabolism among <i>Hydrangea</i> accessions.....	45
4.5.1 Distribution of phenylpropanoid metabolites in <i>Hydrangea</i> accessions	45
4.5.2 Relationship between PD and other metabolites in <i>Hydrangea</i> accessions	48
4.5.3 Differences in expression patterns of genes involved in PPP and associated pathways	51
4.5.4 Relationship between genes and metabolites involved in phenylpropanoid pathway and related pathways	59
4.6 Validation of candidate gene expression using quantitative real-time-PCR (qRT-PCR)	67
4.7 The efficacy of β -Glucosidase digestion in augmenting PD and HD levels.....	71
4.8 Impact of drought stress on coumarin concentrations in <i>H. macrophylla</i> accessions	73
4.9 Impact of high-light intensity on coumarin concentrations in <i>H. macrophylla</i> accessions	77
5 Discussion.....	81
5.1 Concentrations of PD in <i>H. macrophylla</i> depend on the developmental stage	82

5.2 β -Glucosidase-mediated digestion increases the bioavailability of PD and HD in leaves.....	84
5.3 Regulation of PD and HD biosynthesis in <i>Hydrangea</i> depends on accession-specific expression of genes involved in phenylpropanoid, flavonoid and stilbenoid biosynthesis	86
5.4 <i>Hydrangeas</i> affected by drought stress produce more PD, HD and coumarins	91
5.5 PD and HD concentrations are enhanced in <i>Hydrangeas</i> in plants grown in at high light intensities.....	93
6 Conclusion	96
7 References.....	97
8 Appendix	127
9 Abbreviations	145
10 Acknowledgement.....	148
11 Curriculum Vitae.....	149
12 Eidesstattliche Erklärung/Declaration on oath.....	150
13 Erklärung über bestehende Vorstrafen und anhängige Ermittlungsverfahren/Declaration concerning Criminal Record and Pending Investigations	151

1 Summary

In today's health-conscious world, the pursuit of a sugar-free or low-calorie diet has led to the widespread use of artificial sweeteners in various food and beverage products. While these sugar substitutes promise guilt-free sweetness without calories, there is growing concern about their potential ill effects on human health. In contrast, natural sweeteners offer a safer and healthier alternative, providing a sweet taste without the risks associated with artificial counterparts. One such promising natural sweetener is phyllodulcin (PD), derived from *Hydrangea macrophylla*, a flowering plant native to Japan and Korea. PD is significantly sweeter than sucrose and it presents a calorie-free alternative to traditional sugars, making it appealing those seeking to reduce their sugar intake. Considering its utility, the present research was designed to investigate the physiology, biochemistry and genetics of PD enrichment in *H. macrophylla*. The research began by optimizing the extraction of PD from plant tissue through a drying process. After achieving this, 14 accessions with varying concentrations of PD and its precursor, hydrangenol (HD), were selected by a screening of a panel of 182 accessions. Out of these 14 accessions, 5 were cultivated in a greenhouse from the initial cutting stage to senescence to determine the optimal developmental stage in the plant's life cycle for maximizing PD extraction. Young leaves from 110 days-old plants were identified to contain highest concentrations of PD. To assess the degree of PD enrichment during tissue processing, the enzyme β -glucosidase was supplied to fresh or dried tissues, resulting in improved phyllodulcin extraction efficiency that can be further optimized for industrial-scale production. Additionally, the present study unveiled a positive linear correlation between PD and other metabolites in the same biochemical pathway, in particular phenylalanine, p-coumaric acid, umbelliferone, resveratrol, and naringenin. When comparing the metabolite profiles of accessions with high and low PD production, it was observed that high-PD accessions displayed higher concentrations of flavonoids, stilbenes, and polyketides, indicating the distinct metabolic diversity of these accessions. By conducting a comparative transcriptome analysis between high and low PD-producing plants, the study identified key genes most likely involved PD biosynthesis, including *PAL1*, *C4H*, *4CL1*, *F6'H1*, *PKS*, *PKC*, *CHS*, *DBR*, *KR*, *ROMT*, *CTAS*, *F3'5'H*, and *CHI*, which were upregulated in plants with higher phyllodulcin production. Conversely, *C3'H*, *HCT*, *CCoAOMT*, *COMT*, *CSE*, *SGT*, and *F3H* were downregulated in plants

with higher phyllodulcin production. Finally, the research explored the impact of environmental factors, specifically drought stress and high-light intensity, on the biochemical composition of *Hydrangea* plants and their influence on PD enrichment. It was observed that under these two stress conditions, both PD and HD, accumulated in stress-affected plants. Overall, this study provides an in-depth investigation into the various physiological, biochemical, and genetic aspects enhancing biosynthesis of natural sweetener PD in *H. macrophylla*, positioning it as a potential alternative to artificial sweeteners. In conclusion, by integrating metabolic and transcriptomic data and investigating the effects of external stress factors on PD production in *H. macrophylla*, this study provides new insights into the biochemistry and molecular regulation of PD and HD biosynthesis.

2 Introduction

2.1 Phenylpropanoid biosynthesis in plants

The sessile nature of plants has led to the evolution of diverse metabolic pathways that enabled them to respond to environmental stimuli and establish sophisticated relationships with co-evolving species through the production of specialized biomolecules that are generally not involved in the primary metabolism (Dixon, 2001; Hartmann, 2007; Weng *et al.*, 2021). These secondary metabolites (SMs) contain an array of over 200,000 diverse chemical compounds originating from multiple biosynthetic pathways (Dixon, 2001; Schwab, 2003; Viladomat and Bastida, 2015). However, the origins of most of these biomolecules are credited to phenylpropanoid biosynthesis. Phenylpropanoids are a group of organic compounds that originate from the amino acid L-phenylalanine through a deamination process facilitated by L-phenylalanine ammonia lyase (PAL). This nonoxidative deamination of phenylalanine transforms it into trans-cinnamate and directs carbon flow into various branches of the general phenylpropanoid metabolism (Dixon *et al.*, 2002; Vogt, 2010). Therefore, the phenylpropanoid pathway (PPP) serves as the central route, starting from phenylalanine and leading to the production of an activated hydroxycinnamic acid derivative through the actions of PAL, cinnamate 4-hydroxylase (C4H), and 4-coumarate: coenzyme A ligase (4CL). The formation of 4-coumaroyl CoA is a pivotal branching point within the central phenylpropanoid biosynthesis in plants (Schneider *et al.*, 2003). The direction in which this biomolecule is channeled determines the accumulation of specific metabolites in plants (Fraser and Chapple, 2011). Certain pathways, such as those responsible for proanthocyanidins, tannins, and flavonoids, diverge from phenylpropanoid metabolism shortly after the production of 4-coumaroyl CoA (Winkel-Shirley, 2001; Dixon *et al.*, 2005). Conversely, other pathways, including those leading to phenylpropenes, coumarins, lignins, and lignans, share some intermediate compounds within the phenylpropanoid metabolism (Lewis and Davin, 1999; Boerjan *et al.*, 2003; Dudareva *et al.*, 2004; Vogt, 2010). A wide range of bioactive molecules with therapeutic properties can be observed as downstream products of these polyhydroxylated rings. These include flavonoids, stilbenes, isoflavonoids, and other polyketides such as 3,4-dihydroisocoumarins and melleins (Dixon & Piva, 1995; Austin & Noel, 2002; Noel *et al.*, 2005; Dewick, 2009; Noor *et al.*, 2020; Reveglia *et al.*, 2020). Some of the essential biomolecules that help plants

respond to external stimuli branch out from these enzyme-mediated reactions. A visual representation of the PPP is given in Figure 1.

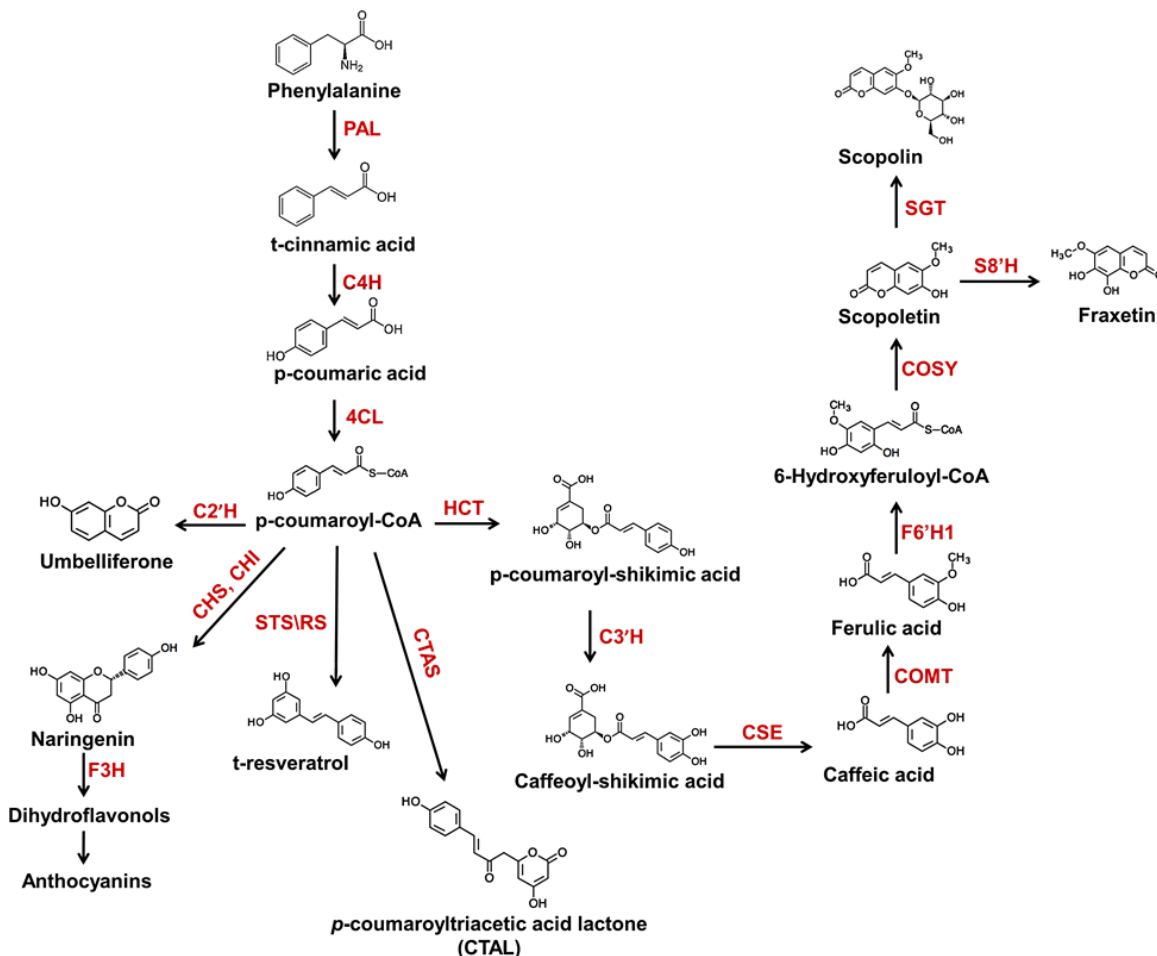


Figure 1. Scheme of phenylpropanoid metabolism in plants leading to the formation of coumarins, flavonoids and polyketides. Red bold font indicates enzymes. 4CL, 4-coumarate-CoA ligase; C3H, p-coumaroyl shikimate 3' hydroxylase; C4H, cinnamic acid 4-hydroxylase; CHS, chalcone synthase; CHI, chalcone isomerase; COMT, caffeate/5-hydroxyferulate 3-O-methyltransferase; CSE, caffeoyl shikimate esterase; F3H, flavanone 3-hydroxylase; HCT, hydroxycinnamoyl transferase; PAL, phenylalanine ammonia lyase; RS, resveratrol synthase; C2H, cinnamate 2 hydroxylase; F6'H1, feruloyl-CoA 6'-hydroxylase; SGT, scopoletin glucosyl transferase; S8H, scopoletin 8-hydroxylase; CTAS, p-coumaroyltriacetic acid synthase; COSY, coumarin synthase.

2.1.1 Effect of drought stress on phenylpropanoid biosynthesis

Drought, a widespread and complex abiotic stressor in the plant world, is common in arid and semiarid regions worldwide. It typically triggers various changes in plants at morphological, physiological, biochemical, and molecular levels, often negatively impacting both the quality and quantity of plant biomass (Mashilo *et al.*, 2017). Throughout their evolutionary history, plants have developed adaptations to cope with drought conditions, often involving the accumulation of secondary metabolites (SMs)

like terpenes, alkaloids, and phenolic compounds induced by ionic or osmotic stress. However, this increased SM production usually comes at the cost of reduced biomass (Isah, 2019). For example, when exposed to drought stress, species like *Hypericum brasiliense* and *Pisum sativum* experience an increase in phenolic compound concentrations (Dawid and Hille, 2018). This is typically associated with alterations in the phenylpropanoid pathway, where many key genes are activated in response to drought stress. For instance, drought stress leads to the activation of the PAL gene in lettuce plants and the expression of several genes involved in flavonoid biosynthesis in *Scutellaria baicalensis* (Yuan *et al.*, 2012). Drought stress has been found to influence the biosynthesis of phenolic acids and flavonoids, resulting in increased levels of these compounds (Rezayian., 2018; Gharibi *et al.*, 2019). These phenolic compounds serve as antioxidants and help protect plants by detoxifying the harmful H₂O₂ molecules generated during drought stress (Nichols *et al.*, 2015). Conversely, drought can therefore be exploited to generate these phenylpropanoids from plants. Drought stress induction has been performed on bell peppers to extract SMs that are industrially relevant (Junker *et al.*, 2018). The research findings offer evidence indicating that drought stress induces the accumulation of secondary metabolites (SMs) in plants. This phenomenon can be leveraged for the extraction of substantial quantities of these metabolites from plants.

2.1.2 Effect of light stress on phenylpropanoid biosynthesis

Plants possess the ability to respond to changes in light radiation by both accumulating and releasing a range of secondary metabolites (SMs), including phenolic compounds, triterpenoids, and flavonoids, many of which are valued for their antioxidant properties (Jaakola and Hohtola, 2010). Research has demonstrated that the intensity of light radiation plays a role in regulating the levels of various phenolic phenylpropanoid derivatives in *Xanthium* species. Specifically, compared to prolonged exposure to high light, shorter periods of light exposure result in a significant reduction of caffeoylquinic acids by approximately 40% and a nearly two-fold increase in the reduction of flavonoid aglycone content (Taylor, 1965). In *Ipomoea batatas*, a significant increase in phenolic acids (e.g., hydroxybenzoic acids and hydroxycinnamic) and flavonoids (e.g., flavonols, anthocyanins, and catechins) content was observed after a long period of high-intensity light exposure (Carvalho *et al.*, 2010). In general, a light intensity between 200 and 300 $\mu\text{mol m}^{-2} \text{s}^{-1}$ is suitable for plants grown in controlled

environments. Exposing a plant to higher light intensities results in higher accumulation of anthocyanins by activation of cryptochromes (Folta and Carvalho, 2015; Bian *et al.*, 2015). Light Emitting Diodes (LEDs), emitting high-intensity lights have been used to enhance the biosynthesis of therapeutic metabolites, specifically phenolics in orchids (Yeow *et al.*, 2020). A similar study has shown that high light intensities were used to produce terpenoids by enhancing the mevalonic acid pathway in *Solanum lycopersicum* (Saadat *et al.*, 2022). These investigations offer compelling evidence that exposure to light stress leads to the accumulation of secondary metabolites (SMs) in plants. Furthermore, this phenomenon can be harnessed to extract significant quantities of these metabolites from plant sources.

2.2 Coumarins: Structure and Functions

Coumarins belong to the polyphenol class of secondary metabolites (SMs) and are derived from the phenylpropanoid pathway (PPP) (Bourgaud *et al.*, 2006). They constitute a substantial group of phenolic compounds characterized by a benzene ring fused to an α -pyrone ring, which can be classified into different types based on their chemical structure (Rettie *et al.*, 1992). Since the initial discovery of coumarin in the plant *Coumarouna odorata*, more than 1300 of these 1,2-benzopyrone derivatives have been identified in various organisms, including insects, liverworts, marine sponges, lichens, bacteria, fungi, and plants (Egan *et al.*, 1990; Iranshahi *et al.*, 2009; Reveglia *et al.*, 2020). In the plant kingdom, coumarins have been reported in approximately 150 different species spanning nearly 30 different families, including Apiaceae, Caprifoliaceae, Clusiaceae, Guttiferae, Nyctaginaceae, Oleaceae, Rutaceae, and Umbelliferae. The distribution of these bioactive molecules within plant tissues, whether it's in leaves, seeds, fruits, roots, latex, etc., depends on the specific type of coumarin, the plant species, and its developmental stage (Venugopala *et al.*, 2013). Environmental factors significantly influence the accumulation of coumarin in plant tissues. Extensive research has been conducted to gain insights into these low molecular weight natural compounds, revealing their broad impacts not only on plant systems but also on the surrounding environment. This includes coumarins' ability to facilitate iron acquisition from soils in *Nicotiana* (Kai *et al.*, 2006; Rajniak *et al.*, 2018; Lefèvre *et al.*, 2018), modify the rhizosphere to create a favorable environment for specific microbes in *Arabidopsis* (Voges *et al.*, 2019), confer resistance to fungal infections in *Brassica* sp. (Tortosa *et al.*, 2018), and scavenge

reactive oxygen species (ROS) under abiotic stress conditions (Fourcroy *et al.*, 2014; Döll *et al.*, 2018). While the plant kingdom remains an important source of chemical compounds, recent studies have highlighted the utility of natural coumarins and their synthetic analogs in various fields, including pharmacology, the food industry, perfumery, and scientific research (Floc'h *et al.*, 2002; Lončar *et al.*, 2020; Sugiyama *et al.*, 2023; Onder *et al.*, 2023). The coumarin biosynthesis pathway branching from the PPP in *Arabidopsis* is depicted in Figure 2.

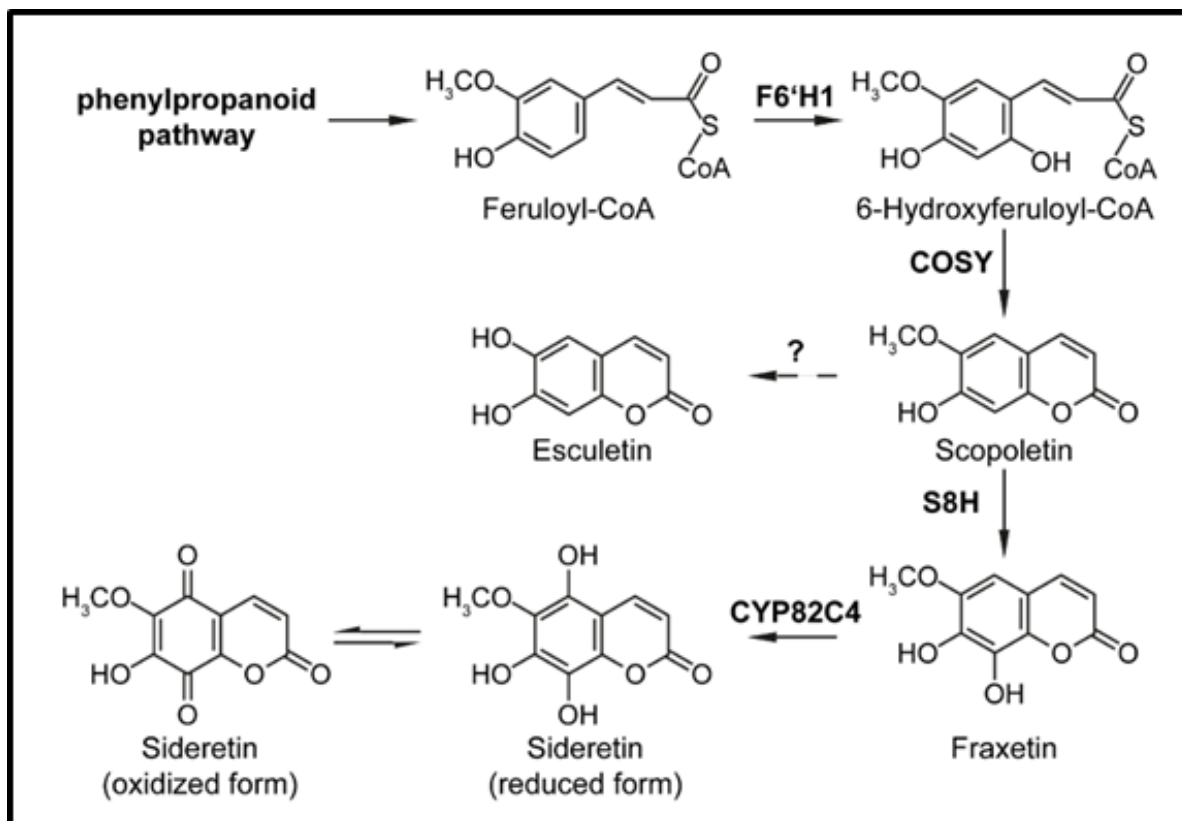


Figure 2. Biosynthesis of coumarins. Biosynthesis of hydroxy coumarins in *Arabidopsis* branching out from general phenylpropanoid pathway. Figure was adopted from Paffrath, (2022).

Isocoumarins represent a class of compounds that are isomeric to coumarins and are characterized by a reversed lactone moiety. They can exhibit a 6,8-dioxygenated pattern, a 3-un substituted phenyl ring, or a 3-alkyl chain (C1-C17) (Saeed *et al.*, 2014; Pal and Pal, 2018) (Figure 3A). While coumarins typically originate from the phenylpropanoid pathway, as seen in compounds like umbelliferone (7-hydroxy coumarin), isocoumarins have their roots in the polyketide biosynthetic pathway (Wu *et al.*, 2016; Song *et al.*, 2017). As a result, these biologically active molecules are commonly categorized under polyketides (Reveglia *et al.*, 2020). Within the realm of isocoumarins, 3,4-dihydroisocoumarins (DHCs) form a subgroup distinguished by the

presence of saturated analogs at the C-3/C-4 positions (Figure 3B). DHCs constitute a relatively limited yet fascinating category of secondary compounds produced by specific plants, fungi, insects, and other organisms. Natural DHC structures exhibit various modifications within their fundamental framework, including O-glucosylation and methylation. These modifications significantly influence their chemical and biological properties (Saddiqa *et al.*, 2017). Consequently, gaining a deeper understanding of how plants synthesize these isocoumarins holds promise for expanding their industrial applications, particularly in the agricultural and pharmaceutical sectors (Robe *et al.*, 2021; Kim *et al.*, 2023). Researchers have directed their attention towards the Cornales genus to identify DHCs with unique medicinal and nutritional properties.

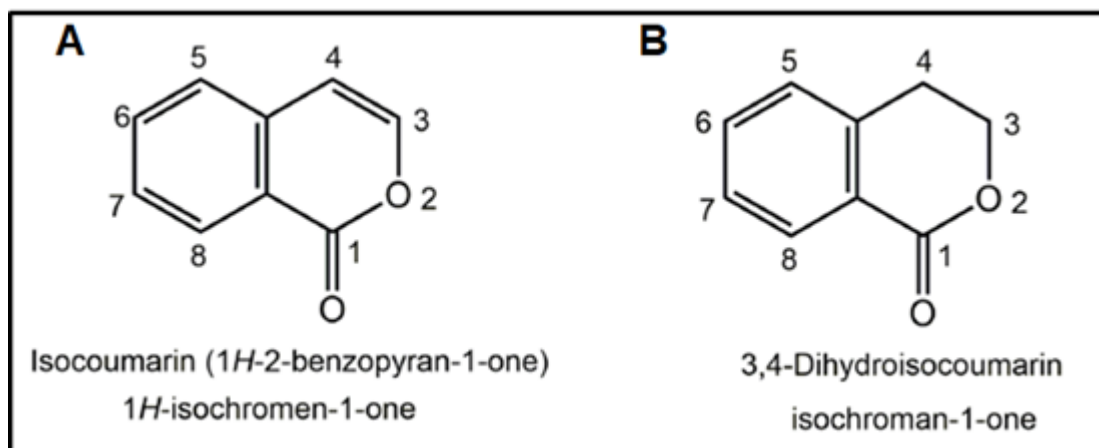


Figure 3. Structure of isocoumarins. (A, B) General chemical structures of (A) isocoumarin, (B) 3,4 dihydroisocoumarin skeletons. Figure was adopted from Noor *et al.*, 2020.

2.3 Physiology and biochemical profile of *H. macrophylla*

2.3.1 Physiology and growth habits of *H. macrophylla*

H. macrophylla are ornamental plants native to hilly areas of Japan, which was introduced into Europe in the late 17th century by Sir Joseph Banks and they are now considered the most commercially significant *Hydrangea* species among the other 22 recognized species (Wilson, 1923; Griffith, 1994; Wu *et al.*, 2021). In *Hydrangea* breeding, the primary traits of significance include distinctive inflorescence structures and a wide range of flower colors that cater to various markets. These traits encompass the ability to induce flowering (enabling reblooming in landscape varieties and year-round flower production for florist *Hydrangeas*), resilience to drought and sunlight for landscape breeding, and resistance to powdery mildew for plants grown in

greenhouses and outdoor landscapes (Rinehart *et al.*, 2016). *Hydrangea* species can be propagated through seeds, although the seeds are sometimes very small, and this method of sexual propagation results in variability among genotypes. The most prevalent techniques for commercially propagating *Hydrangeas* are stem cuttings and tissue culture through micropropagation (Ruffoni *et al.*, 2013).

Hydrangeas thrive in soil or substrate conditions where the pH level falls within the range of 5.5 to 6.5. Some species can even adapt to or prefer alkaline soils or substrates with pH levels around 7.0 or higher. Mineral nutrient deficiencies in *Hydrangea* depend on the taxonomic lineage of the plant. Inadequate levels of nitrogen (N) result in the yellowing of older leaves turning chlorotic, and possibly showing signs of tip dieback. Younger leaves, on the other hand, exhibit reddish margins and tend to stay smaller. Sulfur (S) deficiency shares some similarities with nitrogen deficiency, including reduced shoot elongation resulting in shorter internodes. Calcium (Ca) deficiency is characterized by younger leaves appearing light green to yellow, and they may become necrotic or distorted. Phosphorus (P) deficiencies manifest as reduced growth of the shoot and a purplish tint in older leaves. *Hydrangeas*, particularly *H. macrophylla* are considered to have high water demand with an approximate consumption of 0.2 liters per day and plant, emphasizing its dependency on ample water supply (Owen *et al.*, 2016). These physiological parameters are exploited and manipulated while growing *Hydrangeas* at large scale.

2.3.2 Biochemical profile of *Hydrangea* species

Hydrangeas exhibit a rich biochemical profile featuring a wide array of biomolecules with therapeutic and non-therapeutic properties. Traditional medicine has long utilized *H. macrophylla* to address various ailments, including insect stings, allergies, sore throats, malarial fever, and diabetes. Additionally, scientific studies have illuminated the anti-inflammatory and immune-modulating properties inherent in *Hydrangeas* (Lee *et al.*, 2022; Agustini *et al.*, 2023). Upon subjecting *H. macrophylla* to biochemical analysis, researchers have uncovered a treasure trove of compounds. These include dihydro-isocoumarin derivatives, stilbenic acids, stilbenoids, flavonols, and more (Wellmann *et al.*, 2022). Notably, a particular isocoumarin called Thunberginol C (ThmC) and its glycoside forms have demonstrated antimicrobial, antioxidative, photoaging prevention, stress reduction, and brain cell protection properties (Shin *et al.*, 2019; Duy *et al.*, 2020; Lee *et al.*, 2022). The exploration of *Hydrangea's*

biochemical makeup goes back to 1916 when the first 3,4-dihydroisocoumarin hydrangenol (HD) was extracted from these plants. HD exhibited multifaceted therapeutic potential, including antifungal, anti-allergic, antidiabetic, anti-inflammatory, and anti-angiogenic properties. This early investigation led to the discovery of another noteworthy biomolecule, phyllodulcin (PD), by Asahina and Ueno in the same year (Asahina and Ueno, 1916; Reveglia *et al.*, 2020). Furthermore, *Hydrangea* flowers are known for containing delphinidin 3-glucoside, an anthocyanin capable of chelating aluminum in the presence of co-pigments like 3-caffeoylquinic acid. This interaction produces the distinctive blue coloration observed under acidic pH conditions (Takeda *et al.*, 1985; Schreiber *et al.*, 2011). *Hydrangeas* also house a diverse array of coumarins and their derivatives, including umbelliferone, skimmin (umbelliferone-7-3-o-glucoside), daphnetin-8-monomethylether, hydrangeic acid, lunurarin and its glucosides, scopoletin, scopolin, quercetin and kaempferol derivatives, cyanogenic glycosides, and resveratrol derivatives (Suzuki *et al.*, 1978; Yoshikawa *et al.*, 1999a; Yoshikawa *et al.*, 1999b; Wellmann *et al.*, 2022). These collective findings underscore the remarkable diversity of metabolites present in *Hydrangeas*, making them a valuable resource for academic research and industrial applications.

2.4 Phyllodulcin

Phyllodulcin (PD) is a unique dihydroisocoumarin (DHC) compound exclusively found within *H. macrophylla* (Figure 4). In Japan, a traditional sweet herbal tea called Amacha is brewed which contains PD from dried leaves of *H. macrophylla*. This tea is renowned for its distinctively sweet flavor, along with associated health benefits (Bassoli *et al.*, 2008). Notably, R-(+)-PD is known to be exceptionally sweet, approximately 400–800 times sweeter than sucrose. The molecule's sweet taste is attributed to the presence of the ortho-hydroxy methoxyphenyl (isovanillyl) unit (Bassoli *et al.*, 2008; Kim *et al.*, 2018; Ciçek, 2020). In the leaves of *Hydrangea*, PD is naturally present in the form of phyllodulcin- β -D-glucosides (Figure 4). When the plant experiences various stressors such as drying, wounding, or senescence, native glucosidases within the plant hydrolyze these glucosides, converting PD to its aglycone form, which possesses a pleasantly sweet, minty taste. This enzymatic hydrolysis process has been harnessed in Japan for many years, involving methods like crushing, hand rolling, high-temperature drying, and fermentation of *Hydrangea* leaves to create sweet-tasting beverages (Ujihara *et al.*, 1995; Jung *et al.*, 2016; Kim

et al., 2017). Furthermore, PD has exhibited a range of beneficial properties, including anti-bacterial, anti-malarial, antifungal, anti-ulcer, and anti-inflammatory effects, both in traditional and modern medicine.

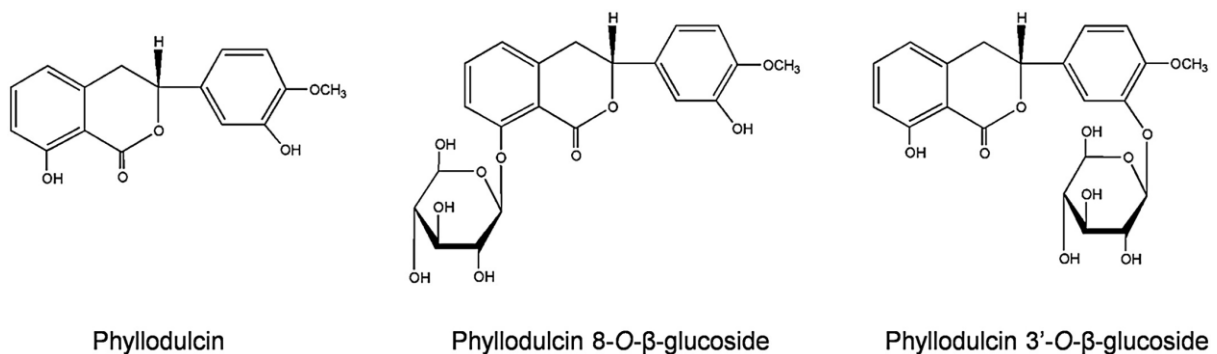


Figure 4. Structure of phyllodulcin and its conjugates. Chemical structures of phyllodulcin, and its glycoside forms, phyllodulcin 8-O-β-glucoside and as phyllodulcin 3'-O-β-glucoside found in *H. macrophylla*. Figure was adopted from Jung *et al.* (2016).

2.4.1 Health benefits of phyllodulcin

Recent studies on animal models have shown a wide range of potential health benefits from the consumption of PD. PD has the ability to penetrate the blood-brain barrier (BBB) and be distributed throughout the brain. Hence, it can be a candidate for understanding the effects of Alzheimer's disease (Cho *et al.*, 2023). The administration of phyllodulcin to mice led to enhancements in their blood lipid levels and glucose levels (Zhang *et al.*, 2007). In animal trials, PD was able to decrease the weight of subcutaneous fat and the expression of adipogenesis and lipogenesis-related genes in mice (Kim *et al.*, 2017). A work on bovine adrenocortical cells reported that low concentrations of PD inhibited phosphodiesterase activity through enhanced cyclic AMP-induced steroidogenesis, thus postulating its ability to avert attack of bronchial asthma and/or minor exacerbation of heart failure (Kawamura *et al.*, 2002). These findings indicate that phyllodulcin has the potential to serve as a beneficial treatment option for metabolic disorders associated with obesity and may be utilized as a substitute sweetener with therapeutic properties, which is highly beneficial for the population suffering from type 2 diabetes, overweight and obesity (Zhang *et al.*, 2007; Kim *et al.*, 2017). Regarding such immense therapeutic potential, approaches to study this natural molecule in detail are limited by the lack of cost-efficient extraction methods and time-consuming synthetic approaches.

2.4.2 Biosynthesis of phyllodulcin in *H. macrophylla*

Phyllodulcin, a type of 3,4 dihydroisocoumarin, is believed to originate from the phenylpropanoid pathway. Early investigations, aided by the use of labeled ^{14}C compounds, indicated that the initiation of PD biosynthesis occurs through L-phenylalanine and cinnamic acid (Basyouni *et al.*, 1964; Kindle and Billek, 1964; Yagi *et al.*, 1977). These studies also suggested that branching from p-coumaric acid was a possible route for PD biosynthesis, and hydrangenol (HD) could serve as a precursor in this pathway. This conclusion was drawn based on the incorporation ratio of labeled carbon, which indicated that the introduction of the C-3' hydroxy group in phyllodulcin occurs after the formation of hydrangenol. Additionally, it was reported that three molecules of malonyl CoA condense to form a tetraketide intermediate, likely involved in hydrangenol biosynthesis (Ibrahim and Towers, 1960).

In 1999, researchers identified an enzyme called p-coumaroyltriacytic acid synthase (CTAS) in *H. macrophylla*. This enzyme catalyzes three consecutive decarboxylation reactions of p-coumaroyl-CoA and malonyl-CoAs, ultimately leading to the production of p-coumaroyltriacytic acid (CTA) tetraketide, which is further converted into p-coumaroyltriacytic acid lactone (CTAL) (Akiyama *et al.*, 1999). Although an enzyme responsible for stilbene carboxylic acid biosynthesis in *Hydrangea* wasn't detected, it was suggested that CTAS, in association with a hypothetical polyketide cyclase and ketoreductase, might be involved in hydrangic acid formation (Akiyama *et al.*, 1999; Austin and Noel, 2003). Another research group that reported the enzyme stilbenecarboxylate synthase (STCS), which prefers dihydro p-coumaric acid to produce stilbene carboxylates like 5-hydroxy-lunularic acid, also suggested this reduction step (Eckermann *et al.*, 2003). Hydrangic acid could potentially lead to the formation of HD, and subsequently PD, as PD may be derived from HD through C-3' hydroxylation and C-4'O-methylation (Yagi *et al.*, 1977). In parallel, Thunberginols, synthesized from resveratrol, have also been proposed to be linked to PD biosynthesis (Çiçek *et al.*, 2018; Preusche *et al.*, 2022). While these studies lay the foundation for deciphering the PD biosynthetic pathway in *Hydrangea*, a comprehensive understanding would require further research into the genes, enzymes, and potential intermediates involved in this pathway. Figure 5 illustrates the biosynthetic pathway responsible for the production of documented stilbene carboxylates, which are

anticipated to serve as intermediate compounds in the biosynthesis of PD, as outlined in the existing literature.

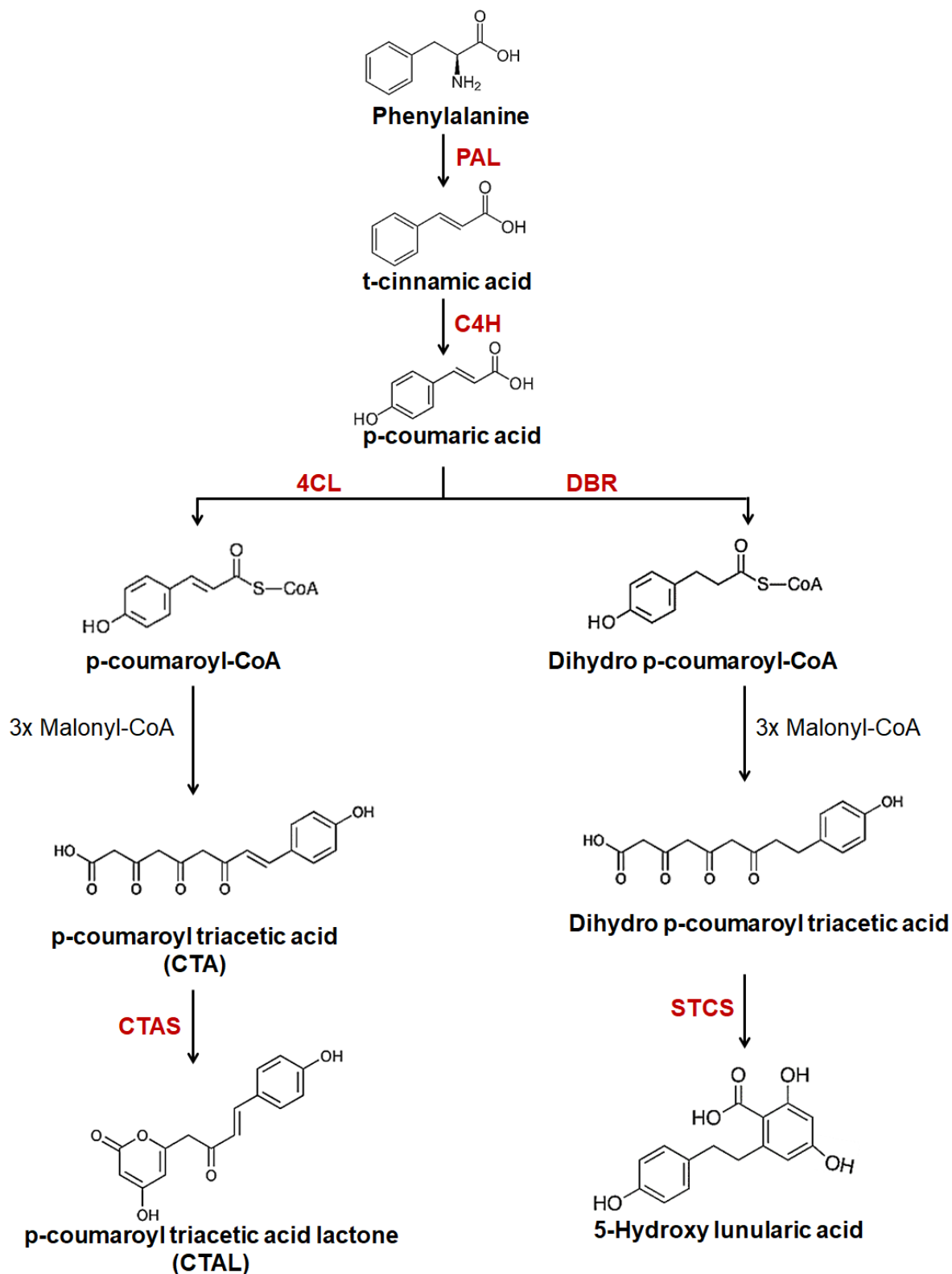


Figure 5. Scheme of stilbene carboxylate biosynthesis reported in *Hydrangea* sp. Red bold font indicates enzymes. 4CL, 4-coumarate-CoA ligase; C4H, cinnamic acid 4-hydroxylase; PAL, phenylalanine ammonia lyase; CTAS, p-coumaroyltriacetic acid synthase; STCS, stilbene carboxylate synthase; DBR, double bond reductase

2.5 Use of phyllodulcin as a natural sweetener

In the late 18th century, following the discovery of saccharin, the first artificial sweetener, the global food industry began searching for chemical compounds that not only provided sweetness but were also cost-effective (O'Brien-Nabors, 2011). However, concerns regarding the safety of consuming and producing these chemicals have arisen. For instance, well-known FDA-approved sweeteners like saccharin, aspartame, cyclamate, or their metabolic products have all been linked to increased health risks in various ways. It's important to note that the approval and use of these sweeteners vary from one country to another (Prince *et al.*, 1970; Weihrauch and Diehl, 2004; Debras *et al.*, 2022; Riboli *et al.*, 2023). In recent times, there's a growing consumer preference for natural ingredients, leading to a higher demand for natural, calorie-free, or zero-calorie sweeteners. This shift in consumer demand is also reflected in scientific literature, with an increase in research on sugar substitutes and a substantial rise in publications concerning natural sweeteners (Dubois and Prakash, 2012; Philippe *et al.*, 2014; Çiçek *et al.*, 2020). One commonly proposed structural element believed to be present in sweet-tasting compounds, referred to as the "glucophore," plays a crucial role in imparting sweetness to these substances. This feature is a key factor in determining the relative sweetness of a molecule, and chemists have used this concept when developing new artificial sweeteners, often drawing inspiration from natural sweeteners (Shallenberger and Acree, 1967; Brich, 1987; Çiçek *et al.*, 2020). Research on PD and its analogs aimed to uncover the structure-activity relationships underlying their sweetening properties. Within these compounds, the ortho-hydroxymethoxyphenyl (isovanillyl) component plays a pivotal role in eliciting the sweet taste, and it can be modified to some extent while retaining its effectiveness. These compounds interact with taste receptors on the tongue and activate the brain regions responsible for perceiving sweetness (Shallenberger and Acree, 1967; Bassoli *et al.*, 2002). Studies have indicated that PD is between 400 and 800 times sweeter than sucrose and has a refreshing taste (Yamato *et al.*, 1977; Bassoli *et al.*, 2008). Furthermore, purified phyllodulcin has shown no mutagenicity, and its acute oral toxicity in mice is greater than 2 grams per kilogram of body weight, indicating that PD can be safely ingested without posing a risk of toxicity (Izawa *et al.*, 2010). Despite these favorable characteristics, the potential use of PD as a natural sweetener has been limited primarily due to the lack of large-scale industrial

production. The use of PD as a natural sweetener is not a new concept. PD is well-known in Japan as both an oral refrigerant and a sweetener. It is a key component in the preparation of a sweet tea called Amacha (甘茶), which is a traditional Japanese beverage made from the leaves of *H. macrophylla* and is typically served during the Hanamatsuri celebration, marking the birth of Buddha (Yasuda *et al.*, 2004; Moll *et al.*, 2021). Fresh *Hydrangea* leaves are not considered sweet; however, during the tea-making process, which includes hand-rolling and high-temperature drying, the distinct minty sweet taste of PD is developed as a result of the bioconversion of phyllo dulcin within the leaves (Ujihara *et al.*, 1995). Previous studies have revealed that non-sweet phyllo dulcin- β -D-glucosides present in fresh *Hydrangea* leaves are converted into their aglycone, phyllo dulcin, during the heating process (Suzuki *et al.*, 1977a; Zehnter and Gerlach, 1995). This conversion process is primarily mediated by the action of β -glucosidase (Zehnter and Gerlach, 1995; Ujihara *et al.*, 1995). Additionally, the concentration of PD in harvested *Hydrangea* leaves was found to increase directly proportional to the length of storage, particularly up to five days when stored at 25°C under humid conditions. However, there is a suggestion that the β -glucosidase enzyme in *Hydrangea* might have a broader optimal temperature range, potentially contributing to its heightened enzymatic activity (Jung *et al.*, 2016). Therefore, the main challenge in producing PD from plant leaves lies in the bioconversion of its glycoside form to its active non-glycoside form. This conversion can be achieved by drying the plant tissue in large batches at a high temperature. The yield of PD can be further increased by treating the plant tissue with the enzyme β -glucosidase. In principle, both of these methods break the β -glucoside bond and release free PD from its glucoside form.

Metabolic engineering using microbial systems can be a valuable approach for upscaling the production of natural products. Similar work to express important genes involved in the steviol glycoside biosynthetic pathway has been done in *E. coli* (Wang *et al.*, 2016; Moon *et al.*, 2020). Successful microbial engineering relies on a detailed biochemical and genetic understanding of the target compound's biosynthesis in the native organism. This includes knowledge of the genes, enzymes, and intermediate biomolecules involved. Once the enzymes responsible for producing a specific compound are identified and comprehensively studied, the next challenge involves two main steps. First, the development of a genetically engineered microbial strain

capable of producing the target compound. Second, the optimization of this engineered strain for maximum efficiency in sweetener production, regardless of the carbon source used. Engineering complex pathways for secondary metabolites in microbes, particularly for large-scale production, is a highly intricate undertaking (Philippe *et al.*, 2014). Nonetheless, recent advancements in the metabolic engineering of compounds like artemisinic acid and hydroxylated taxanes offer encouraging prospects (Ajithkumar *et al.*, 2010; Paddon *et al.*, 2013). Transcriptome profiling enables the simultaneous analysis of gene expression dynamics, providing a comprehensive view of cell physiology and regulatory processes. This technology has significantly advanced the field of metabolic engineering by allowing the systematic examination of cell metabolism at a holistic level (Shi *et al.*, 2013). Therefore, by identifying potential genes involved in PD biosynthesis through transcriptome profiling and expressing these genes in a microbial system like *E. coli*, it becomes possible to scale up PD production to an industrial level.

2.6 Aim of the present work

To date, several studies have explored the biosynthesis of phenylpropanoids in *H. macrophylla*, but these investigations were conducted independently. They did not consider the closely associated metabolites linked to pathways relevant to phyllo dulcin biosynthesis. Understanding the dynamics of these metabolites in response to changing environmental conditions is crucial for comprehending how phyllo dulcin (PD) and hydrangenol (HD) are metabolized within the plant. Moreover, from an industrial as well as scientific viewpoint, it is important to understand how environmental factors can be manipulated to enhance PD biosynthesis in *H. macrophylla*. Additionally, determining the growth stage, at which PD and HD are most abundant is essential for optimizing the harvesting time to efficiently collect leaves rich in these compounds. Furthermore, investigation is needed to understand how leaf processing might impact PD and HD concentrations. Lastly, a thorough understanding of the PD biosynthetic pathway, including the genes, enzymes and metabolites involved is included in this study.

To close these gaps, a large variety of *H. macrophylla* accessions were screened for their enrichment of PD and HD. These lines were preselected from a pool of accessions provided by Koetterheinrich Hortensienkulturen (Ms. Frauke Engel) on the basis of their ornamental trait and aesthetic appeal. To identify the growth stage with

the highest PD content, selected plants were cultivated under controlled greenhouse conditions throughout their life cycle. A pre-treatment method involving leaf drying and enzyme treatment to enhance PD concentrations before extraction was implemented. A comprehensive analysis of the transcriptome and metabolome of *H. macrophylla* accessions with differing PD and HD contents was conducted. This analysis aimed to unravel the differences in metabolites and gene expression in plants with contrasting PD enrichment. Metabolomic analysis involved quantifying biomolecules using liquid chromatography tandem mass spectrometry (LC-MS/MS), while transcriptome analysis encompassed RNA sequencing followed by weighted gene co-expression network analysis (WGCNA), Kyoto Encyclopedia of Genes and Genomes (KEGG) pathway analysis, and Gene Ontology (GO) term analysis of the RNA sequences. Additionally, *H. macrophylla* accessions were exposed to abiotic stress conditions, specifically drought stress and high-light stress, to investigate alterations in the metabolite profile, including PD and HD concentrations. Collectively, these experiments offered insights into the natural and induced variation of PD concentrations from various perspectives.

3 Materials and methods

3.1 Plant material and sample processing

Fresh, fully expanded young upper leaves from 182 *Hydrangea macrophylla* accessions were obtained from Koetterheinrich Hortensienkulturen (Lengerich, Germany) and subsequently screened for phyllostulcin (PD) and hydrangenol (HD) concentration after drying the leaf tissue. Thirteen accessions were selected and were chosen for further experiments. The accessions used for the screening are listed in appendix 11.

From the selected 13 accessions, five accessions of *H. macrophylla* namely, VAR-552, VAR-746, VAR-553, VAR-212 and VAR-163, were grown from the cutting stage in the greenhouse at IPK-Gatersleben under controlled conditions, including an 18-hour photoperiod with a light intensity of $200 \mu\text{mol m}^{-2} \text{s}^{-1}$, temperature maintained at 21/19°C (day/night), and relative humidity set at 60%. Daily randomization and grouping of the plants were carried out.

The plants were allowed to grow for a total of 145 days, and five developmental stages were selected for the analysis: 20, 50, 75, 110 days from the initial cutting taken from the mother plants and planted in the soil to the stage of senescence after flowering. At each of these stages, fully expanded leaves, stems, roots, and later flowers from six replicates were harvested. The harvested materials were divided into two portions for separate analysis:

1. One portion of fresh tissues underwent a drying process at a temperature of 40°C for 48 hours, after which they were finely ground into a powder. The resulting powder was then placed into plastic containers and stored in a low-moisture environment.
2. The other portion was frozen immediately after harvesting, ground to a fine powder and stored in plastic vials at -80°C until they were needed for analysis.

3.2 Chemicals

LC-MS grade acetonitrile, methanol, and n-hexane used in this experiment were procured from Carl Roth (Karlsruhe, Germany). Formic acid was obtained from Thermo Fisher Scientific (Massachusetts, United States), and ultrapure water with a resistivity exceeding $18.2 \text{ M}\Omega\text{-cm}$ was produced using the Milli-Q® IQ 7000 Purification System. Analytical standards essential for the quantitative measurements

of phyllodulcin (PD) and hydrangenol (HD) were provided by Symrise AG, (Holzminden, Germany). Additionally, the analytical standards required for phenylpropanoid analysis were purchased from Sigma Aldrich (St. Louis, Missouri, United States).

3.3 Extraction and concentration of PD and HD

Both PD and HD were extracted with slight modifications to an existing method that included drying and fermentation steps, specifically using Accelerated Solvent Extraction (ASE) as described by Lee *et al.* (2008) and Jung *et al.* (2016). In this procedure, powdered tissue, both fresh and dried, was separately subjected to extraction to quantify the PD and HD concentrations under each condition. In both cases, 5-10 mg of ground tissue was fermented with 0.2 mL of ultrapure water for 2 hours at 40°C. Following this, 1.8 mL of methanol was added to the mixture, and it was further incubated in an ultrasonic bath for an additional 2 hours at 40°C. The supernatant was separated by centrifugation at 13,000× g for 10 minutes, and 1 mL of methanol was added to the sediment, which was then vortexed for 1 hour. The supernatant from this fraction was combined with the previous fraction after centrifugation at 13,000× g for 10 minutes. The final mixture was collected and passed through Strata C-18-E columns (55 µm, 70 Å, 100 mg/ml, Phenomenex, Germany) that had been preconditioned using 1 mL of methanol, and subsequently eluted with 1 mL of methanol. The final volume was collected and subjected to LC-MS analysis.

3.4 Extraction of phenolic compounds

For the extraction of phenolics, including p-coumaric acid, trans-cinnamic acid, caffeic acid, ferulic acid, naringenin, and trans-resveratrol, a liquid extraction using methanol was carried out with slight modifications based on the method described by Irakli *et al.* (2021). Approximately 5-10 mg of finely ground plant tissue was combined with 1 mL of 80% methanol and agitated in an ultrasonic bath for 1 hour at 30°C. The resulting extract was then subjected to centrifugation at 13,000× g for 10 minutes at 4°C, and the extraction process was repeated once more. The supernatant was subsequently filtered through a membrane filter with a porosity of 0.45 µm and collected in new Eppendorf tubes for further analysis.

3.5 Extraction of coumarins

The extraction of scopolin, scopoletin, esculin, esculetin, fraxetin, and umbelliferone was performed with slight modifications based on a previously published method (Perkowska *et al.*, 2021). Initially, 1 mL of methanol was added to the finely ground and powdered samples. These samples were then subjected to sonication for 1 hour, followed by incubation in darkness at 4°C for an additional 2 hours. After this incubation period, all the samples underwent centrifugation at 13,000 × g for 10 minutes, and the resulting supernatants were carefully transferred to new Eppendorf tubes. To further process the extracts, they were first dried for 2 hours in an incubator at 45°C and then for an additional 2 hours in a vacuum centrifuge. Subsequently, 100 µL of 80% methanol was added to the dried extracts to dissolve the samples, and they were left to incubate overnight at 4°C. The following day, the extracts were vortexed for 10 minutes and separated into 50 µL aliquots. These samples were stored at -20°C until they were ready for analysis via LC-MS.

3.6 Extraction and quantification of carbohydrates

The method employed for assessing soluble sugars and starch levels in the leaves was adapted from the procedure outlined by Ahkami *et al.* (2013) with some modifications. Initially, 50 mg of fully expanded leaves were subjected to homogenization in liquid nitrogen. Extracts were prepared by using 0.7 mL of 80% (v/v) ethanol, followed by an incubation period at 80°C for 60 minutes at 600 rpm. Subsequently, the crude extracts underwent centrifugation at 14,000 rpm at 4°C for 5 minutes, and the resulting supernatant was carefully collected in new Eppendorf tubes. The residual pellet was washed twice with 1 mL of 100% ethanol. To convert starch into glucose, 0.2 mL of 0.2 N KOH was added, followed by an overnight incubation at 4°C. This was followed by neutralization with 0.07 mL of acetic acid 1N, maintaining a pH range of 6.5-7.5. Sample digestion was facilitated using 0.1 mL of a buffer containing 2 mg·mL⁻¹ amyloglucosidase in 50 mM sodium acetate at pH 5.2, followed by an overnight incubation at 37°C. Starch concentration was subsequently calculated based on the glucose concentration in the samples after starch breakdown. The determination of glucose, fructose, and sucrose levels was carried out through a photometric assay that involved the use of hexokinase, phosphoglucosomerase, and invertase enzymes, with the oxidation of NAD to NADH (Nicotinamide adenine dinucleotide) being monitored at a maximum wavelength of 340 nm.

3.7 Extraction and quantification of amino acids

The ethanol extracts obtained from the sugar measurements were utilized for amino acid analysis following the methodology described by Mayta *et al.* (2018). In this process, NMR-purified fluorescing reagent AQC (6-aminoQuinolyl-N hydroxysuccinimidyl carbamate) sourced from BIOSYNTH AG in Switzerland was employed as the derivatization agent. The AQC reagent was prepared by dissolving 3 mg of AQC in 1 mL of acetonitrile, followed by incubation for 10 minutes at 55°C. The derivatization of amino acids involved the use of 0.01 mL of the extract or standard mixture, 0.01 mL of AQC, and 0.08 mL of 0.2M boric acid at pH 8.8. This mixture was subjected to a 10-minute incubation at 55°C. The separation of 20 different soluble amino acids was achieved through ultra-pressure reversed-phase chromatography (UPLC) using the Acquity H-Class machine by Waters GmbH in Germany, equipped with a fluorescent (FLR) detector. A reversed-phase C18 column (Luna Omega, 1.6 µm, 2.1x100 mm, from Phenomenex, Germany) was employed for chromatographic separation, with a flow rate of 0.6 mL/min for a total runtime of 6 minutes and a column temperature of 40°C. The chromatographic gradient was created using eluent A concentrate, eluent B, and eluent C, with the addition of high-purity water as per the manufacturer's instructions (Bioanalytics Gatersleben, <http://www.bioanalytics-gatersleben.de>). Amino acids were detected at excitation and emission wavelengths of 266 and 473 nm, respectively. For quantification, a calibration curve was generated using a standard mix containing 20 amino acids at concentrations ranging from 0.5 to 20 nmol/mL. Data acquisition and final qualitative and quantitative analysis were performed using Empower 3 software from Waters GmbH in Germany.

3.8 UPLC-MS analysis

UPLC–MS analyses were performed on Agilent 1290 UPLC system coupled to Agilent 6490 Triple Quadrupole Mass spectrometer (Agilent Technologies, Waldbronn Germany). The chromatographic separation was performed using ZORBAX RRHD Eclipse Plus C18, 95Å, 2.1 x 50 mm, 1.8 µm column (Agilent Technologies, Santa Clara, USA) at a flow rate of 0.45 mL/min and a column temperature of 40°C. 1µL of the injected samples were eluted using a gradient of solvent A (water) and B (acetonitrile), both with 0.1 % formic acid (v/v). The initial percentage of B was 10 %, which was linearly increased to 80 % in 5 min, then re-equilibrated with original conditions in 6th min. ESI-MS/MS analysis was conducted in positive and negative

ionization modes by using nitrogen as drying and nebulizing gas. The gas flow was set at 12.0 l/min at 250°C and the nebulizer pressure was 30 psi. The capillary voltage was 2 kV and a dwell time of 20. The collision energy ranged from 9 to 69 eV depending on the masses estimated using MassHunter optimizer software using MS₂ Selected Ion Monitoring (SIM). To improve sensitivity, accuracy and specifically select parent ion and daughter ions corresponding to the mass of the molecules of interest, Multiple reactions monitoring (MRM) was performed. 14 essential metabolites in the pathway were selected for quantification and calibration curve was set up from a range between 0.01- 50 µg per ml. Agilent MassHunter software (B.07.01, Agilent Technologies, United States) was used for data acquisition and final qualitative and quantitative analysis. A detailed description of the analysis is added to the results chapter.

3.9 RNA isolation, sequencing and analysis

To isolate total RNA from the plant tissues, the Spectrum™ Plant Total RNA Kit, obtained from Sigma Aldrich, was employed following the manufacturer's guidelines, and it was found to be highly effective for isolating RNA from *Hydrangea* tissues. Total RNA was isolated and analyzed from three replicates of 14 selected accessions, each with varying levels of PD and HD concentration. The quality of RNA was assessed using NanoDrop™ 2000c spectrophotometry from Thermo Scientific™, with a 10µL volume collected and used for sequencing. RNA integrity was further evaluated using the RNA Nano 6000 Assay Kit on the Bioanalyzer 2100 system by Agilent Technologies in California, USA. For cDNA library preparation and transcriptome sequencing, Novogene Co conducted the procedures using the NEBNext® Ultra™ RNA Library Prep Kit for Illumina® (NEB, USA). Initially, mRNA was purified from total RNA using poly-T oligo-attached magnetic beads, followed by fragmentation. Subsequently, the first and second strands of cDNA were synthesized using a random hexamer primer and M-MuLV Reverse Transcriptase (RNase H-) along with DNA Polymerase I and RNase H, respectively. cDNA fragments of lengths between 370 to 420 bp were selected after purifying library fragments using the AMPure XP system from Beckman Coulter in Beverly, USA. PCR was then carried out with Phusion High-Fidelity DNA polymerase, Universal PCR primers, and Index (X) Primer. The quality of the libraries was assessed using the Agilent Bioanalyzer 2100 system. Upon library preparation, 150 bp pair end reads were generated after clustering. The reference

genome and gene model annotation files were downloaded directly from <https://plantgarden.jp>. Indexing of the reference genome and read alignment to the reference genome were performed using Hisat2 v2.0.5. The mapped reads from each sample were assembled using StringTie (v1.3.3b) (Pertea *et al.*, 2015) in a reference-based approach. FeatureCounts v1.5.0-p3 was utilized to count the number of reads mapped to each gene. Differential expression analysis was conducted using the DESeq2 R package (v1.20.0). The resulting p-values were adjusted using the Benjamini and Hochberg's approach to control the False Discovery Rate (FDR), represented as p_{adj} value. Significantly differentially expressed genes were identified with a corrected p-value of 0.05 and an absolute fold change of 2 as the threshold.

To gain insights into the functional significance of differentially expressed genes, Gene Ontology (GO) enrichment analysis was performed using the clusterProfiler R package, with GO terms exhibiting corrected p-values below 0.05 considered significantly enriched by the differentially expressed genes. Additionally, KEGG (Kyoto Encyclopedia of Genes and Genomes) pathway enrichment analysis was conducted to assign each gene to its respective pathways.

3.10 Validation of gene expression using qRT-PCR

The RevertAid First Strand cDNA Synthesis Kit from Thermo Scientific was utilized to perform cDNA synthesis, and 0.3 μ g of total RNA was employed as the starting material. This synthesis process was initiated using oligo(dT) primers. The primers for the quantitative real-time polymerase chain reaction (qRT-PCR) were created through primer design software Primer3, and they were subsequently synthesized by the company Metabion in Germany. The list of primers designed for validation with qRT-PCR are represented in table 1. Specific criteria during the primer design process included achieving a melting temperature (T_m) within the range of $60 \pm 1^\circ\text{C}$, designing primers with a length between 18 and 25 base pairs, preferably located close to the 3'-end of the target sequence, and ensuring a GC content between 40% and 60%. This strategy aimed to generate PCR products that are unique and relatively short, ranging from 60 to 150 base pairs in length. To analyze gene expression levels, the cDNA samples were employed in qPCR, which was conducted using the CFX384 TouchTM system from Bio-Rad. For the qPCR reactions, the iQ SYBR Green Supermix from Bio-Rad (Hercules, CA, USA) was used. The samples underwent examination in triplicates, following this procedure: an initial activation cycle was

carried out for 3 minutes at 95°C; this was followed by 40 amplification cycles, with each cycle comprising 15 seconds at 95°C and then 30 seconds at either 58°C or 60°C, depending on the specific primer used. Subsequently, a single melting curve cycle was executed, spanning from 65°C to 95°C, with increments of 0.5°C every 5 seconds. The Ct (Cycle threshold) values obtained were exported from the Bio-Rad CFX Manager Software (Version 3.1, Bio-Rad Laboratories) and were employed to calculate the efficiency of PCR amplification. Normalization factors were calculated using glyceraldehyde-3-phosphate dehydrogenase (GAPDH) as reference gene. PCR amplification efficiency was determined following the guidelines outlined in prior instructions (Bustin *et al.*, 2009). Only experiments exhibiting an efficiency falling within the range of 90% to 110% were considered. Normalization factors were calculated using geNORM (Vandesompele *et al.*, 2002). The expression levels of genes between different study groups of accessions having varying metabolite contents were represented as foldchange using the formula:

$$\text{Fold change} = \frac{\left(\frac{2^{-C_t^{GOI}}}{NF}\right)_{\text{target sample}}}{\left(\frac{2^{-C_t^{GOI}}}{NF}\right)_{\text{reference sample}}}$$

where NF is the calculated normalization factor, C_t is the cycle threshold, and GOI is the investigated gene of interest.

Table 1. List of qRT-PCR primers used for validation.

Gene	Forward primer 5'→3'	Reverse primer 5'→3'
Glyceraldehyde-3-phosphate dehydrogenase - <i>GADPH</i>	GGCTGAGACTGGAGCGGAAT	CAAACATGGGGGCGTCTTTGC
Double Bond Reductase - <i>DBR</i>	ACCGTTGTGCCTTACATCAG	ACGGCCACTAAAGAGTCCAA
Dihydroflavonol 4-reductase - <i>DFR</i>	ATGTTGGACGCCTCTCCATC	CACAAGTCCACACCCAAGAG
p-Coumaroyl tri acetic acid synthase - <i>CTAS</i>	CAGGCAAAAGTGGGTCTGAA	GAAAAACACACATGCGCTGG
Polyketide Cyclase - <i>PKC</i>	TGCAGCCCATTCCAAATCAG	TGATGAAGGACCTTTTCGGGA
Phenylalanine ammonia-lyase 1 – <i>PAL1</i>	ATCAGAGAGTGCCGGTCTTT	ACCGGACTTTTCTCTCCTGTC
4-coumarate CoA ligase – <i>4CL</i>	TGGTTCCAAGATCTCCGAGG	GAGCTTTTGGGATTGCGTCT
Keto reductase - <i>KR</i>	GGTAGCCCTGAATATGTGCG	GTCGACACGATGTGGGTAGT
Hydroxycinnamoyl transferase - <i>HCT</i>	AGATGGACTTTCAGCCCTCC	GAGGATGGTCCGATCGATGA
Caffeoyl-CoA 3-O-methyltransferase - <i>CCoAOMT</i>	GGCATGGAGCACAAGATCAA	GGGCTTGTGACGTCATAA
Caffeic acid O-methyltransferase - <i>COMT</i>	GTGTCGATCGGAAGGCCATA	ATGCGACAGCACAAGGTAAC

3.11 Gene co-expression analysis

WGCNA is a data-driven method that discovers co-clustered gene sets (modules) based on weighted correlations between gene transcripts. For the construction of gene co expression networks, weighted gene co-expression network analysis (WGCNA) was performed on 22,980 genes having high variance among the accessions which were obtained from RNA sequencing of *Hydrangea* accessions. The WGCNA (version 1.72-1) R software package is a comprehensive collection of R functions for performing various aspects of weighted correlation network analysis. This R package included functions for network construction, module detection, gene selection,

calculations of topological properties, data simulation, visualization, and interfacing with external software (Langfelder and Horvath, 2012).

3.12 Drought stress experiment

Five selected accessions of *H. macrophylla* namely VAR-552, VAR-746, VAR-553, VAR-212 and VAR-163 were grown under drought stress. Initially, all the plants were grown in the green house of IPK-Gatersleben under the following conditions: 18-h photoperiod with $200 \mu\text{mol m}^{-2} \text{s}^{-1}$ light intensity, 21/19 °C (day/night) temperature and 60% relative humidity for 10 days from cutting stage. After the 10th day the plants were separated into two batches. 12 plants of each accessions were grown under ambient growth conditions and watered regularly. These plants were used as control plants. Similarly, 12 plants of the same accessions were watered to the brim of the pot and allowed to completely drain. After complete drain, each day the moisture content of soil was monitored using moisture meter (Delta T devices Ltd. England). A reference water of 450ml was added to maintain equal water conditions until all the plants reached desired soil moisture. After 24 days all these plants attained 5% soil moisture. These plants were randomized daily and soil moisture content was monitored. The plants were maintained for 20 more days under this moisture until harvest. The top fully expanded leaves were harvested. One portion of the harvested leaves were dried in oven at 40°C for 48 hours and second portion was frozen in liquid nitrogen and stored at -80°C until analysis.

3.13 Light stress experiment

Five selected accessions of *H. macrophylla* namely VAR-552, VAR-746, VAR-553, VAR-212 and VAR-163 were grown under high light intensity to induce light stress. 6 biological replicates of each accessions were grown under normal growth conditions within the greenhouse for 10 days (18hrs photoperiod with $150 \mu\text{mol m}^{-2} \text{s}^{-1}$ ($150 \mu\text{E m}^{-2} \text{s}^{-1}$) light intensity, 21/19 °C (day/night) temperature and 60% relative humidity). On the 11th day treatment 6 plants each were shifted to two different growth chamber both having same growth conditions but differed in light intensity. The six control plants were grown under $150 \mu\text{E m}^{-2} \text{s}^{-1}$ of light intensity and six treatment plants were grown under $600 \mu\text{E m}^{-2} \text{s}^{-1}$. The plants were regularly watered normally until harvest. After 22 days the treatment plants started to show pigmentation and plants in both the chambers were harvested. One portion of the harvested leaves were dried in oven at

40°C for 48 hours and second portion was frozen in liquid nitrogen and stored at -80°C until analysis.

3.14 β -glucosidase digestion

To convert the glucoside forms of PD and HD into their active forms, a digestion step was carried out using almond β -Glucosidase procured from Sigma Aldrich (G-0395), with slight modifications adapted from Cowan *et al.* (2021). Approximately 5-7 mg of homogenized leaf powder (fresh and dried) was placed in 2ml Eppendorf tubes. Next, 150 μ L of 0.2% w/v β -glucosidase (Almond) in 0.1M citrate buffer (pH 5.6) (containing trisodium citrate) was added to the tubes. These tubes were then placed in an incubation block and shaken for 1 hour at 35°C.

Following the 1-hour incubation, 1 mL of methanol was introduced to the samples, and they were shaken for an additional 1 hour. Subsequently, the tubes were centrifuged for 15 minutes at 13,000 \times g, and the resulting supernatant was carefully separated. This supernatant was used for the extraction of PD and HD as described in section 3.3.

3.15 Statistical analysis

Statistical analysis was carried out using GraphPad Prism 9.5.1 (GraphPad Software Inc.) and R (version 4.0.3). For multiple comparison analysis, a one-way ANOVA with post hoc Tukey's test ($p \leq 0.05$) was conducted. To assess the significance of differences between the control and treatment groups, paired sample t-tests were performed.

4 Results

4.1 Analysis of metabolites in *H. macrophylla* via UPLC-MS/MS

To study the concentrations of different metabolites in different accessions, leaf extracts were subjected to UPLC-MS/MS analysis. To separate these metabolites from the matrix, chromatographic separation was performed using a reverse-phase column and all samples were analyzed in positive and negative mode electrospray ionization (+/-ESI). A scan range of 10-500 was used to acquire the m/z ratio of metabolites. In an MS/MS experiment, mass-selected precursor ions are induced to dissociate into product ions, which are then mass analyzed by a second analyzer. Once multiple reaction monitoring (MRM) transitions were decided, the calibration curves were derived for injections of known amounts of each metabolite. Five different concentrations of these molecules were used to prepare a calibration curve and the absolute quantification was performed using a single MRM transition for each analyte (Appendix 1-3). A good linearity was achieved for all metabolites with a correlation coefficient of above 0.9145 with the concentration ranges 0.01-50 µg/mL. The limit of quantification (LOQ) for the coumarins were measured by triplicate injections of the standard solutions based on signal to noise ratio of 10.

MassHunter optimizer software was used to select precursor ions using MS² Selected Ion Monitoring (SIM), product ions using product ion scan for each precursor ion and optimum collision energy for each transition using MRM acquisition mode (Table 2). Product ions were selected as the most abundant ions in a composite product ion scan spectrum obtained for a given precursor ion at multiple collision energies. With the collision energy of 13 eV, [PD+H]⁺ fragmented into a product having m/z of 269.1 [M-OH]⁺, indicating the loss of hydroxyl group (-OH, molar mass = 17g/mol) (Figure 6A). This fragment showed highest abundance among all other fragments. Similarly, at a collision energy of 13 eV, [HD+H]⁺ fragmented into a characteristic m/z of 239.1 [M-OH]⁺ with highest abundance (Figure 6B). [Naringenin+H]⁺, dissociated into a fragment containing characteristic m/z of 152.9 at a collision energy of 25 eV. This most abundant fragment was a result of the formation of [M+H - C₈H₈O]⁺ ions (Figure 6C). [Resveratrol+H]⁺ at a collision energy of 17 eV, gave a characteristic fragment of m/z 135 indicating the formation of an ion species - [M+H - C₆H₆O]⁺ (Figure 6D). Similar fragmentation pattern was observed also in previous studies (Claeys *et al.*, 1996; Flamini and Vedova, 2004).

Table 2. Transitions of ions used for quantification of metabolites. The transition of ions used for quantification and mode of ionizations, QIT, collision energies (CE) of corresponding transition in eV and retention time (t_R) in minutes of the 14 metabolites analyzed in leaf extracts of *Hydrangea* accessions.

Sl.no	Molecule	QIT	CE (eV)	t_R (min)	Ionization
1	Phyllodulcin	287.1→269.1	13	4.036	Positive
2	Hydrangenol	257.1→239.0	13	3.933	Positive
3	Naringenin	273.1→152.9	25	2.460	Positive
4	Resveratrol	229.1→135.0	17	2.777	Positive
5	Umbelliferone	163.0→118.9	17	2.093	Positive
6	Caffeic acid	179.0→135.0	14	1.296	Negative
7	Ferulic acid	193.1→134.1	18	2.194	Negative
8	trans-Cinnamic acid	147.0→103.1	10	3.134	Negative
9	<i>p</i> -Coumaric acid	163.0→119.0	14	1.952	Negative
10	Scopolin	355.1→193.0	9	0.926	Positive
11	Scopoletin	193.1→133.0	21	2.160	Positive
12	Esculin	341.1→179.0	13	0.611	Positive
13	Esculetin	179.1→122.9	25	1.238	Positive
14	Fraxetin	209.5→149.0	21	1.738	Positive

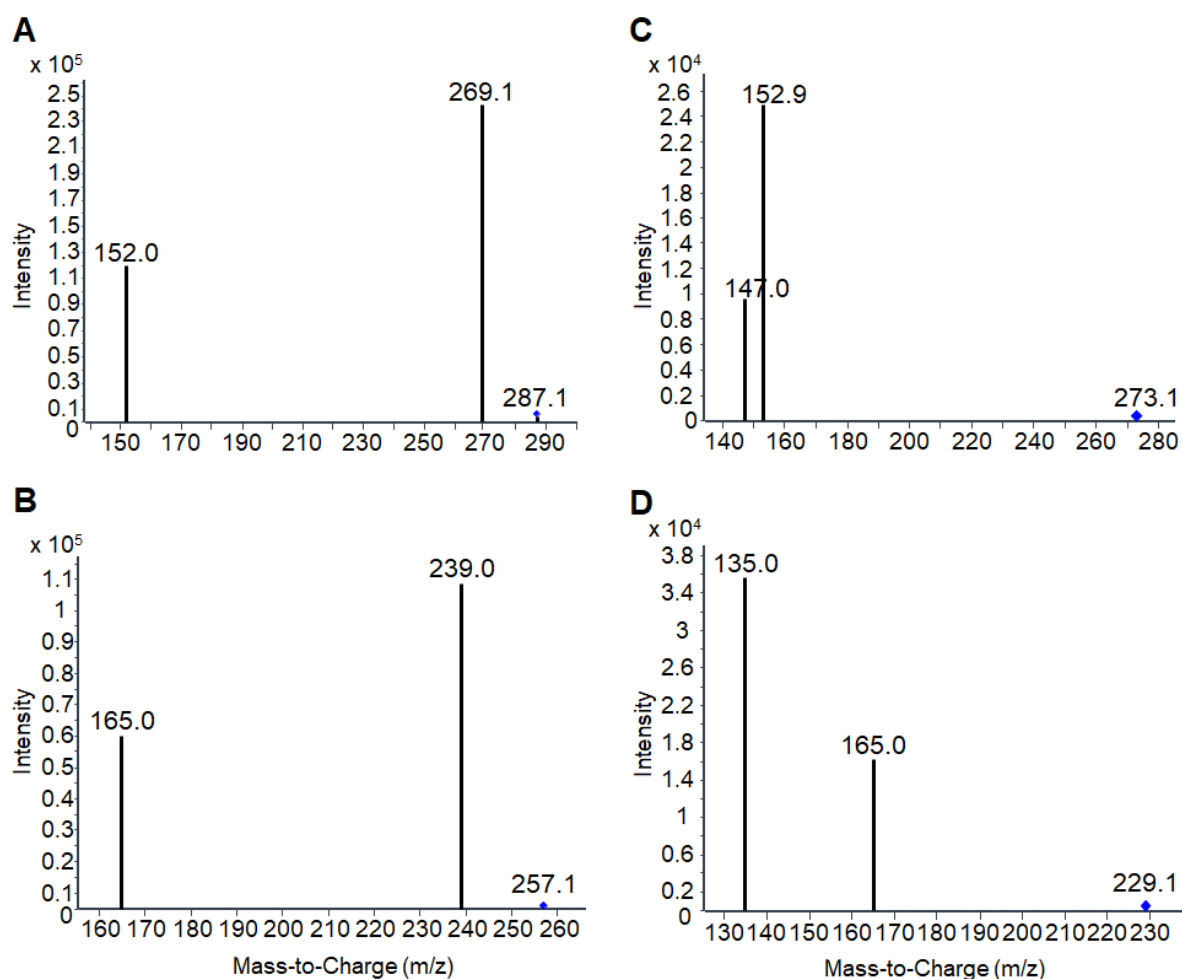


Figure 6. Mass spectra (MS/MS) of product ions obtained from MRM. (A-D) Fragmentation patterns of (A) PD, (B) HD, (C) naringenin and (D) resveratrol in positive ionization mode. The protonated $[M + H]^+$ is represented by the blue dot. The collision energy of each transition was determined by MS₂ Selected Ion Monitoring (SIM). Each bar represents the intensity of the fragmented ion with specific m/z and the ion with the highest abundance was selected as quantifier and the lowest intensities were used as qualifiers.

The negative mode ionization of $[\text{trans-cinnamic acid-H}]^-$ with a collision energy of 10 eV gave rise to characteristic fragment of m/z 103.1 with highest abundance (Figure 7A). This fragment was formed by the loss of CO₂ (Meisser Redeuil *et al.*, 2009). Similarly, it was possible to identify the $[\text{p-coumaric acid-H}]^-$ based on the peak corresponding to the characteristic fragment of m/z 119 using a collision energy of 14eV (A. Santos *et al.*, 2021) (Figure 7B). In the negative mode at low collision energies of 14eV and 18eV, $[\text{caffeic acid-H}]^-$ and $[\text{ferulic acid}]^-$ formed decarboxylation products with high abundance (Figure 7C, D). $[\text{M-H-CO}_2]^-$ at m/z 135 for caffeic acid, and $[\text{M-H-CO}_2-\text{CH}_3]^-$ at m/z 134.1 for ferulic acid (Alonso-Salces *et al.*, 2009).

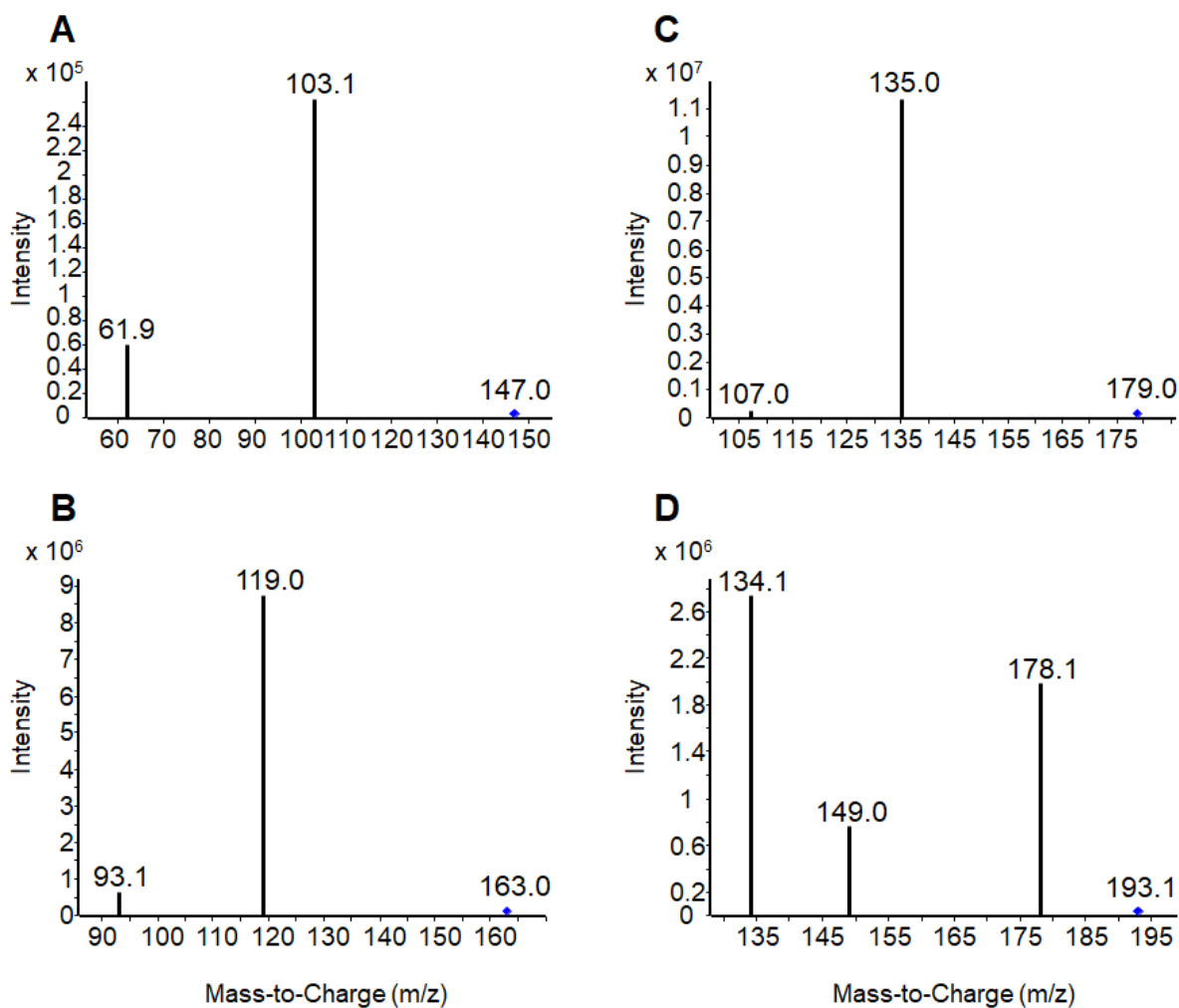


Figure 7. Mass spectra (MS/MS) of product ions obtained from MRM. (A-D) Fragmentation patterns of (A) trans-cinnamic acid, (B) para-coumaric acid, (C) caffeic acid and (D) ferulic acid in negative ionization mode. The deprotonated $[M - H]^-$ is represented by the blue dot. The collision energy of each transition was determined by MS₂ Selected Ion Monitoring (SIM). Each bar represents the intensity of fragmented ion with specific m/z and the ion with the highest abundance was selected as quantifier and the lowest intensities were used as qualifiers.

At a collision energy of 9 eV, the precursor ion of $[\text{Scopolin}+H]^+$ fragmented to produce a characteristic fragment with m/z of 193 (Figure 8A). This fragment was formed by the removal of $-C_6H_{10}O_5$ group from the parent molecule (Xiao *et al.*, 2019). Using the product ion scan mode, the most abundant fragment was recorded at m/z 133 for $[\text{scopoletin}+H]^+$ (Figure 8B). This characteristic fragment m/z 133 was formed from the removal of $-COCH_3OH$ from the parent molecule (Zeng *et al.*, 2015). Similarly, $[\text{Umbelliferone}+H]^+$ due to collision induced dissociation at 17 eV, fragmented to a characteristic m/z of 118.9 showing high abundance (Figure 8C). The loss of neutral CO_2 should attribute to the formation of this highly abundant species (Wang *et al.*, 2014). The collision energy of 13eV and 25 eV was used to fragment the precursor

ions of [Esculin+H]⁺ and [Esculetin+H]⁺ respectively (Figure 8D, E). The fragmentation resulted in characteristic product ions with m/z 179 and 122.9 respectively. Similar fragmentation pattern was also observed in earlier studies (Yang *et al.*, 2017). Under a collision energy of 21 eV, [Fraxetin+H]⁺ fragmented to produce a characteristic fragment with m/z 149 (Figure 8F). In the fragmentation pattern of [Fraxetin+H]⁺, m/z 149 was found to be the highest abundant product (Zhao *et al.*, 2014). This quantitative ion transition (QIT) derived from MRM was used to quantitate the metabolites and the retention times (tR) during chromatographic separation were used to demarcate each metabolite in the samples.

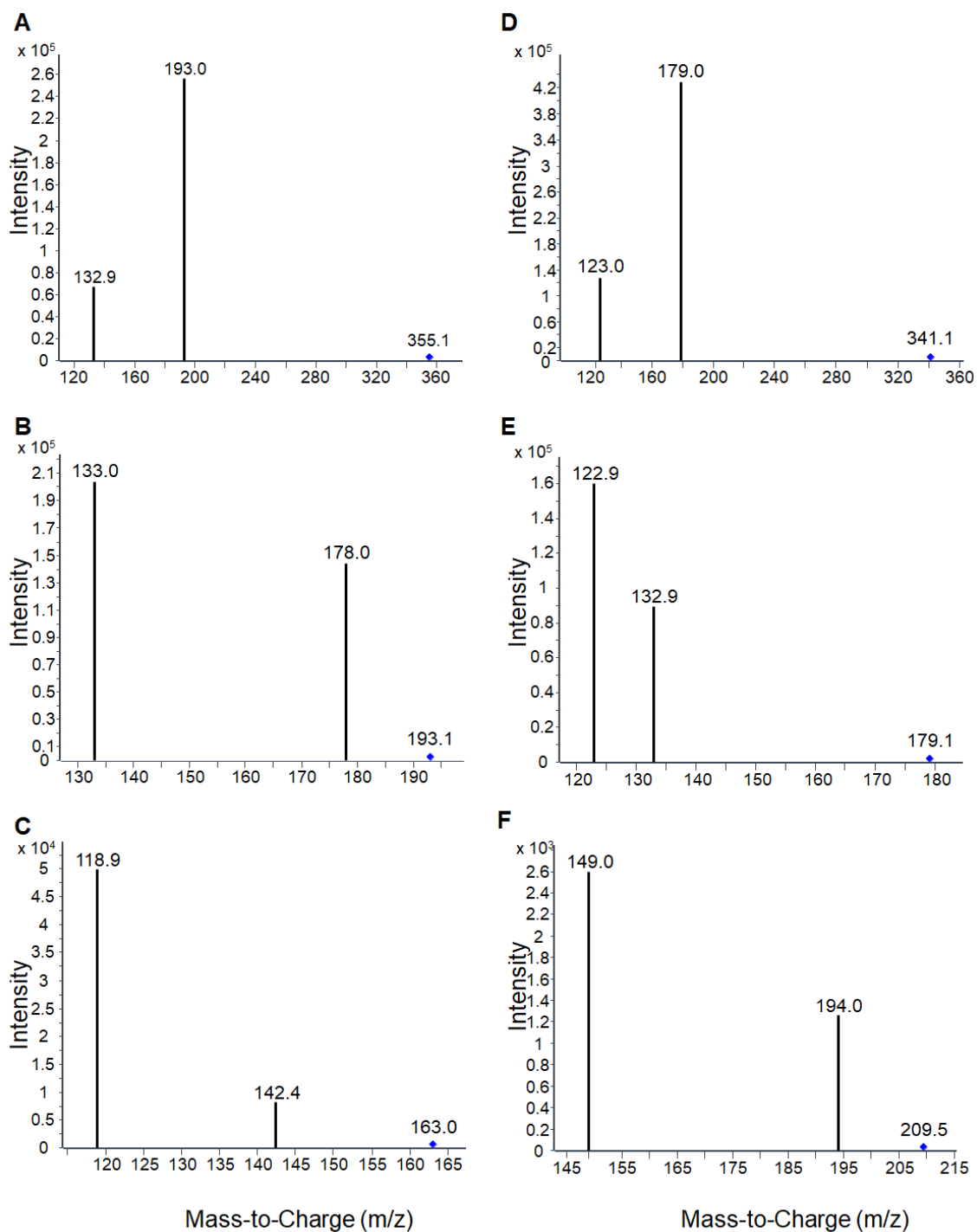


Figure 8. Mass spectra (MS/MS) of product ions obtained from MRM. (A-F) Fragmentation pattern of (A) scopolin, (B) scopoletin, (C) umbelliferone, (D) esculin, (E) esculetin and (F) fraxetin in positive ionization mode. The protonated $[M + H]^+$ is represented by the blue dot. The collision energy of each transition was determined by MS₂ Selected Ion Monitoring (SIM). Each bar represents the intensity of fragmented ion with specific m/z and the ion with the highest abundance was selected as quantifier and the lowest intensities were used as qualifiers.

This mass spectrometric analysis provided an overall detail about the fragmentation pattern of selected metabolites in leaf extracts of *Hydrangea* accessions and provide a reliable analysis condition for the rapid detection of these metabolites.

4.2 Screening and selection of *H. macrophylla* accessions based on phyllodulcin (PD) and hydrangenol (HD) content

To investigate the distribution of specific dihydroisocoumarins and select plants with varying phyllodulcin (PD) content, a total of 182 accessions of *H. macrophylla* were utilized in this study, all of which were provided by Koetterheinrich Hortensienkulturen (Appendix 11). The primary objective was to quantify the concentrations of PD and hydrangenol (HD) in these accessions to identify those plant accessions that contain high PD and/or high HD and to use them for further studies and crosses in the next generation to increase the PD content for biochemical pathway analysis and industrial use (Figure 9). Leaf tissues from all accessions were harvested and subsequently dried at 40°C for 48 hours as an initial screening step. LC-MS analysis was then conducted to quantify both PD and HD concentrations across all desired accessions. The measured PD concentrations among the different accessions in this study ranged from 1.366 to 38.343 mg g⁻¹ DW, while HD concentrations spanned from 1.285 to 28.807 mg g⁻¹ DW (Figure 9). Based on these measurements, the accessions were categorized into four distinct classes (study groups) according to their PD and HD concentrations, and these accessions were recommended for further breeding efforts aimed at enhancing isocoumarin concentrations in future progenies.

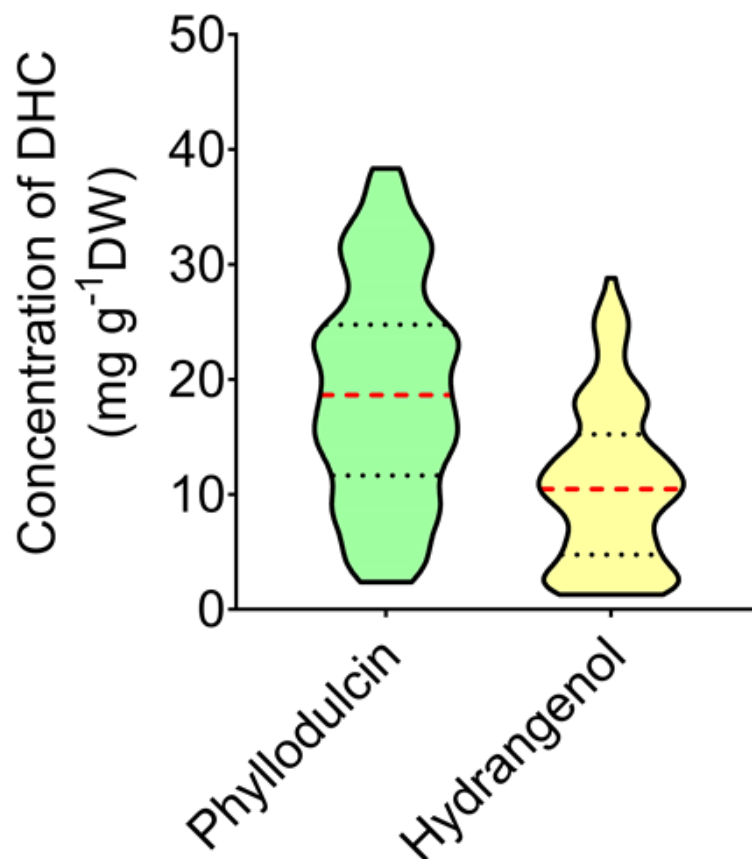


Figure 9. Screening and selection of *Hydrangea* accessions based on phylloidalcin (PD) and hydrangenol (HD) levels. The red dotted line in the violin plot represents median observations while black dotted line represents the 3rd and 1st quartile. Of the 182 accessions studied, 14 accessions with high PD, high PD/HD, high HD, low PD/HD and *H. paniculata* as negative control were selected for further experiments.

Specifically, 13 accessions were selected based on their PD content (Table 3). Additionally, *Hydrangea paniculata*, a species known to contain no detectable PD or HD, was included as a reference variety (negative control). The PD and HD concentrations of all the selected accessions were evaluated in both freshly harvested leaves and leaves that had been dried at 40°C for 48 hours (Figure 10A-D). A comparison of freshly harvested leaves with dried leaves revealed that the dried leaves of the selected accessions contained significantly higher levels of PD and HD compared to their fresh counterparts. Notably, PD and HD were not detected in *H. paniculata*.

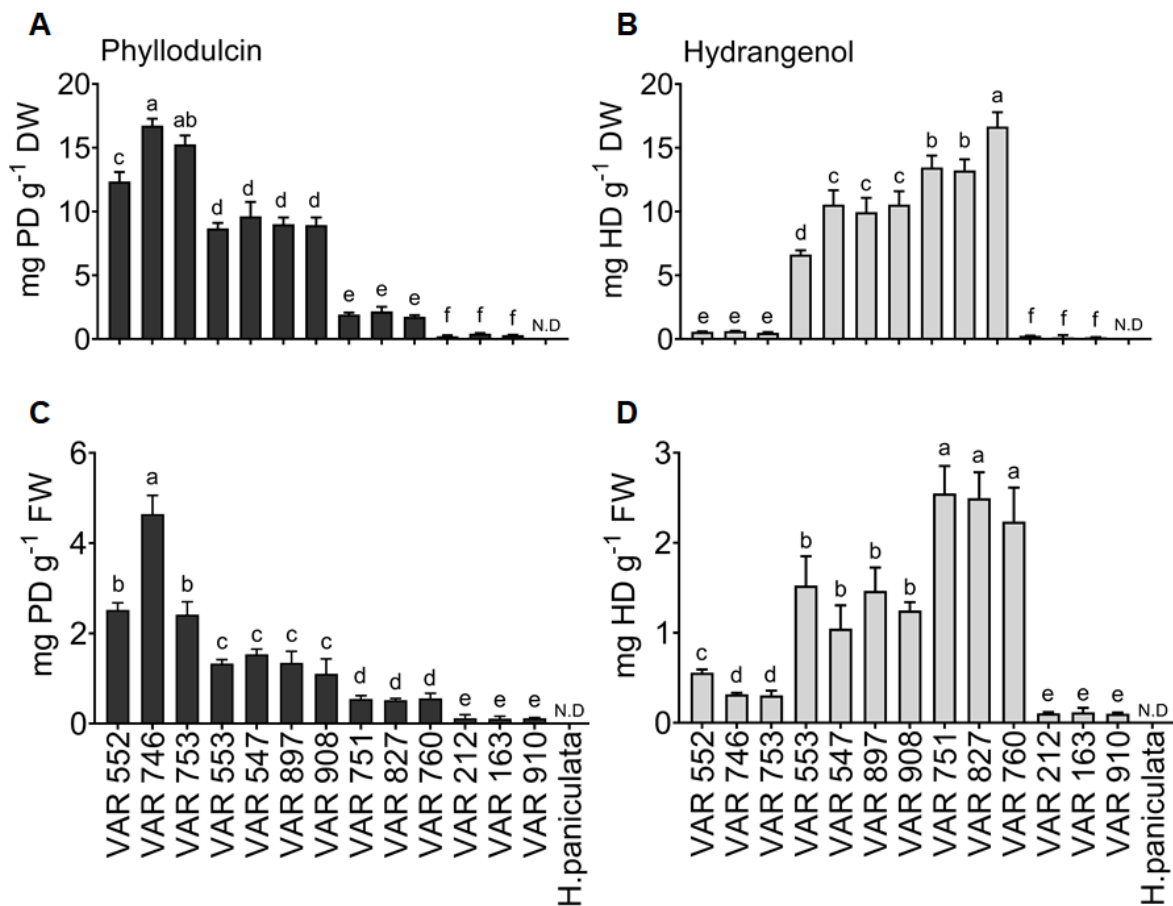


Figure 10. Phyllodulcin (PD) and hydrangenol (HD) concentrations in selected *Hydrangea* accessions. (A) PD and (B) HD concentrations in dried leaves of selected accessions. (C) PD and (C) HD concentrations in freshly harvested leaves of selected accessions. Analysis was performed on fully expanded, young upper leaves. Bars represent means + SE (n=6). Not detected (N.D), indicates the absence of the corresponding metabolite. Different letters denote significant differences among accessions according to one-way ANOVA and post-hoc Tukey's test ($p < 0.05$).

The leaves used for this selection were obtained from plants approximately 75 days after taking cuttings from the mother plant and planting them in the soil. Five out of the 13 selected accessions were cultivated from the cutting stage in the IPK greenhouse to ensure a consistent supply of plant material for the study. These five accessions included two with high PD content (VAR-552 and VAR-746), two with low PD/HD content (VAR-212 and VAR-163), and one with high PD and HD (VAR-553). The screening and selection process of *Hydrangea* accessions served to optimize the research workflow and acted as a valuable resource for developing next-generation crosses with increased PD and HD content. Furthermore, it provided insights into the enhancement of PD and HD concentrations through leaf drying.

Table 3. Categorization of *H. macrophylla* accessions into study groups based on PD and HD concentrations. According to MS-based analysis, the selected accessions were categorized into 4 different study groups based on phyllodulcin (PD) and hydrangenol (HD) concentrations. The stars (*) represent the accessions grown in the green house of IPK.

SI no:	High PD accessions	High HD accessions	High PD/HD accessions	Low PD/HD accessions
1	VAR-552*	VAR-751	VAR-553*	VAR-212*
2	VAR-746*	VAR-827	VAR-547	VAR-163*
3	VAR-753	VAR-760	VAR-897	VAR-910
4			VAR-908	

4.3 Distribution of PD and HD in different plant organs of *H. macrophylla*

To investigate the distribution of PD and HD within the anatomy of *H. macrophylla*, it was imperative to quantify these specific dihydroisocoumarins in various plant organs, including leaves, stems, flowers, and roots. To achieve this, tissues from these organs were harvested from five selected accessions of *H. macrophylla* cultivated in the greenhouse (Table 2). The plants were approximately 85 days after the cuttings were taken from the mother plant and planted in the soil. As the bioavailability of PD and HD is higher in dried tissues compared to freshly harvested tissues, the collected tissues were dried at 40°C for 48 hours before conducting the extraction. Metabolite analysis of different tissue extracts revealed that the concentration of PD in different accessions ranged from 11.37 to 0.73 mg g⁻¹ DW in leaves, 5.88 to 0.35 mg g⁻¹ DW in flowers, 0.81 to 0.10 mg g⁻¹ DW in stems, and 0.62 to 0.11 mg g⁻¹ DW in roots, respectively (Figure 11A-E). A similar trend was observed in the concentrations of HD in different plant tissues, ranging from 5.73 to 0.59 mg g⁻¹ DW in leaves, 4.15 to 0.42 mg g⁻¹ DW in flowers, 0.85 to 0.08 mg g⁻¹ DW in stems, and 1.75 to 0.11 mg g⁻¹ DW in roots, respectively, in different accessions (Figure 12A-E).

In this experiment, the highest concentration of PD was observed in the leaves of VAR-746 (11.37 mg g⁻¹ DW). There were significant differences in the concentrations of PD between leaves and flowers in all accessions. However, the concentrations of PD did not show significant differences between stems and roots in all accessions. Similarly, HD concentrations also showed significant difference between leaves and flowers but not between stem and roots. The highest concentration of HD was found in the leaves

of VAR-553 (6.24 mg g⁻¹ DW). VAR-552 and VAR-746 had higher concentrations of PD compared to HD, whereas VAR-553 had similar concentrations of both PD and HD. In contrast, VAR-212 and VAR-163 contained the lowest concentrations of both PD and HD. These findings suggest that the highest concentrations of PD and HD are primarily located in the leaves, followed by flowers, with stems and roots containing comparatively lower concentrations.

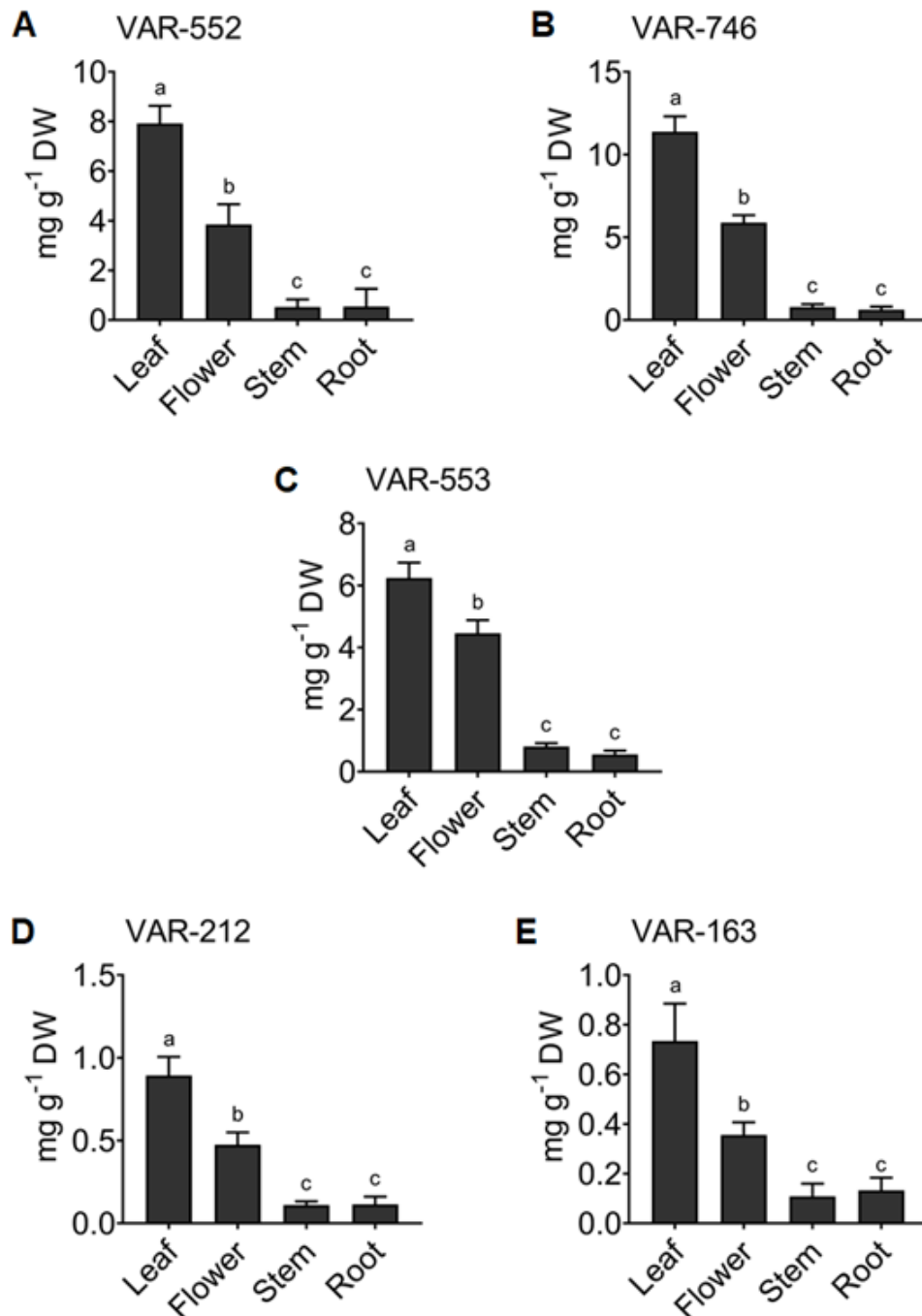


Figure 11. Concentrations of PD in different plant organs of selected *H. macrophylla* accessions. (A-E) PD concentrations in four major organs leaf, flower, stem and roots of *H. macrophylla* accessions (A) VAR-552, (B) VAR-746, (C) VAR-553, (D) VAR-212 and (E) VAR-163. Tissues under study were fully expanded young upper leaves, fully opened flower as whole, stem cuttings of equal length and root tissues. Analysis was performed on tissues dried at 40°C for 48 h. Bars represent means + SE, n= 6 independent biological replicates and standard error. Different letters denote significant differences among accessions according to one-way ANOVA and post-hoc Tukey's test ($p < 0.05$).

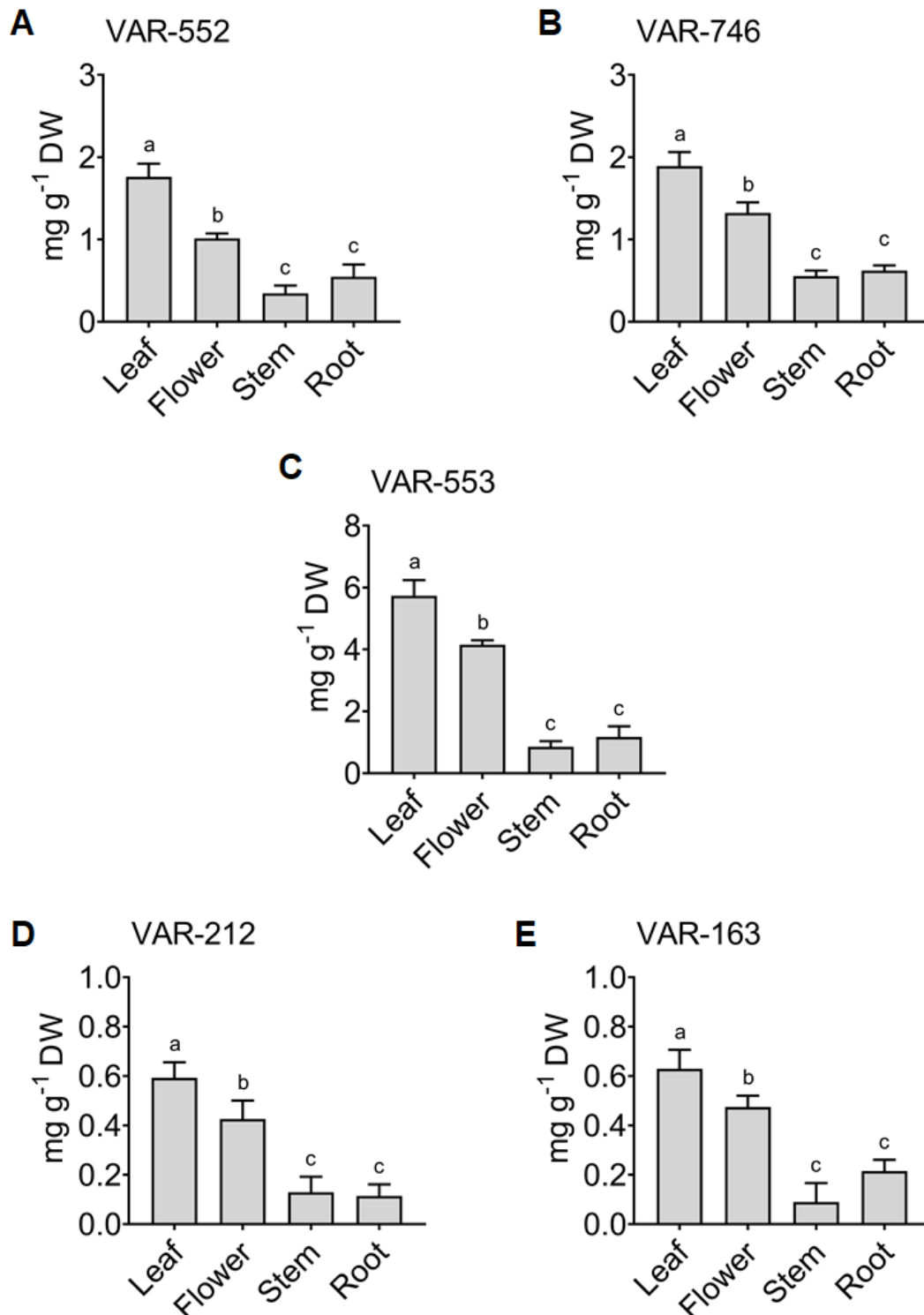


Figure 12. Concentrations of HD in different plant organs of selected *H. macrophylla* accessions. (A-E) HD concentrations in four major organs leaf, flower, stem and roots of *H. macrophylla* accessions (A) VAR-552, (B) VAR-746, (C) VAR-553, (D) VAR-212 and (E) VAR-163. Tissues under study were fully expanded young upper leaves, fully opened flower as whole, stem cuttings of equal length and root tissues. Analysis was performed on tissues dried at 40°C for 48 h. Bars represent means + SE, n= 6 independent biological replicates and standard error. Different letters denote significant differences among accessions according to one-way ANOVA and post-hoc Tukey's test ($p < 0.05$).

4.4 Variation of PD and HD levels at different developmental stages of *H. macrophylla*

To investigate the variations in PD and HD concentrations during different developmental stages of *H. macrophylla*, samples were collected at distinct time points representing various growth stages (20, 50, 75, 110, and 145 days), encompassing vegetative growth, reproductive phases, and post-anthesis stages. The vegetative growth phase of the plant spans approximately from 20 to 75 days after the cuttings were taken from the mother plant and planted in the soil (Figure 13A-C). Given the extended duration of the vegetative growth stage, an additional time point at 50 days was included in the study (Figure 13B). Following 75 days, all accessions began to bud, signifying the onset of the reproductive phase. The period from 75 to 110 days marked the reproductive stage, followed by senescence (Figure 13C, D). From 110 to 145 days, the plant began to wilt, shed leaves, and eventually reached the end of its lifecycle (Figure 13E). To determine at which stage of plant development the concentration of PD and HD is highest, leaf tissue from the fully expanded upper leaves was collected at five specific time points in the plant's lifecycle and subjected to drying at 40°C for 48 hours before conducting biochemical extraction.

During the vegetative phase of the plant (20-75 days), the concentration of PD gradually increased in all accessions (Figure 14A-E). As the plant transitioned into budding and flowering (75-110 days), the concentration of PD continued to rise for all accessions, except VAR-212 and VAR-163, peaking at 110 days (Figure 14). At this stage, accessions VAR-552 (16.89 mg g⁻¹ DW), VAR-746 (18.05 mg g⁻¹ DW), and VAR-553 (15.40 mg g⁻¹ DW) exhibited the highest concentrations of PD. The concentrations of PD in accessions VAR-212 and VAR-163 remained relatively constant during budding and flowering, with a non-significant increasing trend from the 75 days to the 110 days. In the initial 20 days through 75 days, HD concentrations also increased for all accessions (Figure 15A-E). This increase was particularly pronounced in VAR-553, an accession with high PD/HD content. From 75 to 110 days, HD concentrations in accessions VAR-552, VAR-746, and VAR-553 increased and reached a peak at 110 days, while for accessions VAR-212 and VAR-163, HD concentrations remained stable with a non-significant increasing trend from the 75 days to the 110 days. Subsequently, for all accessions, both PD and HD concentrations began to decrease after 110 days (Figure 14, 15). These findings

indicate that there is an increasing trend in PD and HD accumulation as *H. macrophylla* accessions mature, a trend sustained until the end of the reproductive phase. However, with the onset of senescence, the levels of PD and HD declined in all accessions (Figure 14, 15), likely due to the downregulation of primary and secondary metabolism during plant senescence. Overall, these results indicate that the concentration of PD and HD is at maximum during 110 days after the cuttings were taken from the mother plant and planted in the soil which corresponds to reproductive phase of the plant. This stage can be used as an optimal harvest time to obtain maximum concentrations of PD and HD from leaves.

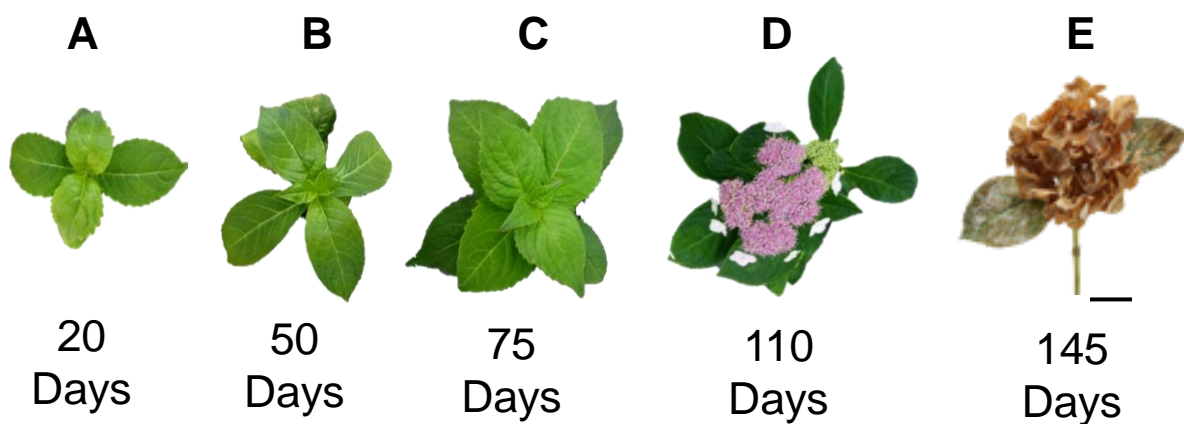


Figure 13. General leaf morphology of *H. macrophylla* at different developmental stages. (A-C) Variation in leaf size and shape of *H. macrophylla* during vegetative plant growth at (A) 20 days, (B) 50 days and (C) 75 days. Changes in leaf structure and fully expanded flowers of *H. macrophylla* during reproductive stage at (D) 110 days. Leaf and flower structure of *H. macrophylla* during plant senescence at (E) 145 days. The point at which the cuttings were taken from mother plant and planted in soil was counted as day 1 and taken as the initial reference point. Bar = 1 cm

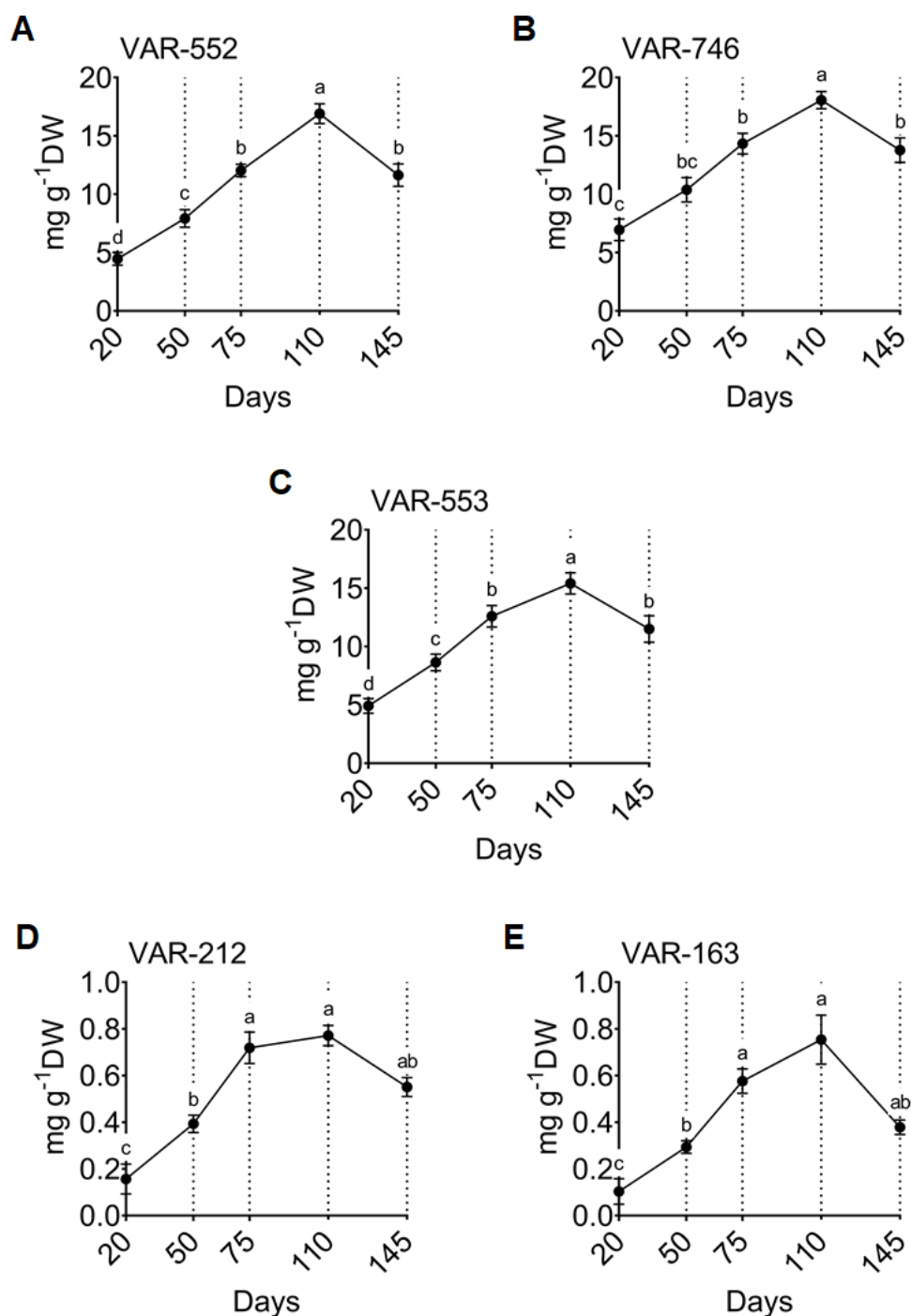


Figure 14. Phylodulcin (PD) accumulation across specific developmental stages in selected *H. macrophylla* accessions. (A-E) PD concentrations of *H. macrophylla* accessions (A) VAR-552, (B) VAR-746, (C) VAR-553, (D) VAR-212 and (E) VAR-163 at five different time points of the plant's lifecycle. 20-75 days correspond to vegetative growth stage, 75-110 days correspond to the reproductive stage and 110-145 correspond to post anthesis stage respectively. Analysis was performed on upper leaf tissues dried at 40°C for 48 h. The solid line represents the trend line connecting the means of 6 independent biological replicates and standard error for each time point. One-way ANOVA was used to estimate the significant differences between each interval at 95% confidence interval (CI). Different letters denote significant differences between stages according to post-hoc Tukey's test ($p < 0.05$).

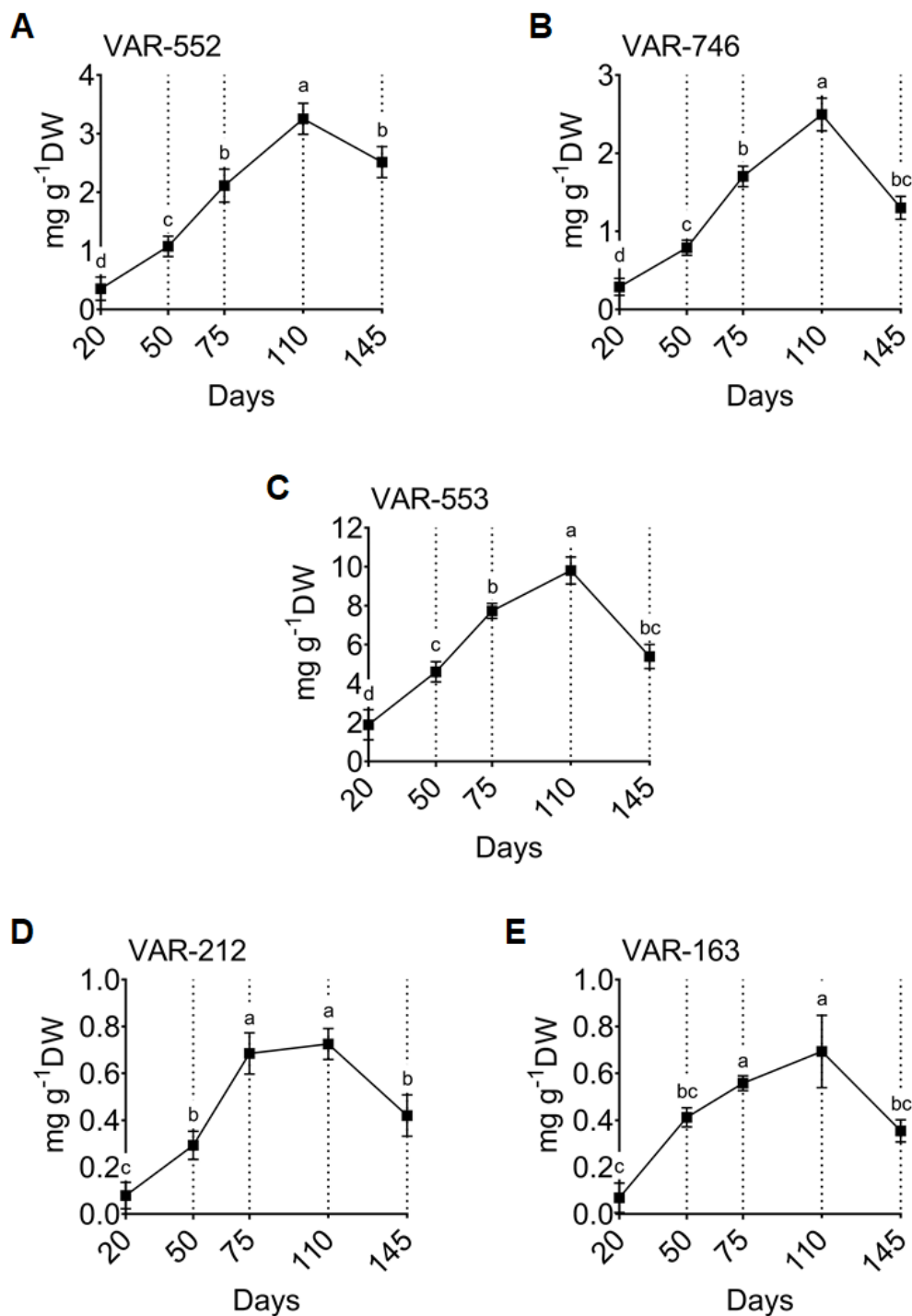


Figure 15. Hydrangenol (HD) accumulation across specific developmental stages in selected *H. macrophylla* accessions. (A-E) HD concentrations of *H. macrophylla* accessions (A) VAR-552, (B) VAR-746, (C) VAR-553, (D) VAR-212 and (E) VAR-163 at five different time points of the plant's lifecycle. 20-75 days correspond to vegetative growth stage, 75-110 days correspond to the reproductive stage and 110-145 correspond to post anthesis stage respectively. Analysis was performed on upper leaf tissues dried at 40°C for 48 h. The solid line represents the trend line connecting the means of 6 independent biological replicates and standard error for each time point. One-way ANOVA was used to estimate the significant differences between each interval at 95% CI. Different letters denote significant differences between stages according to post-hoc Tukey's test ($p < 0.05$).

4.5 Variations in phenylpropanoid metabolism among *Hydrangea* accessions

4.5.1 Distribution of phenylpropanoid metabolites in *Hydrangea* accessions

To investigate the variation in phenylpropanoid metabolism among selected accessions of *H. macrophylla*, the concentrations of 14 closely related phenylpropanoids were analyzed in freshly harvested leaves using LC-MS. Notably, the high PD, high HD, and high PD/HD accessions exhibited significantly elevated concentrations of phenylalanine, which serves as the starting compound in phenylpropanoid metabolism, (Figure 16A). This suggests that these accessions may possess higher levels of the initial precursor required to initiate the phenylpropanoid pathway (PPP). Moving further along the PPP, it was observed that all low PD/HD accessions and *H. paniculata* accumulated notably higher concentrations of trans-cinnamic acid, a derivative of phenylalanine, compared to the other groups (Figure 16B). In plants, the activated p-coumaric acid is branched into various metabolites, including umbelliferone, caffeic acid, naringenin chalcones, and resveratrol. The levels of caffeic acid and ferulic acid were significantly higher in low PD/HD accessions in comparison to all other accessions (Figure 16E, F). Furthermore, moving downstream of the PPP, it became evident that plants with high PD and/or HD concentrations contain significantly higher levels of p-coumaric acid and naringenin compared to low PD/HD accessions and *H. paniculata* (Figure 16C, D). The levels of stilbenoid, particularly resveratrol, were lower in low PD/HD accessions compared to all other plants, and it was not detected in *H. paniculata* (Figure 16G). Among the five different thunberginols, thunberginol C (Thn C) exhibited distinct differences among various *Hydrangea* accessions. The relative abundance of Thn C was lower in low PD/HD accessions compared to all other plants, and it was not detected in *H. paniculata* (Figure 16H).

High PD and/or HD accessions exhibited significantly higher levels of umbelliferone (Figure 17A), whereas the concentrations of scopolin and scopoletin were higher in low PD/HD accessions and *H. paniculata* when compared to high PD accessions (Figure 17B, C). Accessions with PD and HD showed lower levels of esculetin compared to other study groups (Figure 17E), while fraxetin concentrations were lower in high PD accessions than in the other study groups (Figure 17F). These hydroxylated coumarins such as scopolin, scopoletin, esculin, esculetin, and fraxetin are downstream products derived from caffeic acid and ferulic acids (Rajniak et al., 2018;

Schoch *et al.*, 2001; Kai *et al.*, 2006; Vanholme *et al.*, 2019; Yin *et al.*, 2023; Wang *et al.*, 2023).

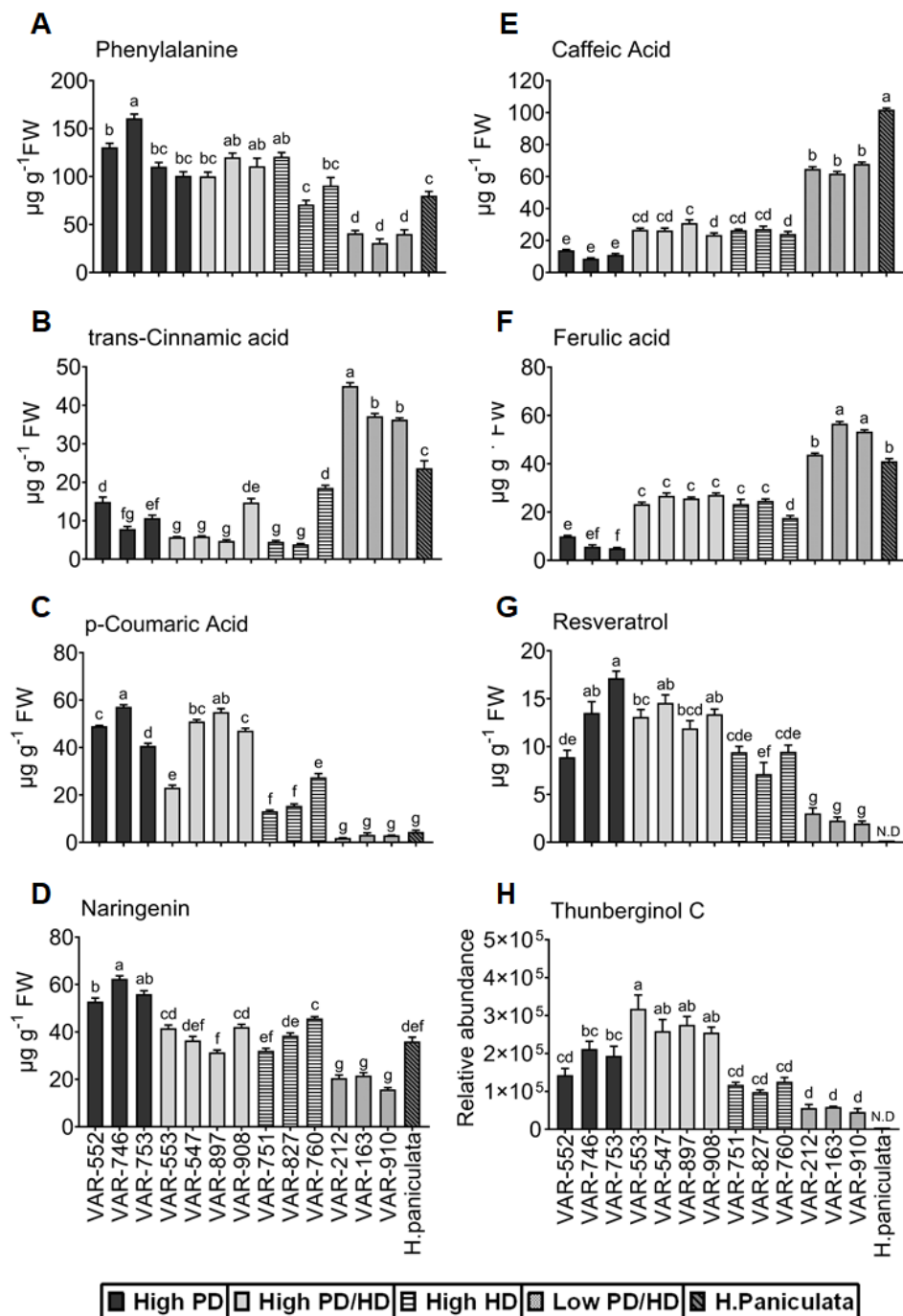


Figure 16. Concentration of selected phenylpropanoids in different *Hydrangea* accessions. (A-H) Concentrations of (A) phenylalanine, (B) trans-cinnamic acid, (C) p-coumaric acid, (D) naringenin, (E) caffeic acid, (F) ferulic acid, (G) resveratrol and (H) thunberginol C in 14 selected accessions of *Hydrangea*. Analysis was conducted on freshly harvested, fully expanded, young upper leaves. Bars represent means + SE, n = 6 biological replicates. Not detected (N.D) indicates the absence of the corresponding metabolite. Different letters denote significant differences among varieties according to one-way ANOVA and post-hoc Tukey's test (p<0.05).

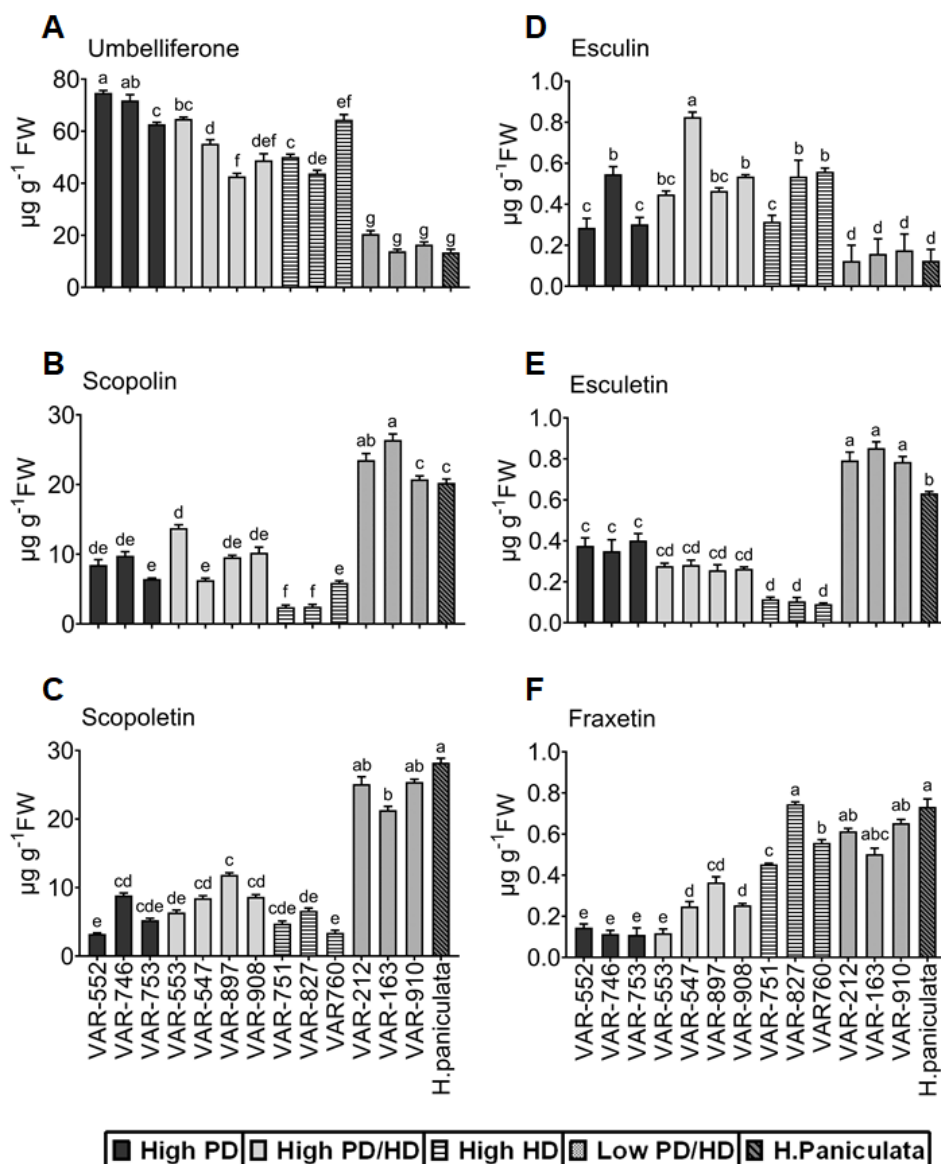


Figure 17. Distribution of coumarins in different *Hydrangea* accessions. (A-F) Biochemical concentrations of (A) umbelliferone, (B) scopolin, (C) scopoletin, (D) esculin, (E) esculetin and (F) fraxetin in 14 selected accessions of *Hydrangea*. Analysis was conducted on freshly harvested, fully expanded, young upper leaves. Bars represent means + SE, n = 6 biological replicates. Not detected (N.D) indicates the absence of the corresponding metabolite. Different letters denote significant differences among varieties according to one-way ANOVA and post-hoc Tukey's test ($p < 0.05$).

These changes observed in the metabolite profiles of different *H. macrophylla* accessions helped predicting the metabolic conversions within the major PPP, ultimately leading to the biosynthesis of PD and HD.

4.5.2 Relationship between PD and other metabolites in *Hydrangea* accessions

To assess the interdependence of various phenylpropanoid intermediates and identify potential contributors to the biosynthesis of PD, a correlation analysis was conducted using the metabolite concentrations of different *Hydrangea* accessions. Each group of accessions revealed a distinct pattern of the metabolite contents (Figure 18A, B). Pearson's correlation was employed to evaluate this metabolite associations based on correlation coefficient (r) values. The correlation matrix was constructed using the metabolite concentrations of all the accessions (Figure 19). In particular, low PD/HD accessions exhibited higher concentrations of cinnamic acid, caffeic acid, ferulic acid, scopoletin, scopolin, fraxetin, and esculetin compared to all other accessions, while high PD accessions had higher concentrations of umbelliferone, naringenin, and resveratrol (Figure 18B).

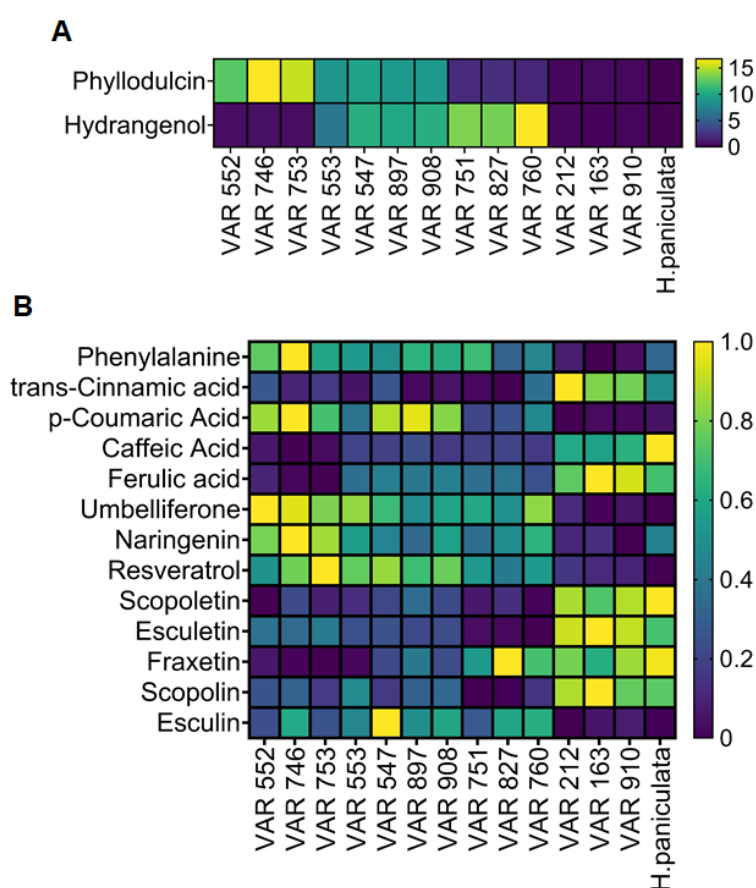


Figure 18. Variation in phenylpropanoid derivatives among *Hydrangea* accessions. (A) Heat map of absolute concentrations of PD and HD in different *Hydrangea* accessions. (B) Heatmap of relative concentrations of 13 metabolites in different *Hydrangea* accessions. Metabolite analysis was performed on freshly harvested fully expanded upper leaves ($n=6$). Yellow colour represents the highest relative concentration and dark violet represents lowest relative concentration of metabolites.

The correlation analysis indicated strong and positive correlations between PD concentrations and the concentrations of naringenin, resveratrol, umbelliferone, p-coumaric acid, esculin, and phenylalanine (Figure 19). Conversely, there were strong negative correlations between caffeic acid, ferulic acid, trans-cinnamic acid, scopolin, scopoletin, fraxetin, and esculetin with PD concentrations (Figure 19). For HD, there were weak positive correlations with phenylalanine, p-coumaric acid, umbelliferone, resveratrol, and esculin (Figure 19). Conversely, HD concentrations exhibited negative correlations with caffeic acid, ferulic acid, trans-cinnamic acid, esculetin, scopolin, and scopoletin (Figure 19).

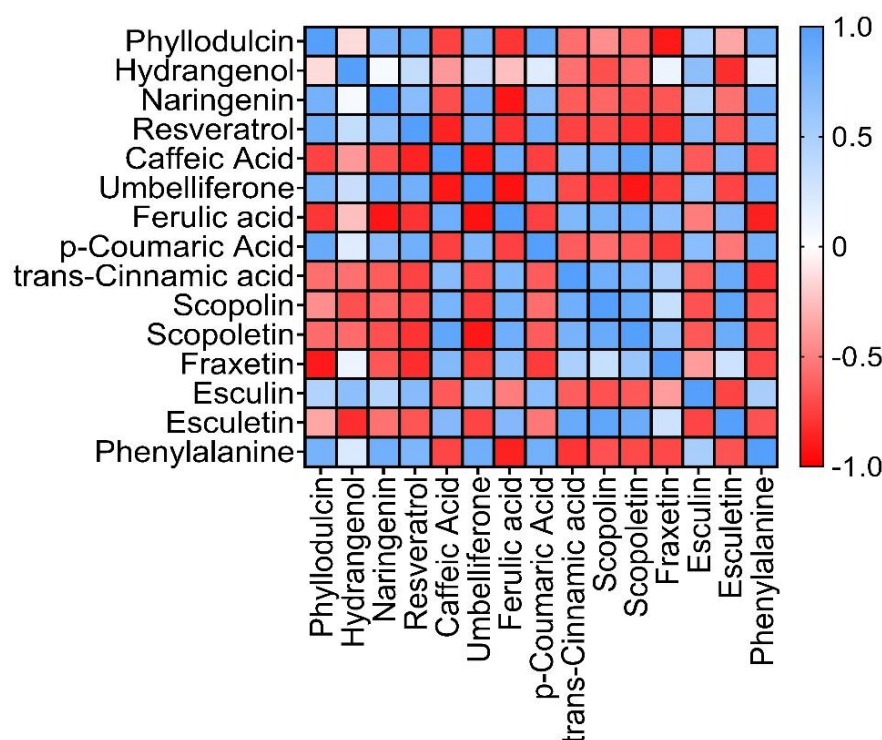


Figure 19. Correlation between phenylpropanoids in *Hydrangea* accessions. Pearson's correlation analysis conducted among 15 metabolite concentrations of different *Hydrangea* accessions. The blue colour represents high positive correlation ($r=1$) and red colour represents high negative correlation ($r=-1$). Metabolite analysis was performed in freshly harvested fully expanded young upper leaves ($n=6$).

Principal component analysis (PCA) was conducted using the concentrations of all selected metabolites in each accession to group accessions based on their biochemical diversity. The principle component 2 (PC2) captured 15.48 % variance in different *Hydrangea* accessions and principal component 1 (PC1) captured 70.25 % variance in metabolite concentrations among accessions. The PCA plot demonstrated that high PD, high PD/HD, low PD/HD, and high HD accessions formed distinct

clusters, indicating that metabolite concentrations were a major factor contributing to the differences among these groups (Figure 20). In the loading plot, the vector angles for PD and HD were nearly orthogonal to each other, suggesting a lack of correlation between their concentrations among the accessions. Accessions VAR-552, VAR-746, and VAR-753 clustered along the PD vector projection, suggesting that PD could be a key factor for this grouping (Figure 20). Similarly, VAR-751, VAR-760, and VAR-827 clustered closer to the HD vector projection, indicating that HD might be responsible for this clustering. Similarly, accessions VAR-212, VAR-163, VAR-910, and *H. paniculata* clustered in proximity to the vectors of trans-cinnamic acid, scopolin, and caffeic acid. On the other hand, VAR-553, VAR-908, VAR-897, and VAR-547 clustered closer to the vectors of esculin, umbelliferone, resveratrol, and phenylalanine (Figure 20).

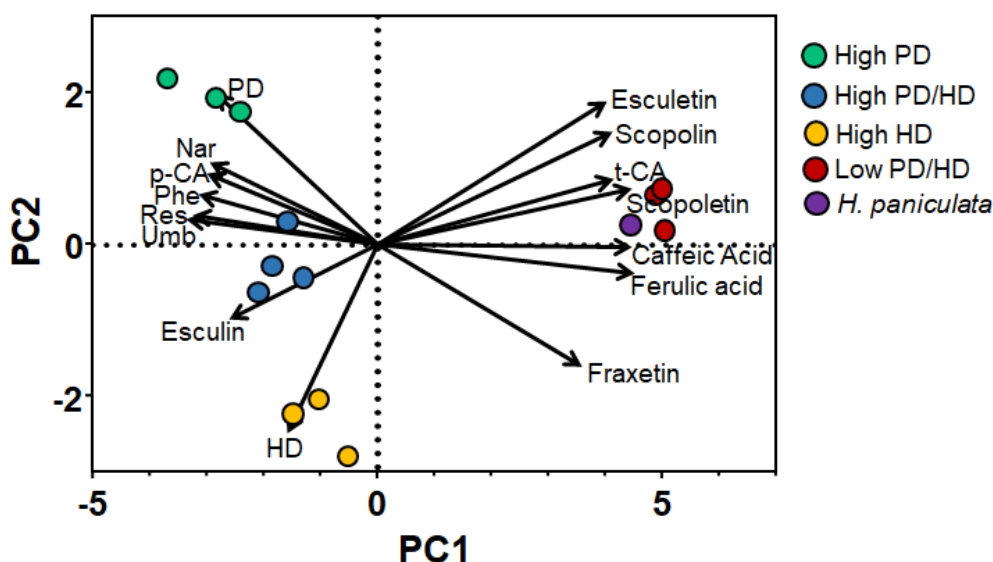


Figure 20. Principle component analysis biplot of *Hydrangea* accessions. PCA biplot representing different *Hydrangea* accessions as PCA plot and metabolite concentrations as loading plot. Each dot represents different *Hydrangea* accessions and arrows represent eigenvectors of 15 metabolites. The abbreviations Nar, p-CA, Phe, Res, Umb and t-CA represents naringenin, p-coumaric acid, phenylalanine, resveratrol, umbelliferone and trans cinnamic acid respectively. Metabolite analysis was performed in freshly harvested fully expanded young upper leaves (n=6).

Taking these analyses together provides an overall understanding of the distribution of different metabolites among various groups of *Hydrangea* accessions and their relationships with each other. As PD positively correlates strongly with naringenin, resveratrol, p-coumaric acid, phenylalanine and umbelliferone it can be expected that the pathway related these metabolites have strong influence on PD biosynthesis. Conversely, as cinnamic acid, caffeic acid, ferulic acid, scopolin, scopoletin, fraxetin

and esculetin are showing strong negative correlation with PD, these metabolites are expected to belong to a competitive pathway which is unrelated to PD biosynthesis.

4.5.3 Differences in expression patterns of genes involved in PPP and associated pathways

To investigate the genetic regulation of the phenylpropanoid pathway (PPP) and associated pathways in various *Hydrangea* accessions sorted by their biochemical content, a transcriptome analysis was conducted. This analysis focused on selected accessions with high PD, high HD, high PD/HD ratios, low PD/HD and *H. paniculata* as a negative control.

The clustering of genes using heat maps revealed distinct gene expression patterns among the different accessions. Notably, *H. paniculata*, which lacked PD and HD, displayed markedly different gene expression compared to other varieties containing trace amounts of PD and HD (Figure 21A). Thus, comparing the transcriptomes of accessions with high PD, high HD, or high PD/HD to those with low PD allowed for clear differentiation in gene expression patterns.

Gene Ontology function classification categorized the genes obtained from RNA sequencing into three major classes: biological process, cellular component, and molecular function. The majority of genes were associated with biological processes and molecular functions (Figure 21B). Among biological processes, metabolic and cellular processes were highly represented. In the molecular functions category, genes related to binding and catalytic activity were predominant.

To streamline the analysis, transcriptomes of accessions with high PD, high PD/HD, and high HD were compared to those of low PD accessions, specifically VAR-163, VAR-910, and *H. paniculata*. Differentially expressed genes were identified, revealing a significant number of both upregulated and downregulated genes (>3000) when comparing accessions with high and low isocoumarin concentrations (Figure 22A-C). In the comparison with *H. paniculata*, there were more upregulated genes than downregulated ones, potentially indicating species-specific differences in gene regulation due to evolutionary drift (Figure 23) (Breschi *et al.*, 2016).

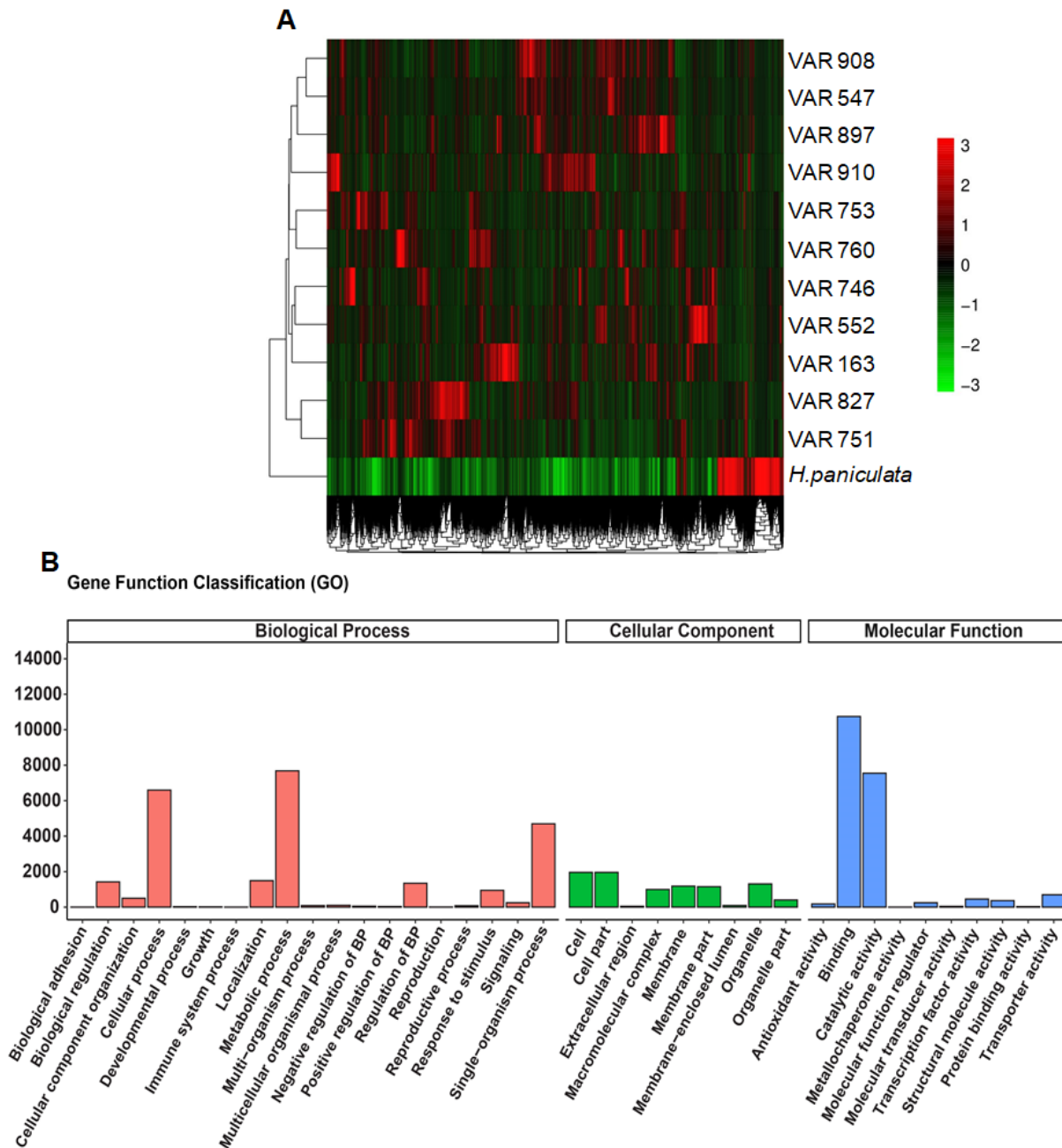


Figure 21. Differences in expression pattern of genes in *Hydrangea* accessions. (A) Heatmap indicating the relative gene expression patterns in *H. paniculata* and 11 different accessions of *H. macrophylla*. Homogenized expression data using fpkm values of the genes were used to conduct hierarchical clustering. The green colour represents downregulated genes and red colour represents upregulated genes (B) Gene Ontology (GO) annotation classification statistics graph classified according to biological process, cellular component and molecular functions. The 38 most significant terms were selected for display. The data was obtained from full length transcriptome of leaf tissues of all *Hydrangea* accessions under study subjected to RNA sequencing. Only GO terms with $p_{adj} < 0.05$ are represented.

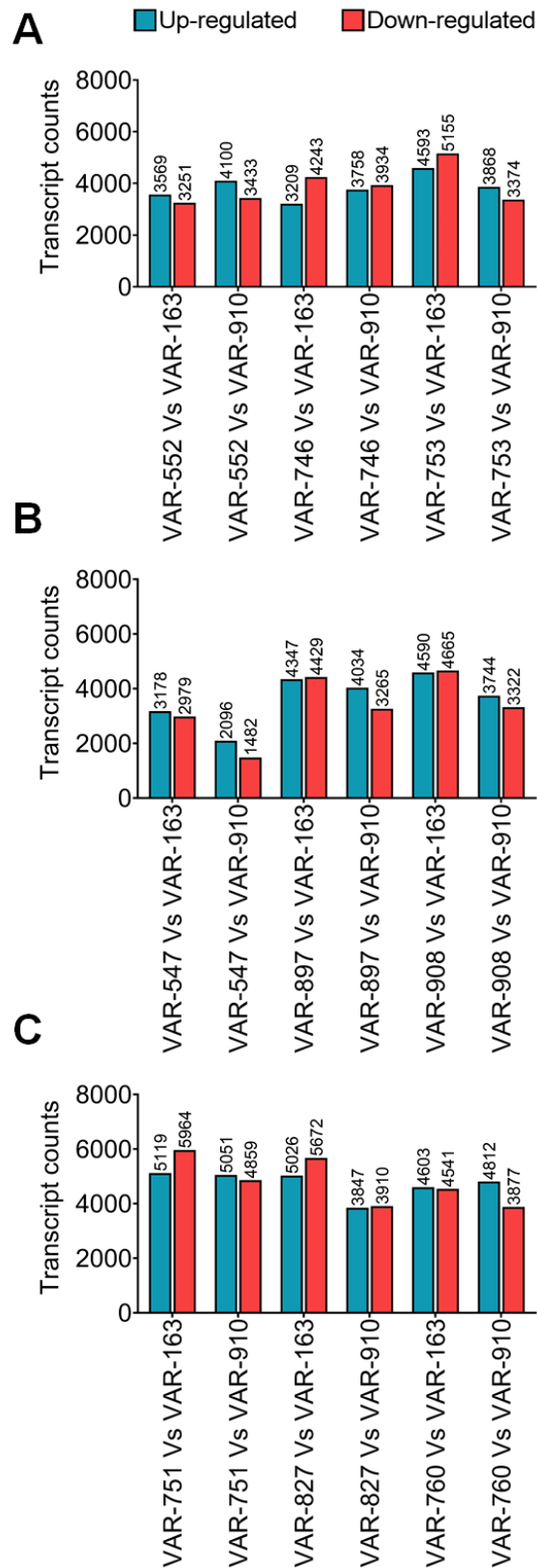


Figure 22. Differentially expressed genes in different *H. macrophylla* study group comparison. (A-C) The differentially expressed upregulated and downregulated transcript counts in (A) High PD vs Low PD/HD accessions, (B) High PD/HD vs Low PD/HD accessions, (C) High HD vs Low PD/HD accessions.

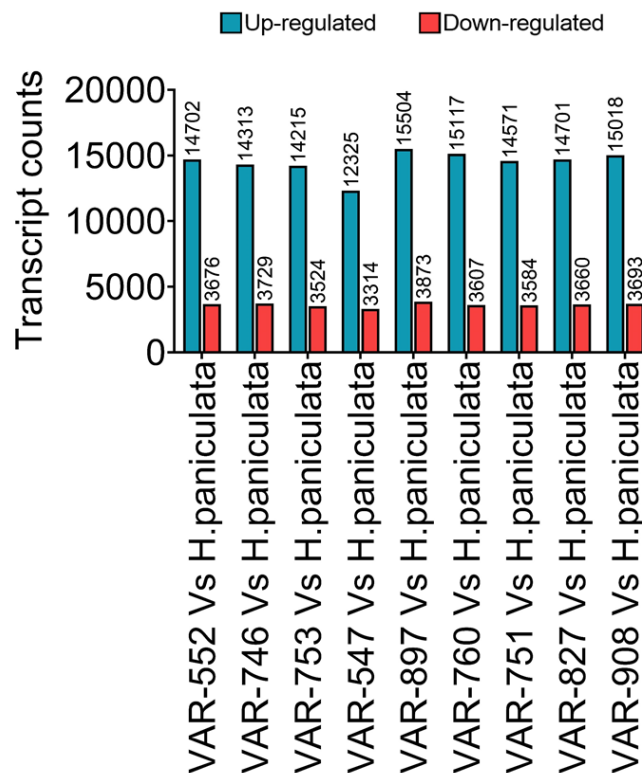


Figure 23. Differentially expressed genes in *H. macrophylla* and *H. paniculata* comparison. (A) The differentially expressed, upregulated and downregulated transcript counts in High PD, High PD/HD, High HD accessions vs *H. paniculata*.

Additionally, KEGG enrichment analysis was performed to assign differentially expressed genes in each study group to various biochemical pathways. In most comparisons, except for VAR-751 vs. VAR-163 and VAR-751 vs. VAR-910 (Appendix 5), pathways related to phenylpropanoid biosynthesis, flavonoid biosynthesis, flavone and flavonol biosynthesis, and stilbenoid, diarylheptanoid, and gingerol biosynthesis ranked among the top 20 most highly expressed metabolic pathways with a corrected p-value (p_{adj}) < 0.05. Contrarily, these pathways were not significantly enriched while comparing the transcriptome profiles of accessions containing PD and/or HD with *H. paniculata* (Appendix 6-10).

Specifically, when comparing VAR-552 to VAR-163 and VAR-910, phenylpropanoid biosynthesis and flavonoid biosynthesis were the most enriched pathways (Figure 24A, B). In the comparison with VAR-746, stilbene biosynthesis and flavonoid biosynthesis were highly enriched (Appendix 11), while VAR-753 displayed enrichment in stilbene and phenylpropanoid biosynthesis pathways (Appendix 12). This suggests that accessions with high PD, high HD, and high PD/HD have more active phenylpropanoid, stilbene, and flavonoid metabolism compared to low PD/HD

accessions. Comparisons of VAR-547 and VAR-897 to VAR-163 and VAR-910 also revealed enrichment in flavonoid and phenylpropanoid biosynthesis pathways (Figure 25A, B; Appendix 13). Similarly, VAR-908, VAR-827, and VAR-760 comparisons to VAR-163 and VAR-910 showed significant enrichment in flavonoid and phenylpropanoid biosynthesis pathways (Figures 26A, B; Appendix 14,15). These results indicate that differentially expressed genes associated with flavonoid biosynthesis, phenylpropanoid biosynthesis, and stilbene biosynthesis are highly enriched while comparing the transcriptome of an accession containing high PD and/or HD with that of a low PD and/or HD. This shows the influence of genes associated with these pathways in biosynthesis of PD. By studying these genes related to these three pathways, a comprehensive understanding of the biosynthesis of PD and metabolites which are closely associated with it in *Hydrangeas* can be developed.

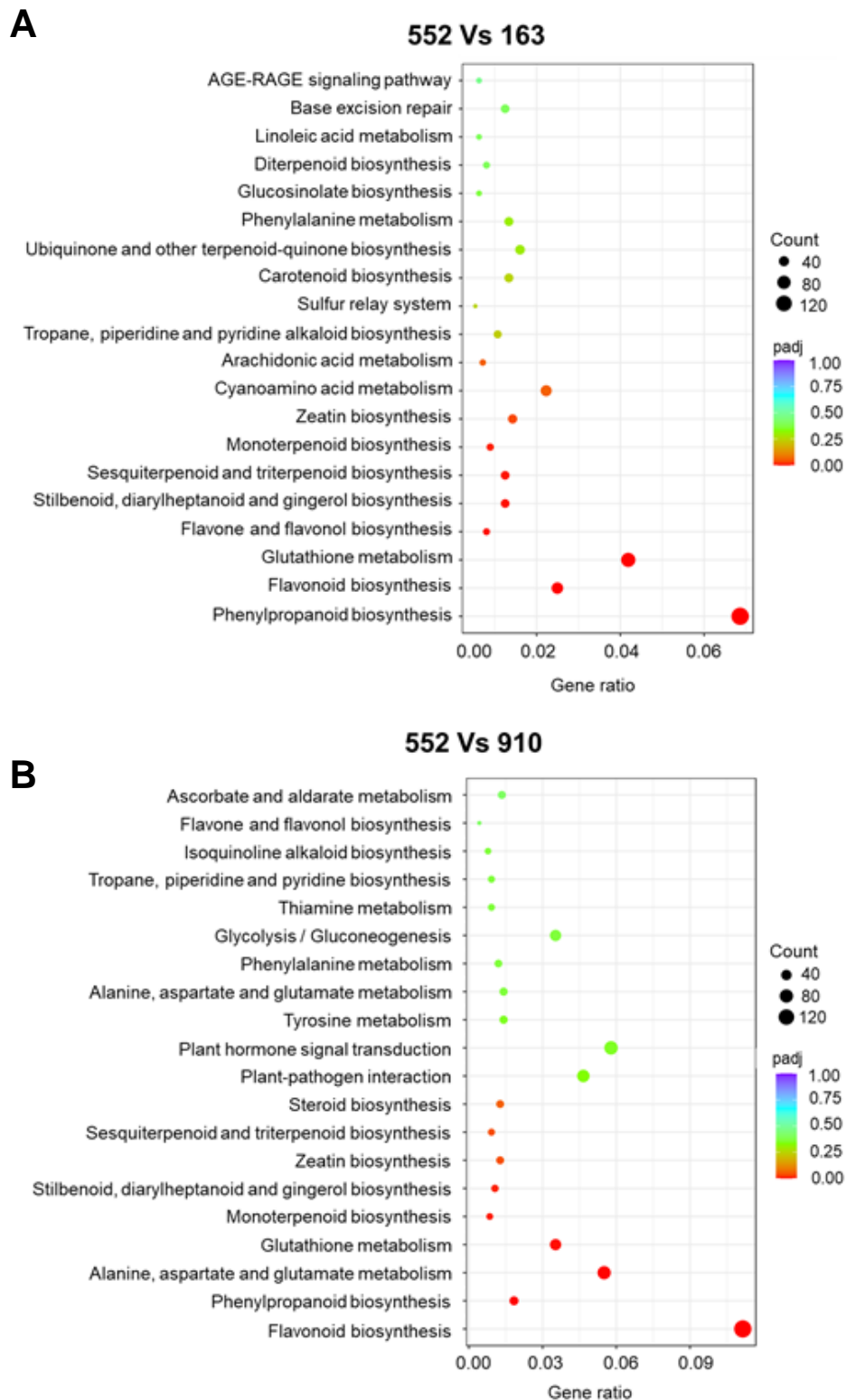


Figure 24. The assignment of genes to different metabolic pathways in high and low PD/HD accessions of *H. macrophylla*. (A, B) Dot plot of KEGG enrichment analysis showing the gene ratio (the percentage of total DEGs) assigned to the top 20 metabolic pathways in the study group (A) VAR-552 and VAR-163 and (B) VAR-552 and VAR-910. The dot sizes represent the gene counts and color of the dot is based on p-value adjusted to sample distribution (p_{adj} value) and indicates significance of pathway enrichment. KEGG annotates genes at the pathway level.

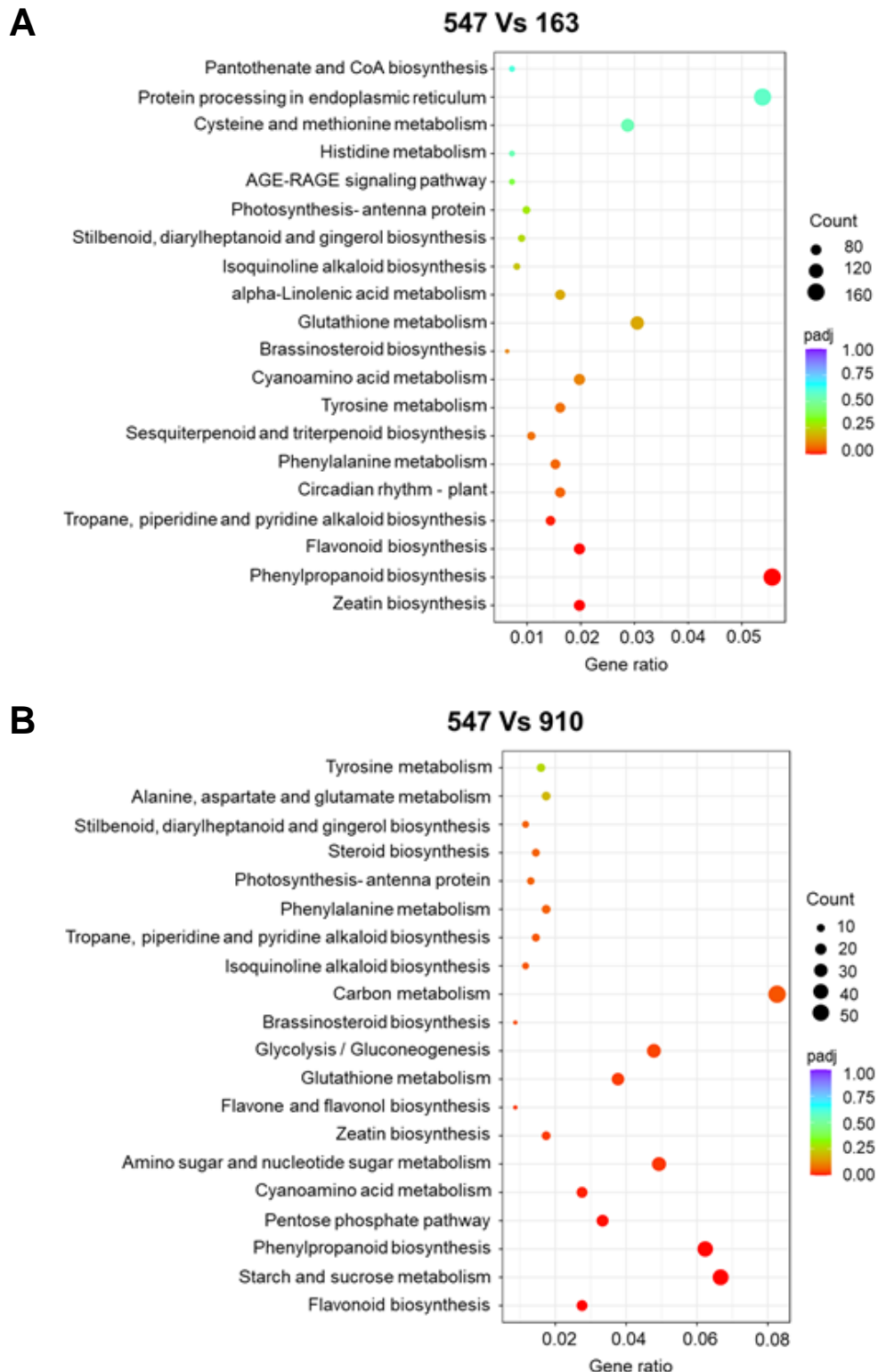


Figure 25. The assignment of genes to different metabolic pathways in high PD/HD and low PD/HD accessions of *H. macrophylla*. (A, B) Dot plot of KEGG enrichment analysis showing the gene ratio (the percentage of total DEGs) assigned to the top 20 metabolic pathways in the study group (A) VAR-547 and VAR-163 and (B) VAR-547 and VAR-910. The dot sizes represent the gene counts and color of the dot is based on p-value adjusted to sample distribution (p_{adj} value) and indicates significance of pathway enrichment. KEGG annotates genes at the pathway level.

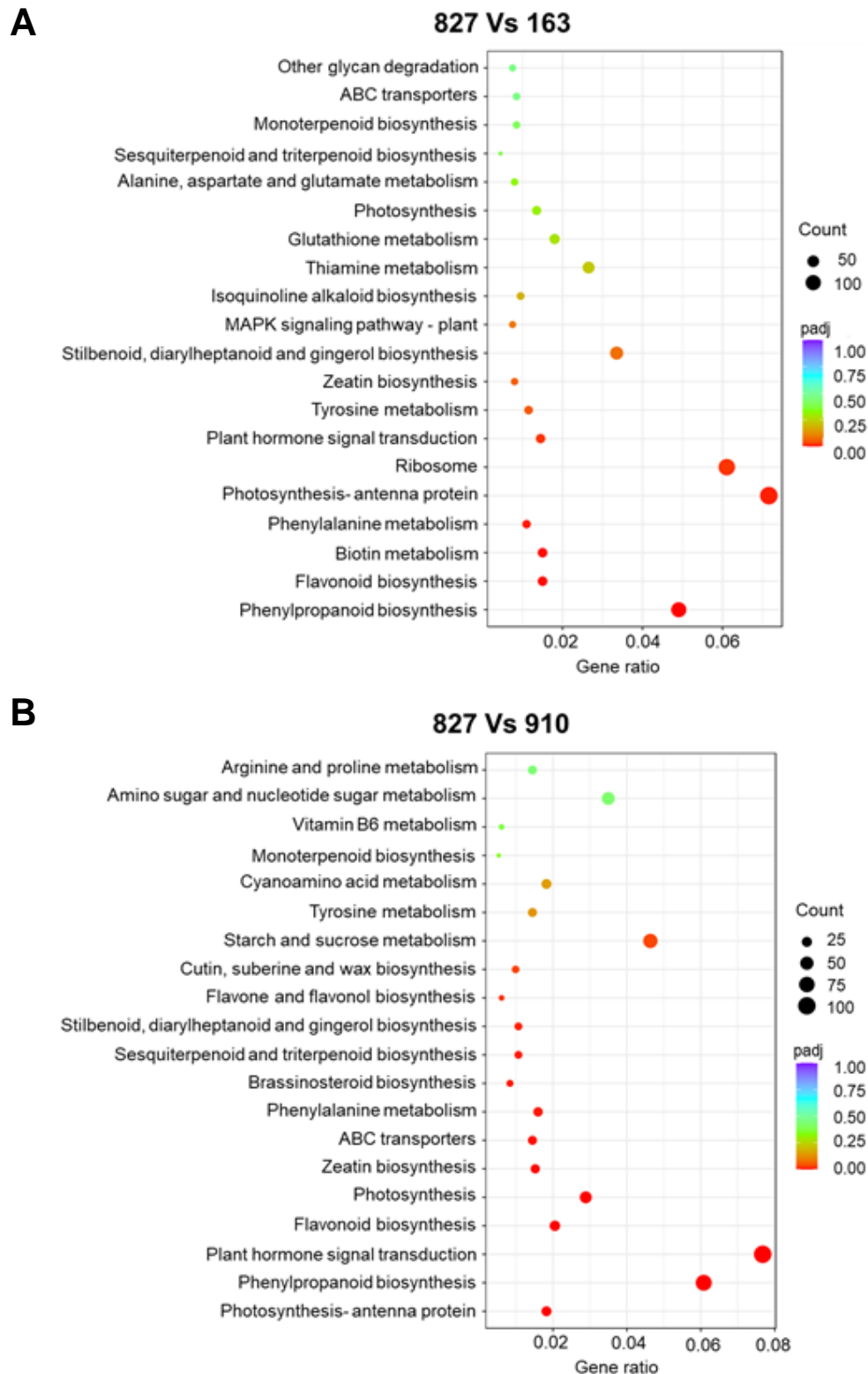


Figure 26. The assignment of genes to different metabolic pathways in high HD and low PD/HD accessions of *H. macrophylla*. (A, B) Dot plot of KEGG enrichment analysis showing the *gene ratio* (the percentage of total DEGs) assigned to the top 20 metabolic pathways in the study group (A) VAR-827 and VAR-163 and (B) VAR-827 and VAR-910. The dot sizes represent the gene counts and color of the dot is based on p-value adjusted to sample distribution (p_{adj} value) and indicates significance of pathway enrichment. KEGG annotates genes at the pathway level.

4.5.4 Relationship between genes and metabolites involved in phenylpropanoid pathway and related pathways

To investigate the relationship between genes in the phenylpropanoid pathway and associated pathways with metabolite concentrations, a Weighted Gene Correlation Network Analysis (WGCNA) was performed, followed by correlating the eigengenes with metabolite levels. WGCNA is an unsupervised analysis method that clusters genes based on their expression patterns, commonly used for studying biological networks through pairwise correlations between variables.

To enhance the network's stability, genes expressed as 0 in all samples were removed, and high-quality genes with a variance cut-off above 0.55 were selected, resulting in 22,980 genes with high variance among the accessions. The WGCNA package was used to calculate the soft threshold power and average mean connectivity, with a power value of 9 found to be most suitable for the analysis. A gene cluster dendrogram tree was constructed, with each branch representing a gene cluster with highly correlated expression levels (Figure 27). The closeness of branches indicates the similarity between gene sets, and genes with similar expression patterns were grouped together in the same module. In total, 85 modules of different colors were obtained, each containing co-expressing genes. Based on module eigengene similarity, 16 final expression modules were selected (Table 4), with the darkolivegreen module containing most genes (5065), and the grey module the least (68). Module eigengene values represent the overall expression level of all genes in each sample and can be correlated with external traits. In this study, external traits were defined by phenylpropanoid metabolite concentrations in each *H. macrophylla* accession.

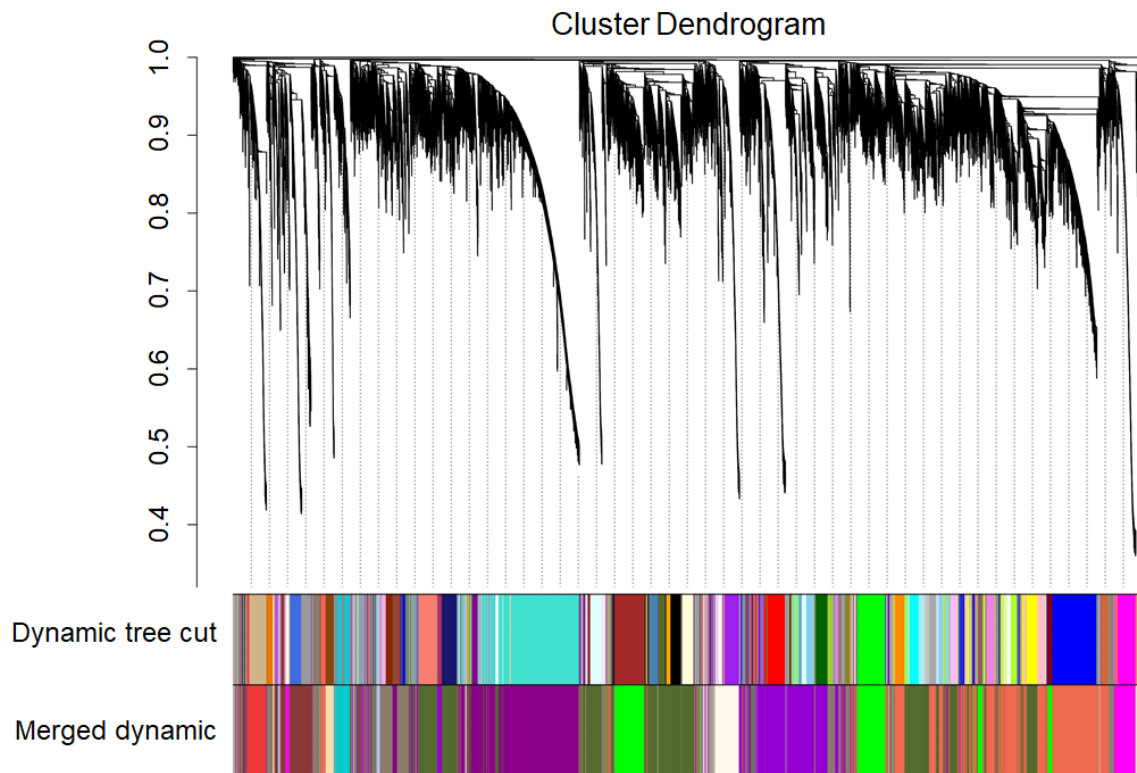


Figure 27. Identification of co expressing genes using weighted gene co-expression network analysis (WGCNA). Gene clustering tree built by hierarchical clustering of adjacency-based dissimilarity to detect 85 co-expression clusters with corresponding color assignments represented as dynamic tree cut. Modules with strongly correlated eigengenes were amalgamated based on threshold to assign highly co-expressed genes into 16 separate modules indicated as merged dynamic. Color bars reflect module assignments before and after the merging of closed modules. Each color represents a module and the gray module indicates no co-expression among the genes. The branches of the tree correspond to a cluster of gene sets with highly correlated expression levels. Analysis was done on 22,980 genes obtained from RNA sequencing of 11 *H. macrophylla* accessions.

Table 4. Number of genes grouping in individual co-expression modules. Based on a soft thresholding power of 9, the strongly co-expressing genes were clustered into final 16 modules. In total 22,980 genes obtained from the RNA sequencing of different accessions of Hydrangea containing varying amounts of PD and HD were used to construct a co-expression network analysis by WGCNA.

SI no:	Module colour	Gene count
1	darkolivegreen	5065
2	coral2	4153
3	darkmagenta	3294
4	darkviolet	2508
5	green	1907
6	bisque4	1656
7	indianred4	923
8	floralwhite	906
9	magenta	768
10	brown2	553
11	darkturquoise	432
12	navajowhite1	379
13	lightsteelblue	172
14	antiquewhite	123
15	thistle	73
16	grey	68
	TOTAL	22,980

Pearson's correlation was performed to estimate module-metabolite relationships. Modules magenta, navajowhite1, brown2, darkolivegreen, floralwhite, darkmagenta, indianred4, lightsteelblue, antiquewhite4, bisque4, darkturquoise, and green, showed significant positive correlations ($p < 0.05$) with certain metabolite concentrations (Figure 28), indicating a positive linear relationship between metabolite concentrations and genes in these modules.

Module-metabolite relationships revealed that genes in the floralwhite, bisque4, lightsteelblue, and darkolivegreen modules exhibited high positive correlations with PD concentration (Figure 28). Additionally, modules floralwhite, darkturquoise, green,

and magenta correlated with HD concentrations. Phenylalanine concentrations positively correlated with modules lightsteelblue and floralwhite, while p-coumaric acid concentrations positively correlated with darkolivegreen, floralwhite, lightsteelblue, antiquewhite, and bisque4 (Figure 28). Modules navajowhite1 and brown2 displayed high positive correlations with trans-cinnamic acid, caffeic acid, ferulic acid, and esculetin concentrations, while umbelliferone and naringenin concentrations positively correlated with the floralwhite module. Resveratrol concentrations positively correlated with bisque4 and darkturquoise, while scopoletin concentrations correlated positively with navajowhite1, brown2, and indianred4. Fraxetin concentrations showed a positive correlation with the darkmagenta module. Notably, the floralwhite module correlated positively with PD, HD, phenylalanine, p-coumaric acid, umbelliferone, and naringenin, suggesting a common regulatory network for these metabolites (Figure 28). By examining genes within modules highly correlated with each metabolite, it is possible to identify genes involved in the biosynthesis of these metabolites.

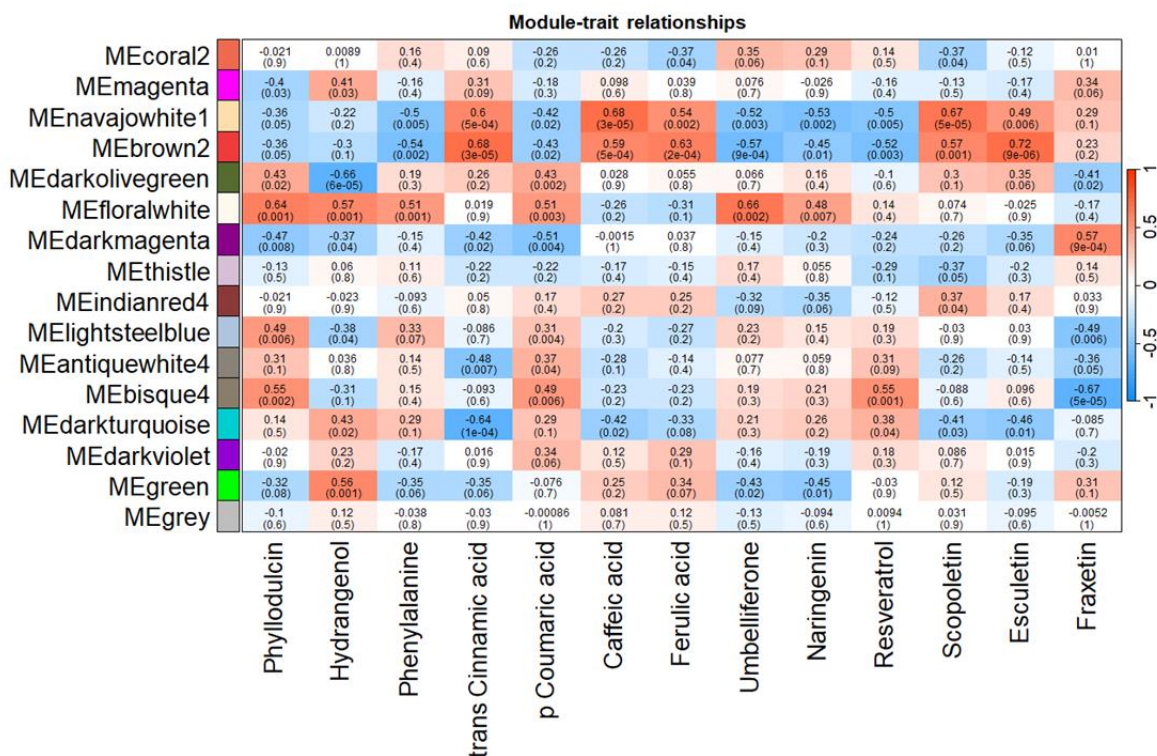


Figure 28. Identifying module-external trait relationship using correlation analysis. The correlation of co-expressing gene modules with 13 metabolite concentrations in different accessions of *H. macrophylla*. Modules significantly associated with the traits were identified at a p-value < 0.05. Numbers inside the blocks represents Pearson’s correlation coefficients and numbers inside brackets represent p-value. Red and blue colors denote positive and negative correlations between metabolite concentration and gene expression, respectively.

When comparing the transcriptomes of high PD, high PD/HD, and high HD groups with low PD/HD accessions, the most common and enriched pathways were related to flavonoid biosynthesis, phenylpropanoid biosynthesis, and stilbene biosynthesis. By searching for genes in modules highly correlated with metabolite concentrations and related to these three metabolic pathways, 22 genes were identified. To understand the regulation of the phenylpropanoid pathway, the expression levels of these genes were analyzed in different study groups individually (Figure 29).

It was found that the gene encoding the enzyme phenylalanine ammonia-lyase (*PAL1*), responsible for converting phenylalanine to trans-cinnamic acid, was highly upregulated in accessions containing PD and/or HD. This enzyme was found in the darkolivegreen module, which positively correlated with PD and para-coumaric acid concentrations. The darkolivegreen module also showed a positive correlation with trans-cinnamic acid. The gene encoding the enzyme cinnamate 4-hydroxylase (*C4H*), which acts on the next step of the pathway, converting trans-cinnamic acid to para-coumaric acid, showed high expression levels in accessions containing PD and/or HD. This enzyme was found in the lightsteelblue module, which correlated positively with PD and para-coumaric acid (Figure 28, 29).

Genes for the enzyme 4-coumarate-CoA ligase 1 (*4CL1*), responsible for converting para-coumaric acid into para-coumaroyl CoA, had high expression levels in PD and/or HD accessions. This enzyme had several analogues, with two showing significant expression differences among study groups. These analogues were present in two different modules, darkolivegreen and floralwhite, both of which correlated with PD. The floralwhite module also correlated positively with HD, phenylalanine, para-coumaric acid, umbelliferone, and naringenin (Figure 28, 29).

The gene of the enzyme hydroxycinnamoyl transferase (*HCT*), which converts para-coumaroyl-CoA into para-coumaroyl shikimate, showed downregulation in high PD and/or HD accessions. The genes coding for HCT were found in the brown2 module. The gene for the next enzyme 4-coumarate 3-hydroxylase, *C3H*, which converts para-coumaroyl shikimate to caffeoyl shikimate, was also downregulated in high PD and/or HD accessions. *C3H* was found in the brown2 module, which correlated with caffeic acid and ferulic acid concentrations (Figure 28, 29).

The gene *CSE*, coding for the enzyme caffeoyl shikimate esterase which converts caffeoyl shikimate to caffeic acid, showed downregulation in high PD and/or HD

accessions and correlated with the navajowhite1 module. The gene for the enzyme caffeate 3-O-methyltransferase (*COMT*), responsible for converting caffeic acid into ferulic acid, was also downregulated in high PD and/or HD accessions and correlated with the darkviolet module (Figure 28, 29).

The genes for the enzymes hydroxycinnamoyl transferase and caffeoyl-CoA O-methyltransferase (*HCT* and *CCoAOMT* respectively) involved in converting caffeoyl shikimate into caffeoyl-CoA and then into feruloyl-CoA, respectively, both showed downregulation in high PD and/or HD accessions. *CCoAOMT* correlated with the brown2 module (Figure 28, 29).

The genes for the enzyme feruloyl-CoA 6'-hydroxylase (*F6'H2*), which converts feruloyl CoA into 6'-hydroxyferuloyl CoA, showed upregulation in high PD and/or HD accessions and correlated with the navajowhite1, darkolivegreen, and floralwhite modules (Figure 28, 29).

The genes of enzyme responsible for converting scopoletin into scopolin, scopoletin glucosyltransferase (*SGT*) showed downregulation in high PD and/or HD accessions and correlated with the brown2 module (Figure 28, 29).

The genes coding for enzymes in the flavonoid biosynthesis and downstream metabolites, namely chalcone synthase (*CHS*), chalcone isomerase (*CHI*), flavonoid 3',5'-hydroxylase (*F3'5'H*), dihydroflavonol 4-reductase (*DFR*), and flavonoid 3',5'-methyltransferase (*FOMT*), showed upregulation in PD and/or HD accessions, except for flavonoid 3'-hydroxylase (*F3'H*), which was downregulated. The genes involved in stilbene biosynthesis and associated pathway, such as p-coumaroyltriacyclic acid synthase (*CTAS*), resveratrol di-O-methyltransferase (*ROMT*), keto reductase (*KR*), type III polyketide synthase (*PKS*) and polyketide cyclase (*PKC*), were upregulated in high PD and/or HD accessions. These enzymes were distributed across the modules floralwhite, bisque4 and darkolivegreen (Figure 28, 29).

When comparing the same set of genes in *H. paniculata* and *H. macrophylla* accessions, it was observed that genes involved in flavonoid metabolism and stilbene metabolism were highly expressed in *H. macrophylla* accessions with high PD and/or HD. However, enzymes responsible for the initial steps of phenylpropanoid metabolism were less expressed in all *H. macrophylla* accessions (Figure 30). The genes for the enzyme CTAS showed particularly high expression levels in high PD and/or HD accessions of *H. macrophylla* but was absent in *H. paniculata*. These

results provide insights into the regulation of the phenylpropanoid pathway and its associated pathways in different *Hydrangea* accessions.

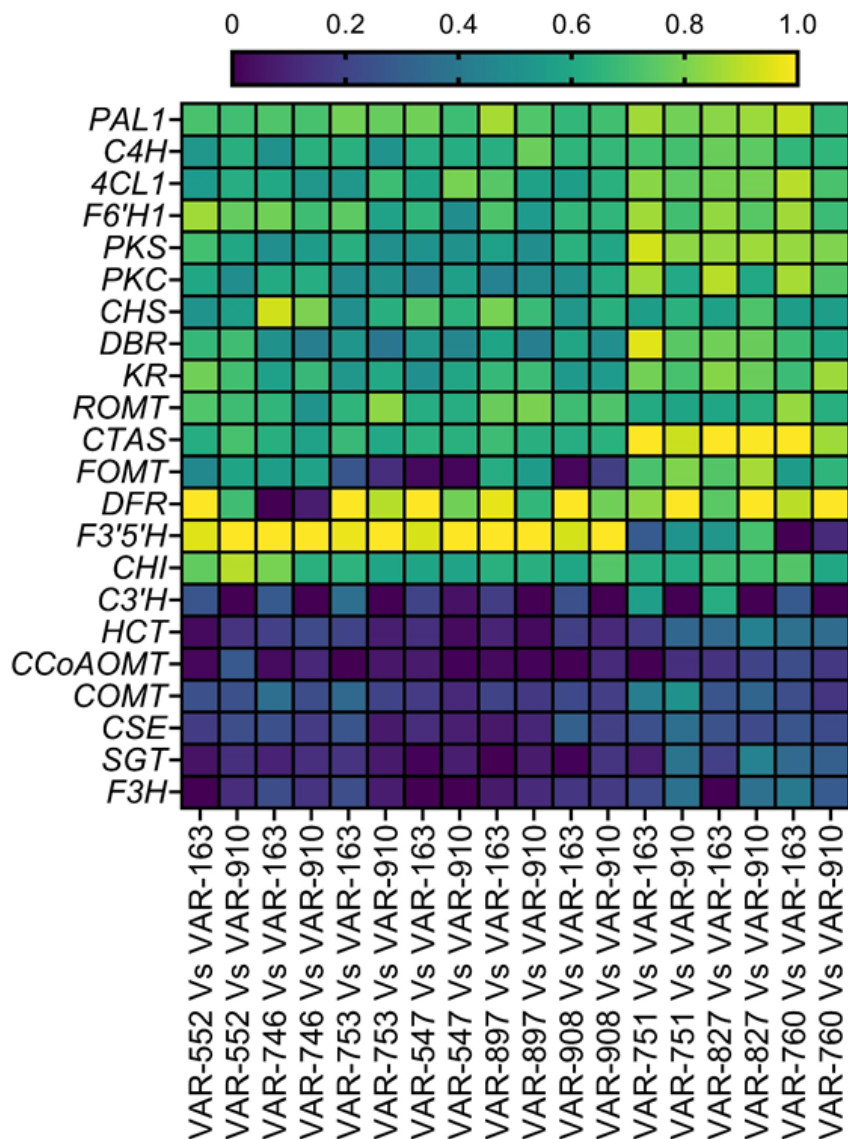


Figure 29. Expression patterns of module-specific genes involved in the PPP and associated pathways in *H. macrophylla* accessions. Heatmap of selected genes involved in PPP, flavonoid biosynthetic pathway and stilbene biosynthetic pathway. Differentially expressed genes were selected based on module-trait relationships derived from WGCNA, where each gene was present in a module, which correlated to individual metabolite concentrations ($p_{adj} < 0.05$). Each square black represents the normalized log-fold2 change values of specific gene in each study group. The comparison was between a high PD and/or HD accession with low PD/HD accessions (VAR-163 and VAR-910). Yellow represents the highest relative expression level of the gene and dark violet represents the lowest relative expression level of the gene.

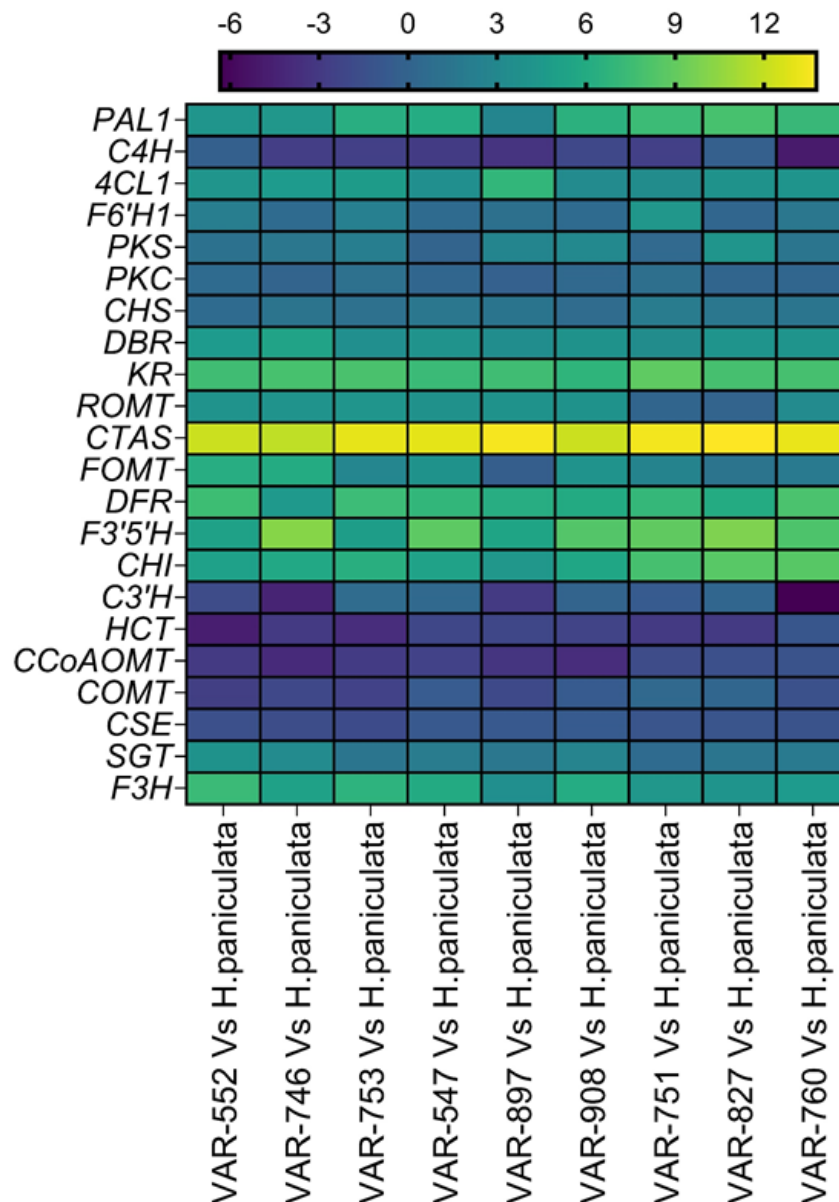


Figure 30. Expression patterns of module-specific genes involved in the PPP and associated pathways in *H. macrophylla* and *H. paniculata* accessions. Heatmap of selected genes involved in PPP, flavonoid biosynthetic pathway and stilbene biosynthetic pathway while comparing *H. macrophylla* and *H. paniculata*. Differentially expressed genes were selected based on module-trait relationships derived from WGCNA, where each gene was present in a module, which correlated to individual metabolite concentrations ($p_{adj} < 0.05$). Each square black represents the normalized log-fold2 change values of specific gene in each study group. The comparison was between a high PD and/or HD accession with low PD/HD accessions (VAR-163 and VAR-910). Yellow represents the highest relative expression level of the gene and dark violet represents the lowest relative expression level of the gene.

4.6 Validation of candidate gene expression using quantitative real-time-PCR (qRT-PCR)

For the validation of the RNA sequencing data, the sequences of 10 candidate genes, involved in phenylpropanoid biosynthesis, flavonoid biosynthesis and stilbenoid biosynthesis, which showed varying expression levels in all experimental groups, were subjected to quantitative real-time PCR using specifically designed primers (Table 1). The selected genes were *DFR*, *DBR*, *CTAS*, *PKC*, *4CL*, *PAL1*, *KR*, *HCT*, *CCoAOMT* and *COMT*. For the present study the best suitable internal reference gene (housekeeping gene) was identified as glyceraldehyde 3-phosphate dehydrogenase (*GADPH*) which was also reported in earlier studies (Zhang *et al.*, 2022). The gene expression levels were expressed as foldchange and log₂ transformed by comparing the same study groups as that of RNA sequencing experiment.

By studying the expression levels of genes using qPCR it was observed that genes *DBR*, *CTAS*, *PKC*, *4CL*, *PAL1* and *KR* were upregulated when comparing the transcriptome of high PD and/or HD accessions with that of a low PD and HD accessions (Figure 31-33). Similarly, in the genes *HCT*, *CCoAOMT* and *COMT* involved in caffeic acid synthesis and related downstream metabolites was found downregulated while comparing the same set of accessions (Figure 31-33). The gene *DFR* was found downregulated while comparing accession VAR-746 with VAR-163 and VAR-910 (Figure 31C, D).

While comparing these results with fold-change values of genes obtained from transcriptome profiling, it was observed that the expression levels of transcriptome and RT-qPCR analyses were quite similar to each other, indicating that the genes studied are involved in the metabolic pathways associated with PD biosynthesis.

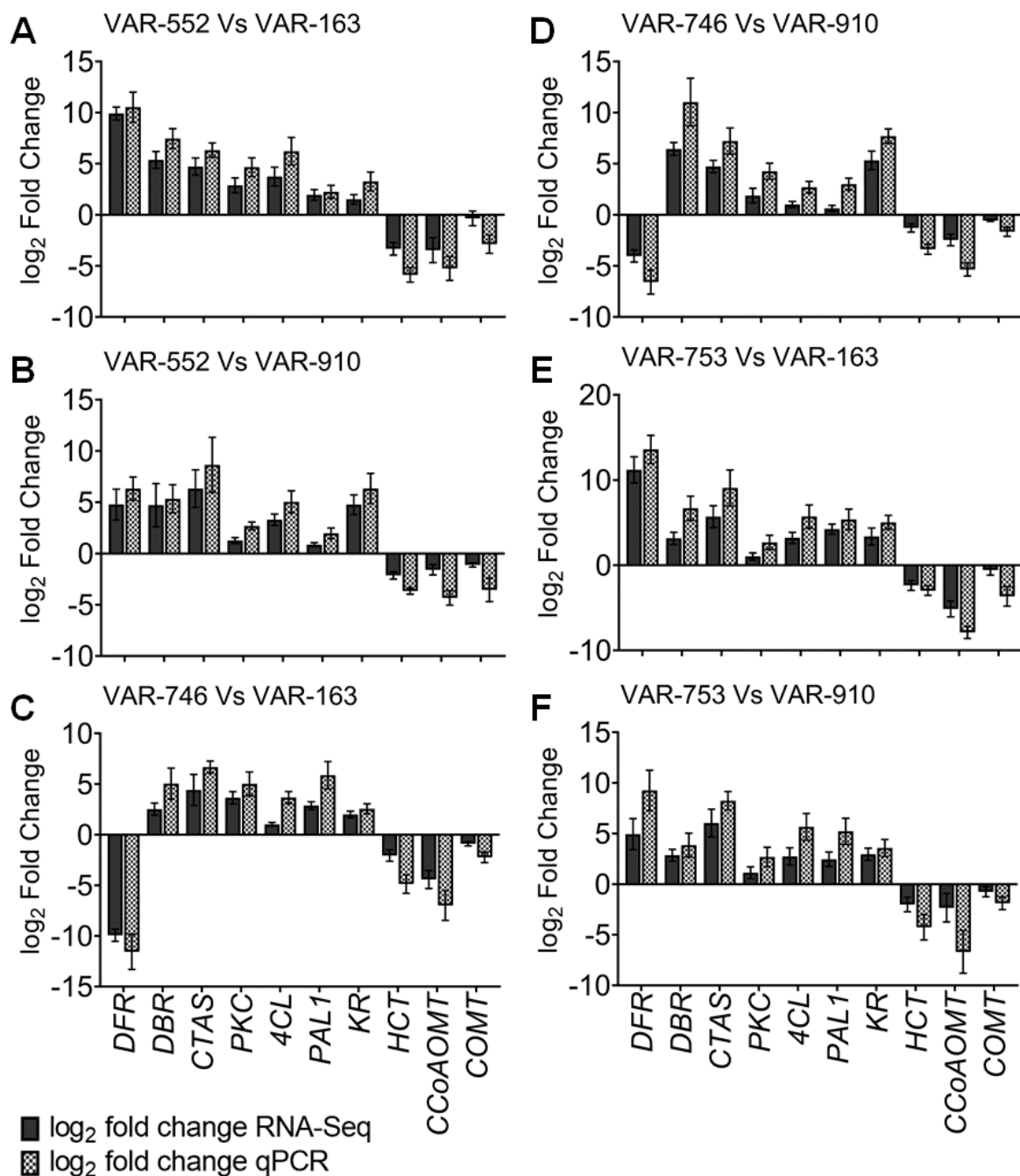


Figure 31. Validation of RNAseq data with qRT-PCR. (A-F) The expression of genes involved in the metabolic pathways associated with PD biosynthesis while comparing accessions (A) VAR-552 and VAR-163, (B) VAR-552 and VAR-910, (C) VAR-746 and VAR-163 and (D) VAR-746 and VAR-910, (E) VAR-753 and VAR-163 and (F) VAR-753 and VAR-910. Ten representative genes namely *DFR*, *DBR*, *CTAS*, *PKC*, *4CL*, *PAL1*, *KR*, *HCT*, *CCoAOMT* and *COMT* were chosen to validate the expression of genes obtained from RNAseq using RT-qPCR. Bars indicate means \pm SE ($n=3$) of log₂ fold-change obtained from respective experiments. Positive values represent upregulation and negative values represent downregulation. The gene *GADPH* was used as internal reference gene.

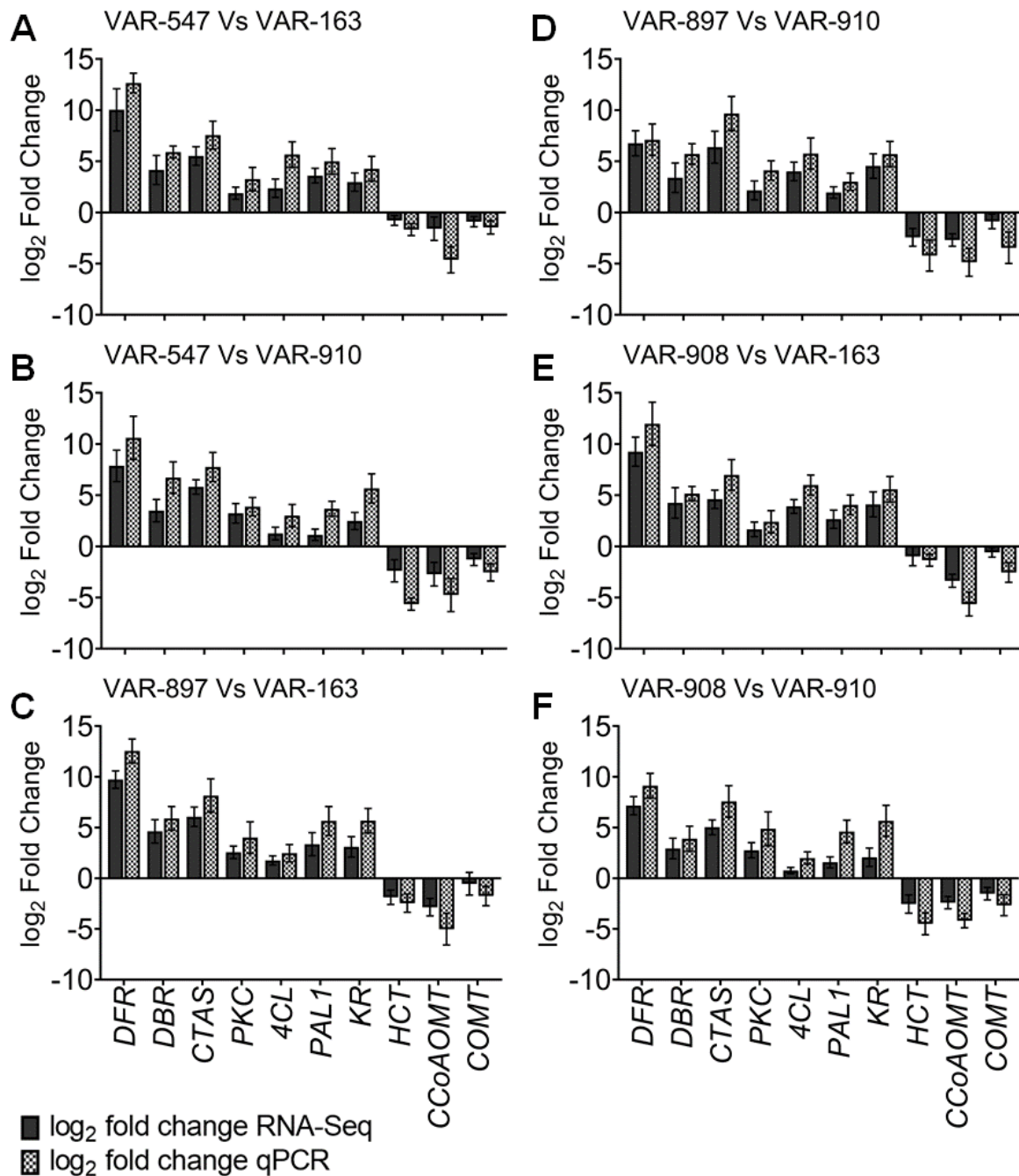


Figure 32. Validation of RNAseq data with qRT-PCR. (A-F) The expression of genes involved in the metabolic pathways associated with PD biosynthesis while comparing accessions (A) VAR-547 and VAR-163, (B) VAR-547 and VAR-910, (C) VAR-897 and VAR-163 and (D) VAR-897 and VAR-910, (E) VAR-908 and VAR-163 and (F) VAR-908 and VAR-910. Ten representative genes namely *DFR*, *DBR*, *CTAS*, *PKC*, *4CL*, *PAL1*, *KR*, *HCT*, *CCoAOMT* and *COMT* were chosen to validate the expression of genes obtained from RNAseq using RT-qPCR. Bars indicate mean \pm SE (n=3) of log₂ fold-change obtained from respective experiments. Positive values represent upregulation and negative values represent downregulation. The gene *GADPH* was used as internal reference gene.

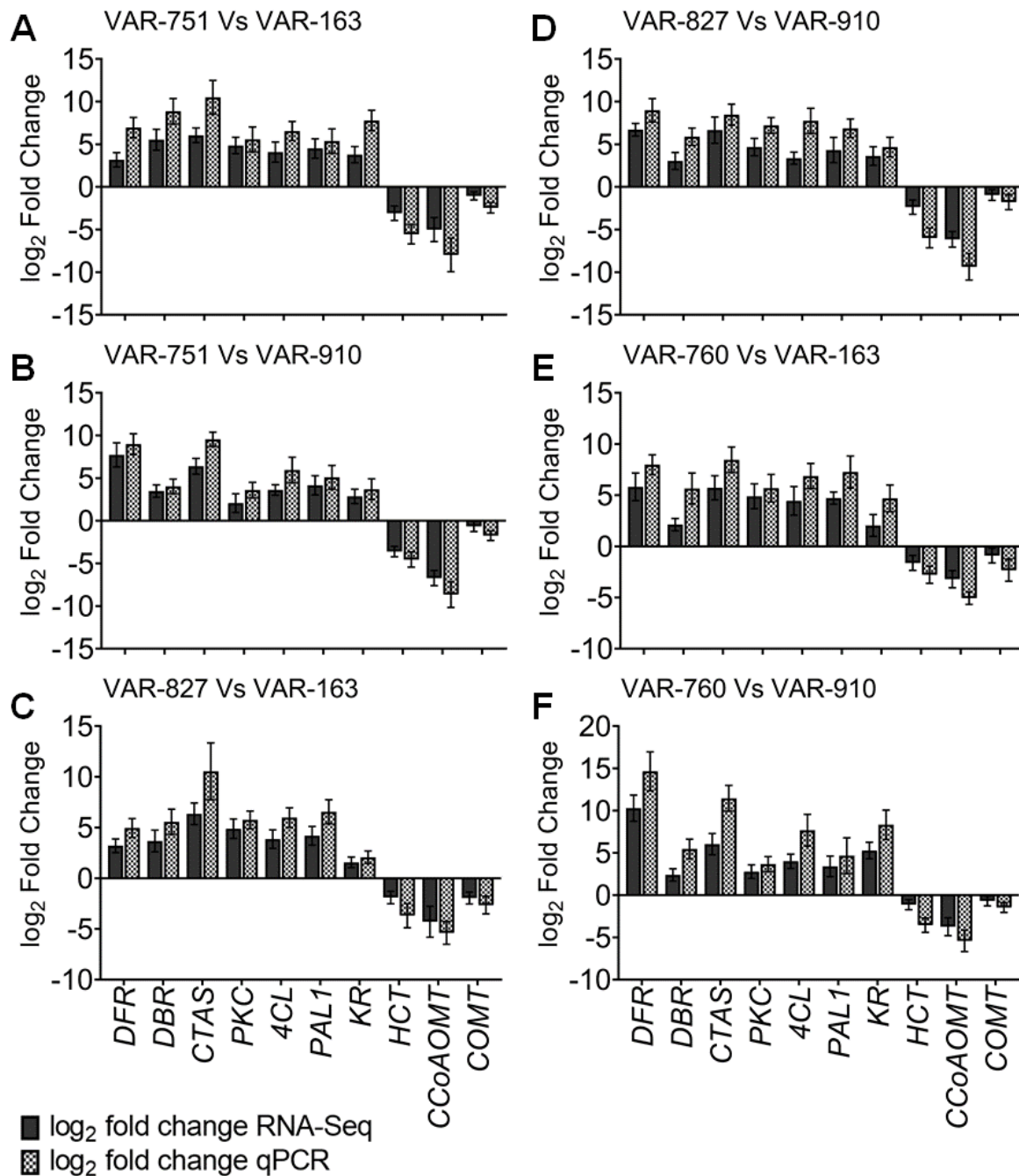


Figure 33. Validation of RNAseq data with qRT-PCR. (A-F) The expression of genes involved in the metabolic pathways associated with PD biosynthesis while comparing accessions (A) VAR-751 and VAR-163, (B) VAR-751 and VAR-910, (C) VAR-827 and VAR-163 and (D) VAR-827 and VAR-910, (E) VAR-760 and VAR-163 and (F) VAR-760 and VAR-910. Ten representative genes namely *DFR*, *DBR*, *CTAS*, *PKC*, *4CL*, *PAL1*, *KR*, *HCT*, *CCoAOMT* and *COMT* were chosen to validate the expression of genes obtained from RNAseq using RT-qPCR. Bars indicate mean \pm SE (n=3) of log₂ fold-change obtained from respective experiments. Positive values represent upregulation and negative values represent downregulation. The gene *GADPH* was used as internal reference gene.

4.7 The efficacy of β -Glucosidase digestion in augmenting PD and HD levels

To investigate the underlying mechanism of how bioactive PD and HD accumulate in dried leaves, freshly harvested and dried leaf tissues from selected accessions were externally supplied β -glucosidase enzyme and subsequently performed biochemical extraction followed by LC-MS analysis. Quantification of PD and HD after the enzyme treatment revealed that when fresh leaf material was treated with β -glucosidase, there was an increase in the levels of active PD and HD (Figure 34A-J). This increase was consistent across all accessions, demonstrating a significant difference between PD and HD levels in fresh leaf material and fresh leaf material treated with β -glucosidase. Similarly, when dry leaf material was treated with β -glucosidase, there was also a notable increase in active PD and HD levels (Figure 34A-J). This increase was found to be significant for all varieties treated with the enzyme. When comparing the differences between enzyme-treated fresh and dried tissues, it was observed that there were no significant differences between them. This suggests that through enzyme treatment, all the detectable glucoside forms present in the tissue may have been converted into their active forms. This work provides a solid basis on how enzymatic digestion with β -glucosidase can effectively enrich the PD and HD concentrations in tissues aiding in better during extraction.

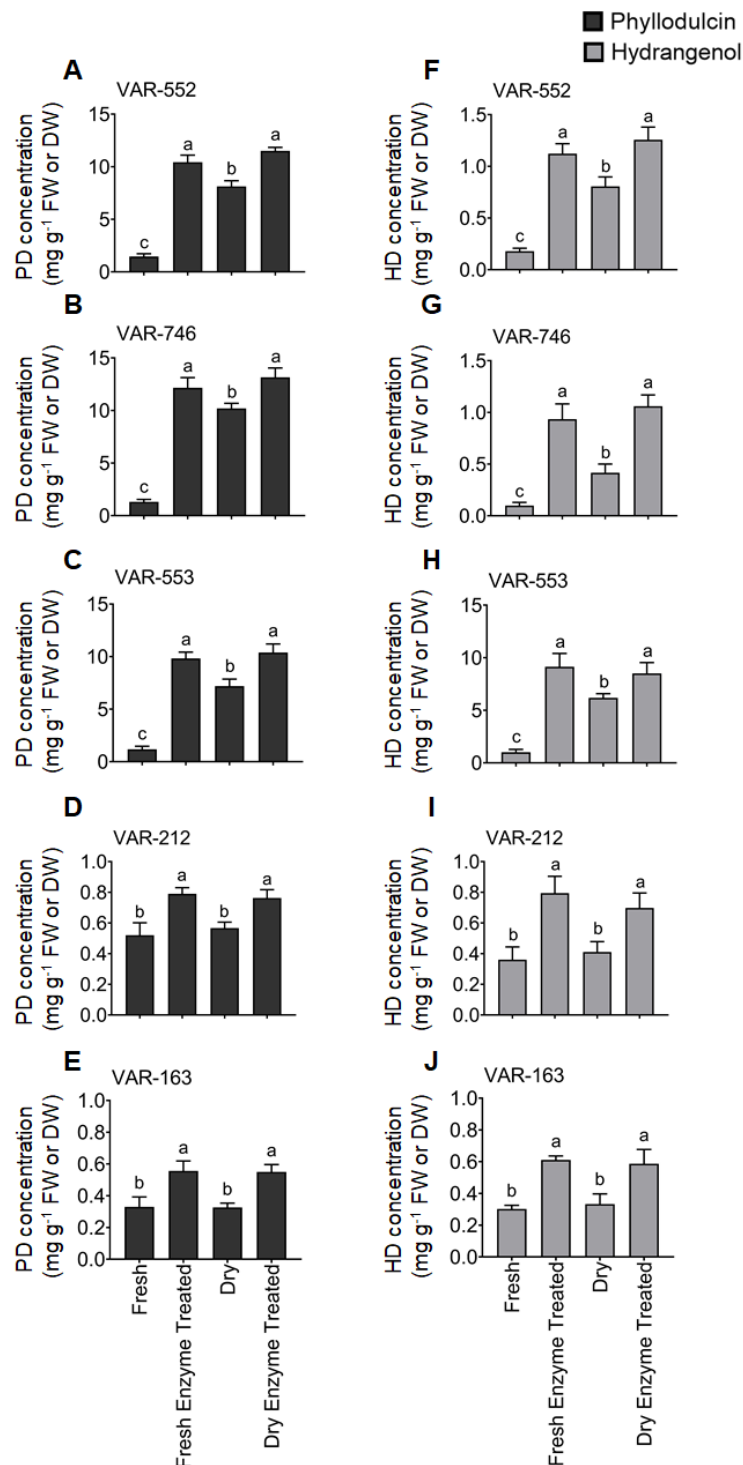


Figure 34. Effect of enzymatic digestion of leaf tissue with β -glucosidase on PD and HD yield. (A-E) Changes in PD concentrations of freshly harvested and oven dried leaves when (A) VAR-552, (B) VAR-746, (C) VAR-553, (D) VAR-212 and (E) VAR-163 was treated with the enzyme β -glucosidase. (F-G) Changes in HD concentrations of freshly harvested and dried leaves when (F) VAR-552, (G) VAR-746, (H) VAR-553, (I) VAR-212 and (J) VAR-163 was treated with the enzyme β -glucosidase. Analysis was done on fully expanded upper leaves. Black bars represent the level of PD and grey bars show the level of HD. Bars represent means of 6 independent biological replicates and standard error. Different letters denote significant differences among varieties according to one-way ANOVA and post-hoc Tukey's test ($p < 0.05$). FW and DW indicate fresh and dried weights of tissues used for respective enzymatic digestions.

4.8 Impact of drought stress on coumarin concentrations in *H. macrophylla* accessions

To investigate the impact of drought stress on the coumarin profile of various *Hydrangea* accession groups, a study was conducted using five selected *H. macrophylla* accessions. These accessions were categorized into high PD (VAR-552 and VAR-746), high PD/HD (VAR-553), and low PD/HD (VAR-212 and VAR-163) groups. The plants were initially grown in well-watered soil conditions for ten days in greenhouse. On the 11th day, the control plants were separated from the treatment group and received regular watering as before. The treatment group continued to grow for an additional 24 days under controlled conditions until all plants reached a soil moisture level of 5% soil moisture, determined through moisture meter. The plants were then maintained under these conditions for an additional 20 days until harvest. Visually, the drought affected plants grown at 5% soil moisture exhibited narrow leaf lamina, less expanded top leaves, and weaker stems compared to the plants grown at normal watering conditions (Figure 35A-E). These differences in morphology between the control and treatment plants were likely due to variations in soil moisture levels (Tan *et al.*, 2023; Schrieber *et al.*, 2023).

To comprehensively assess the treatment's effects, leaf extracts from both control and treatment plants were subjected to mass spectrometric analysis to quantify seven different coumarins, along with naringenin and resveratrol. Additionally, fluorescence detection was used to study the dynamics of free amino acids in the samples.

The analysis revealed that the amino acids phenylalanine (Figure 36A) and proline (Figure 36B) as well as phenylpropanoids such as PD (Figure 37A), HD (Figure 37B), resveratrol (Figure 37C), naringenin (Figure 37D), scopoletin (Figure 37E), scopolin (Figure 37F), and fraxetin (Figure 37I) were present at higher concentrations in drought-affected plants compared to unaffected plants in all studied *H. macrophylla* accessions. However, the concentrations of esculin (Figure 37G) and esculetin (Figure 37H) were higher in plants grown under well-watered conditions. Notably, there was no significant difference in esculin concentrations between control and treatment plants in VAR-163.

The highest PD concentration (15.68 mg g⁻¹ dry weight) was observed in VAR-746, while the highest HD concentration (12.35 mg g⁻¹ dry weight) was found in VAR-553, both of which were grown under 5% soil moisture-induced drought conditions (Figure

37A, B). In the study, the highest scopolin concentrations were detected in drought-induced VAR-212 (Figure 37F), while the highest scopoletin concentrations were found in drought-affected VAR-163 (Figure 37E). The highest esculin concentration was observed in VAR-552 grown under well-watered conditions (Figure 37G), and the highest esculetin levels were found in well-watered VAR-212 and VAR-163 (Figure 37H). Fraxetin concentration was highest in VAR-552 exposed to drought conditions (Figure 37I). Naringenin concentration was highest in VAR-746 and VAR-553 subjected to drought stress (Figure 37D), while resveratrol concentration peaked in VAR-746 grown under drought conditions (Figure 37C).

These findings suggest that under conditions of abiotic stress with limited water availability, plants tend to synthesize more coumarins like scopolin, scopoletin, fraxetin, and dihydroisocoumarins like PD and HD. This phenomenon aligns with previous research in other plant species, such as *Melilotus*, which reported an increase in coumarin concentration under drought stress due to the upregulation of coumarin biosynthetic genes, including regulatory elements of the *BGLU* gene family (Zhang *et al.*, 2023; Wu *et al.*, 2022). These coumarins may assist plants in coping with stress through various mechanisms, including the scavenging of reactive oxygen species (ROS) produced during stressful conditions. The higher accumulation of coumarins in this experiment may also be attributed to this protective mechanism.

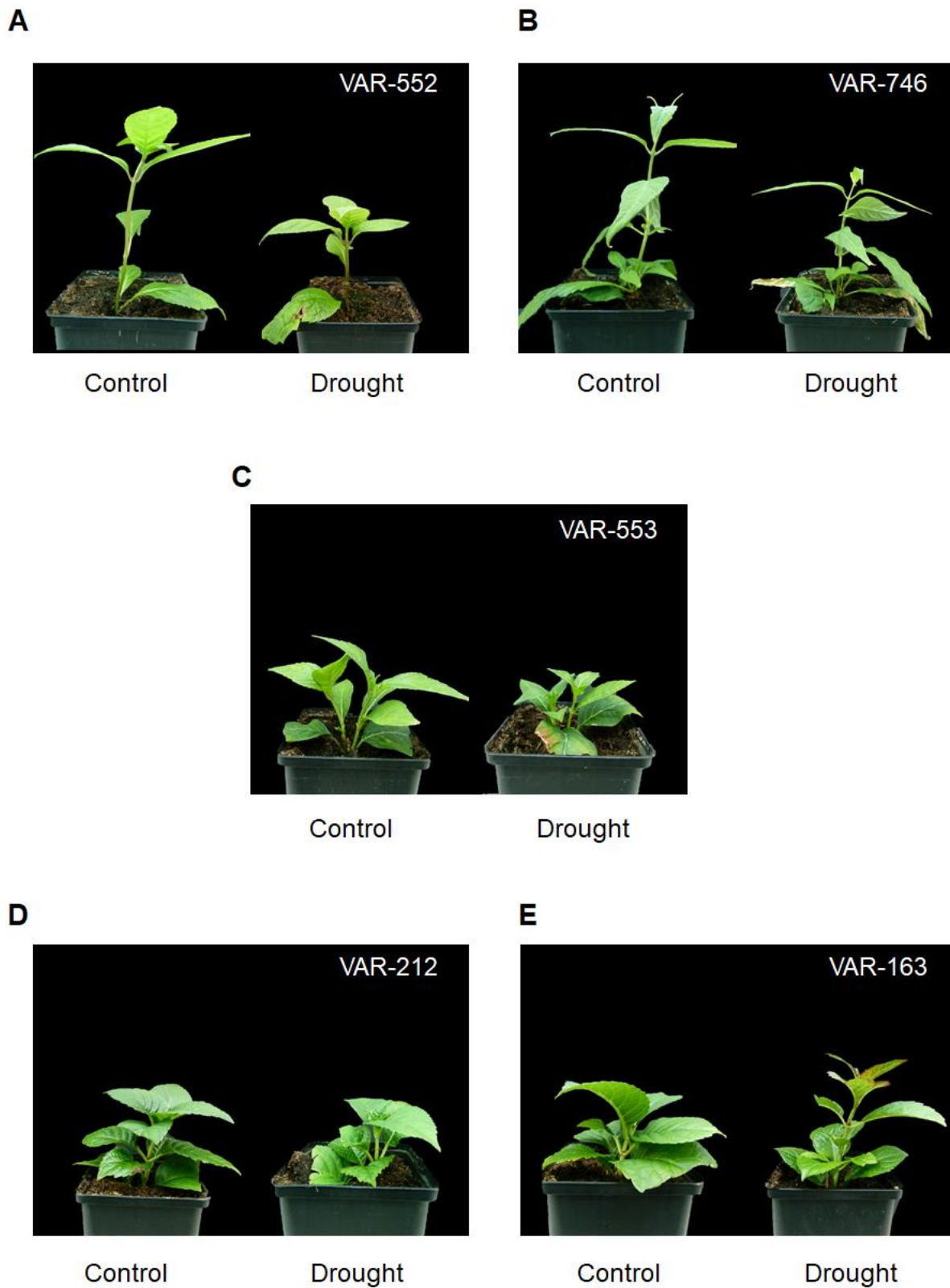


Figure 35. Effect of drought on the visual appearance of different *H. macrophylla* accessions. (A-E) Visual appearance of shoots in (A, B) high-PD accessions, (C) high-PD/HD accessions and (D, E) low-PD/HD accessions grown under well-watered conditions (control) or drought conditions. Plants were subjected to drought stress for 20 days.

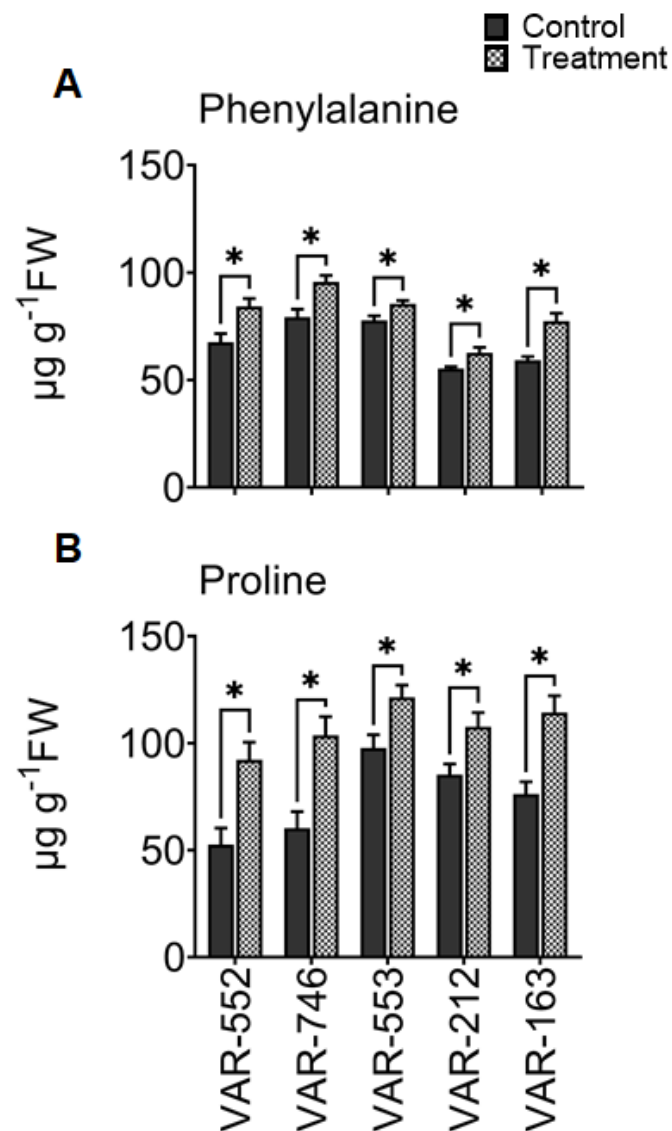


Figure 36. Concentrations of selected amino acids in *Hydrangea* plants grown under sufficient water supply and drought stress. (A, B) Concentrations of (A) phenylalanine and (B) proline, in leaf tissues of well-watered plants and drought-stressed plants. Analysis was done on fully expanded top leaves. Bars represent means + SE, n = 8 independent biological replicates and standard error. Asterisks indicate significant differences at $p < 0.05$ according to Student t-test.

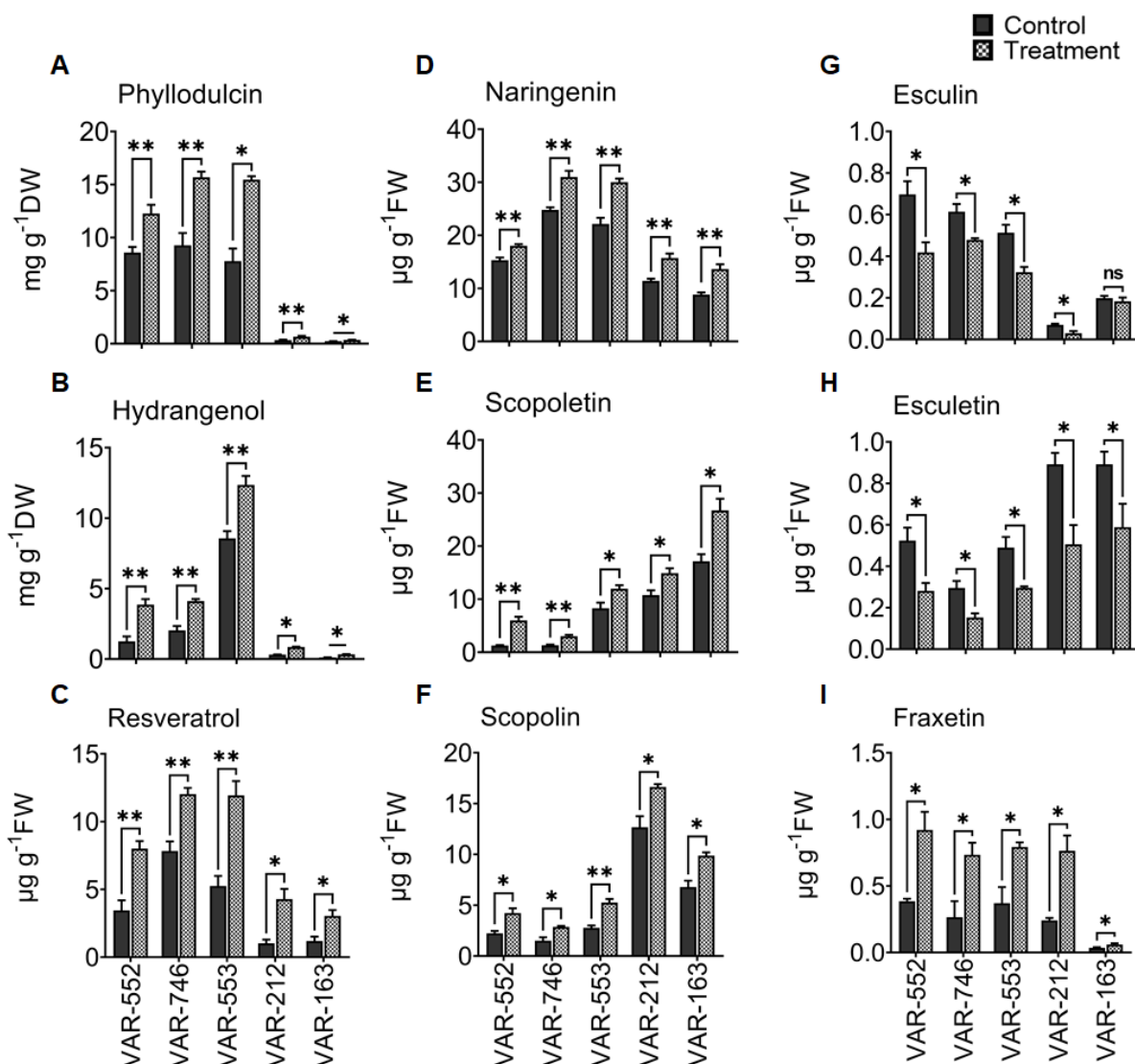


Figure 37. Concentrations of PD, HD, and associated metabolites in *Hydrangea* plants grown under sufficient water supply or drought stress. (A-I) Concentrations of (A) PD, (B) naringenin, (C) esculin, (D) HD, (E) scopoletin, (F) esculetin, (G) resveratrol, (H) scopolin and (I) fraxetin in leaf tissue of well-watered plants compared to drought affected plants. Analysis was done on fully expanded top leaves. Bars represent means + SE, n= 8 independent biological replicates and standard error. Single and double asterisks indicate significant differences at p<0.05 and p<0.01 respectively according to Student t-test. ns: not significant.

4.9 Impact of high-light intensity on coumarin concentrations in *H. macrophylla* accessions

To investigate the impact of high light intensities on the coumarin profile of *Hydrangea*, we conducted an experiment using five selected *H. macrophylla* accessions. These accessions included those with high PD concentration (VAR-552 and VAR-746), high PD/HD (VAR-553), and low PD/HD (VAR-212 and VAR-163). The plants were initially grown under normal light conditions, with a light intensity of 150 µmol m⁻² s⁻¹ (150 µE

$\text{m}^{-2} \text{s}^{-1}$), an 18-hour photoperiod and at a temperature of 21/19 °C (day/night), and 60% relative humidity for ten days. On the 11th day, both control and treatment plants were shifted to growth chambers with the same temperature and humidity conditions but with different light intensities: 150 $\mu\text{E m}^{-2} \text{s}^{-1}$ for control and 600 $\mu\text{E m}^{-2} \text{s}^{-1}$ for treatment. To prevent confounding effects, the plants were randomized daily. After 22 days under these conditions, the leaves of the plants grown at 600 $\mu\text{E m}^{-2} \text{s}^{-1}$ exhibited yellow and purple pigmentation, which varied depending on the accession (Figure 38A-E). At this stage, both control and treatment plants were removed from the chambers, and the leaves were harvested. The leaves were dried at 40°C for 48 hours, after which biochemical extraction of PD and HD was performed. The extraction of other metabolites was carried out on fresh leaf tissue.

Subsequent LC-MS analysis of leaf extracts revealed that PD (Figure 39A), HD (Figure 39B), resveratrol (Figure 39C), and naringenin (Figure 39D) had higher concentrations in treatment plants compared to control plants. However, there were no significant differences in esculin (Figure 39G) and fraxetin (Figure 39I) concentrations between control and treatment conditions. The extent of changes in concentrations of esculin, scopoletin (Figure 39E), and scopolin (Figure 39F) were dependent on the accession. Specifically, accessions VAR-552, VAR-212, and VAR-163 showed significant differences in scopoletin and esculin concentrations between control and treatment accessions (Figure 39E, H). Scopolin concentrations were higher in control compared to light stressed accessions VAR-212 and VAR-163 (Figure 39F).

In summary, this experiment suggests that in *H. macrophylla* accessions, high light intensities enhance dihydroisocoumarin, stilbene, and flavonoid accumulation.

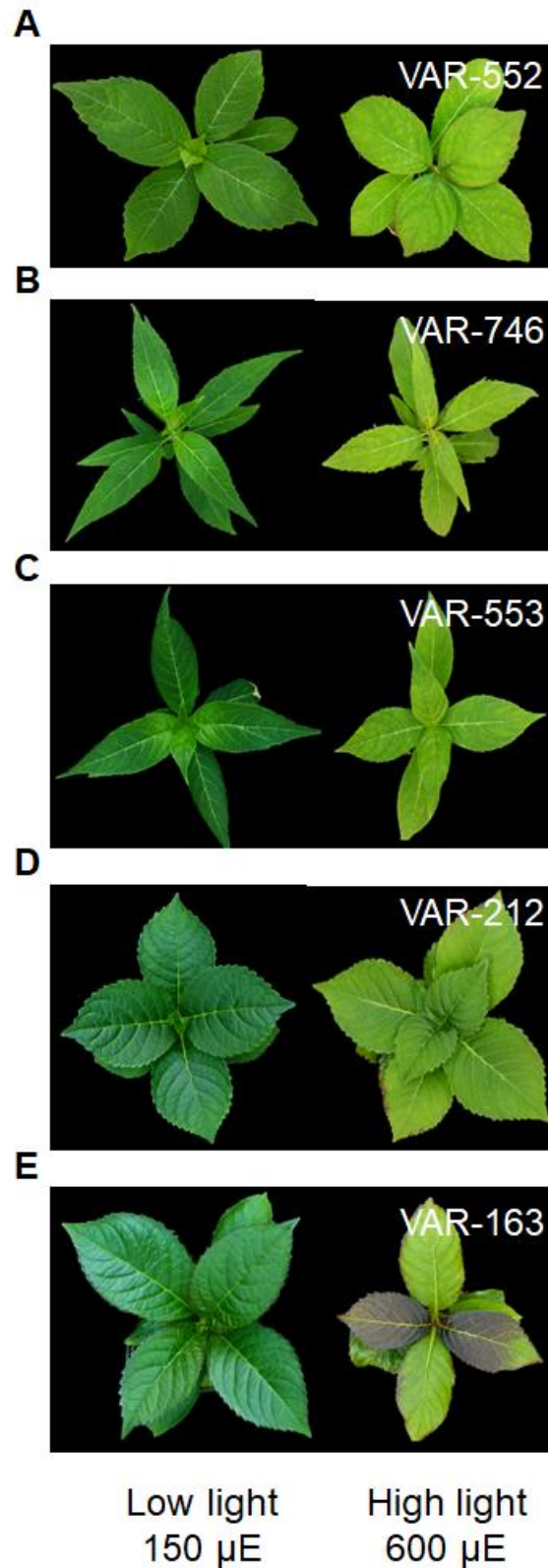


Figure 38. Effect of light intensity on the visual appearance of leaves of different *H. macrophylla* accessions. (A-E) Visual changes in leaf colour in (A, B) high PD accessions, (C) high PD/HD accessions and (D, E) low PD/HD accessions grown under $150 \mu\text{E m}^{-2} \text{s}^{-1}$ (low light) and $600 \mu\text{E m}^{-2} \text{s}^{-1}$ (high light) conditions. Plants were subjected to light stress for 22 days.

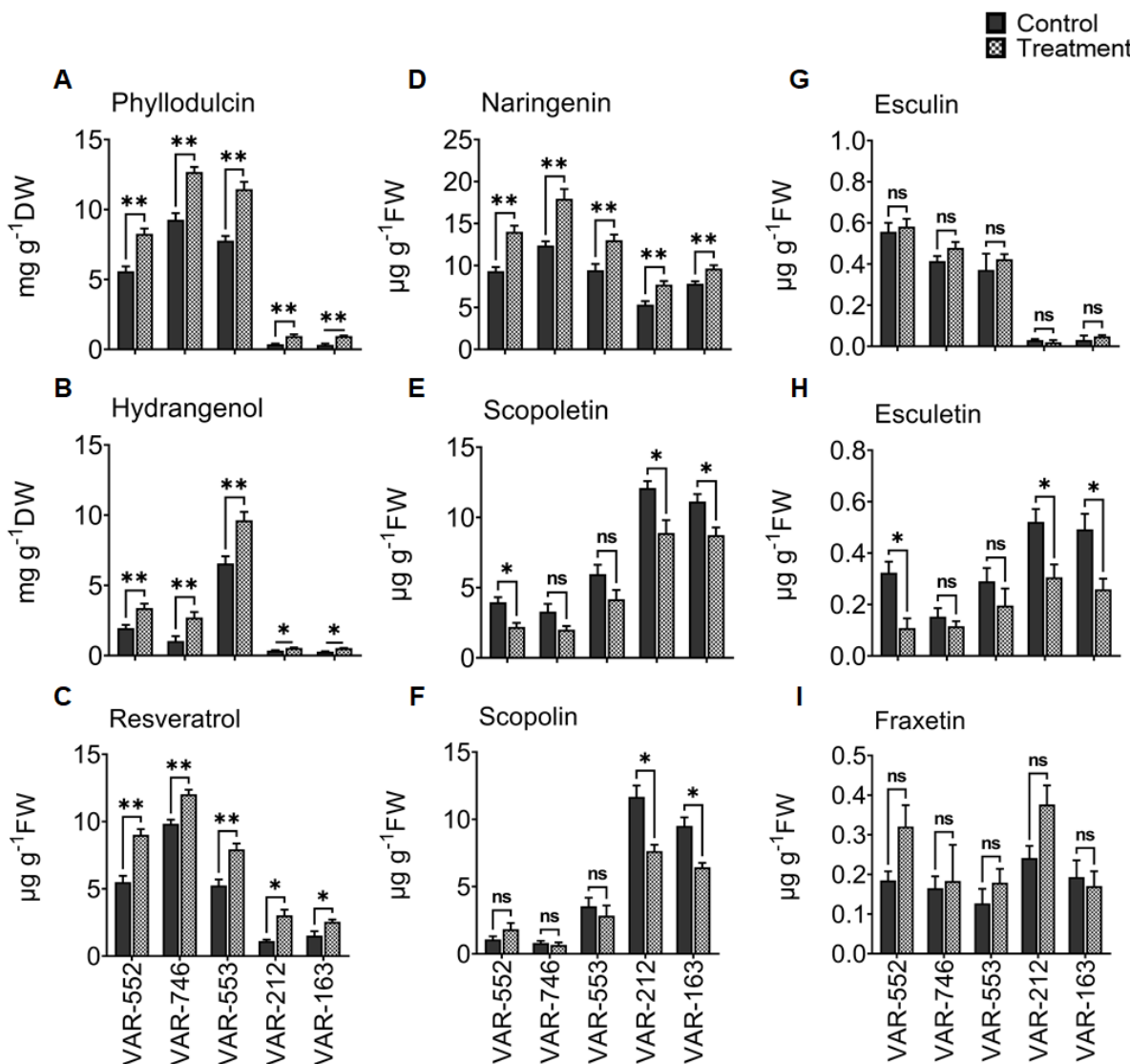


Figure 39. Concentrations of PD, HD and associated metabolites in *Hydrangea* plants grown under different light intensities. (A-I) Concentrations of (A) PD, (B) HD, (C) resveratrol, (D) naringenin, (E) scopoletin, (F) scopolin, (G) esculin, (H) esculetin and (I) fraxetin in leaf tissue of plants grown in $150\mu\text{E m}^{-2} \text{s}^{-1}$ compared to plants grown in $600\mu\text{E m}^{-2} \text{s}^{-1}$ to induce light stress. Analysis was done on fully expanded top leaves. Bars represent means + SE, $n = 8$ independent biological replicates and standard error. Single and double asterisks indicate significant differences at $p < 0.05$ and $p < 0.01$ respectively according to Student t-test. ns: not significant.

5 Discussion

In the modern era, where food safety is of highest concern, use of artificial sweeteners in food industry is still controversial. The recent classification of aspartame, an FDA-approved and widely used synthetic sweetener, into the International Agency for Research on Cancer (IARC) group 2B as “possibly carcinogenic to humans” poses an important question of whether these molecules may continue to be used to enhance the taste of foods (Riboli *et al.*, 2023). This scientific curiosity has led researchers to explore a safer and healthier option of mining the plant kingdom for natural sweeteners (Mora and Dando, 2021; Castro-Muñoz *et al.*, 2022). An alternative to sweeteners and sugar substitutes is stevioglycoside, a natural sweetener derived from the Stevia plant. Stevioglycosides are exceptionally sweet (up to 300 times sweeter than sucrose), low in calories (0.21 kcal/g), and non-cariogenic. However, concerns about the safety of stevioglycosides have led to the establishment of a uniform daily intake limit (ADI) of 4 mg/kg by EFSA (European Food Safety Authority) and JECFA (Joint Expert Committee on Food Additives) due to potential health effects from the degradation product steviol (Pezzuto *et al.*, 1985; Philippe *et al.*, 2014). Currently produced in China, the extraction process for stevioglycosides requires a substantial amount of water, includes the use of formaldehyde for preservation (not permitted in Germany), and involves controversial practices like the use of aluminum salts during precipitation. This process chemically alters the plant material and deviates from the natural composition of *Stevia rebaudiana*. This departure from naturalness could be deemed deceptive, potentially violating food regulations (DGE/Dokumentationsband_2014.pdf). As an alternative, phyllo dulcin offers a promising option, as it involves using molasses directly from the leaves rather than isolating the active ingredient phyllo dulcin.

Phyllo dulcin (PD), the sweet component of *H. macrophylla* is 600 to 800 times sweeter than sucrose and has the potential to be used as a natural sweetener in a wider scale (Yamato *et al.*, 1975; Yasuda *et al.*, 2004; Kim *et al.*, 2017; Preusche *et al.*, 2022; Tsukioka and Nakamura, 2023; Cho *et al.*, 2023). The antidiabetic, antiulcer and antifungal effects along with potential to reduce SARS-CoV-2 infection of PD in *H. macrophylla* extracts and its role in Japanese traditional medicine further justifies the importance of studying the biochemical profile and the genetic regulation of PD biosynthesis in the plant (Nozawa *et al.*, 1981; Zhang *et al.*, 2007; Yano *et al.*, 2023).

So far, the relationship between metabolites and genes in *Hydrangea* varieties has not been addressed together in a single frame, especially by giving preference to PD. Therefore, the work described in this thesis was directed to increase the natural production of PD and identify the associated biosynthetic pathway.

5.1 Concentrations of PD in *H. macrophylla* depend on the developmental stage

Knowing the optimum stage at which the plant produces the highest concentrations of bioactive molecules and the tissue in which these biomolecules can be extracted economically are crucial factors need to be addressed in phytochemistry. To find out at which developmental stage and in which tissue the plant produces the highest concentrations of phyllodulcin, different plant organs and developmental stages were studied by quantifying it using LC-MS (Figure 6A). These analyses were important to ensure that the correct tissue and developmental stage were harvested for optimum PD and HD extraction. After initial screening, 5 out of 14 accessions were grown in green house of IPK from initial cutting to senescence for 145 days (Figure 9, 10; Table 3). By analyzing different plant organs, it was concluded that the highest concentration of PD and HD was found in leaves, hence leaves were used as study material (Figure 11, 12). The performed developmental study showed that the highest concentration of PD and HD in high PD accessions (VAR-552 and VAR-746) and a high PD/HD accession (VAR-553) were obtained when the plants were close to maturity of 110 days at the end of flowering (Figure 14A-C, 15A-C). In contrast, there was a low concentration of PD in accessions VAR-212 and VAR-163. For low PD accessions, VAR-212 and VAR-163, the PD and HD concentrations did not significantly change from 75 to 110 days but rather showed a non-significant increasing trend (Figure 14D, E; 15D, E). Overall, these results indicate that in the upper leaves of *H. macrophylla*, PD concentrations do not remain constant throughout the plant's life but rather exhibits a steady increase from the vegetative stage to the reproductive stage and then decrease after flowering (Figure 14A-E).

Leaves serve as the primary structures in plants responsible for photosynthesis and hold significant importance in the plant's lifecycle. Additionally, leaves can function as synthetic and storage organs for secondary metabolites. The concentration of these metabolites in medicinal plant leaves can be influenced by factors such as the age of the leaves, the season in which they are harvested and the growth stage of the plant (Li *et al.*, 2016c; Vazquez-Leon *et al.*, 2017; Gomes *et al.*, 2019). Previous studies

have shown that within *Hydrangea* sp. the younger leaves from the top had higher PD concentrations compared to the lower older leaves (Ujihara *et al.*, 1995; Moll *et al.*, 2021b). It has also been recorded that in a span of 3 months, phylodulcin-8-0-D-glucose is enzymatically hydrolyzed to PD resulting in higher abundance in the plant (Suzuki *et al.*, 1981). However, the precise growth stage of the plants in the experiment was not mentioned to allow a comparison with the current study.

Since the phenylpropanoid metabolism exhibits extreme plasticity in response to different developmental stages, the biochemical composition of medicinal plants varies substantially due to the same factor. In *Hypericum organifolium*, the level of flavonoid derivatives hypericin, quercitrin and quercetin reached a peak at budding and flowering stage and then declined during later stages (Kazlauskas and Bagdonaite, 2004; Çirak *et al.*, 2007). In *Gentiana pneumonanthe*, the concentrations of bioactive secoiridoid glycosides swertiamarin, gentiopicrin and mangiferin increased from vegetative growth to flowering and dropped post anthesis (Popović *et al.*, 2021). A similar trend for stilbenes was observed in grapes Chinese wild grapes during berry development (Li *et al.*, 2020). *Scutellaria baicalensis*, *Polygala tenuifolia*, *Astragalus compactus* and some *Cannabis* sp. also showed the same dynamics in phenylpropanoid derivatives (Gatto *et al.*, 2008; Teng *et al.*, 2009; Naghiloo *et al.*, 2012b; Xu *et al.*, 2018; Richins *et al.*, 2018).

The production and accumulation of secondary metabolites in plants, primarily serving protective and defensive roles, represent a dynamic process shaped by various factors related to plant adaptation and acclimation (Fineblum *et al.*, 1995). This phenomenon can be attributed to two primary factors: firstly, "ontogenetic drift," which involves changes in the plant's size and developmental stage as it matures (Evans, 1972; Peng *et al.*, 2010). Secondly, "ontogenetic trajectories" influenced by the pressures of natural selection also play a significant role (Barton and Boege, 2017). The synthesis of specific secondary metabolites in plants is often closely tied to particular stages of their development, exhibiting distinct temporal patterns. These patterns can be influenced by various factors, including growth, reproduction, and environmental conditions (Sampaio *et al.*, 2016). It's important to note, however, that the relationship between metabolite production and plant development is not always straightforward. There are instances where the highest levels of a particular metabolite can be observed at different developmental stages than initially expected (Baraldi *et al.*,

2008). This complexity underscores that plant secondary metabolite production is a multifaceted and adaptable process, influenced by genetic variability, environmental signals, and evolutionary pressures. In summary, concentration of both PD and HD in *H. macrophylla* accessions peaking at 110 days could be mainly because of the channeling of a pool of precursor metabolites towards secondary metabolism during later stages of the plant's lifecycle. The gradual increase and peak accumulation of flavonoid precursor naringenin and stilbene resveratrol (secondary metabolites) at 110 days also supports this hypothesis (Appendix 4). These secondary metabolites help the plant to overcome biotic and abiotic stresses which is imperative for the plant's survival. For VAR-212 and VAR-163, which are categorized as low PD/HD accessions, it is conceivable that these accessions reached a saturation point in terms of their maximum PD and HD production by 75 days (Figure 14D, E; 15D, E). Beyond this point, it may not have been possible for these accessions to further increase their PD or HD concentrations. This could provide an explanation for why the PD and HD concentrations remained relatively stable from the 75 days to the 110 days in these accessions (Figure 14,15). Consequently, for industrial-scale extraction of these biomolecules, it is advisable to harvest the young upper leaves at this particular developmental stage for the optimum extraction of both PD and HD.

5.2 β -Glucosidase-mediated digestion increases the bioavailability of PD and HD in leaves

Plants have a mechanism for storing highly reactive biochemical compounds in a less active form by conjugating them with glucose or other sugar molecules. This conjugation reduces the internal toxicity and reactivity of these compounds, allowing for their safe storage in vacuolar cell compartments. This process serves as a form of internal detoxification in plants (Wari *et al.*, 2022; Aboshi *et al.*, 2023). However, when plants undergo drying, experience physical damage (wounding), or go through senescence, these glycosides are converted into their active forms by the removal of the sugar moiety. This conversion process is catalyzed by an enzyme called β -glucosidase (Vassao *et al.*, 2018; Wari *et al.*, 2021). The efficiency of β -glucosidase is influenced by temperature, with its maximum activity typically occurring within the range of 30-45 °C, although this can vary depending on the plant species.

In the leaves of *H. macrophylla* PD and HD exist in glucoside forms (Glc), which encompass compounds like phyllodulcin-8-O-Glc, phyllodulcin-3'-O-Glc, hydrangenol-

8-O-Glc, and hydrangenol-4'-O-Glc, as reported in various studies (Suzuki *et al.*, 1977; Yoshikawa *et al.*, 1994; Ujihara *et al.*, 1995; Zehnter and Gerlach, 1995; Akiyama *et al.*, 1999; Liu *et al.*, 2013; Wellmann *et al.*, 2022) (Figure 4). To extract the total content of PD and HD within the tissue, it is essential to convert these glucoside forms into their active, non-bound forms. Traditionally, this conversion is achieved by drying and rolling the leaf tissue to activate the intrinsic β -glucosidase enzyme, which breaks down these compounds. However, in this study, external supplementation of β -glucosidase was employed to convert all the bound PD and HD glucosides into their active forms.

When freshly harvested leaves from VAR-552, VAR-746 and VAR-553 were dried at 40°C for 48 hours, there was a noticeable increase in the concentrations of PD and HD in the dried tissue compared to the fresh tissue (Figure 10; 34A-C, F-H). Some reports suggest that PD and HD glucosides initially exist in this conjugated form, and the sugar component within them can undergo enzymatic hydrolysis, particularly by β -glucosidase, either during storage or as part of post-harvest processing (Suzuki *et al.*, 1977; Zehnter and Gerlach, 1995; Ujihara *et al.*, 1995; Jung *et al.*, 2016). Similar processes have been observed for other metabolites such as plant cytokinins and steviol glycosides, which also increase in concentration through such enzymatic conversion (Chranioti *et al.*, 2016; Pokorná *et al.*, 2020). Therefore, this could explain the higher concentration of PD and HD observed in the dried leaf tissues in the present study. For low PD accessions like VAR-212 and VAR-163, there was no significant difference in the concentrations of PD and HD between fresh and dried tissues (Figure 34D, E; 34I, J). This lack of variation could be attributed to the fact that the low levels of PD and HD glucosides were not effectively converted into their active forms by the native enzymes, likely due to their low initial concentrations. Consequently, similar concentrations were observed in both fresh and dried tissues.

When freshly harvested tissues underwent external enzyme digestion, there was a notable increase in the levels of PD and HD across all accessions (Figure 34). This augmentation suggested that the concentration of externally supplied enzyme was sufficient to convert all the glucoside forms of PD and HD into their active states. This increase was more pronounced than what occurred during the drying process because, while drying, residual glucoside forms may remain inaccessible to the enzyme due to spatial separation or their presence in concentrations below the

enzyme's minimal substrate concentration level required for effective action. In the case of dried tissue subjected to external enzyme digestion, any residual glucoside forms of PD and HD that remained unaffected by native enzymes were transformed into their active states. Consequently, higher concentrations of PD and HD were observed in enzyme-treated dried tissue compared to oven-dried tissue for all accessions (Figure 34). Notably, the concentrations of PD and HD in enzyme-treated fresh tissues and enzyme-treated dried tissues did not exhibit significant differences (Figure 34). This suggests that through enzyme treatment of tissues, the glucoside-conjugated forms were effectively converted into their physiologically active forms, leaving minimal to no conjugated PD and HD in the tissue. Consequently, enzyme treatment emerges as a viable option for the comprehensive extraction of PD and HD in both their glucoside-conjugated and free forms. However, it is essential to consider the cost-effectiveness of this approach in smaller-scale studies. At an industrial scale, where large batches can be digested simultaneously, coupled with methods for enzyme recovery, this technique can become more practical and productive (Singh *et al.*, 2016).

5.3 Regulation of PD and HD biosynthesis in *Hydrangea* depends on accession-specific expression of genes involved in phenylpropanoid, flavonoid and stilbenoid biosynthesis

Understanding the biosynthesis of PD and HD in *Hydrangeas* holds promise for unlocking a broad spectrum of bioactive compounds with diverse applications, ranging from the food industry to medical science. Earlier studies have shed light on the branching of the phenylpropanoid pathway (PPP), which leads to PD production (Figure 1, 5). Investigations involving ¹⁴C-labelled compounds have indicated that downstream gallic acid accumulates more labeled carbon, suggesting that the initiation of the pathway commences with L-phenylalanine and cinnamic acid (Basyouni *et al.*, 1964; Kindle and Billek, 1964; Yagi *et al.*, 1977). These studies also pointed towards p-coumaric acid, rather than caffeic acid (which is synthesized from activated p-coumaric acid in plants), as the likely precursor for PD biosynthesis (Figure 5). This insight is valuable as it suggests that during PD biosynthesis, the branch leading to caffeic acid is less favoured.

In the present study, a comparative transcriptome analysis between accessions characterized by high PD and/or HD concentrations and those with low PD/HD levels

revealed the significant enrichment of three metabolic pathways: phenylpropanoid biosynthesis, flavonoid biosynthesis, and stilbene biosynthesis, as indicated by KEGG enrichment analysis (Figure 24-26; Appendix 11-15). The differences in gene expression of *H. macrophylla* accessions and *H. paniculata* was clearly observable through hierarchical clustering (Figure 21A). The enrichment of GO terms specifically to the metabolic process indicate the transcripts related to these biological processes are expressed among accessions (21B). Furthermore, the genes of enzymes associated with these pathways exhibited correlations with the concentrations of the investigated metabolites, as determined through Weighted Gene Co-expression Network Analysis (WGCNA) (Figure 28). Notably, in accessions with high PD and/or HD levels, there was an observed elevation in phenylalanine concentrations (Figure 16A). Additionally, a positive correlation was evident between the concentrations of PD, HD, and phenylalanine, confirming the essential role of phenylalanine in PD biosynthesis, with accessions possessing higher phenylalanine are producing more PD (Figure 19). Accessions with high PD and/or HD concentrations also displayed increased levels of p-coumaric acid (Figure 16C) when quantified using LC-MS (Figure 7B), and these concentrations positively correlated with PD and HD levels (Figure 19). The higher expression levels of *4CL* in high PD and/or HD accessions, compared to low PD/HD accessions, can be attributed to the activation of p-coumaric acid to p-coumaroyl CoA, which is a crucial molecule in the pathway (Figure 29; 31-33). These findings underscore the significant influence of p-coumaroyl CoA in PD and HD biosynthesis. Conversely, a negative correlation was observed between PD and HD concentrations and metabolites such as caffeic acid, ferulic acid, scopolin, scopoletin, and esculetin, while no correlation was found in the case of fraxetin (Figure 19). This suggests that these metabolites may have limited to no impact on PD and HD biosynthesis. It is also noteworthy that the concentrations of these biomolecules (except for fraxetin) were generally low in accessions characterized by high PD and/or HD levels during quantification (Figure 8; 16E, F; 17B-F).

At the transcriptome level, the expression levels of *HCT* (p-coumaroyl CoA → p-coumaroyl shikimate, caffeoyl shikimate → caffeoyl CoA), *C3H* (p-coumaroyl shikimate → caffeoyl shikimate), *CCoAOMT* (caffeoyl CoA → feruloyl CoA), *CSE* (caffeoyl shikimate → caffeate), *COMT* (caffeate → ferulate) and *SGT* (scopoletin → scopolin) were found to be downregulated in accessions with high PD and/or HD levels compared to those with low PD/HD levels (Figure 29). This suggests that in low PD/HD

accessions, there is a higher abundance of metabolites associated with caffeic and ferulic acid, which are part of a pathway biochemically distant from PD and HD biosynthesis (Yagi *et al.*, 1977).

The metabolites umbelliferone, naringenin, and resveratrol displayed a positive correlation with PD and HD concentrations (Figure 19). This suggests that these metabolites might indeed be associated with PD and HD biosynthesis. Moreover, accessions characterized by high PD and/or HD levels exhibited elevated concentrations of these aforementioned metabolites, along with thunberginol C (Figure 17A; 16D, G, H). At the transcriptome level, genes of the enzymes CHS (p-coumaroyl CoA → naringenin chalcone), CHI (naringenin chalcone → naringenin), F3'5'H (dihydrokaempferol → dihydromyricetin), DFR (dihydromyricetin → leucodelphinidin), ROMT (resveratrol → pinostilbene → pterostilbene) and FOMT showed upregulation in high PD and/or HD accessions and downregulation in low PD/HD accessions (Figure 29). By integrating the metabolite and transcriptome data, it can be inferred that accessions with high PD and/or HD levels exhibit enhanced flavonoid biosynthesis (involving metabolites derived from naringenin chalcone) and stilbene biosynthesis (involving metabolites derived from resveratrol) compared to low PD/HD accessions. Notably, previous studies have reported a diverse range of metabolites in *Hydrangeas* (Brown *et al.*, 1964; Wellmann *et al.*, 2022; Yoon *et al.*, 2023; Yano *et al.*, 2023). However, the present research successfully incorporates the underlying genetic changes, specifically in terms of enzymatic regulation, that underlie these metabolic diversities.

p-Coumaroyltriacyclic acid synthase (CTAS) is an enzyme that plays a pivotal role in the conversion of p-coumaroyl CoA into p-coumaroyltriacyclic acid lactone (CTAL). Prior studies have hypothesized that CTAS, in conjunction with a cyclase and a ketoreductase, can facilitate the synthesis of hydrangeic acid. Subsequently, hydrangeic acid may undergo further modifications within the plant, ultimately leading to the formation of hydrangenol (Akiyama *et al.*, 1999; Austin and Noel, 2003; Eckermann *et al.*, 2003). In the current research, notably higher transcript levels of CTAS were observed in accessions characterized by high PD and/or HD concentration, with the highest expression detected in accessions containing both PD and HD (Figure 29; 31-33). With the help of transcriptome analysis and RT-qPCR, the present study revealed upregulation of type III-polyketide synthases (PKS),

ketoreductase (*KR*), polyketide cyclase (*PKC*), and double-bond reductase (*DBR*) in high PD and/or HD accessions (Figure 29; 31-33). Intriguingly, it was noted that *CTAS* was absent in *H. paniculata* and *PKC* along with *KR* exhibited elevated expression levels when comparing all *H. macrophylla* accessions with *H. paniculata*, where PD and HD are not detected (Figure 30). This observation suggests that these enzymes likely play a central role in the biosynthesis of PD and HD. The abundance of these enzymes, particularly *KR* and *PKC*, may potentially form a multi-enzyme complex responsible for the synthesis of stilbene carboxylic acid (hydrangeic acid), in line with a hypothesis raised in previous research (Akiyama *et al.*, 1999; Austin and Noel, 2003). A similar enzyme series involving type-III PKS, *KR*, and tetraketide cyclase was proposed to be responsible for the production of lunularic acid, another stilbene carboxylic acid, in *Cannabis sativa* L (Gülck and Møller, 2020).

The literature offers several alternative pathways for the biosynthesis of PD and HD, and one intriguing hypothesis revolves around the role of thunberginols in this biosynthetic pathway. Thunberginols and hydrangenol have been identified as catabolic products in the feces of rats fed with PD (as reported by Yasuda *et al.*, 2004 and Preusche *et al.*, 2022). Moreover, a proposed biosynthetic pathway starting from resveratrol → dihydro resveratrol → 5-hydroxy-lunularic acid → thunberginol C has been suggested (as described by Çiçek *et al.*, 2018). A type-III polyketide synthase (*PKS*) responsible for conversion of dihydro-paracoumaroyl-CoA to dihydroresveratrol was reported in *Cannabis sativa* L. (Boddington *et al.*, 2022). In the current study, higher concentrations of resveratrol were observed in accessions with high PD and/or HD levels when compared to those with low PD/HD levels (Figure 16G). The enzyme responsible for downstream processing of resveratrol, *ROMT*, also displayed increased expression levels in accessions with high PD and/or HD compared to low PD/HD accessions (Figure 29). Simultaneously, a greater relative abundance of thunberginol C was found in accessions with high PD and/or HD levels compared to those with low PD/HD levels (Figure 16H). It's noteworthy, however, that resveratrol and thunberginol C were not detected in the *H. paniculata* accession. It is essential to mention that 5-hydroxy-lunularic acid, a metabolite involved in the same pathway, could not be evaluated due to the unavailability of a reference standard at the time of the study and the challenges associated with proper chromatographic separation. Nevertheless, previous reports have indeed mentioned the presence of 5-hydroxy-lunularic acid and its closely associated metabolites in *Hydrangeas* (Gorham, 1977

and Bojack *et al.*, 2022). By incorporating the findings from metabolomic and transcriptomic data in the present research, coupled with an extensive review of relevant literature pertaining to the subject, a speculative pathway outlining the biosynthesis of PD was devised and is represented in figure 40.

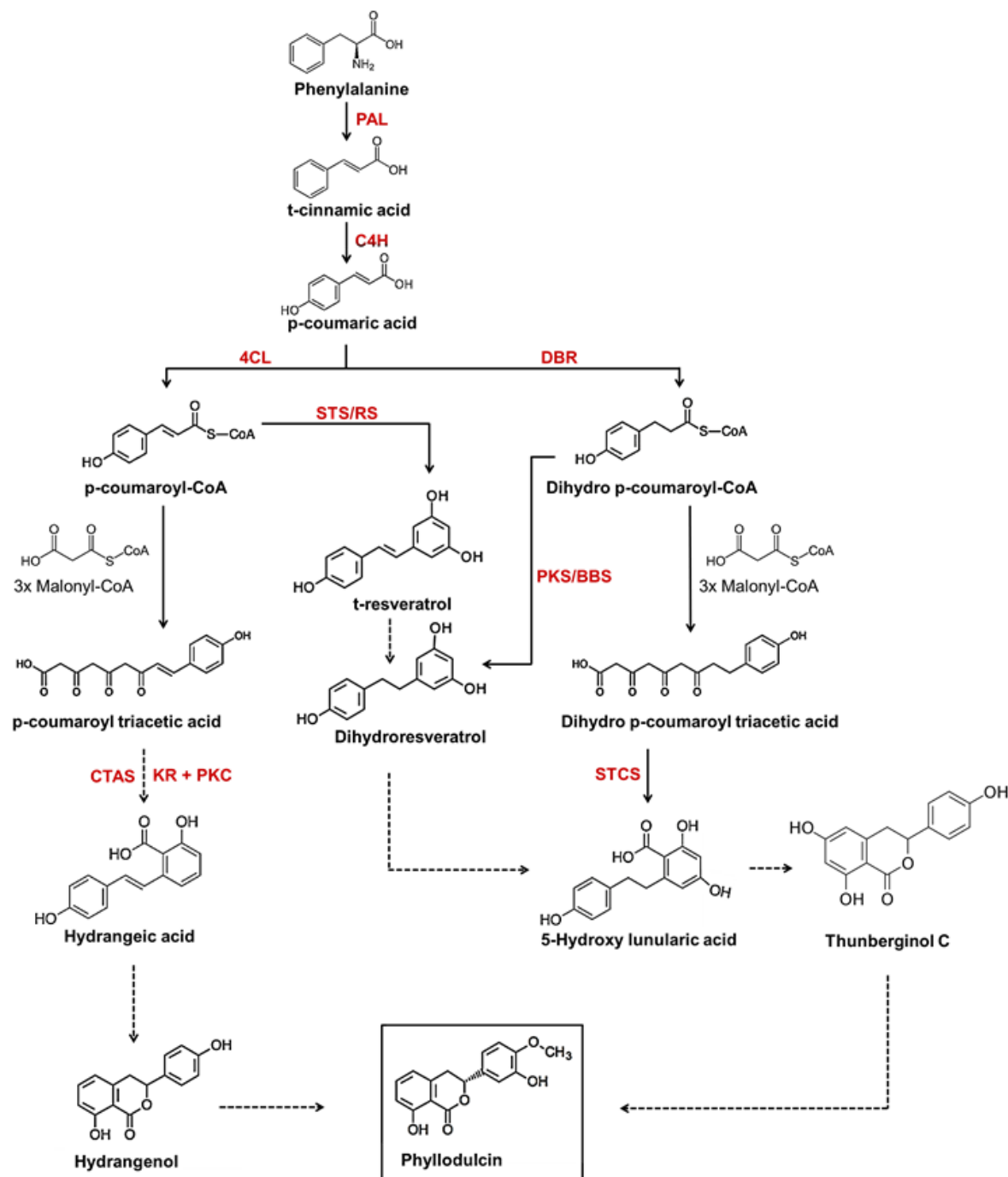


Figure 40. A proposed biosynthesis pathway of phyllodulcin. Enzymes in each step are represented in red fonts and metabolites are represented in black fonts. The solid lines or dashed lines represent known/reported or proposed steps in the pathway respectively. The enzymes are abbreviated as follows, PAL, phenylalanine ammonia-lyase; C4H, cinnamate-4-hydroxylase; 4CL, 4-coumarate-CoA ligase; DBR, double-bond reductase; STS, stilbene synthases; RS, resveratrol synthase; PKS, type-III polyketide synthase; BBS, bibenzyl synthase; KR, ketoreductase; PKC, polyketide cyclase; CTAS, p-coumaroyltriacetic acid synthase; STCS, stilbenecarboxylate synthase.

These findings collectively indicate that in low PD/HD *H. macrophylla* accessions, there is a substantial diversion of metabolic flux away from dihydroisocoumarin biosynthesis. Conversely, in accessions containing PD, HD, or both PD and HD, the metabolic flux is directed towards dihydroisocoumarin biosynthesis. This clear differentiation among accessions based on their biochemical concentrations is evident in the PCA biplot (Figure 20) and metabolite heatmap (Figure 18). Specifically, naringenin, phenylalanine, resveratrol, umbelliferone, and, to some extent, esculin are responsible for the distinctions observed in high PD accessions. Similarly, esculetin, scopolin, trans-cinnamic acid, scopoletin, caffeic acid, and ferulic acid contribute to the characteristics of accessions with low PD/HD (Figure 20). These shifts in metabolic pathways, coupled with variations in the expression of key genes within the pathway, culminate in the accumulation of PD and HD in different *H. macrophylla* accessions. To further validate and gain a real-time understanding of these findings, a transgenic approach involving the overexpression of these key genes in low PD/HD accessions could be employed, allowing for an in-depth exploration of the metabolite profile changes, which can additionally be exploited for the industrial scale production of PD.

5.4 *Hydrangeas* affected by drought stress produce more PD, HD and coumarins

Plants constantly face changing environmental conditions and frequent exposure to various stresses and stimuli. These factors necessitate plants to allocate their energy and carbon resources to adapt to these challenging conditions and trigger specific signaling pathways to mitigate the resulting damage (Dixon and Paiva, 1995; Verma and Shukla, 2015; Zhu, 2016). Under drought stress, when roots are impaired in water uptake, plants tend to accumulate certain amino acids to interact with enzymes to preserve protein structure and enzyme activities, ion transport, and serve as an energy source (Rai and Sharma, 1991; Yoshida et al., 1997; Kavi Kishor et al., 2005; Hildebrandt et al., 2015). In the case of *Hydrangea* accessions grown at 5% soil moisture, a higher accumulation of the amino acids phenylalanine and proline were observed in drought-affected plants compared to those receiving regular watering (Figure 36A, B). A similar trend with phenylalanine has been reported in citrus, poplar, melon, and artichoke (Zandalinas et al., 2017; Jia et al., 2020; Zhao et al., 2021; Chevilly et al., 2021). Furthermore, proline tends to accumulate in plants under stress conditions and functions as an osmoprotectant (Figure 36B) (Sánchez et al., 1998; Alexieva et al., 2001; Zulfiqar et al., 2020). Amino acids are a vital nitrogen source for

plants, and specific amino acids may help delay protein degradation under drought conditions (Bowne *et al.*, 2012; Rabara *et al.*, 2017). Phenylalanine, for instance, influences osmotic adjustment and serves as a precursor for numerous essential secondary metabolites (e.g., phenylpropanoids, flavonoids, catechin, and kaempferol), contributing to enhanced plant drought tolerance (Yamada *et al.*, 2008, Barchet *et al.* 2013; Frelin *et al.*, 2017). This phenomenon could also elucidate the presence of elevated concentrations of naringenin and resveratrol in drought-affected plants, both of which are phenylpropanoid derivatives originating from phenylalanine (Figure 37C, D). An increase in resveratrol and its glycosides has been independently reported in grapes under drought stress (Griesser *et al.*, 2015). Additionally, genes encoding enzymes such as PAL, C4H, 4CL, and CHS, involved in the biosynthesis of these metabolites, were also observed to be upregulated under drought stress (Baldassarini *et al.*, 2018; Cheng *et al.*, 2018). Similar to these observations, an increase in scopolin and scopoletin was noted in citrus plants exposed to drought, contributing to the plant's ability to overcome drought stress (Zandalinas *et al.*, 2017). Scopoletin and scopolin are derived from ferulic acid, and reports suggest that enzymes like HCT, COMT, and CCoAOMT are upregulated under drought stress (Chen *et al.*, 2019b; Hu *et al.*, 2019c). Drought stress has also been known to elevate esculetin content in plants, such as *Fraxinus ornus*. It was observed that esculetin concentrations in leaves correlate with its capacity to scavenge H₂O₂ (Lee *et al.*, 2007; Fini *et al.*, 2012). Interestingly, in our study, the concentrations of esculin and esculetin were higher in well-watered plants compared to those exposed to drought. This observation aligns with existing literature, as esculin does not possess significant ROS scavenging activity, and during drought, the plant may redirect energy towards other pathways. However, the high concentration of esculetin in normally watered plants could be attributed to the plant's regular phenylpropanoid metabolism. Changes in fraxetin content may also be due to its reducing potential (Döll *et al.*, 2018; Tsai *et al.*, 2018).

This study revealed a strong positive correlation between PD and HD concentrations and phenylalanine levels (Figure 19). Interestingly, in this experiment, phenylalanine, PD and HD exhibited significant increases under drought stress conditions (Figure 36A; 37A, B). Furthermore, existing reports indicate that drought stress leads to the upregulation of phenylpropanoid metabolism, flavonoid metabolism, and stilbene metabolism (Yamada *et al.* 2008; Barchet *et al.* 2013; Griesser *et al.*, 2015; Frelin *et*

al. 2017), all of which are pathways linked to PD and HD biosynthesis (Figure 24-26; Appendix 11-15). Consequently, it can be inferred that the increase in PD and HD levels under drought stress may be attributed to the heightened concentration of phenylalanine and the upregulation of genes associated with the phenylpropanoid, flavonoid biosynthetic, and stilbene biosynthetic pathways observed indirectly by enhanced biosynthesis of naringenin and resveratrol (Figure 36A; 37C, D). With this outcome, the present study contributes to a better understanding of the impact of abiotic stress factor drought on the accumulation of so far little studied in *Hydrangea* species.

5.5 PD and HD concentrations are enhanced in *Hydrangeas* in plants grown in at high light intensities.

Light availability, encompassing various wavelengths and intensities, is a fundamental abiotic factor profoundly influencing plant life. It not only sustains photosynthesis but also regulates the synthesis of secondary metabolites, collectively shaping plant growth, health, and adaptability within their ecosystems (Zhang *et al.*, 2015; Li *et al.*, 2018). Previous studies on plants like *Ocimum basilicum*, *Valerianella locusta*, and *Lactuca sativa* have reported that higher light intensities lead to increased accumulation of flavanols (Rodriguez *et al.*, 2014; Vaštakaitė *et al.*, 2015; Brazaitytė *et al.*, 2015; Długosz-Grochowska *et al.*, 2017). Similarly, lettuce exposed to high light intensities displayed maximum anthocyanin levels (Nicole *et al.*, 2016).

In this study, *H. macrophylla* plants cultivated under high light intensity ($600\mu\text{E m}^{-2} \text{s}^{-1}$) displayed a significant increase in naringenin accumulation (Figure 39D). Naringenin, a major intermediate compound, undergoes various hydroxylation reactions to produce diverse anthocyanidins. Subsequent glycosylation and other modifications result in the formation of anthocyanins (Li *et al.*, 2016; Zha and Koffas, 2017). Downstream products of naringenin, including kaempferol, naringenin, and myricetin, were also detected in the leaves of *Labisia pumila* grown under high light intensity (Karimi *et al.*, 2013). The increase in naringenin is often attributed to its antioxidant properties, as it helps counteracting harmful reactive oxygen species (ROS) generated during high light conditions. Moreover, naringenin aids in preventing DNA damage by inhibiting thymine dimerization and protects essential enzymes such as NAD/NADP from photodamage. It also forms a protective shield beneath the epidermal layer, safeguarding cellular components (Daayf and Lattanzio, 2009;

Naikoo *et al.*, 2019). This may explain the development of yellow/purple pigmentation observed on the leaves of treated plants, which could result from anthocyanin and other flavonoid derivatives, which protect the tissue against UV (Figure 38).

Recent studies on peanut sprouts have demonstrated that high light intensities lead to increased production of phenolic compounds and resveratrol (Chung *et al.*, 2021). The current study yielded a similar observation regarding the concentration of resveratrol, with plants exposed to high-light stress showing a higher accumulation of resveratrol (Figure 39C). This rise in resveratrol levels can be attributed to its effectiveness as a scavenger of ROS and reactive nitrogen species (RNS) generated during metabolic processes. Resveratrol plays a crucial role in maintaining the oxidation-reduction balance in cells by supporting antioxidant enzymes such as catalase, superoxide dismutase, and glutathione peroxidase (Robb *et al.*, 2008; Kavas *et al.*, 2013; Cordova-Gomez *et al.*, 2013). While the concentrations of esculetin, scopoletin, and scopolin did not exhibit consistent changes under high light intensity across all accessions, low PD/HD accessions tended to accumulate less of these biomolecules under high light intensities (Figure 39E, F, H). This could be attributed to the increased demand for flavonoids to scavenge the elevated ROS production. Consequently, the metabolic flux may have shifted away from the biosynthesis of methoxy coumarins and toward the production of flavonoids and stilbenes. This redirection of metabolic pathways may also explain why esculin and fraxetin did not display significant differences between control and treatment groups (Figure 39G, I).

Recent genetic and biochemical studies have shed light on the intricate interplay between the jasmonic acid (JA) pathway and light responses in plants. Components of the JA pathway, such as the JA co-receptors COI1 and JAZ proteins, along with MYC2 and JAR1, have been found to influence various aspects of light responses. Conversely, elements of light signaling, including photoreceptor phytochromes, have been shown to impact JA-regulated gene expression and responses. This reciprocal interaction between the two signaling pathways has been extensively documented (Hsieh *et al.*, 2000; Robson *et al.*, 2010; Cheng *et al.*, 2011; Kazan and Manners, 2011). Moreover, it has been reported that anthocyanin biosynthesis is often controlled synergistically by both light and JA under light stress conditions (Vázquez-Flota and De Luca, 1998; Curtin *et al.*, 2003; Devoto *et al.*, 2005). A recent study on *Hydrangeas* demonstrated that the biosynthesis of PD and HD increased when plants were

externally supplied with methyl jasmonates (MeJA). The researchers observed that HD levels doubled after three applications of MeJA, with an immediate increase after just one application (Preusche *et al.*, 2022). Considering this information, it can be inferred that JA biosynthesis is influenced by incident light levels, and in turn, JA enhances PD and HD biosynthesis. The present study revealed a significant increase in PD and HD concentrations when plants were grown under high light intensity compared to normal light intensity (Figure 39A, B). This phenomenon may be attributed to two key factors. First, the upregulation of phenylpropanoid biosynthesis, flavonoid biosynthesis, and stilbene biosynthesis, especially under high light intensity, could contribute to increased PD and HD production (Długosz-Grochowska *et al.*, 2017; Chung *et al.*, 2021). Enzymes involved in these three pathways were found to be relevant to PD and HD biosynthesis (Figure 24-26; Appendix 11-15). Second, the biosynthesis of jasmonates in plants under high light intensity may also play a role in enhancing PD and HD biosynthesis (Preusche *et al.*, 2022). It's plausible that these two processes occur simultaneously and jointly contribute to the observed increase in PD and HD levels. A deeper understanding of the concentrations of JA or MeJA within the plant would help elucidate the crosstalk between dihydroisocoumarin biosynthesis, JA signaling, and high light intensities, further advancing research in this area. This study also provides valuable insights into the optimal light intensity for cultivating large batches of *Hydrangeas* to achieve elevated concentrations of PD, suitable for industrial-scale extraction.

6 Conclusion

While previous research has laid a solid foundation, this thesis recognized the need for a more comprehensive understanding of dihydroisocoumarin biosynthesis at the genetic level and a detailed exploration of metabolite dynamics in *Hydrangea* under abiotic stress conditions. Within the scope of this study, it became evident that *H. macrophylla* accessions with elevated levels of PD, HD, or both exhibited distinct metabolite profiles compared to accessions with low PD and HD concentration. Metabolic pathways involving caffeic acid, ferulic acid, and their derivatives, including scopolin, scopoletin, esculetin, and fraxetin, appeared to be predominant in accessions with low PD and HD concentrations. Conversely, the metabolism of phenylalanine, umbelliferone, p-coumaric acid, naringenin, resveratrol, and thunberginol C appeared to be particularly active in accessions containing PD, HD, or both. A correlation analysis between PD, HD, and these metabolites provided valuable insights into their interrelationships. Transcriptome analysis identified specific genes involved in the phenylpropanoid biosynthesis, flavonoid biosynthesis, and stilbene biosynthesis pathways that play a pivotal role in PD and HD biosynthesis. Furthermore, the discovery of cyclase and ketoreductase genes that were upregulated in accessions with high PD, HD, or both could potentially help unravel the biosynthetic pathway leading to PD and HD production. Additionally, based on metabolite levels and gene expressions, a hypothetical pathway from resveratrol to thunberginol was proposed, suggesting its potential association with PD and HD biosynthesis. The study also highlighted the significance of processing freshly harvested *Hydrangea* leaves, either through drying or with the use of β -glucosidase enzymes, to remove the glucoside moiety and liberate bioactive PD and HD. This knowledge could facilitate the scaling up of PD and HD production. Finally, the understanding of how PD and HD biosynthesis is enhanced under drought stress and high light intensities holds promise for cultivating *Hydrangeas* under these conditions to extract these valuable biomolecules on a larger scale.

7 References

- Aboshi, T., Ittou, K., Galis, I., Shinya, T., & Murayama, T. (2023). Glucosylation prevents autotoxicity of stress inducible DOPA in maize seedlings. *Plant Growth Regulation*, 101(1), 159–167. <https://doi.org/10.1007/s10725-023-01009-w>
- Agustini, D. M., Hermawati, E., Mujahidah, N. N., & Riga, R. (2023). Coumarin Derivatives from *Hydrangea macrophylla* and Evaluation of Their Cytotoxic Activity. *Chemistry Africa*, 6(4), 1747–1751. <https://doi.org/10.1007/s42250-023-00619-1>
- Ahkami, A. H., Melzer, M., Ghaffari, M. R., Pollmann, S., Ghorbani Javid, M., Shahinnia, F., Hajirezaei, M. R., & Druerge, U. (2013). Distribution of indole-3-acetic acid in *Petunia hybrida* shoot tip cuttings and relationship between auxin transport, carbohydrate metabolism and adventitious root formation. *Planta*, 238(3), 499–517. <https://doi.org/10.1007/s00425-013-1907-z>
- Ajikumar, P. K., Xiao, W.-H., Tyo, K. E. J., Wang, Y., Simeon, F., Leonard, E., Mucha, O., Phon, T. H., Pfeifer, B., & Stephanopoulos, G. (2010). Isoprenoid Pathway Optimization for Taxol Precursor Overproduction in *Escherichia coli*. *Science (New York, N.Y.)*, 330(6000), 70–74. <https://doi.org/10.1126/science.1191652>
- Akiyama, T., Shibuya, M., Liu, H. M., & Ebizuka, Y. (1999). p-Coumaroyltriacytic acid synthase, a new homologue of chalcone synthase, from *Hydrangea macrophylla* var. *Thunbergii*. *European Journal of Biochemistry*, 263(3), 834–839. <https://doi.org/10.1046/j.1432-1327.1999.00562.x>
- Alexieva, V., Sergiev, I., Mapelli, S., & Karanov, E. (2001). The effect of drought and ultraviolet radiation on growth and stress markers in pea and wheat. *Plant, Cell & Environment*, 24(12), 1337–1344. <https://doi.org/10.1046/j.1365-3040.2001.00778.x>
- Alonso-Salces, R. M., Guillou, C., & Berrueta, L. A. (2009). Liquid chromatography coupled with ultraviolet absorbance detection, electrospray ionization, collision-induced dissociation and tandem mass spectrometry on a triple quadrupole for the on-line characterization of polyphenols and methylxanthines in green coffee beans. *Rapid Communications in Mass Spectrometry*, 23(3), 363–383. <https://doi.org/10.1002/rcm.3884>

- Asahina, Y., & Ueno, S. (1916). Phyllodulcin, a chemical constituent of Amacha (*Hydrangea thunbergii* Sieb). *J. Pharm. Soc. Jpn*, 36, 146.
- Austin, M. B., & Noel, J. P. (2003). The chalcone synthase superfamily of type III polyketide synthases. *Natural Product Reports*, 20(1), 79–110. <https://doi.org/10.1039/B100917F>
- Baraldi, R., Isacchi, B., Predieri, S., Marconi, G., Vincieri, F., & Bilia, A. (2008). Distribution of artemisinin and bioactive flavonoids from *Artemisia annua* L. during plant growth. *Biochemical Systematics and Ecology*, 36, 340–348. <https://doi.org/10.1016/j.bse.2007.11.002>
- Barchet, G. L. H., Dauwe, R., Guy, R. D., Schroeder, W. R., Soolanayakanahally, R. Y., Campbell, M. M., & Mansfield, S. D. (2014). Investigating the drought-stress response of hybrid poplar genotypes by metabolite profiling. *Tree Physiology*, 34(11), 1203–1219. <https://doi.org/10.1093/treephys/tpt080>
- Barton, K., & Boege, K. (2017). Future directions in the ontogeny of plant defence: Understanding the evolutionary causes and consequences. *Ecology Letters*, 20. <https://doi.org/10.1111/ele.12744>
- Bassoli, A., Laureati, M., Borgonovo, G., Morini, G., Servant, G., & Pagliarini, E. (2008). Iovanillic Sweeteners: Sensory Evaluation and In Vitro Assays with Human Sweet Taste Receptor. *Chemosensory Perception*, 1(3), 174.
- Bassoli, A., Merlini, L., & Morini, G. (2002). Iovanillyl sweeteners. From molecules to receptors. *Pure and Applied Chemistry*, 74(7), 1181–1187. <https://doi.org/10.1351/pac200274071181>
- Bian, Z. H., Yang, Q. C., & Liu, W. K. (2015). Effects of light quality on the accumulation of phytochemicals in vegetables produced in controlled environments: A review. *Journal of the Science of Food and Agriculture*, 95(5), 869–877. <https://doi.org/10.1002/jsfa.6789>
- Billek, G., & Kindl, H. (1961). Zur Biosynthese pflanzlicher Stilbene, 1. Mitt.: Zur Biosynthese des Hydrangenols (Vorläufige Mitteilung). *Monatshefte für Chemie und*

verwandte Teile anderer Wissenschaften, 92(2), 493–497.
<https://doi.org/10.1007/BF01153905>

Birch, G. G. (1987). Sweetness and sweeteners. *Endeavour*, 11(1), 21–24.
[https://doi.org/10.1016/0160-9327\(87\)90165-7](https://doi.org/10.1016/0160-9327(87)90165-7)

Boddington, K. F., Soubeyrand, E., Van Gelder, K., Casaretto, J. A., Perrin, C., Forrester, T. J. B., Parry, C., Al-Abdul-Wahid, M. S., Jentsch, N. G., Magolan, J., Bozzo, G. G., Kimber, M. S., Rothstein, S. J., & Akhtar, T. A. (2022). Bibenzyl synthesis in *Cannabis sativa* L. *The Plant Journal*, 109(3), 693–707.
<https://doi.org/10.1111/tpj.15588>

Boerjan, W., Ralph, J., & Baucher, M. (2003). Lignin Biosynthesis. *Annual Review of Plant Biology*, 54(1), 519–546.
<https://doi.org/10.1146/annurev.arplant.54.031902.134938>

Bojack, G., Brown, R. W., Dittgen, J., Heinemann, I., Helmke, H., Hills, M. J., Hohmann, S., Holstein, P. M., Schmutzler, D., & Frackenhohl, J. (2022). Synthesis and SAR of 2,3-Dihydro-1-benzofuran-4-carboxylates: Potent Salicylic Acid-Based Lead Structures against Plant Stress. *European Journal of Organic Chemistry*, 2022(14), e202200087. <https://doi.org/10.1002/ejoc.202200087>

Bourgaud, F., Hehn, A., Labat, R., Doerper, S., Gontier, E., Kellner, S., & Matern, U. (2006). Biosynthesis of coumarins in plants: A major pathway still to be unravelled for cytochrome P450 enzymes. *Phytochemistry Reviews*, 5(2), 293–308.
<https://doi.org/10.1007/s11101-006-9040-2>

Bowne, J. B., Erwin, T. A., Juttner, J., Schnurbusch, T., Langridge, P., Bacic, A., & Roessner, U. (2012). Drought responses of leaf tissues from wheat cultivars of differing drought tolerance at the metabolite level. *Molecular Plant*, 5(2), 418–429.
<https://doi.org/10.1093/mp/ssr114>

Brazaitytė, A., Viršilė, A., Jankauskienė, J., Sakalauskienė, S., Samuolienė, G., Sirtautas, R., Novičkovas, A., Dabašinskas, L., Miliauskienė, J., Vaštakaitė, V., Bagdonavičienė, A., & Duchovskis, P. (2015). Effect of supplemental UV-A irradiation

- in solid-state lighting on the growth and phytochemical content of microgreens. *International Agrophysics*, 29(1), 13–22. <https://doi.org/10.1515/intag-2015-0004>
- Breschi, A., Djebali, S., Gillis, J., Pervouchine, D. D., Dobin, A., Davis, C. A., Gingeras, T. R., & Guigó, R. (2016). Gene-specific patterns of expression variation across organs and species. *Genome Biology*, 17(1), 151. <https://doi.org/10.1186/s13059-016-1008-y>
- Brown, S. A., Towers, G. H. N., & Chen, D. (1964). Biosynthesis of the coumarins—V.: Pathways of umbelliferone formation in *Hydrangea macrophylla*. *Phytochemistry*, 3(4), 469–476. [https://doi.org/10.1016/S0031-9422\(00\)88023-1](https://doi.org/10.1016/S0031-9422(00)88023-1)
- Bustin, S. A., Benes, V., Garson, J. A., Hellemans, J., Huggett, J., Kubista, M., Mueller, R., Nolan, T., Pfaffl, M. W., Shipley, G. L., Vandesompele, J., & Wittwer, C. T. (2009). The MIQE guidelines: Minimum information for publication of quantitative real-time PCR experiments. *Clinical Chemistry*, 55(4), 611–622. <https://doi.org/10.1373/clinchem.2008.112797>
- Carvalho, I., Cavaco, T., Carvalho, L., & Duque, P. (2010). Effect of photoperiod on flavonoid pathway activity in sweet potato (*Ipomoea batatas* (L.) Lam.) leaves. *Food Chemistry*, 118, 384–390. <https://doi.org/10.1016/j.foodchem.2009.05.005>
- Castro-Muñoz, R., Correa-Delgado, M., Córdova-Almeida, R., Lara-Nava, D., Chávez-Muñoz, M., Velásquez-Chávez, V. F., Hernández-Torres, C. E., Gontarek-Castro, E., & Ahmad, M. Z. (2022). Natural sweeteners: Sources, extraction and current uses in foods and food industries. *Food Chemistry*, 370, 130991. <https://doi.org/10.1016/j.foodchem.2021.130991>
- Chen, K., Song, M., Guo, Y., Liu, L., Xue, H., Dai, H., & Zhang, Z. (2019). MdMYB46 could enhance salt and osmotic stress tolerance in apple by directly activating stress-responsive signals. *Plant Biotechnology Journal*, 17(12), 2341–2355. <https://doi.org/10.1111/pbi.13151>
- Cheng, L., Han, M., Yang, L., Li, Y., Sun, Z., & Zhang, T. (2018). Changes in the physiological characteristics and baicalin biosynthesis metabolism of *Scutellaria*

baicalensis Georgi under drought stress. *Industrial Crops and Products*, 122, 473–482. <https://doi.org/10.1016/j.indcrop.2018.06.030>

Cheng, Z., Sun, L., Qi, T., Zhang, B., Peng, W., Liu, Y., & Xie, D. (2011). The bHLH transcription factor MYC3 interacts with the Jasmonate ZIM-domain proteins to mediate jasmonate response in *Arabidopsis*. *Molecular Plant*, 4(2), 279–288. <https://doi.org/10.1093/mp/ssq073>

Cho, E., Jeon, S. J., Jeon, J., Yi, J. H., Kwon, H., Kwon, H.-J., Kwon, K. J., Moon, M., Shin, C. Y., & Kim, D. H. (2023). Phyllodulcin improves hippocampal long-term potentiation in 5XFAD mice. *Biomedicine & Pharmacotherapy = Biomedecine & Pharmacotherapie*, 161, 114511. <https://doi.org/10.1016/j.biopha.2023.114511>

Chranioti, C., Chanioti, S., & Tzia, C. (2016). Comparison of spray, freeze and oven drying as a means of reducing bitter aftertaste of steviol glycosides (derived from *Stevia rebaudiana* Bertoni plant) – Evaluation of the final products. *Food Chemistry*, 190, 1151–1158. <https://doi.org/10.1016/j.foodchem.2015.06.083>

Chung, I.-M., Lee, C., Hwang, M. H., Kim, S.-H., Chi, H.-Y., Yu, C. Y., Chelliah, R., Oh, D.-H., & Ghimire, B. K. (2021). The Influence of Light Wavelength on Resveratrol Content and Antioxidant Capacity in *Arachis hypogaeas* L. *Agronomy*, 11(2), Article 2. <https://doi.org/10.3390/agronomy11020305>

Çiçek, S. S., Vitalini, S., & Zidorn, C. (2018). Natural Phenylidihydroisocoumarins: Sources, Chemistry and Bioactivity. *Natural Product Communications*, 13, 279–288. <https://doi.org/10.1177/1934578X1801300306>

Çirak, C., Radusiene, J., Ivanauskas, L., & Janulis, V. (2007). Variation of bioactive secondary metabolites in *Hypericum organifolium* during its phenological cycle. *Acta Physiologiae Plantarum*, 29, 197–203. <https://doi.org/10.1007/s11738-007-0024-7>

Claeys, M., Li, Q., van den Heuvel, H. and Dillen, L., 1996, Mass spectrometric studies on flavonoidglucosides. In: *Applications of Modern Mass Spectrometry in Plant Sciences*. R.P Newton and T.J. Walton (Eds.), Clarendon Press, Oxford, 182-194.

- Cordova-Gomez, M., Galano, A., & Alvarez-Idaboy, J. (2013). Piceatannol, a better peroxy radical scavenger than resveratrol. *RSC Advances*, 3, 20209. <https://doi.org/10.1039/c3ra42923g>
- Cowan, M. F., Blomstedt, C. K., Møller, B. L., Henry, R. J., & Gleadow, R. M. (2021). Variation in production of cyanogenic glucosides during early plant development: A comparison of wild and domesticated sorghum. *Phytochemistry*, 184, 112645. <https://doi.org/10.1016/j.phytochem.2020.112645>
- Curtin, C., Zhang, W., & Franco, C. (2003). Manipulating anthocyanin composition in *Vitis vinifera* suspension cultures by elicitation with jasmonic acid and light irradiation. *Biotechnology Letters*, 25(14), 1131–1135. <https://doi.org/10.1023/a:1024556825544>
- Dawid, C., & Hille, K. (2018). Functional Metabolomics—A Useful Tool to Characterize Stress-Induced Metabolome Alterations Opening New Avenues towards Tailoring Food Crop Quality. *Agronomy*, 8(8), Article 8. <https://doi.org/10.3390/agronomy8080138>
- Debras, C., Chazelas, E., Srour, B., Druesne-Pecollo, N., Esseddik, Y., Edelenyi, F., S. de, Agaësse, C., Sa, A. D., Lutchia, R., Gigandet, S., Huybrechts, I., Julia, C., Kesse-Guyot, E., Allès, B., Andreeva, V. A., Galan, P., Hercberg, S., Deschasaux-Tanguy, M., & Touvier, M. (2022). Artificial sweeteners and cancer risk: Results from the NutriNet-Santé population-based cohort study. *PLOS Medicine*, 19(3), e1003950. <https://doi.org/10.1371/journal.pmed.1003950>
- Devoto, A., Ellis, C., Magusin, A., Chang, H.-S., Chilcott, C., Zhu, T., & Turner, J. G. (2005). Expression profiling reveals COI1 to be a key regulator of genes involved in wound- and methyl jasmonate-induced secondary metabolism, defence, and hormone interactions. *Plant Molecular Biology*, 58(4), 497–513. <https://doi.org/10.1007/s11103-005-7306-5>
- Dewick, P. M. (2009). *Medicinal natural products: A biosynthetic approach* (3rd edition). Wiley, A John Wiley and Sons, Ltd., Publication.
- Dixon, R. A. (2001). Natural products and plant disease resistance. *Nature*, 411(6839), 843–847. <https://doi.org/10.1038/35081178>

- Dixon, R. A., Achnine, L., Kota, P., Liu, C.-J., Reddy, M. S. S., & Wang, L. (2002). The phenylpropanoid pathway and plant defence—a genomics perspective. *Molecular Plant Pathology*, 3(5), 371–390. <https://doi.org/10.1046/j.1364-3703.2002.00131.x>
- Dixon, R. A., Xie, D.-Y., & Sharma, S. B. (2005). Proanthocyanidins – a final frontier in flavonoid research? *New Phytologist*, 165(1), 9–28. <https://doi.org/10.1111/j.1469-8137.2004.01217.x>
- Dixon, R., & Paiva, N. (1995). Stress-Induced Phenylpropanoid Metabolism. *The Plant Cell*, 7(7), 1085–1097.
- Długosz-Grochowska, O., Wojciechowska, R., Kruczek, M., & Habela, A. (2017). Supplemental lighting with LEDs improves the biochemical composition of two *Valerianella locusta* (L.) cultivars. *Horticulture, Environment, and Biotechnology*, 58(5), 441–449. <https://doi.org/10.1007/s13580-017-0300-4>
- Döll, S., Kuhlmann, M., Rutten, T., Mette, M. F., Scharfenberg, S., Petridis, A., Berreth, D.-C., & Mock, H.-P. (2018). Accumulation of the coumarin scopolin under abiotic stress conditions is mediated by the *Arabidopsis thaliana* THO/TREX complex. *The Plant Journal: For Cell and Molecular Biology*, 93(3), 431–444. <https://doi.org/10.1111/tpj.13797>
- Dong, N.-Q., & Lin, H.-X. (2021). Contribution of phenylpropanoid metabolism to plant development and plant–environment interactions. *Journal of Integrative Plant Biology*, 63(1), 180–209. <https://doi.org/10.1111/jipb.13054>
- Dudareva, N., Pichersky, E., & Gershenzon, J. (2004). Biochemistry of Plant Volatiles. *Plant Physiology*, 135(4), 1893–1902. <https://doi.org/10.1104/pp.104.049981>
- Eckermann, C., Schröder, G., Eckermann, S., Strack, D., Schmidt, J., Schneider, B., & Schröder, J. (2003). Stilbenecarboxylate biosynthesis: A new function in the family of chalcone synthase-related proteins. *Phytochemistry*, 62(3), 271–286. [https://doi.org/10.1016/s0031-9422\(02\)00554-x](https://doi.org/10.1016/s0031-9422(02)00554-x)
- Egan, D., O’Kennedy, R., Moran, E., Cox, D., Prosser, E., & Thornes, R. D. (1990). The pharmacology, metabolism, analysis, and applications of coumarin and coumarin-

related compounds. *Drug Metabolism Reviews*, 22(5), 503–529.
<https://doi.org/10.3109/03602539008991449>

El-Basyouni, S. Z., Chen, D., Ibrahim, R. K., Neish, A. C., & Towers, G. H. N. (1964). The biosynthesis of hydroxybenzoic acids in higher plants. *Phytochemistry*, 3(4), 485–492. [https://doi.org/10.1016/S0031-9422\(00\)88025-5](https://doi.org/10.1016/S0031-9422(00)88025-5)

Evans, G. C. (1972). *The Quantitative Analysis of Plant Growth*. University of California Press.

Fineblum, W., & Rausher, M. (1995). Tradeoff between resistance and tolerance to herbivore damage in a morning glory. *Nature*, 377, 517–520.
<https://doi.org/10.1038/377517a0>

Fini, A., Guidi, L., Ferrini, F., Brunetti, C., Ferdinando, M. D., Biricolti, S., Pollastri, S., Calamai, L., & Tattini, M. (2012). Drought stress has contrasting effects on antioxidant enzymes activity and phenylpropanoid biosynthesis in *Fraxinus ornus* leaves: An excess light stress affair? *Journal of Plant Physiology*, 169(10), 929.

Flamini, R., & Vedova, A. D. (2004). Fast determination of the total free resveratrol content in wine by direct-exposure-probe, positive-ion chemical ionization and collision-induced-dissociation mass spectrometry. *Rapid Communications in Mass Spectrometry*, 18(17), 1925–1931. <https://doi.org/10.1002/rcm.1569>

Floc'h, F., Mauger, F., Desmurs, J.-R., Gard, A., Bagneris, F., & Carlton, B. (2002). *Coumarin in Plants and Fruits: Implication in Perfumery*. 27.

Folta, K. M., & Carvalho, S. D. (2015). Photoreceptors and Control of Horticultural Plant Traits. *HortScience*, 50(9), 1274–1280.
<https://doi.org/10.21273/HORTSCI.50.9.1274>

Fourcroy, P., Sisó-Terraza, P., Sudre, D., Savirón, M., Reyt, G., Gaymard, F., Abadía, A., Abadía, J., Álvarez-Fernández, A., & Briat, J.-F. (2014). Involvement of the ABCG37 transporter in secretion of scopoletin and derivatives by *Arabidopsis* roots in response to iron deficiency. *New Phytologist*, 201(1), 155–167.
<https://doi.org/10.1111/nph.12471>

- Francesc, V., & Bastida, J. (2015). General Overview of Plant Secondary Metabolism. In *Plant Biology and Biotechnology: Plant Diversity, Organization, Function and Improvement* (Vol. 1, pp. 539–568). https://doi.org/10.1007/978-81-322-2286-6_21
- Fraser, C. M., & Chapple, C. (2011). The Phenylpropanoid Pathway in Arabidopsis. *The Arabidopsis Book*, 2011(9). <https://doi.org/10.1199/tab.0152>
- Frelin, O., Dervinis, C., Wegrzyn, J., Davis, J. M., & Hanson, A. (2017). Drought stress in *Pinus taeda* L. induces coordinated transcript accumulation of genes involved in the homogentisate pathway. *Tree Genetics & Genomes*, 13, 27. <https://doi.org/10.1007/s11295-017-1115-2>
- Gatto, P., Vrhovsek, U., Muth, J., Segala, C., Romualdi, C., Fontana, P., Pruefer, D., Stefanini, M., Moser, C., Mattivi, F., & Velasco, R. (2008). Ripening and Genotype Control Stilbene Accumulation in Healthy Grapes. *Journal of Agricultural and Food Chemistry*, 56(24), 11773–11785. <https://doi.org/10.1021/jf8017707>
- Gharibi, S., Sayed Tabatabaei, B. E., Saeidi, G., Talebi, M., & Matkowski, A. (2019). The effect of drought stress on polyphenolic compounds and expression of flavonoid biosynthesis related genes in *Achillea pachycephala* Rech.f. *Phytochemistry*, 162, 90–98. <https://doi.org/10.1016/j.phytochem.2019.03.004>
- Ghasemzadeh, A., Jaafar, H. Z. E., & Rahmat, A. (2010). Synthesis of Phenolics and Flavonoids in Ginger (*Zingiber officinale* Roscoe) and Their Effects on Photosynthesis Rate. *International Journal of Molecular Sciences*, 11(11), 4539–4555. <https://doi.org/10.3390/ijms11114539>
- Gomes, A. F., Almeida, M. P., Leite, M. F., Schwaiger, S., Stuppner, H., Halabalaki, M., Amaral, J. G., & David, J. M. (2019). Seasonal variation in the chemical composition of two chemotypes of *Lippia alba*. *Food Chemistry*, 273, 186–193. <https://doi.org/10.1016/j.foodchem.2017.11.089>
- Gorham, J. (1977). Lunularic acid and related compounds in liverworts, algae and *Hydrangea*. *Phytochemistry*, 16(2), 249–253. [https://doi.org/10.1016/S0031-9422\(00\)86795-3](https://doi.org/10.1016/S0031-9422(00)86795-3)

- Griesser, M., Weingart, G., Schoedl-Hummel, K., Neumann, N., Becker, M., Varmuza, K., Liebner, F., Schuhmacher, R., & Forneck, A. (2015). Severe drought stress is affecting selected primary metabolites, polyphenols, and volatile metabolites in grapevine leaves (*Vitis vinifera* cv. Pinot noir). *Plant Physiology and Biochemistry: PPB*, 88, 17–26. <https://doi.org/10.1016/j.plaphy.2015.01.004>
- Griffiths, M. *The New Royal Horticultural Society Dictionary: Index of Garden Plants*; Macmillan Press Ltd.: London, UK, 1994.
- Gülck, T., & Møller, B. L. (2020). Phytocannabinoids: Origins and Biosynthesis. *Trends in Plant Science*, 25(10), 985–1004. <https://doi.org/10.1016/j.tplants.2020.05.005>
- Hartmann, T. (2007). From waste products to ecochemicals: Fifty years research of plant secondary metabolism. *Phytochemistry*, 68(22–24), 2831–2846. <https://doi.org/10.1016/j.phytochem.2007.09.017>
- Hsieh, H. L., Okamoto, H., Wang, M., Ang, L. H., Matsui, M., Goodman, H., & Deng, X. W. (2000). FIN219, an auxin-regulated gene, defines a link between phytochrome A and the downstream regulator COP1 in light control of Arabidopsis development. *Genes & Development*, 14(15), 1958–1970.
- Hu, P., Zhang, K., & Yang, C. (2019). BpNAC012 Positively Regulates Abiotic Stress Responses and Secondary Wall Biosynthesis1[OPEN]. *Plant Physiology*, 179(2), 700–717. <https://doi.org/10.1104/pp.18.01167>
- Ibrahim, R. K., & Towers, G. H. N. (1960). Studies of hydrangenol in *Hydrangea macrophylla* ser.: I. isolation, identification, and biosynthesis from c14-labelled compounds. *Canadian Journal of Biochemistry and Physiology*, 38(1), 627–634. <https://doi.org/10.1139/y60-077>
- Irakli, M., Skendi, A., Bouloumpasi, E., Chatzopoulou, P., & Biliaderis, C. G. (2021). LC-MS Identification and Quantification of Phenolic Compounds in Solid Residues from the Essential Oil Industry. *Antioxidants*, 10(12), Article 12. <https://doi.org/10.3390/antiox10122016>
- Iranshahi, M., Sahebkar, A., Takasaki, M., Konoshima, T., & Tokuda, H. (2009). Cancer chemopreventive activity of the prenylated coumarin, umbelliprenin, in vivo.

European Journal of Cancer Prevention, 18(5), 412.
<https://doi.org/10.1097/CEJ.0b013e32832c389e>

Isah, T. (2019). Stress and defense responses in plant secondary metabolites production. *Biological Research*, 52(1), 39. <https://doi.org/10.1186/s40659-019-0246-3>

Izawa, K., Amino, Y., Kohmura, M., Ueda, Y., & Kuroda, M. (2010). 4.16—Human–Environment Interactions – Taste. In H.-W. (Ben) Liu & L. Mander (Eds.), *Comprehensive Natural Products II* (pp. 631–671). Elsevier. <https://doi.org/10.1016/B978-008045382-8.00108-8>

Jaakola, L., & Hohtola, A. (2010). Effect of latitude on flavonoid biosynthesis in plants. *Plant, Cell & Environment*, 33(8), 1239–1247. <https://doi.org/10.1111/j.1365-3040.2010.02154.x>

Jung, C.-H., Kim, Y., Kim, M.-S., Lee, S., & Yoo, S.-H. (2016). The establishment of efficient bioconversion, extraction, and isolation processes for the production of phyllodulcin, a potential high intensity sweetener, from sweet *Hydrangea* leaves (*Hydrangea macrophylla Thunbergii*). *Phytochemical Analysis*, 27(2), 140–147. <https://doi.org/10.1002/pca.2609>

Junker, L., Genzel, F., Büchenschütz, J., Thiele, B., Wormit, A., & Wiese-Klinkenberg, A. (2018). Targeted induction of plant secondary metabolism in horticultural plants by controlled stress applications. *Plant Biology Europe 2018*.

Kai, K., Shimizu, B., Mizutani, M., Watanabe, K., & Sakata, K. (2006). Accumulation of coumarins in *Arabidopsis thaliana*. *Phytochemistry*, 67(4), 379–386. <https://doi.org/10.1016/j.phytochem.2005.11.006>

Karimi, E., Jaafar, H. Z., Ghasemzadeh, A., & Ibrahim, M. H. (2013). Light intensity effects on production and antioxidant activity of flavonoids and phenolic compounds in leaves, stems and roots of three varieties of *Labisia pumila* Benth. *Australian Journal of Crop Science*, 7, 1016–1023.

- Kavas, G. O., Ayril, P. A., & Elhan, A. H. (2013). The effects of resveratrol on oxidant/antioxidant systems and their cofactors in rats. *Advances in Clinical and Experimental Medicine: Official Organ Wroclaw Medical University*, 22(2), 151–155.
- Kawamura, M., Kagata, M., Masaki, E., & Nishi, H. (2002). Phyllodulcin, a Constituent of “Amacha”, Inhibits Phosphodiesterase in Bovine Adrenocortical Cells. *Pharmacology & Toxicology*, 90(2), 106–106. <https://doi.org/10.1034/j.1600-0773.2002.900209.x>
- Kazan, K., & Manners, J. M. (2011). The interplay between light and jasmonate signalling during defence and development. *Journal of Experimental Botany*, 62(12), 4087–4100. <https://doi.org/10.1093/jxb/err142>
- Kazlauskas, S., & Bagdonaite, E. (2004). Quantitative analysis of active substances in St. John’s wort (*Hypericum perforatum* L.) by the high performance liquid chromatography method. *Medicina (Kaunas, Lithuania)*, 40, 975–981.
- Kim, C. Y., Mitchell, A. J., Kastner, D. W., Albright, C. E., Gutierrez, M. A., Glinkerman, C. M., Kulik, H. J., & Weng, J.-K. (2023). Emergence of a proton exchange-based isomerization and lactonization mechanism in the plant coumarin synthase COSY. *Nature Communications*, 14(1), Article 1. <https://doi.org/10.1038/s41467-023-36299-1>
- Kim, E., Lim, S.-M., Kim, M.-S., Yoo, S.-H., & Kim, Y. (2017). Phyllodulcin, a Natural Sweetener, Regulates Obesity-Related Metabolic Changes and Fat Browning-Related Genes of Subcutaneous White Adipose Tissue in High-Fat Diet-Induced Obese Mice. *Nutrients*, 9(10), 1049. <https://doi.org/10.3390/nu9101049>
- Kishor, P. B. K., Amrutha, R., Laxmi, P. S., Naidu, K. R., Sambasiva Rao, K. R. S., Rao, S., Reddy, K. J., Theriappan, P., & Sreenivasulu, N. (2005). Regulation of proline biosynthesis, degradation, uptake and transport in higher plants: Its implications in plant growth and abiotic stress tolerance. *Curr Sci*, 88, 424–438.
- Langfelder P, Horvath S (2012). “Fast R Functions for Robust Correlations and Hierarchical Clustering.” *Journal of Statistical Software*, 46(11), 1–17

- Lattanzio, V., Cardinali, A., & Linsalata, V. (2012). Recent Advances in Polyphenol Research, Volume 3. In *Recent Advances in Polyphenol Research, Volume 3 (Vol. 3)*. <https://doi.org/10.1002/9781118299753.ch1>
- Lee, B.-C., Lee, S. Y., Lee, H. J., Sim, G.-S., Kim, J.-H., Kim, J.-H., Cho, Y.-H., Lee, D.-H., Pyo, H.-B., Choe, T.-B., Moon, D. C., Yun, Y. P., & Hong, J. T. (2007). Antioxidative and photo-protective effects of coumarins isolated from *Fraxinus chinensis*. *Archives of Pharmacal Research*, 30(10), 1293–1301. <https://doi.org/10.1007/BF02980270>
- Lee, J., Kwon, H., Cho, E., Jeon, J., Lee, I.-K., Cho, W.-S., Park, S. J., Lee, S., Kim, D. H., & Jung, J. W. (2022). *Hydrangea macrophylla* and Thunberginol C Attenuate Stress-Induced Anxiety in Mice. *Antioxidants*, 11(2), Article 2. <https://doi.org/10.3390/antiox11020234>
- Lefèvre, F., Fourmeau, J., Pottier, M., Baijot, A., Cornet, T., Abadía, J., Álvarez-Fernández, A., & Boutry, M. (2018). The *Nicotiana tabacum* ABC transporter NtPDR3 secretes O-methylated coumarins in response to iron deficiency. *Journal of Experimental Botany*, 69(18), 4419–4431. <https://doi.org/10.1093/jxb/ery221>
- Lewis, N. G., & Davin, L. B. (1999). 1.25 - Lignans: Biosynthesis and Function. In S. D. Barton, K. Nakanishi, & O. Meth-Cohn (Eds.), *Comprehensive Natural Products Chemistry* (pp. 639–712). Pergamon. <https://doi.org/10.1016/B978-0-08-091283-7.00027-8>
- Li, P., Dong, Q., Ge, S., He, X., Verdier, J., Li, D., & Zhao, J. (2016). Metabolic engineering of proanthocyanidin production by repressing the isoflavone pathways and redirecting anthocyanidin precursor flux in legume. *Plant Biotechnology Journal*, 14(7), 1604–1618. <https://doi.org/10.1111/pbi.12524>
- Li, Q., Lei, S., Du, K., Li, L., Pang, X., Wang, Z., Wei, M., Fu, S., Hu, L., & Xu, L. (2016). RNA-seq based transcriptomic analysis uncovers α -linolenic acid and jasmonic acid biosynthesis pathways respond to cold acclimation in *Camellia japonica*. *Scientific Reports*, 6(1), Article 1. <https://doi.org/10.1038/srep36463>

- Li, R., Xie, X., Ma, F., Wang, D., Wang, L., Zhang, J., Xu, Y., Wang, X., Zhang, C., & Wang, Y. (2017). Resveratrol accumulation and its involvement in stilbene synthetic pathway of Chinese wild grapes during berry development using quantitative proteome analysis. *Scientific Reports*, 7(1), Article 1. <https://doi.org/10.1038/s41598-017-10171-x>
- Li, Y., Kong, D., Liang, H., & Wu, H. (2018). Alkaloid content and essential oil composition of *Mahonia breviflora* cultivated under different light environments. *Journal of Applied Botany and Food Quality*, 91, 171–179. <https://doi.org/10.5073/JABFQ.2018.091.023>
- Li, Y., Kong, D., Lin, X., Xie, Z., Bai, M., Huang, S., Nian, H., & Wu, H. (2015). Quality Evaluation for Essential Oil of *Cinnamomum verum* Leaves at Different Growth Stages Based on GC–MS, FTIR and Microscopy. *Food Analytical Methods*, 9. <https://doi.org/10.1007/s12161-015-0187-6>
- Liu, J., Nakamura, S., Zhuang, Y., Yoshikawa, M., Hussein, G. M. E., Matsuo, K., & Matsuda, H. (2013). Medicinal Flowers. XXXX.1) Structures of Dihydroisocoumarin Glycosides and Inhibitory Effects on Aldose Reductase from the Flowers of *Hydrangea macrophylla* var. *Thunbergii*. *Chemical and Pharmaceutical Bulletin*, 61(6), 655–661. <https://doi.org/10.1248/cpb.c13-00160>
- Lončar, M., Jakovljević, M., Šubarić, D., Pavlić, M., Buzjak Služek, V., Cindrić, I., & Molnar, M. (2020). Coumarins in Food and Methods of Their Determination. *Foods*, 9(5), Article 5. <https://doi.org/10.3390/foods9050645>
- Mashilo, J., Odindo, A. O., Shimelis, H. A., Musenge, P., Tesfay, S. Z., & Magwaza, L. S. (2017). Drought tolerance of selected bottle gourd [*Lagenaria siceraria* (Molina) Standl.] landraces assessed by leaf gas exchange and photosynthetic efficiency. *Plant Physiology and Biochemistry: PPB*, 120, 75–87. <https://doi.org/10.1016/j.plaphy.2017.09.022>
- Mayta, M. L., Lodeyro, A. F., Guiamet, J. J., Tognetti, V. B., Melzer, M., Hajirezaei, M. R., & Carrillo, N. (2018). Expression of a Plastid-Targeted Flavodoxin Decreases Chloroplast Reactive Oxygen Species Accumulation and Delays Senescence in Aging

- Tobacco Leaves. *Frontiers in Plant Science*, 9. <https://www.frontiersin.org/articles/10.3389/fpls.2018.01039>
- Moll, M. D., Vieregge, A. S., Wiesbaum, C., Blings, M., Vana, F., Hillebrand, S., Ley, J., Kraska, T., & Pude, R. (2021). Dihydroisocoumarin Content and Phenotyping of *Hydrangea macrophylla* subsp. *Serrata* Cultivars under Different Shading Regimes. *Agronomy*, 11(9), 1743. <https://doi.org/10.3390/agronomy11091743>
- Moon, J. H., Lee, K., Lee, J. H., & Lee, P. C. (2020). Redesign and reconstruction of a steviol-biosynthetic pathway for enhanced production of steviol in *Escherichia coli*. *Microbial Cell Factories*, 19(1), 20. <https://doi.org/10.1186/s12934-020-1291-x>
- Mora, M. R., & Dando, R. (2021). The sensory properties and metabolic impact of natural and synthetic sweeteners. *Comprehensive Reviews in Food Science and Food Safety*, 20(2), 1554–1583. <https://doi.org/10.1111/1541-4337.12703>
- Naghiloo, S., Movafeghi, A., Delazar, A., Nazemiyeh, H., Asnaashari, S., & Dadpour, M. R. (2012). Ontogenetic variation of volatiles and antioxidant activity in leaves of *Astragalus compactus* Lam. (Fabaceae). *EXCLI Journal*, 11, 436–443.
- Naikoo, M. I., Dar, M. I., Raghieb, F., Jaleel, H., Ahmad, B., Raina, A., Khan, F. A., & Naushin, F. (2019). Role and Regulation of Plants Phenolics in Abiotic Stress Tolerance. *Plant Signaling Molecules*, 157.
- Nichols, S. N., Hofmann, R. W., & Williams, W. M. (2015). Physiological drought resistance and accumulation of leaf phenolics in white clover interspecific hybrids. *Environmental and Experimental Botany*, 119, 40–47. <https://doi.org/10.1016/j.envexpbot.2015.05.014>
- Nicole, C. C. S., Charalambous, F., Martinakos, S., Voort, S. V. D., Li, Z., Verhoog, M., & Krijn, M. (2016). Lettuce growth and quality optimization in a plant factory. *Acta Horticulturae*, 1134, 231–238. <https://doi.org/10.17660/ActaHortic.2016.1134.31>
- Noel, J. P., Austin, M. B., & Bomati, E. K. (2005). Structure–function relationships in plant phenylpropanoid biosynthesis. *Current Opinion in Plant Biology*, 8(3), 249–253. <https://doi.org/10.1016/j.pbi.2005.03.013>

- Noor, A. O., Almasri, D. M., Bagalagel, A. A., Abdallah, H. M., Mohamed, S. G. A., Mohamed, G. A., & Ibrahim, S. R. M. (2020). Naturally Occurring Isocoumarins Derivatives from Endophytic Fungi: Sources, Isolation, Structural Characterization, Biosynthesis, and Biological Activities. *Molecules*, 25(2), Article 2. <https://doi.org/10.3390/molecules25020395>
- Nozawa, K., Yamada, M., Tsuda, Y., Kawai, K., & Nakajima, S. (1981). Antifungal activity of oosponol, oospolactone, phyllo dulcin, hydrangenol, and some other related compounds. *Chemical & Pharmaceutical Bulletin*, 29(9), 2689–2691. <https://doi.org/10.1248/cpb.29.2689>
- O'Brien-Nabors L (Ed): *Alternative Sweeteners*. CRC Press; 2011
- Onder, A., Nahar, L., Cinar, A. S., & Sarker, S. D. (2023). The genus *Seseli* L.: A comprehensive review on traditional uses, phytochemistry, and pharmacological properties. *Journal of Herbal Medicine*, 38, 100625. <https://doi.org/10.1016/j.hermed.2023.100625>
- Owen Jr, J., Fulcher, A., Lebude, A., & Chappell, M. (2016). *Hydrangea* Production: Cultivar Selection and General Practices to Consider When Propagating and Growing *Hydrangea*. <https://doi.org/10.13140/RG.2.2.18534.01608>
- Paddon, C. J., Westfall, P. J., Pitera, D. J., Benjamin, K., Fisher, K., McPhee, D., Leavell, M. D., Tai, A., Main, A., Eng, D., Polichuk, D. R., Teoh, K. H., Reed, D. W., Treynor, T., Lenihan, J., Fleck, M., Bajad, S., Dang, G., Dengrove, D., ... Newman, J. D. (2013). High-level semi-synthetic production of the potent antimalarial artemisinin. *Nature*, 496(7446), 528–532. <https://doi.org/10.1038/nature12051>
- Paffrath, V., 2022. Iron mobilization and reduction by coumarin-type siderophores in roots of *Arabidopsis thaliana* (PhD Thesis) / Vanessa Paffrath ; Gutachter: Nicolaus Wirén, Edgar Peiter, Stephan Clemens. Halle/S., Martin-Luther-Universität Halle-Wittenberg, Naturwissenschaftliche Fakultät I Biowissenschaften, Institut für Biologie (2022) 139 pp

- Pal, S., Chatare, V., & Pal, M. (2011). Isocoumarin and Its Derivatives: An Overview on their Synthesis and Applications. *Current Organic Chemistry*, 15, 782–800. <https://doi.org/10.2174/138527211794518970>
- Peng, Y., Niklas, K. J., Reich, P. B., & Sun, S. (2009). Ontogenetic shift in the scaling of dark respiration with whole-plant mass in seven shrub species. *Functional Ecology*, 24(3), 502.
- Perkowska, I., Siwinska, J., Olry, A., Grosjean, J., Hehn, A., Bourgaud, F., Lojkowska, E., & Ihnatowicz, A. (2021). Identification and Quantification of Coumarins by UHPLC-MS in *Arabidopsis thaliana* Natural Populations. *Molecules*, 26(6), Article 6. <https://doi.org/10.3390/molecules26061804>
- Pezzuto, J. M., Compadre, C. M., Swanson, S. M., Nanayakkara, D., & Kinghorn, A. D. (1985). Metabolically activated steviol, the aglycone of stevioside, is mutagenic. *Proceedings of the National Academy of Sciences of the United States of America*, 82(8), 2478–2482. <https://doi.org/10.1073/pnas.82.8.2478>
- Philippe, R. N., De Mey, M., Anderson, J., & Ajikumar, P. K. (2014). Biotechnological production of natural zero-calorie sweeteners. *Current Opinion in Biotechnology*, 26, 155–161. <https://doi.org/10.1016/j.copbio.2014.01.004>
- Pokorná, E., Hluska, T., Galuszka, P., Hallmark, H. T., Dobrev, P. I., Závěská Drábková, L., Filipi, T., Holubová, K., Plíhal, O., Rashotte, A. M., Filepová, R., Malbeck, J., Novák, O., Spíchal, L., Brzobohatý, B., Mazura, P., Zahajská, L., & Motyka, V. (2021). Cytokinin N-glucosides: Occurrence, Metabolism and Biological Activities in Plants. *Biomolecules*, 11(1), Article 1. <https://doi.org/10.3390/biom11010024>
- Popović, Z., Krstić-Milošević, D., Stefanović Marković, M., Vidaković, V., Matic, R., Janković, J., & Bojovic, S. (2020). Variability of six secondary metabolites in plant parts and developmental stages in natural populations of rare *Gentiana pneumonanthe*. *Plant Biosystems - An International Journal Dealing with All Aspects of Plant Biology*, 155, 1–9. <https://doi.org/10.1080/11263504.2020.1785966>

- Preusche, M., Ley, J., Schulz, M., Hillebrand, S., Blings, M., Theisen, A., & Ulbrich, A. (2022). Culture methods for high hydrangenol and phyllodulcin contents in *Hydrangea macrophylla* subsp. *Serrata* (Thunb.) Makino. *European Journal of Horticultural Science*, 87, 1–12. <https://doi.org/10.17660/eJHS.2022/057>
- Preusche, M., Ulbrich, A., & Schulz, M. (2022). Culturing Important Plants for Sweet Secondary Products under Consideration of Environmentally Friendly Aspects. *Processes*, 10(4), 703. <https://doi.org/10.3390/pr10040703>
- Price, J. M., Biava, C. G., Oser, B. L., Vogin, E. E., Steinfeld, J., & Ley, H. L. (1970). Bladder tumors in rats fed cyclohexylamine or high doses of a mixture of cyclamate and saccharin. *Science (New York, N.Y.)*, 167(3921), 1131–1132. <https://doi.org/10.1126/science.167.3921.1131>
- Rajniak, J., Giehl, R. F. H., Chang, E., Murgia, I., von Wirén, N., & Sattely, E. S. (2018). Biosynthesis of redox-active metabolites in response to iron deficiency in plants. *Nature Chemical Biology*, 14(5), 442–450. <https://doi.org/10.1038/s41589-018-0019-2>
- Redeuil, K., Bertholet, R., Kussmann, M., Steiling, H., Rezzi, S., & Nagy, K. (2009). Quantification of flavan-3-ols and phenolic acids in milk-based food products by reversed-phase liquid chromatography–tandem mass spectrometry. *Journal of Chromatography A*, 1216(47), 8362–8370. <https://doi.org/10.1016/j.chroma.2009.09.056>
- Rettie, A. E., Korzekwa, K. R., Kunze, K. L., Lawrence, R. F., Eddy, A. C., Aoyama, T., Gelboin, H. V., Gonzalez, F. J., & Trager, W. F. (1992). Hydroxylation of warfarin by human cDNA-expressed cytochrome P-450: A role for P-4502C9 in the etiology of (S)-warfarin-drug interactions. *Chemical Research in Toxicology*, 5(1), 54–59. <https://doi.org/10.1021/tx00025a009>
- Reveglia, P., Masi, M., & Evidente, A. (2020). Melleins—Intriguing Natural Compounds. *Biomolecules*, 10(5), Article 5. <https://doi.org/10.3390/biom10050772>

- Rezayian, M., Niknam, V., & Ebrahimzadeh, H. (2018). Differential responses of phenolic compounds of *Brassica napus* under drought stress. *Iranian Journal of Plant Physiology*, 8, 2417–2425. <https://doi.org/10.22034/ijpp.2018.540887>
- Riboli, E., Beland, F. A., Lachenmeier, D. W., Marques, M. M., Phillips, D. H., Schernhammer, E., Afghan, A., Assunção, R., Caderni, G., Corton, J. C., Umbuzeiro, G. de A., Jong, D. de, Deschasaux-Tanguy, M., Hodge, A., Ishihara, J., Levy, D. D., Mandrioli, D., McCullough, M. L., McNaughton, S. A., ... Madia, F. (2023). Carcinogenicity of aspartame, methyleugenol, and isoeugenol. *The Lancet Oncology*, 24(8), 848–850. [https://doi.org/10.1016/S1470-2045\(23\)00341-8](https://doi.org/10.1016/S1470-2045(23)00341-8)
- Richins, R. D., Rodriguez-Urbe, L., Lowe, K., Ferral, R., & O'Connell, M. A. (2018). Accumulation of bioactive metabolites in cultivated medical Cannabis. *PLOS ONE*, 13(7), e0201119. <https://doi.org/10.1371/journal.pone.0201119>
- Rinehart, T.; Wadl, P.; Staton, M. An update on *Hydrangea macrophylla* breeding targets and genomics. In *Proceedings of the III International Symposium on Woody Ornamentals of the Temperate Zone 1191*, Minneapolis, MI, USA, 2–5 August 2016; pp. 217–224
- Robb, E. L., Page, M. M., Wiens, B. E., & Stuart, J. A. (2008). Molecular mechanisms of oxidative stress resistance induced by resveratrol: Specific and progressive induction of MnSOD. *Biochemical and Biophysical Research Communications*, 367(2), 406–412. <https://doi.org/10.1016/j.bbrc.2007.12.138>
- Robe, K., Conejero, G., Gao, F., Lefebvre-Legendre, L., Sylvestre-Gonon, E., Rofidal, V., Hem, S., Rouhier, N., Barberon, M., Hecker, A., Gaymard, F., Izquierdo, E., & Dubos, C. (2021). Coumarin accumulation and trafficking in *Arabidopsis thaliana*: A complex and dynamic process. *New Phytologist*, 229(4), 2062–2079. <https://doi.org/10.1111/nph.17090>
- Robson, F., Okamoto, H., Patrick, E., Harris, S.-R., Wasternack, C., Brearley, C., & Turner, J. G. (2010). Jasmonate and Phytochrome A Signaling in *Arabidopsis* Wound and Shade Responses Are Integrated through JAZ1 Stability[C][W]. *The Plant Cell*, 22(4), 1143–1160. <https://doi.org/10.1105/tpc.109.067728>

- Rodriguez, C., Torre, S., & Solhaug, K. A. (2014). Low levels of ultraviolet-B radiation from fluorescent tubes induce an efficient flavonoid synthesis in Lollo Rosso lettuce without negative impact on growth. *Acta Agriculturae Scandinavica, Section B - Soil & Plant Science*, 64, 178–184. <https://doi.org/10.1080/09064710.2014.905623>
- Ruffoni, B., Sacco, E., & Savona, M. (2013). In vitro propagation of *Hydrangea* spp. *Methods in Molecular Biology* (Clifton, N.J.), 11013, 231–244. https://doi.org/10.1007/978-1-62703-074-8_18
- Saadat, N. P., Aalst, M. van, Brand, A., Ebenhöf, O., Tissier, A., & Matuszyńska, A. B. (2023). Shifts in carbon partitioning by photosynthetic activity increase terpenoid synthesis in glandular trichomes (p. 2022.09.29.510054). *bioRxiv*. <https://doi.org/10.1101/2022.09.29.510054>
- SADDIQA, A., ÇAKMAK, O., & USMAN, M. (2017). Isocoumarins and 3,4-dihydroisocoumarins, amazing natural products: A review. *Turkish Journal of Chemistry*, 41(2), 153–178. <https://doi.org/10.3906/kim-1604-66>
- Saeed, A., & Qasim, M. (2014). Total synthesis of cytotoxic metabolite (±)-desmethyldiaportinol from *Ampelomyces* sp. *Natural Product Research*, 28(3), 185–190. <https://doi.org/10.1080/14786419.2013.866111>
- Sampaio, B. L., Edrada-Ebel, R., & Da Costa, F. B. (2016). Effect of the environment on the secondary metabolic profile of *Tithonia diversifolia*: A model for environmental metabolomics of plants. *Scientific Reports*, 6(1), Article 1. <https://doi.org/10.1038/srep29265>
- Sánchez Jiménez, F. J., Manzanares, M., De Andrés Parlorio, E. F., Tenorio, J. L., & Ayerbe, L. (1998). Turgor maintenance, osmotic adjustment and soluble sugar and proline accumulation in 49 pea cultivars in response to water stress. [https://doi.org/10.1016/S0378-4290\(98\)00125-7](https://doi.org/10.1016/S0378-4290(98)00125-7)
- Santos, R. A., Souza Filho, A. P. S., Cantanhede Filho, A. J., Guilhon, G. M. S. P., & Santos, L. S. (2021). Analysis of phenolic compounds from cowpea (*Vigna unguiculata*) by HPLC-DAD-MS/MS. *Brazilian Journal of Food Technology*, 24, e2020077. <https://doi.org/10.1590/1981-6723.07720>

- Schneider, K., Hövel, K., Witzel, K., Hamberger, B., Schomburg, D., Kombrink, E., & Stuible, H.-P. (2003). The substrate specificity-determining amino acid code of 4-coumarate:CoA ligase. *Proceedings of the National Academy of Sciences*, 100(14), 8601–8606. <https://doi.org/10.1073/pnas.1430550100>
- Schoch, G., Goepfert, S., Morant, M., Hehn, A., Meyer, D., Ullmann, P., & Werck-Reichhart, D. (2001). CYP98A3 from *Arabidopsis thaliana* is a 3'-hydroxylase of phenolic esters, a missing link in the phenylpropanoid pathway. *The Journal of Biological Chemistry*, 276(39), 36566–36574. <https://doi.org/10.1074/jbc.M104047200>
- Schreiber, H. D., Jones, A. H., Lariviere, C. M., Mayhew, K. M., & Cain, J. B. (2011). Role of aluminum in red-to-blue color changes in *Hydrangea macrophylla* sepals. *BioMetals*, 24(6), 1005–1015. <https://doi.org/10.1007/s10534-011-9458-x>
- Schreiber, M., Bazaios, E., Ströbel, B., Wolf, B., Ostler, U., Gasche, R., Schlingmann, M., Kiese, R., & Dannenmann, M. (2023). Impacts of slurry acidification and injection on fertilizer nitrogen fates in grassland. *Nutrient Cycling in Agroecosystems*, 125(2), 171–186. <https://doi.org/10.1007/s10705-022-10239-9>
- Schwab, W. (2003). Metabolome diversity: Too few genes, too many metabolites? *Phytochemistry*, 62(6), 837–849. [https://doi.org/10.1016/s0031-9422\(02\)00723-9](https://doi.org/10.1016/s0031-9422(02)00723-9)
- Shallenberger, R. S., & Acree, T. E. (1967). Molecular Theory of Sweet Taste. *Nature*, 216(5114), Article 5114. <https://doi.org/10.1038/216480a0>
- Shi, S., Chen, T., & Zhao, X. (2013). Comparative Transcriptome Analysis for Metabolic Engineering. In H. S. Alper (Ed.), *Systems Metabolic Engineering: Methods and Protocols* (pp. 447–458). Humana Press. https://doi.org/10.1007/978-1-62703-299-5_22
- Shin, J.-S., Han, H.-S., Lee, S.-B., Myung, D., Lee, K., Lee, S. H., Kim, H. J., & Lee, K.-T. (2019). Chemical Constituents from Leaves of *Hydrangea serrata* and Their Anti-photoaging Effects on UVB-Irradiated Human Fibroblasts. *Biological and Pharmaceutical Bulletin*, 42(3), 424–431. <https://doi.org/10.1248/bpb.b18-00742>

- Silva, F., Vieira, L., Ribas, A., Moro, A., Moreira, D., & Pacheco, A. (2018). Proline accumulation induces the production of total phenolics in transgenic tobacco plants under water deficit without increasing the G6PDH activity. *Theoretical and Experimental Plant Physiology*, 30. <https://doi.org/10.1007/s40626-018-0119-0>
- Singh, G., Verma, A. K., & Kumar, V. (2015). Catalytic properties, functional attributes and industrial applications of β -glucosidases. *3 Biotech*, 6(1), 3. <https://doi.org/10.1007/s13205-015-0328-z>
- Song, R.-Y., Wang, X.-B., Yin, G.-P., Liu, R.-H., Kong, L.-Y., & Yang, M.-H. (2017). Isocoumarin derivatives from the endophytic fungus, *Pestalotiopsis* sp. *Fitoterapia*, 122, 115–118. <https://doi.org/10.1016/j.fitote.2017.08.012>
- Sugiyama, Y., Nakamura, S., Tokuda, Y., Nakano, M., Hattori, Y., Nishiguchi, H., Toda, Y., Hosogi, S., Yamashita, M., Tashiro, K., & Ashihara, E. (2023). 7,8-Dihydroxy-3-(4'-hydroxyphenyl)coumarin inhibits invasion and migration of osteosarcoma cells. *Biochemical and Biophysical Research Communications*, 638, 200–209. <https://doi.org/10.1016/j.bbrc.2022.11.056>
- Suzuki, H., Ikeda, T., Matsumoto, T., & Noguchi, M. (1977). Isolation and Identification of a New Glycoside, Phylodulcin-8-O- β -D-glucose from the Cultured Cells and Fresh Leaves of Amacha (*Hydrangea macrophylla* Seringe var. *Thunbergii* Makino). *Agricultural and Biological Chemistry*, 41(9), 1815–1817. <https://doi.org/10.1271/bbb1961.41.1815>
- Suzuki, H., Ikeda, T., Matsumoto, T., & Noguchi, M. (1978). Polyphenol Components in Cultured Cells of Amacha (*Hydrangea macrophylla* Seringe var. *Thunbergii* Makino). *Agricultural and Biological Chemistry*, 42(6), 1133–1137. <https://doi.org/10.1080/00021369.1978.10863124>
- Suzuki, H., Matsumoto, T., Kisaki, T., & Noguchi, M. (1981). Influences of Cultural Conditions on Polyphenol Formation and Growth of Amacha Cells (*Hydrangea macrophylla* Seringe var. *Thunbergii* Makino) and Changes of Polyphenol Contents in Leaves of Amacha Plant during Growth. *Agricultural and Biological Chemistry*, 45(5), 1067–1077. <https://doi.org/10.1080/00021369.1981.10864663>

- Szabados, L., & Savouré, A. (2010). Proline: A multifunctional amino acid. *Trends in Plant Science*, 15(2), 89–97. <https://doi.org/10.1016/j.tplants.2009.11.009>
- Takeda, K., Kariuda, M., & Itoi, H. (1985). Blueing of sepal colour of *Hydrangea macrophylla*. *Phytochemistry*, 24(10), 2251–2254. [https://doi.org/10.1016/S0031-9422\(00\)83019-8](https://doi.org/10.1016/S0031-9422(00)83019-8)
- Tan, J., Yu, W., Liu, Y., Guo, Y., Liu, N., Fu, H., Di, N., Duan, J., Li, X., & Xi, B. (2023). Correction: Tan *et al.* Response of Fine-Root Traits of *Populus tomentosa* to Drought in Shallow and Deep Soil. *Forests* 2023, 14, 951. *Forests*, 14(8), 1657. <https://doi.org/10.3390/f14081657>
- Taylor, A. O. (1965). Some Effects of Photoperiod on the Biosynthesis of Phenylpropane Derivatives in *Xanthium*. *Plant Physiology*, 40(2), 273–280. <https://doi.org/10.1104/pp.40.2.273>
- Teng, H.-M., Fang, M.-F., Cai, X., & Hu, Z.-H. (2009). Localization and dynamic change of saponin in vegetative organs of *Polygala tenuifolia*. *Journal of Integrative Plant Biology*, 51(6), 529–536. <https://doi.org/10.1111/j.1744-7909.2009.00830.x>
- Tortosa, M., Cartea, M. E., Rodríguez, V. M., & Velasco, P. (2018). Unraveling the metabolic response of *Brassica oleracea* exposed to *Xanthomonas campestris* pv. *Campestris*. *Journal of the Science of Food and Agriculture*, 98(10), 3675–3683. <https://doi.org/10.1002/jsfa.8876>
- Tsai, H.-H., Rodríguez-Celma, J., Lan, P., Wu, Y.-C., Vélez-Bermúdez, I. C., & Schmidt, W. (2018). Scopoletin 8-Hydroxylase-Mediated Fraxetin Production Is Crucial for Iron Mobilization. *Plant Physiology*, 177(1), 194–207. <https://doi.org/10.1104/pp.18.00178>
- Tsukioka, J., & Nakamura, S. (2023). Comparison of Growth in *Hydrangea macrophylla* var. *Thunbergii* Grown in Different Soil pH and Quantitative Analysis of Its Sweetness-Related Constituents. *Chemical & Pharmaceutical Bulletin*, 71(5), 368–373. <https://doi.org/10.1248/cpb.c23-00084>
- Ujihara, M., Shinozaki, M., & Kato, M. (1995). Accumulation of phyllodulcin in sweet-leaf plants of *Hydrangea serrata* and its neutrality in the defence against a specialist

leafmining herbivore. *Researches on Population Ecology*, 37(2), 249–257. <https://doi.org/10.1007/BF02515827>

Vandesompele, J., De Preter, K., Pattyn, F., Poppe, B., Van Roy, N., De Paepe, A., & Speleman, F. (2002). Accurate normalization of real-time quantitative RT-PCR data by geometric averaging of multiple internal control genes. *Genome Biology*, 3(7), research0034.1. <https://doi.org/10.1186/gb-2002-3-7-research0034>

Vanholme, R., Sundin, L., Seetso, K. C., Kim, H., Liu, X., Li, J., De Meester, B., Hoengenaert, L., Goeminne, G., Morreel, K., Haustraete, J., Tsai, H.-H., Schmidt, W., Vanholme, B., Ralph, J., & Boerjan, W. (2019). COSY catalyses trans–cis isomerization and lactonization in the biosynthesis of coumarins. *Nature Plants*, 5(10), Article 10. <https://doi.org/10.1038/s41477-019-0510-0>

Vassão, D. G., Wielsch, N., Gomes, A. M. de M. M., Gebauer-Jung, S., Hupfer, Y., Svatoš, A., & Gershenzon, J. (2018). Plant Defensive β -Glucosidases Resist Digestion and Sustain Activity in the Gut of a Lepidopteran Herbivore. *Frontiers in Plant Science*, 9. <https://www.frontiersin.org/articles/10.3389/fpls.2018.01389>

Vaštakaitė V., Viršilė A., Samuolienė G., Jankauskienė J., Sirtautas R., Dabašinskas L., *et al.* (2015b). The effect of blue light dosage on growth and antioxidant properties of microgreens. *Sodin. Daržininkystė* 34 25–35.

Vázquez-Flota, F. A., & De Luca, V. (1998). Jasmonate modulates development- and light-regulated alkaloid biosynthesis in *Catharanthus roseus*. *Phytochemistry*, 49(2), 395–402. [https://doi.org/10.1016/s0031-9422\(98\)00176-9](https://doi.org/10.1016/s0031-9422(98)00176-9)

Vázquez-León, L. A., Páramo-Calderón, D. E., Robles-Olvera, V. J., Valdés-Rodríguez, O. A., Pérez-Vázquez, A., García-Alvarado, M. A., & Rodríguez-Jimenes, G. C. (2017). Variation in bioactive compounds and antiradical activity of *Moringa oleifera* leaves: Influence of climatic factors, tree age, and soil parameters. *European Food Research and Technology*, 243(9), 1593–1608. <https://doi.org/10.1007/s00217-017-2868-4>

- Venugopala, K. N., Rashmi, V., & Odhav, B. (2013). Review on Natural Coumarin Lead Compounds for Their Pharmacological Activity. *BioMed Research International*, 2013, e963248. <https://doi.org/10.1155/2013/963248>
- Verma, N., & Shukla, S. (2015). Impact of various factors responsible for fluctuation in plant secondary metabolites. *Journal of Applied Research on Medicinal and Aromatic Plants*, 2(4), 105–113. <https://doi.org/10.1016/j.jarmap.2015.09.002>
- Voges, M. J. E. E. E., Bai, Y., Schulze-Lefert, P., & Sattely, E. S. (2019). Plant-derived coumarins shape the composition of an Arabidopsis synthetic root microbiome. *Proceedings of the National Academy of Sciences*, 116(25), 12558–12565. <https://doi.org/10.1073/pnas.1820691116>
- Vogt, T. (2010). Phenylpropanoid biosynthesis. *Molecular Plant*, 3(1), 2–20. <https://doi.org/10.1093/mp/ssp106>
- Wang, B., Liu, X., Zhou, A., Meng, M., & Li, Q. (2014). Simultaneous analysis of coumarin derivatives in extracts of *Radix Angelicae pubescentis* (Duhuo) by HPLC-DAD-ESI-MSⁿ technique. *Analytical Methods*, 6(19), 7996–8002. <https://doi.org/10.1039/C4AY01468E>
- Wang, J., Li, S., Xiong, Z., & Wang, Y. (2016). Pathway mining-based integration of critical enzyme parts for de novo biosynthesis of steviolglycosides sweetener in *Escherichia coli*. *Cell Research*, 26(2), 258–261. <https://doi.org/10.1038/cr.2015.111>
- Wang, Z., Xiao, Y., Chang, H., Sun, S., Wang, J., Liang, Q., Wu, Q., Wu, J., Qin, Y., Chen, J., Wang, G., & Wang, Q. (2023). The Regulatory Network of Sweet Corn (*Zea mays* L.) Seedlings under Heat Stress Revealed by Transcriptome and Metabolome Analysis. *International Journal of Molecular Sciences*, 24(13), Article 13. <https://doi.org/10.3390/ijms241310845>
- Wari, D., Aboshi, T., Shinya, T., & Galis, I. (2022). Integrated view of plant metabolic defense with particular focus on chewing herbivores. *Journal of Integrative Plant Biology*, 64(2), 449–475. <https://doi.org/10.1111/jipb.13204>

- Weihrauch, M. R., & Diehl, V. (2004). Artificial sweeteners—Do they bear a carcinogenic risk? *Annals of Oncology*, 15(10), 1460–1465. <https://doi.org/10.1093/annonc/mdh256>
- Wellmann, J., Hartmann, B., Schwarze, E.-C., Hillebrand, S., Brueckner, S. I., Ley, J., Jerz, G., & Winterhalter, P. (2022). Separation of Dihydro-Isocoumarins and Dihydro-Stilbenoids from *Hydrangea macrophylla* ssp. *Serrata* by Use of Counter-Current Chromatography. *Molecules*, 27(11), Article 11. <https://doi.org/10.3390/molecules27113424>
- Weng, J.-K., Lynch, J. H., Matos, J. O., & Dudareva, N. (2021). Adaptive mechanisms of plant specialized metabolism connecting chemistry to function. *Nature Chemical Biology*, 17(10), 1037–1045. <https://doi.org/10.1038/s41589-021-00822-6>
- Wilson, E. H. (1923). The Hortensias *Hydrangea macrophylla* DC. and *Hydrangea serrata* DC. *Journal of the Arnold Arboretum.*, 4(4), 233–246. <https://doi.org/10.5962/p.317979>
- Winkel-Shirley, B. (2001). Flavonoid Biosynthesis. A Colorful Model for Genetics, Biochemistry, Cell Biology, and Biotechnology. *Plant Physiology*, 126(2), 485–493. <https://doi.org/10.1104/pp.126.2.485>
- Wu, C., Zhu, H., van Wezel, G. P., & Choi, Y. H. (2016). Metabolomics-guided analysis of isocoumarin production by *Streptomyces* species MBT76 and biotransformation of flavonoids and phenylpropanoids. *Metabolomics*, 12, 90. <https://doi.org/10.1007/s11306-016-1025-6>
- Wu, F., Duan, Z., Xu, P., Yan, Q., Meng, M., Cao, M., Jones, C. S., Zong, X., Zhou, P., Wang, Y., Luo, K., Wang, S., Yan, Z., Wang, P., Di, H., Ouyang, Z., Wang, Y., & Zhang, J. (2022). Genome and systems biology of *Melilotus albus* provides insights into coumarins biosynthesis. *Plant Biotechnology Journal*, 20(3), 592–609. <https://doi.org/10.1111/pbi.13742>
- Wu, X., Hulse-Kemp, A. M., Wadl, P. A., Smith, Z., Mockaitis, K., Staton, M. E., Rinehart, T. A., & Alexander, L. W. (2021). Genomic Resource Development for *Hydrangea* (*Hydrangea macrophylla* (Thunb.) Ser.)—A Transcriptome Assembly and

a High-Density Genetic Linkage Map. *Horticulturae*, 7(2), Article 2. <https://doi.org/10.3390/horticulturae7020025>

Xiao, X., Ren, W., Zhang, N., Bing, T., Liu, X., Zhao, Z., & Shangguan, D. (2019). Comparative Study of the Chemical Constituents and Bioactivities of the Extracts from Fruits, Leaves and Root Barks of *Lycium barbarum*. *Molecules*, 24(8), Article 8. <https://doi.org/10.3390/molecules24081585>

Xu, J., Yu, Y., Shi, R., Xie, G., Zhu, Y., Wu, G., & Qin, M. (2018). Organ-Specific Metabolic Shifts of Flavonoids in *Scutellaria baicalensis* at Different Growth and Development Stages. *Molecules*, 23(2), 428. <https://doi.org/10.3390/molecules23020428>

Xuan Duy, L., Le Ba, V., Gao, D., Hoang, V. D., Quoc Toan, T., Yang, S. Y., Duy Quang, D., Kim, Y. H., & Cuong, N. M. (2021). Soluble epoxide hydrolase inhibitors from *Docynia indica* (Wall.) Decne. *Natural Product Research*, 35(23), 5403–5408. <https://doi.org/10.1080/14786419.2020.1774759>

Yagi, A., Ogata, Y., Yamauchi, T., & Nishioka, I. (1977). Metabolism of phenylpropanoids in *Hydrangea serrata* var. *Thunbergii* and the biosynthesis of phyllodulcin. *Phytochemistry*, 16(7), 1098–1100. [https://doi.org/10.1016/S0031-9422\(00\)86751-5](https://doi.org/10.1016/S0031-9422(00)86751-5)

Yamada, T., Matsuda, F., Kasai, K., Fukuoka, S., Kitamura, K., Tozawa, Y., Miyagawa, H., & Wakasa, K. (2008). Mutation of a Rice Gene Encoding a Phenylalanine Biosynthetic Enzyme Results in Accumulation of Phenylalanine and Tryptophan. *The Plant Cell*, 20(5), 1316–1329. <https://doi.org/10.1105/tpc.107.057455>

Yamato, M., Hashigaki, K., Uenishi, J., Yamakawa, I., & Sato, N. (1975). Chemical structure and sweet taste of isocoumarin and related compounds. VI. *Chemical & Pharmaceutical Bulletin*, 23(12), 3101–3105. <https://doi.org/10.1248/cpb.23.3101>

Yang, L., Meng, X., Yu, X., & Kuang, H. (2017). Simultaneous determination of anemoside B4, phellodendrine, berberine, palmatine, obakunone, esculin, esculetin in rat plasma by UPLC–ESI–MS/MS and its application to a comparative

pharmacokinetic study in normal and ulcerative colitis rats. *Journal of Pharmaceutical and Biomedical Analysis*, 134, 43–52. <https://doi.org/10.1016/j.jpba.2016.11.021>

Yano, A., Yuki, S., Kanno, Y., Shiraishi, A., Onuma, H., & Uesugi, S. (2023). Dihydroisocoumarins of *Hydrangea macrophylla* var. *Thunbergia* inhibit binding of the SARS-CoV-2 spike protein to ACE2. *Bioscience, Biotechnology, and Biochemistry*, 87(9), 1045–1055. <https://doi.org/10.1093/bbb/zbad078>

Yasuda, T., Kayaba, S., Takahashi, K., Nakazawa, T., & Ohsawa, K. (2004). Metabolic fate of orally administered phyllo dulcin in rats. *Journal of Natural Products*, 67(9), 1604–1607. <https://doi.org/10.1021/np0400353>

Yeow, L. C., Chew, B. L., & Sreeramanan, S. (2020). Elevation of secondary metabolites production through light-emitting diodes (LEDs) illumination in protocorm-like bodies (PLBs) of *Dendrobium* hybrid orchid rich in phytochemicals with therapeutic effects. *Biotechnology Reports*, 27, e00497. <https://doi.org/10.1016/j.btre.2020.e00497>

Yin, Q., Wu, T., Gao, R., Wu, L., Shi, Y., Wang, X., Wang, M., Xu, Z., Zhao, Y., Su, X., Su, Y., Han, X., Yuan, L., Xiang, L., & Chen, S. (2023). Multi-omics reveal key enzymes involved in the formation of phenylpropanoid glucosides in *Artemisia annua*. *Plant Physiology and Biochemistry*, 201, 107795. <https://doi.org/10.1016/j.plaphy.2023.107795>

Yoon, J. H., Park, S. H., Yoon, S. E., Hong, S. Y., Lee, J. B., Lee, J., & Cho, J. Y. (2023). *Hydrangea serrata* Hot Water Extract and Its Major Ingredient Hydrangenol Improve Skin Moisturization and Wrinkle Conditions via AP-1 and Akt/PI3K Pathway Upregulation. *Nutrients*, 15(11), Article 11. <https://doi.org/10.3390/nu15112436>

Yoshiba, Y., Kiyosue, T., Nakashima, K., Yamaguchi-Shinozaki, K., & Shinozaki, K. (1997). Regulation of Levels of Proline as an Osmolyte in Plants under Water Stress. *Plant and Cell Physiology*, 38(10), 1095–1102. <https://doi.org/10.1093/oxfordjournals.pcp.a029093>

Yoshikawa, M., Ueda, T., Matsuda, H., Yamahara, J., & Murakami, N. (1994). Absolute stereostructures of hydramacrosides A and B, new bioactive secoiridoid glucoside

complexes from the leaves of *Hydrangea macrophylla* Seringe var. *Thunbergii* Makino. *Chemical & Pharmaceutical Bulletin*, 42(8), 1691–1693. <https://doi.org/10.1248/cpb.42.1691>

Yuan, Y., Liu, Y., Wu, C., Chen, S., Wang, Z., Yang, Z., Qin, S., & Huang, L. (2012). Water Deficit Affected Flavonoid Accumulation by Regulating Hormone Metabolism in *Scutellaria baicalensis* Georgi Roots. *PLOS ONE*, 7(10), e42946. <https://doi.org/10.1371/journal.pone.0042946>

Zehnter, R., & Gerlach, H. (1995). Enantiodifferentiation in Taste Perception of the phyllodulcins. *Tetrahedron: Asymmetry*, 6(11), 2779–2786. [https://doi.org/10.1016/0957-4166\(95\)00367-X](https://doi.org/10.1016/0957-4166(95)00367-X)

Zeng, Y., Li, S., Wang, X., Gong, T., Sun, X., & Zhang, Z. (2015). Validated LC-MS/MS Method for the Determination of Scopoletin in Rat Plasma and Its Application to Pharmacokinetic Studies. *Molecules*, 20(10), Article 10. <https://doi.org/10.3390/molecules201018988>

Zha, J., & Koffas, M. A. G. (2017). Production of anthocyanins in metabolically engineered microorganisms: Current status and perspectives. *Synthetic and Systems Biotechnology*, 2(4), 259–266. <https://doi.org/10.1016/j.synbio.2017.10.005>

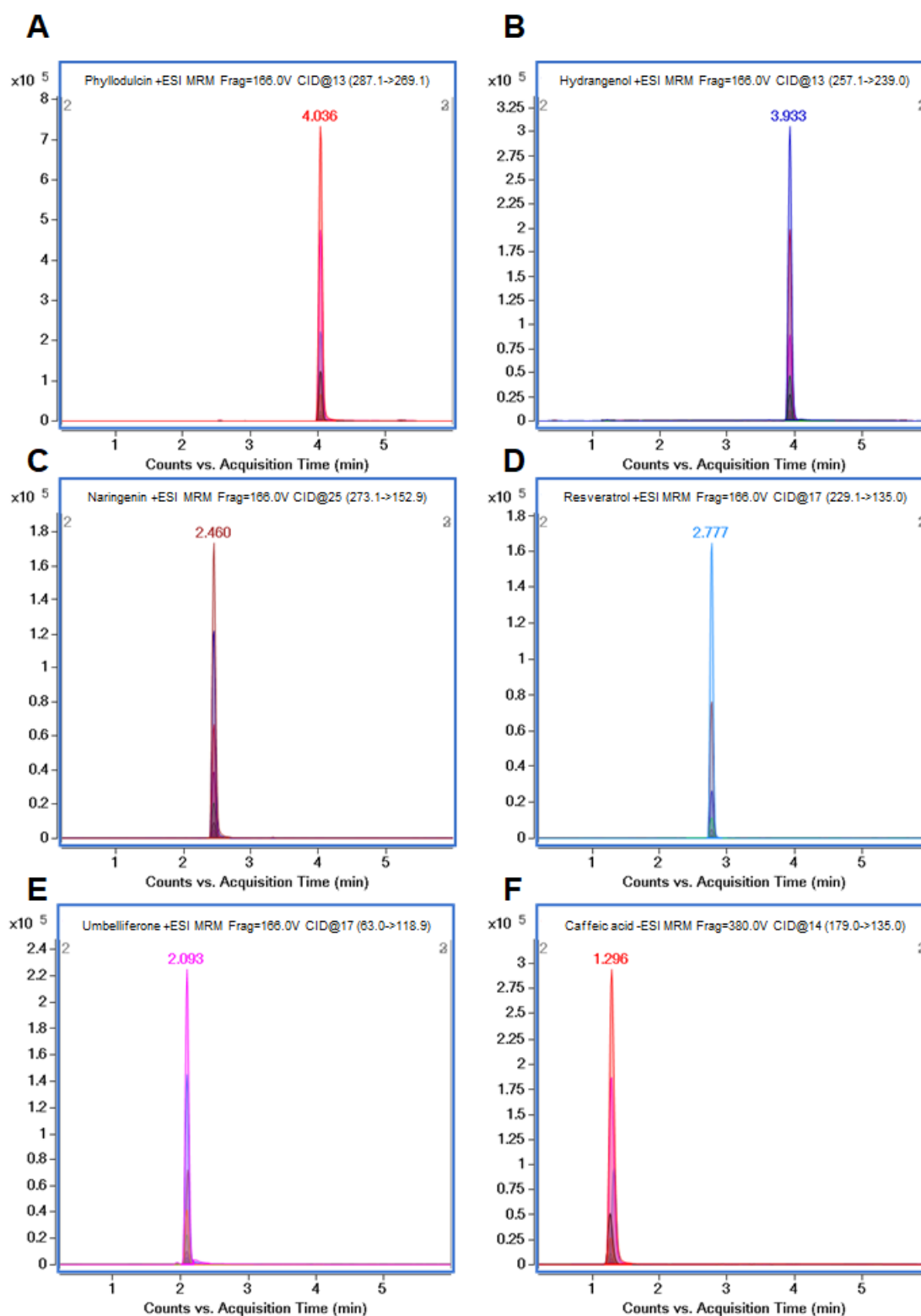
Zhang, G., Yuan, S., Qi, H., Chu, Z., & Liu, C. (2022). Identification of Reliable Reference Genes for the Expression of *Hydrangea macrophylla* ‘Bailmer’ and ‘Duro’ Sepal Color. *Horticulturae*, 8(9), Article 9. <https://doi.org/10.3390/horticulturae8090835>

Zhang, D., Liu, Y., Yang, Z., Song, X., Ma, Y., Zhao, J., Wang, X., Liu, H., & Fan, L. (2023). Widely target metabolomics analysis of the differences in metabolites of licorice under drought stress. *Industrial Crops and Products*, 202, 117071. <https://doi.org/10.1016/j.indcrop.2023.117071>

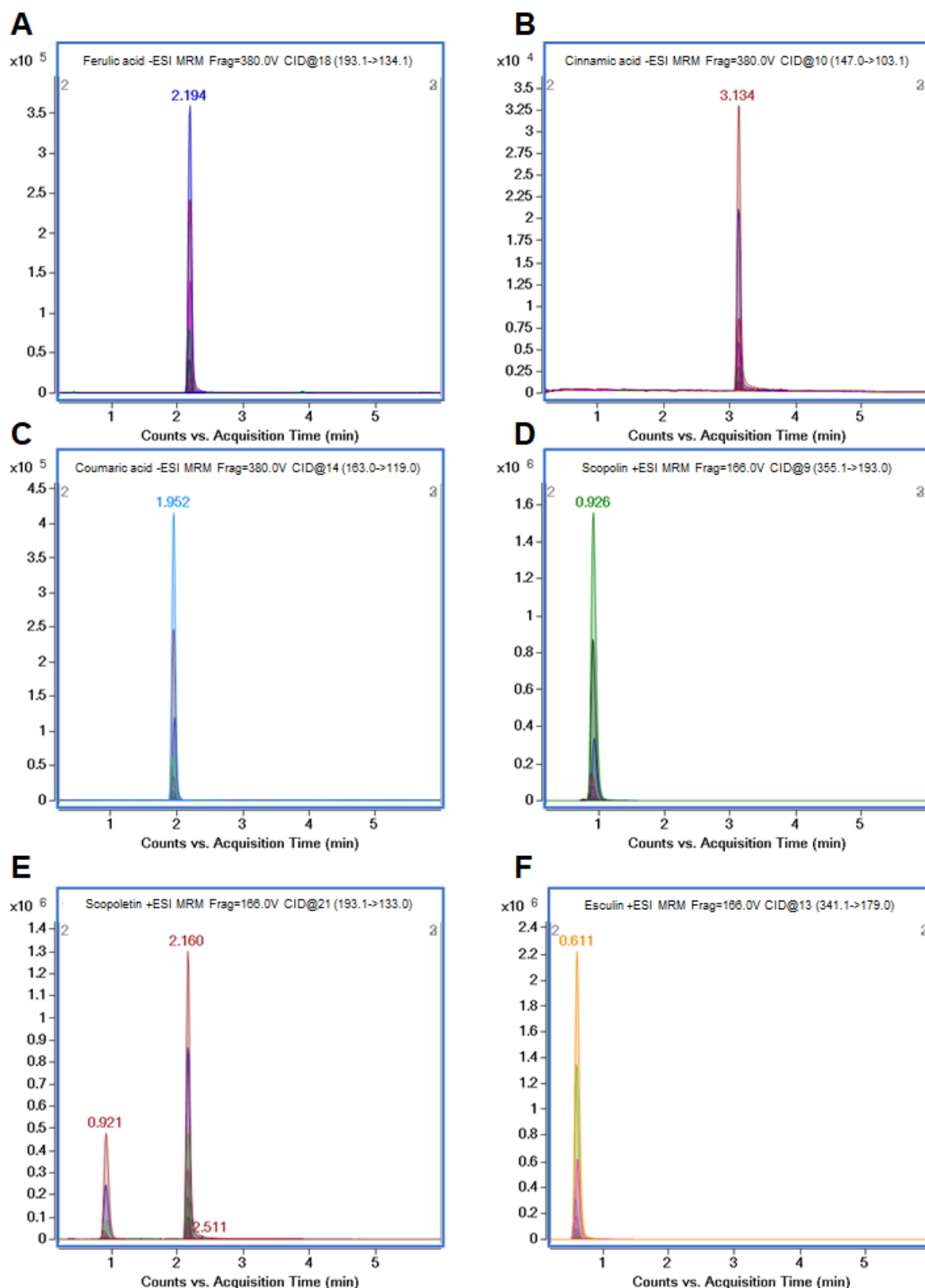
Zhang, H., Matsuda, H., Kumahara, A., Ito, Y., Nakamura, S., & Yoshikawa, M. (2007). New type of anti-diabetic compounds from the processed leaves of *Hydrangea macrophylla* var. *Thunbergii* (*Hydrangeae Dulcis Folium*). *Bioorganic & Medicinal Chemistry Letters*, 17(17), 4972–4976. <https://doi.org/10.1016/j.bmcl.2007.06.027>

- Zhang, L. X., Guo, Q. S., Chang, Q. S., Zhu, Z. B., Liu, L., & Chen, Y. H. (2015). Chloroplast ultrastructure, photosynthesis and accumulation of secondary metabolites in *Glechoma longituba* in response to irradiance. *Photosynthetica*, 53(1), 144–153. <https://doi.org/10.1007/s11099-015-0092-7>
- Zhao, T., He, J., Wang, X., Ma, B., Wang, X., Zhang, L., Li, P., Liu, N., Lu, J., & Zhang, X. (2014). Rapid detection and characterization of major phenolic compounds in *Radix Actinidia chinensis* Planch by ultra-performance liquid chromatography tandem mass spectrometry. *Journal of Pharmaceutical and Biomedical Analysis*, 98, 311–320. <https://doi.org/10.1016/j.jpba.2014.05.019>
- Zhu, J.-K. (2016). Abiotic Stress Signaling and Responses in Plants. *Cell*, 167(2), 313–324. <https://doi.org/10.1016/j.cell.2016.08.029>
- Zulfiqar, F., Akram, N. A., & Ashraf, M. (2019). Osmoprotection in plants under abiotic stresses: New insights into a classical phenomenon. *Planta*, 251(1), 3. <https://doi.org/10.1007/s00425-019-03293-1>
- Çiçek, S. S. (2020). Structure-Dependent Activity of Plant-Derived Sweeteners. *Molecules*, 25(8), Article 8. <https://doi.org/10.3390/molecules25081946>

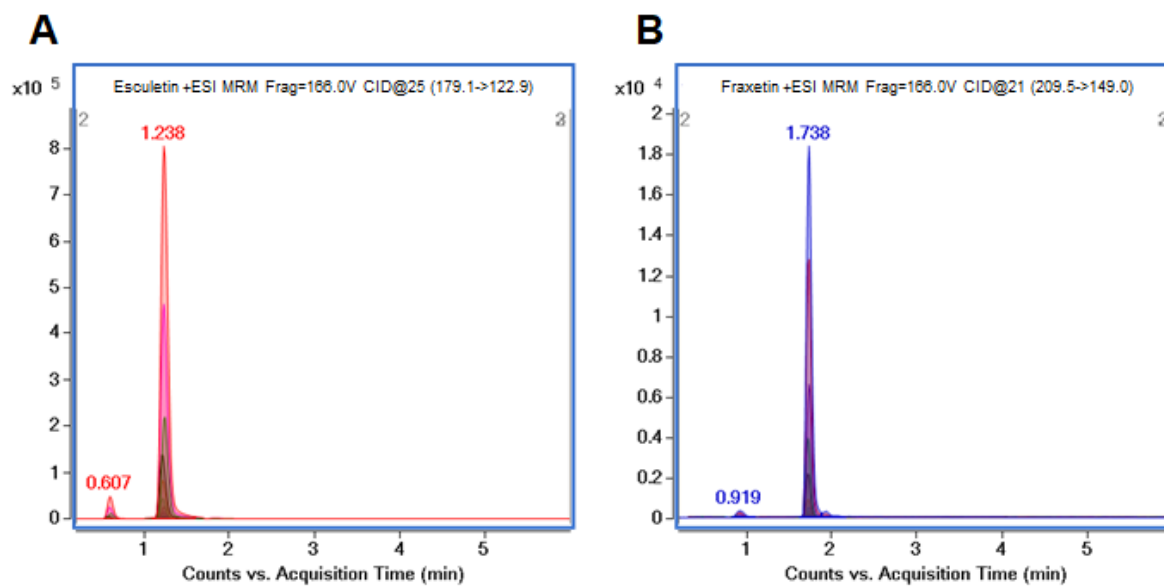
8 Appendix



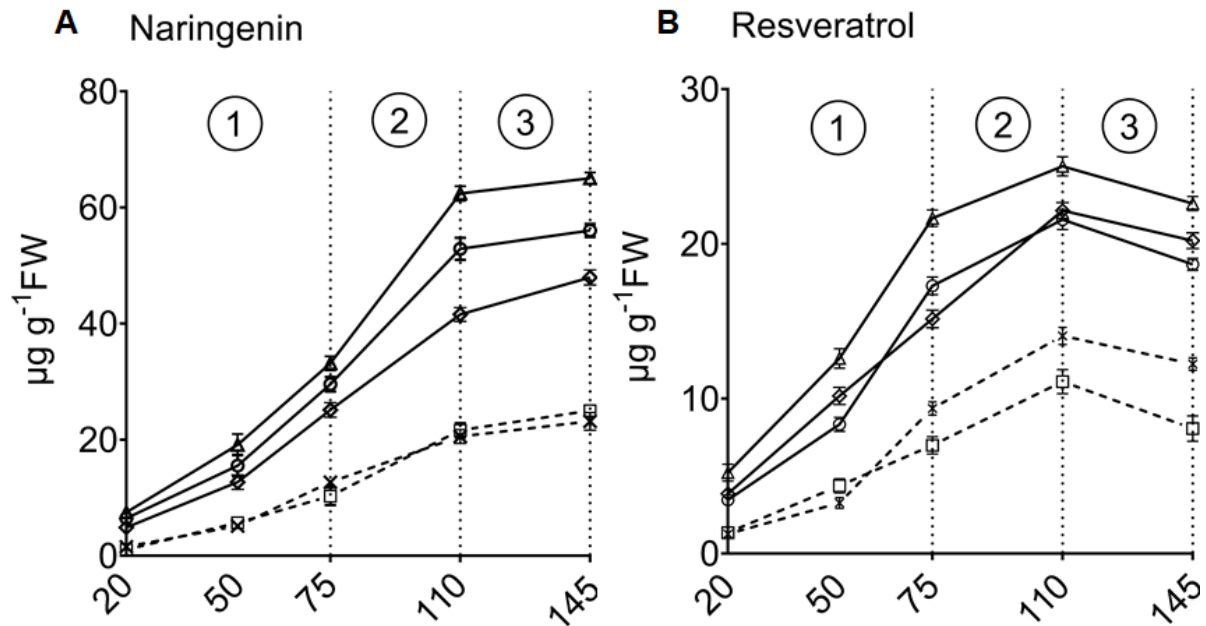
Appendix 1. Total Ion Current (TIC) MRM of phenylpropanoids. TIC MRM of product ions of (A) PD, (B) HD, (C) naringenin and (D) resveratrol, (E) umbelliferone, (F) caffeic acid in respective ionization modes. The collision energy of each transition was determined by MS2 Selected Ion Monitoring (SIM). Each peak represents the intensity of fragmented ion at m/z detected at specific retention times.



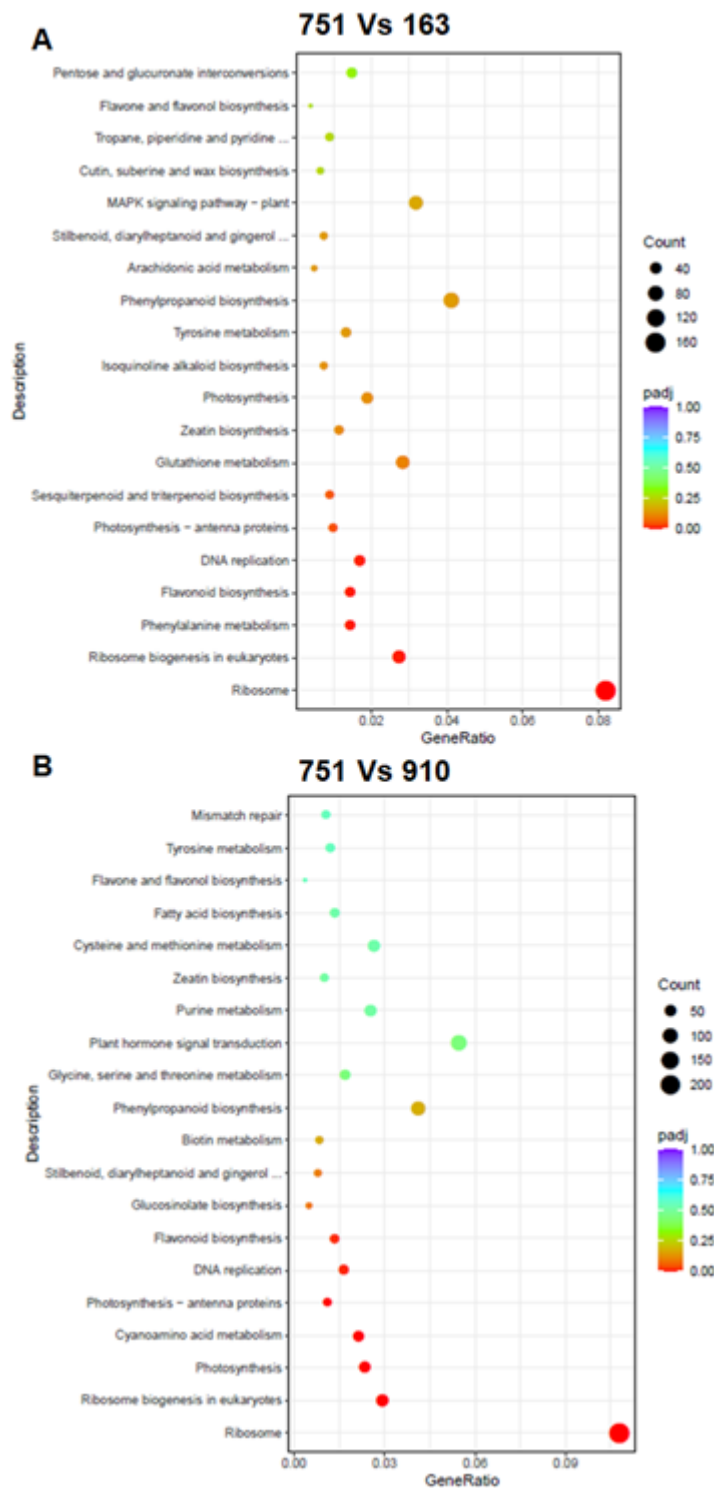
Appendix 2. Total Ion Current (TIC) MRM of phenylpropanoids. TIC MRM of product ions of (A) ferulic acid, (B) cinnamic acid, (C) coumaric acid, (D) scopolin, (E) scopoletin and (F) esculin in respective ionization modes. The collision energy of each transition was determined by MS2 Selected Ion Monitoring (SIM). Each peak represents the intensity of fragmented ion at m/z detected at specific retention times.



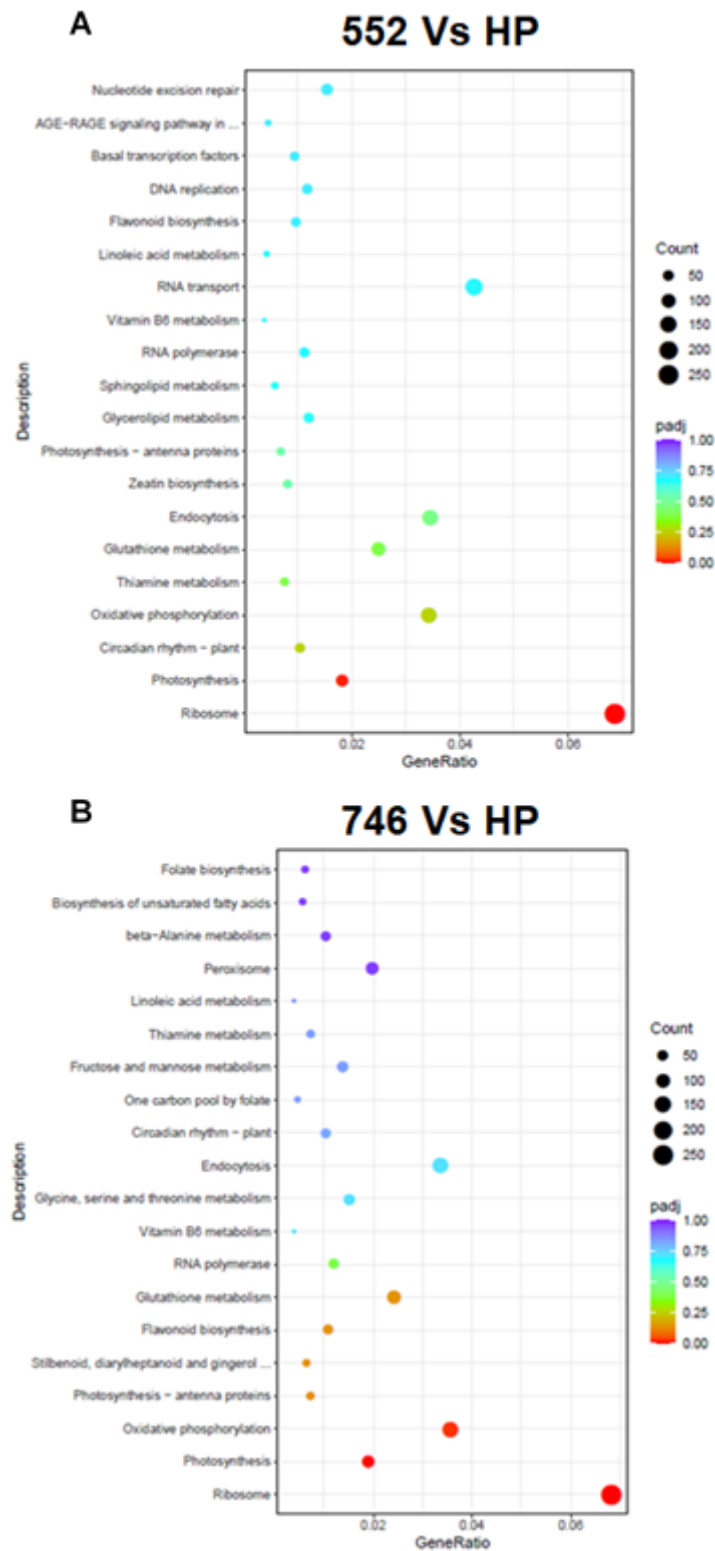
Appendix 3. Total Ion Current (TIC) MRM of phenylpropanoids. TIC MRM of product ions of (A) esculetin and (B) fraxetin in respective ionization modes. The collision energy of each transition was determined by MS2 Selected Ion Monitoring (SIM). Each peak represents the intensity of fragmented ion at m/z detected at specific retention times.



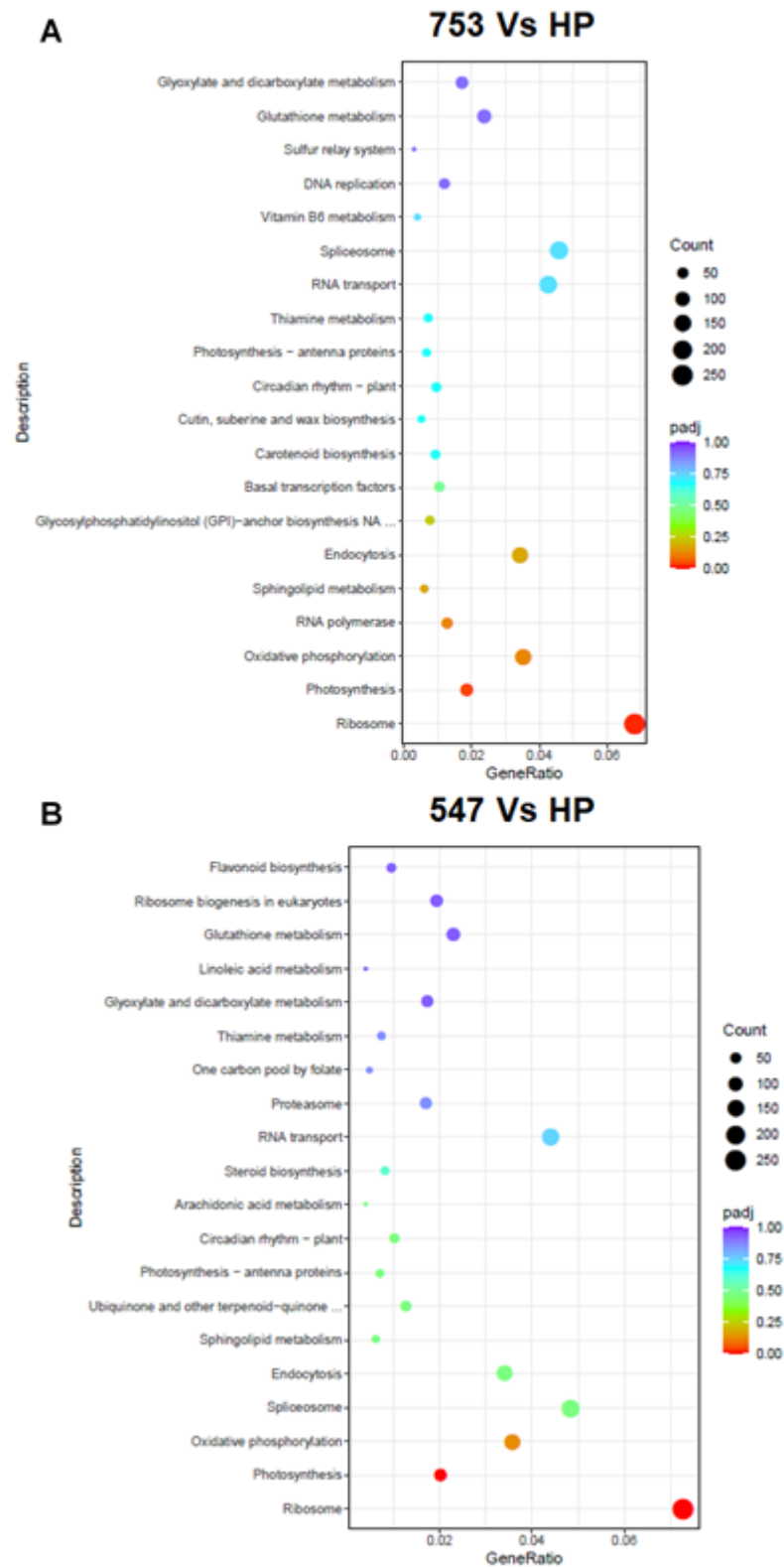
Appendix 4. Naringenin and resveratrol accumulation across specific developmental stages in selected *H. macrophylla* accessions. Concentrations (A) naringenin and (B) resveratrol in selected *H. macrophylla* accessions namely, VAR-552, VAR-746, VAR-553, VAR-212 and VAR-163 at five different time points of the plant's lifecycle. 20-75 days represent vegetative growth stage (1), 75-110 days indicate reproductive stages (2) and 110-145 indicate post anthesis stage respectively (3). Analysis was performed on young upper leaf tissues dried at 40°C for 48 h. The solid line represents the trend line connecting the means of 6 independent biological replicates and standard error for each time point. One-way ANOVA was used to estimate the significant differences between each interval at 95% CI.



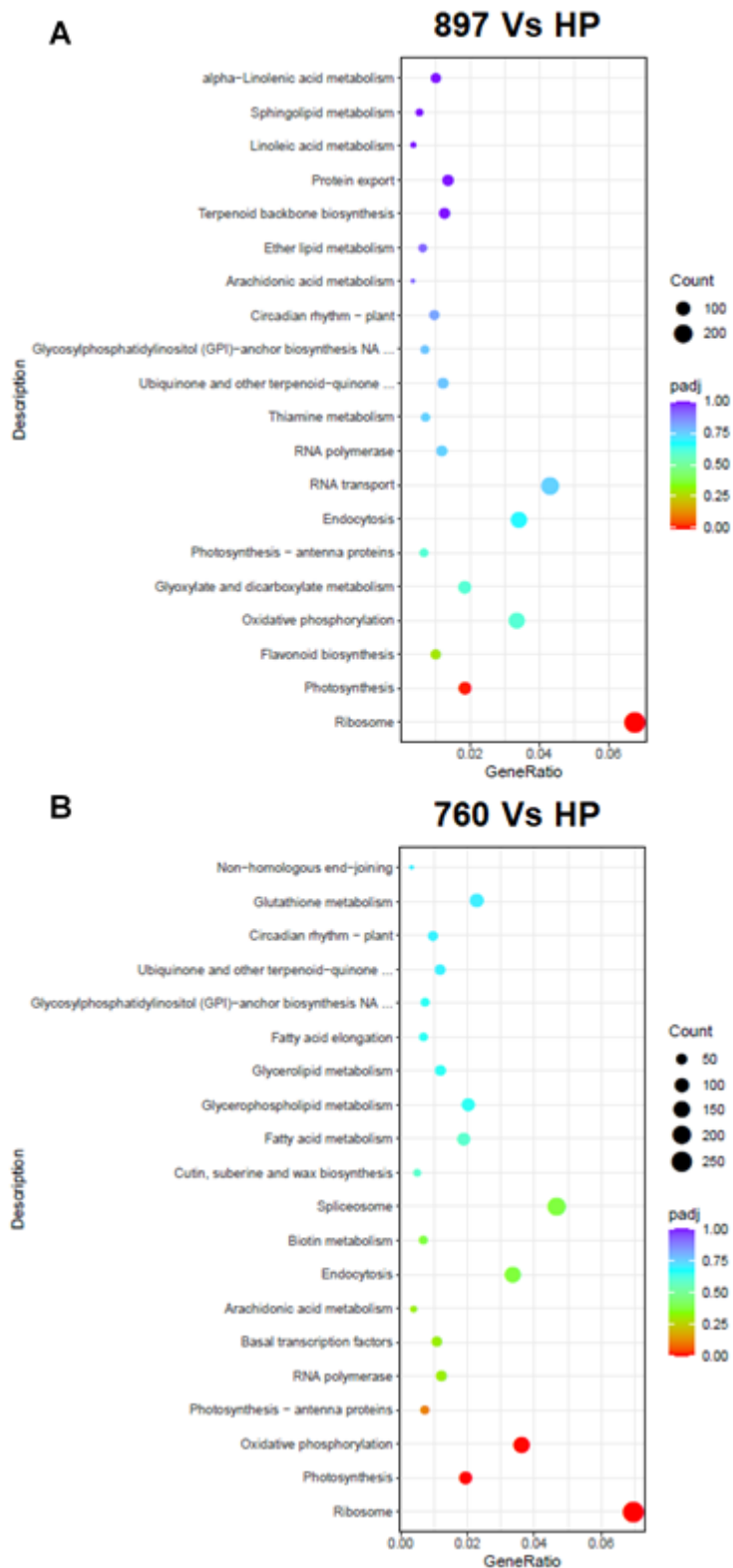
Appendix 5. The assignment of genes to different metabolic pathways in high HD and low PD/HD accessions of *H. macrophylla*. (A, B) Dot plot of KEGG enrichment analysis showing the gene ratio (the percentage of total DEGs) assigned to the top 20 metabolic pathways in the study group (A) VAR-751 and VAR-163 and (B) VAR-751 and VAR-910. The dot sizes represent the gene counts and color of the dot is based on p-value adjusted to sample distribution (p_{adj} value) and indicates significance of pathway enrichment. KEGG annotates genes at the pathway level.



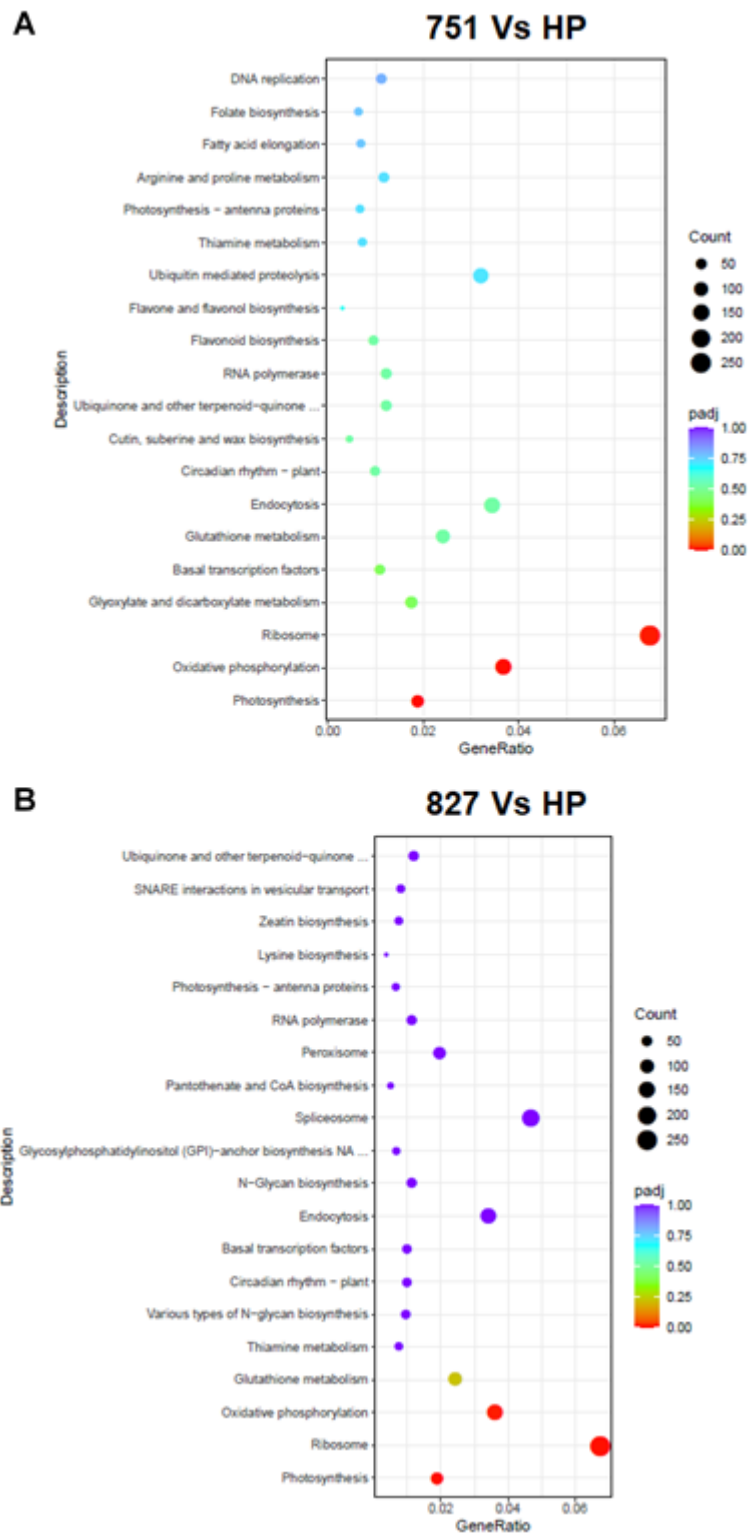
Appendix 6. The assignment of genes to different metabolic pathways in high and low PD/HD accessions of *H. macrophylla* and *H. paniculata*. (A, B) Dot plot of KEGG enrichment analysis showing the gene ratio (the percentage of total DEGs) assigned to the top 20 metabolic pathways in the study group (A) VAR-552 and *H. paniculata* and (B) VAR-746 and *H. paniculata*. The dot sizes represent the gene counts and color of the dot is based on p-value adjusted to sample distribution (p_{adj} value) and indicates significance of pathway enrichment. KEGG annotates genes at the pathway level.



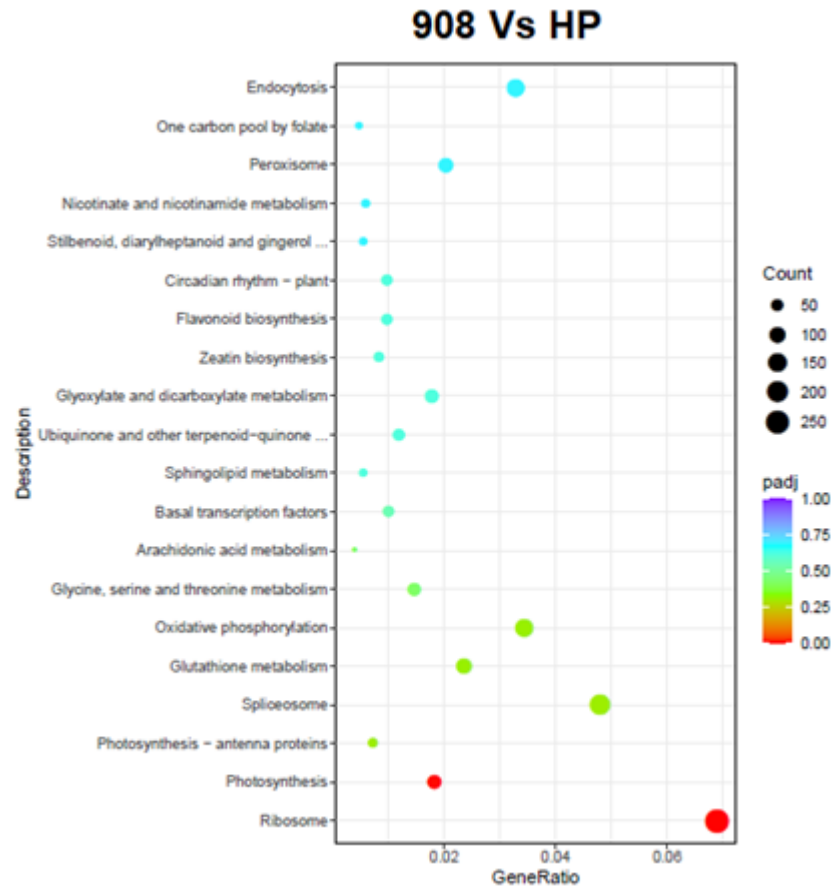
Appendix 7. The assignment of genes to different metabolic pathways in high and low PD/HD accessions of *H. macrophylla* and *H. paniculata*. (A, B) Dot plot of KEGG enrichment analysis showing the gene ratio (the percentage of total DEGs) assigned to the top 20 metabolic pathways in the study group (A) VAR-753 and *H. paniculata* and (B) VAR-547 and *H. paniculata*. The dot sizes represent the gene counts and color of the dot is based on p-value adjusted to sample distribution (p_{adj} value) and indicates significance of pathway enrichment. KEGG annotates genes at the pathway level.



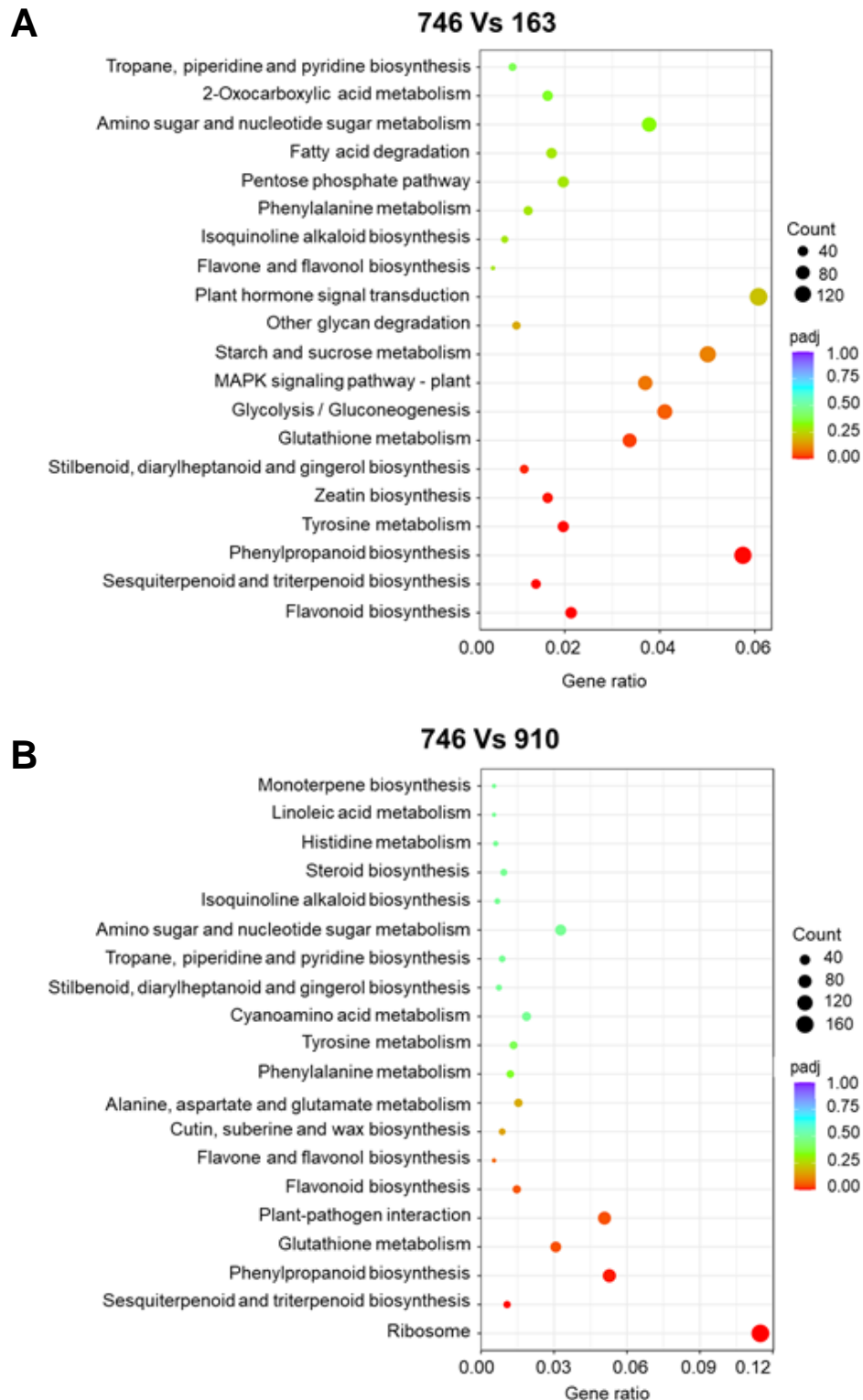
Appendix 8. The assignment of genes to different metabolic pathways in high and low PD/HD accessions of *H. macrophylla* and *H. paniculata*. (A, B) Dot plot of KEGG enrichment analysis showing the gene ratio (the percentage of total DEGs) assigned to the top 20 metabolic pathways in the study group (A) VAR-897 and *H. paniculata* and (B) VAR-760 and *H. paniculata*. The dot sizes represent the gene counts and color of the dot is based on p-value adjusted to sample distribution (p_{adj} value) and indicates significance of pathway enrichment. KEGG annotates genes at the pathway level.



Appendix 9. The assignment of genes to different metabolic pathways in high and low PD/HD accessions of *H. macrophylla* and *H. paniculata*. (A, B) Dot plot of KEGG enrichment analysis showing the gene ratio (the percentage of total DEGs) assigned to the top 20 metabolic pathways in the study group (A) VAR-751 and *H. paniculata* and (B) VAR-827 and *H. paniculata*. The dot sizes represent the gene counts and color of the dot is based on p-value adjusted to sample distribution (p_{adj} value) and indicates significance of pathway enrichment. KEGG annotates genes at the pathway level.

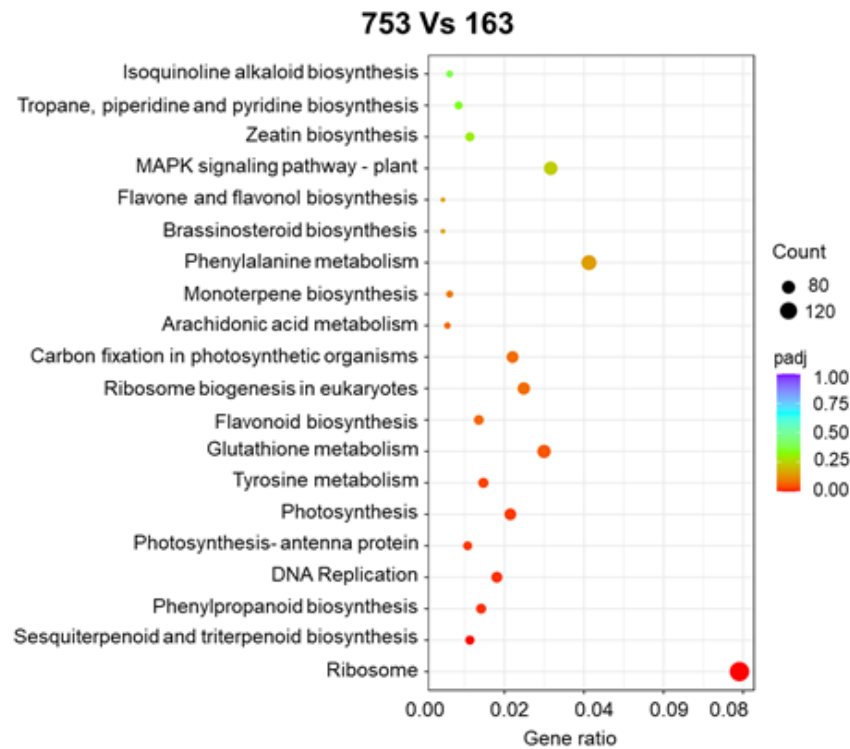


Appendix 10. The assignment of genes to different metabolic pathways in high and low PD/HD accessions of *H. macrophylla* and *H. paniculata*. Dot plot of KEGG enrichment analysis showing the gene ratio (the percentage of total DEGs) assigned to the top 20 metabolic pathways in the study group VAR-908 and *H. paniculata*. The dot sizes represent the gene counts and color of the dot is based on p-value adjusted to sample distribution (p_{adj} value) and indicates significance of pathway enrichment. KEGG annotates genes at the pathway level.

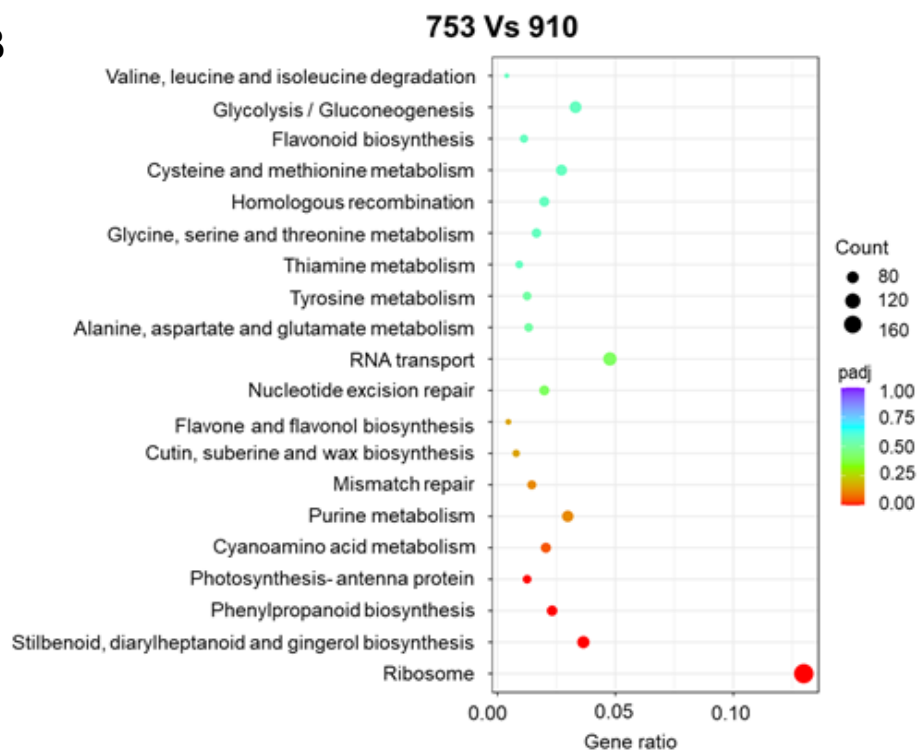


Appendix 11. The assignment of genes to different metabolic pathways in high and low PD/HD accessions of *H. macrophylla*. (A, B) Dot plot of KEGG enrichment analysis showing the gene ratio (the percentage of total DEGs) assigned to the top 20 metabolic pathways in the study group (A) VAR-746 and VAR-163 and (B) VAR-746 and VAR-910. The dot sizes represent the gene counts and color of the dot is based on p-value adjusted to sample distribution (p_{adj} value) and indicates significance of pathway enrichment. KEGG annotates genes at the pathway level.

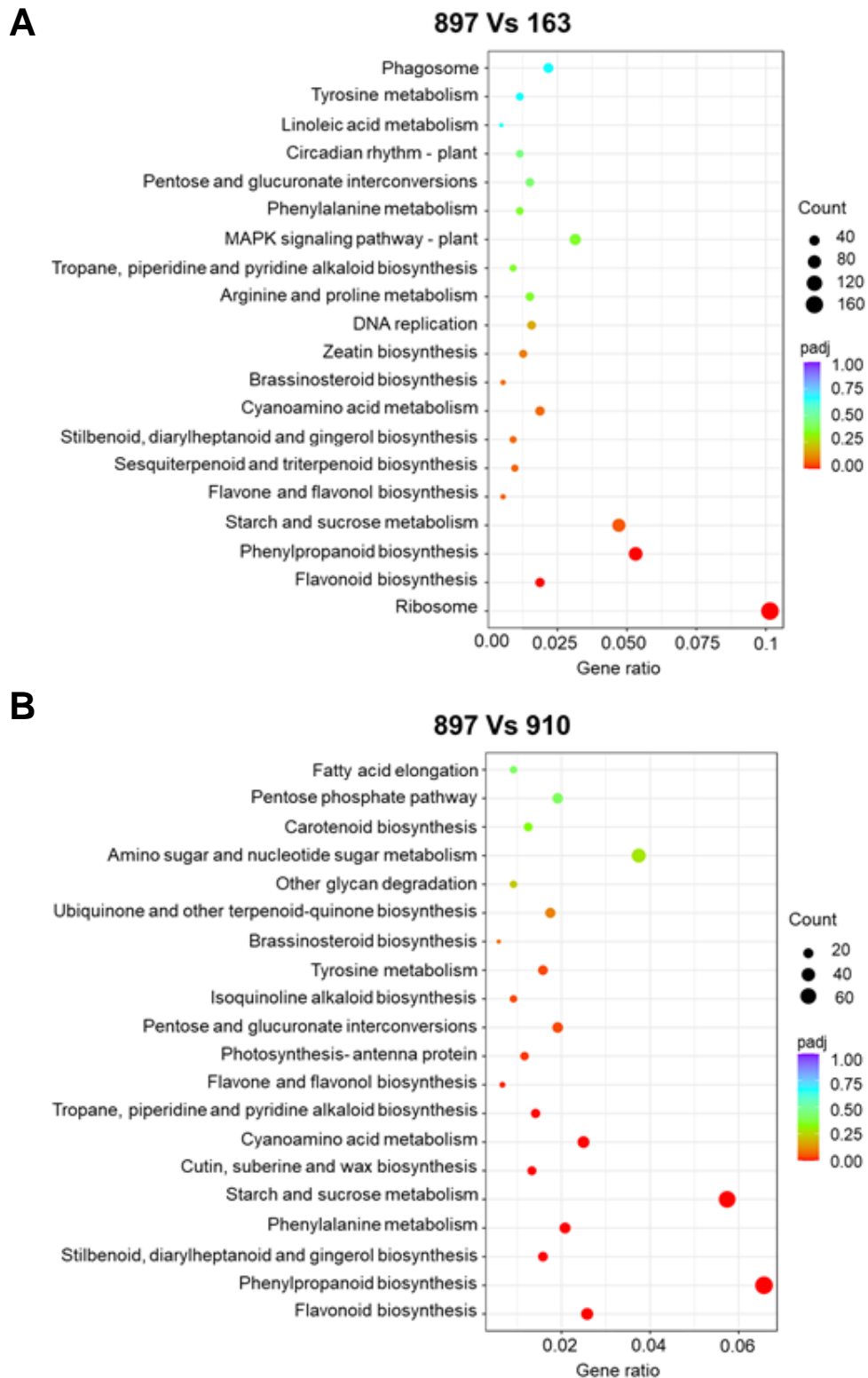
A



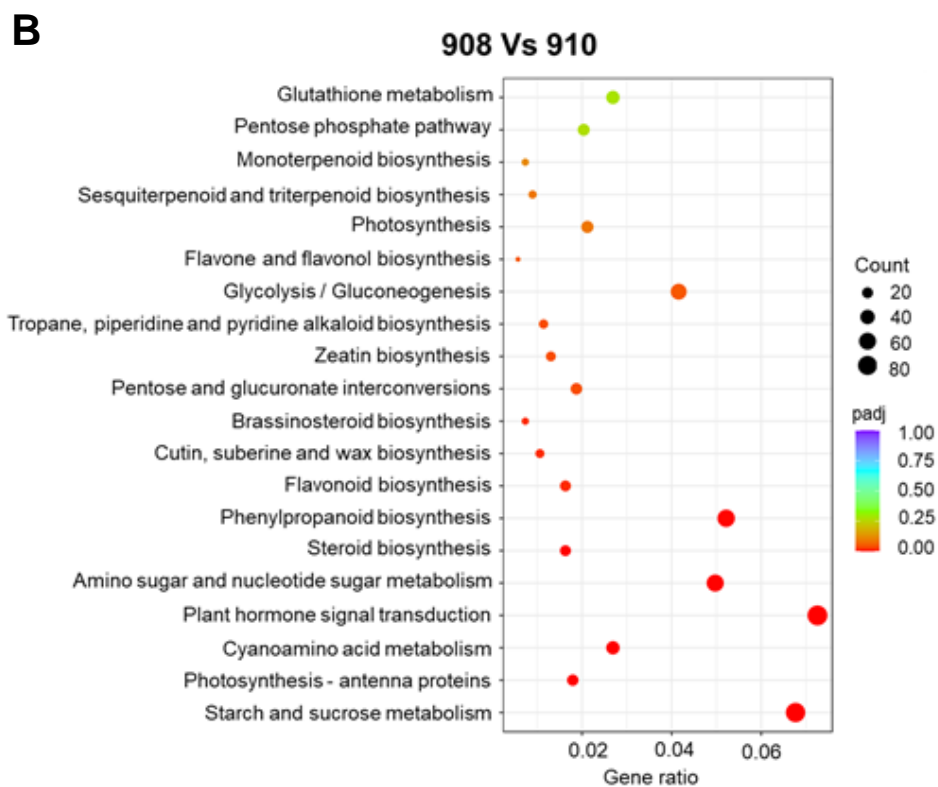
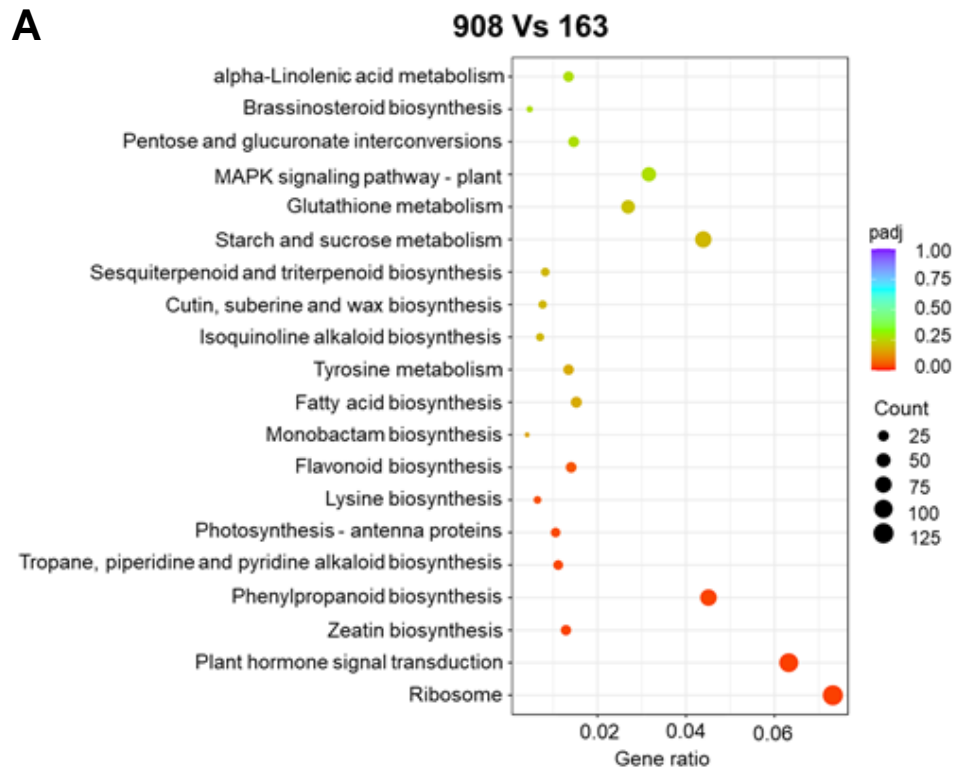
B



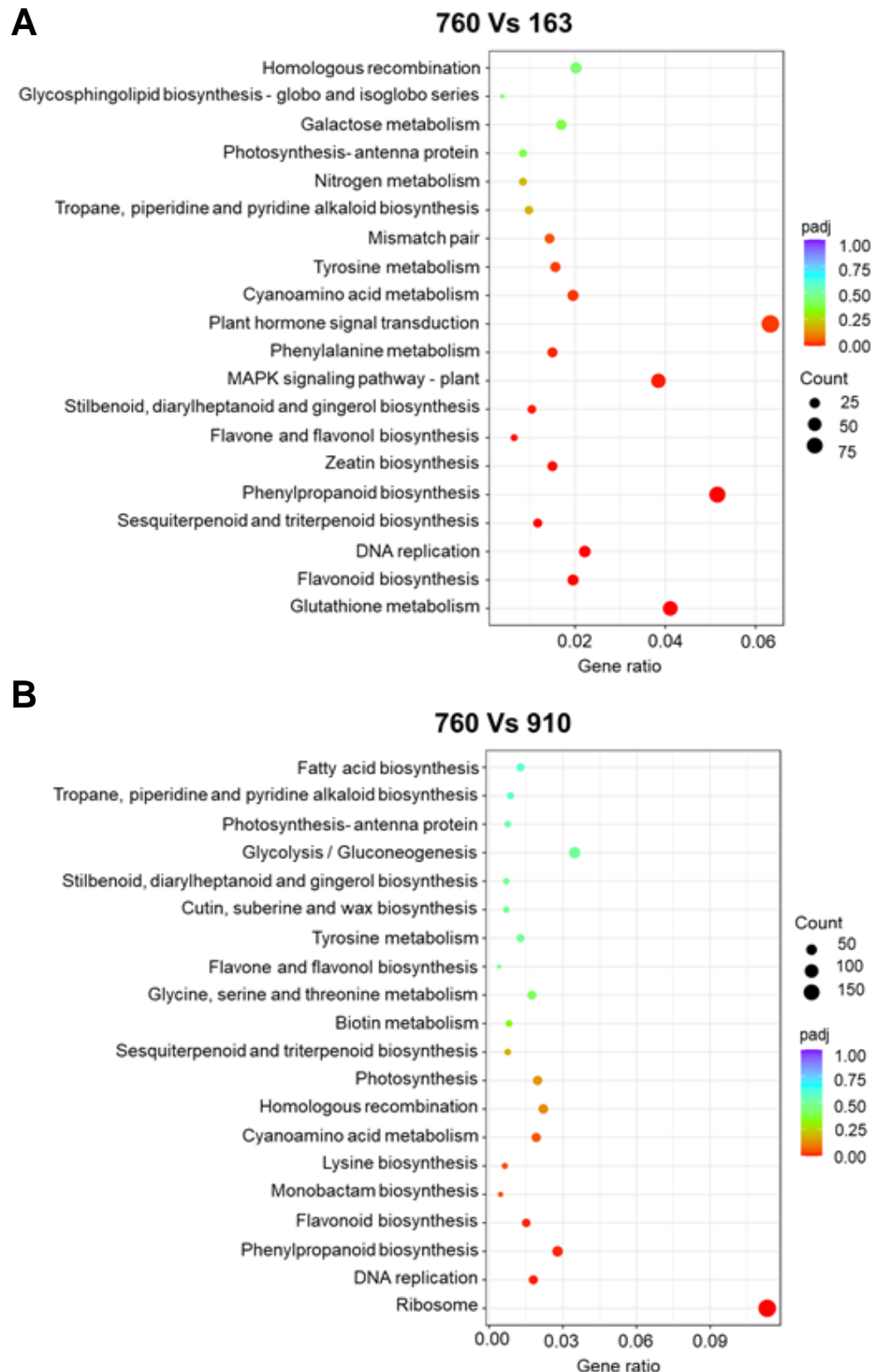
Appendix 12. The assignment of genes to different metabolic pathways in high and low PD/HD accessions of *H. macrophylla*. (A, B) Dot plot of KEGG enrichment analysis showing the gene ratio (the percentage of total DEGs) assigned to the top 20 metabolic pathways in the study group (A) VAR-753 and VAR-163 and (B) VAR-753 and VAR-910. The dot sizes represent the gene counts and color of the dot is based on p-value adjusted to sample distribution (p_{adj} value) and indicates significance of pathway enrichment. KEGG annotates genes at the pathway level.



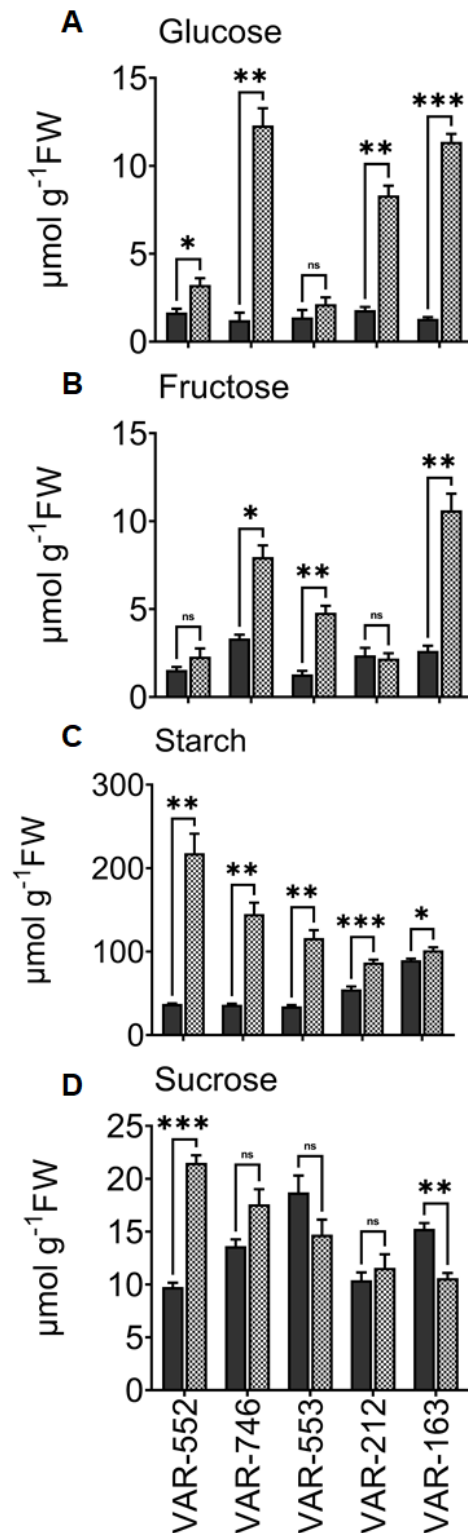
Appendix 13. The assignment of genes to different metabolic pathways in high PD/HD and low PD/HD accessions of *H. macrophylla*. (A, B) Dot plot of KEGG enrichment analysis showing the gene ratio (the percentage of total DEGs) assigned to the top 20 metabolic pathways in the study group (A) VAR-897 and VAR-163 and (B) VAR-897 and VAR-910. The dot sizes represent the gene counts and color of the dot is based on p-value adjusted to sample distribution (p_{adj} value) and indicates significance of pathway enrichment. KEGG annotates genes at the pathway level.



Appendix 14. The assignment of genes to different metabolic pathways in high PD/HD and low PD/HD accessions of *H. macrophylla*. (A, B) Dot plot of KEGG enrichment analysis showing the gene ratio (the percentage of total DEGs) assigned to the top 20 metabolic pathways in the study group (A) VAR-908 and VAR-163 and (B) VAR-908 and VAR-910. The dot sizes represent the gene counts and color of the dot is based on p-value adjusted to sample distribution (p_{adj} value) and indicates significance of pathway enrichment. KEGG annotates genes at the pathway level.



Appendix 15. The assignment of genes to different metabolic pathways in high HD and low PD/HD accessions of *H. macrophylla*. (A, B) Dot plot of KEGG enrichment analysis showing the *gene ratio* (the percentage of total DEGs) assigned to the top 20 metabolic pathways in the study group (A) VAR-760 and VAR-163 and (B) VAR-760 and VAR-910. The dot sizes represent the gene counts and color of the dot is based on p-value adjusted to sample distribution (p_{adj} value) and indicates significance of pathway enrichment. KEGG annotates genes at the pathway level.



Appendix 16. Concentrations of sugars in *Hydrangea* plants grown under sufficient water supply and 5 % soil moisture to induce drought. (A-D) The difference between (A) glucose, (B) fructose, (C) starch and (D) sucrose in leaf tissue of well-watered plants compared to drought affected plants. Analysis was done on fully expanded young upper leaves. Bars represent means +SE, n= 6 independent biological replicates and standard error. Single and double asterisks indicate significant differences at $p < 0.05$, $p < 0.01$ according to Student t-test; ns: not significant.

Appendix 11. List of *H. macrophylla* accessions used for primary screening. Green filled cells represent the 14 accessions selected for experiments.

VAR-0908_000 (VAR 908)	VAR-0553_001 (VAR 553)	VAR-0897_000 (VAR 897)
VAR-0553_002	VAR-0552_000 (VAR 552)	VAR-0552_001
VAR-0828_000	VAR-0766_001	VAR-0158_000
VAR-0547_000 (VAR-547)	VAR-0542_000	VAR-0536_000
VAR-0749_000	VAR-0556_000	VAR-0912_000
VAR-0765_000	VAR-0906_000	VAR-0583_000
VAR-0556_001	VAR-0836_000	VAR-0571_000
VAR-0844_000	VAR-0535_000	VAR-0576_000
VAR-0879_001	VAR-0768_000	VAR-0827_001
VAR-0827_000 (VAR 827)	VAR-0556_002	VAR-0539_000
VAR-0582_000	VAR-0562_000	VAR-0561_000
VAR-0751_000 (VAR 751)	VAR-0580_000	VAR-0560_000
VAR-0574_000	VAR-0260_002	VAR-0763_000
VAR-0550_000	VAR-0575_000	VAR-0561_001
VAR-0750_000	VAR-0747_000	VAR-0573_000
VAR-0566_000	VAR-0921_000	VAR-0446_000
VAR-0846_000	VAR-0547_002	VAR-0567_000
VAR-0555_000	VAR-0564_000	VAR-0706_000
VAR-0915_000	VAR-0132_002	VAR-0438_000
VAR-0746_000 (VAR 746)	VAR-0768_001	VAR-0569_000
VAR-0750_001	VAR-0212_001	VAR-0843_000
VAR-0009_000	VAR-0922_001	VAR-0856_000
VAR-0097_000	VAR-0837_000	VAR-0452_000
VAR-0146_000	VAR-0440_000	VAR-0163_000 (VAR 163)
VAR-0579_000	VAR-0543_000	VAR-0823_000
VAR-0771_000	VAR-0260_000	VAR-0538_000
VAR-0758_000	VAR-0554_000	VAR-0913_000
VAR-0551_000	VAR-0754_000	VAR-0290_000
VAR-0755_000	VAR-0745_000	VAR-0565_000

VAR-0436_000	VAR-0919_000	VAR-0762_000
VAR-0347_000	VAR-0893_000	VAR-0118_000
VAR-0756_000	VAR-0707_000	VAR-0904_000
VAR-0922_002	VAR-0578_000	VAR-0255_000
VAR-0548_000	VAR-0581_000	VAR-0808_000
VAR-0616_000	VAR-0708_000	VAR-0808_001
VAR-0491_000	VAR-0905_000	VAR-0069_000
VAR-0348_000	VAR-0258_000	VAR-0753_001 (VAR 753)
VAR-0142_000	VAR-0766_000	VAR-0856_001
VAR-0540_000	VAR-0890_000	VAR-0145_000
VAR-0256_000	VAR-0010_000	VAR-0704_000
VAR-0741_000	VAR-0544_000	VAR-0549_000
VAR-0559_000	VAR-0068_000	VAR-0577_000
VAR-0572_000	VAR-0584_000	VAR-0364_000
VAR-0477_000	VAR-0132_000	VAR-0769_000
VAR-0879_002	VAR-0757_000	VAR-0568_000
VAR-0439_000	VAR-0537_000	VAR-0615_000
VAR-0823_001	VAR-0259_000	VAR-0811_000
VAR-0492_000	VAR-0918_000	VAR-0748_000
VAR-0761_000	VAR-0907_000	VAR-0770_000
VAR-0131_000	VAR-0770_001	VAR-0570_000
VAR-0493_000	VAR-0758_002	VAR-0447_000
VAR-0039_000	VAR-0418_000	VAR-0920_000
VAR-0856_002	VAR-0772_000	VAR-0451_000
VAR-0744_000	VAR-0835_000	VAR-0760_000 (VAR 760)
VAR-0212_000 (VAR 212)	VAR-0917_000	VAR-0879_003
VAR-0163_001	VAR-0437_000	VAR-0901_000
VAR-0891_000	VAR-0910_000 (VAR 910)	VAR-0894_000
VAR-0898_000	VAR-0896_000	VAR-0857_000
VAR-0758_001	VAR-0900_000	VAR-0119_000
VAR-0824_001	VAR-0911_000	VAR-0899_000
VAR-0895_000	VAR-0563_000	

9 Abbreviations

%	Percentage
°C	Degree Celsius
µg	Microgram
4CL	4-coumarate: coenzyme A ligase
Å	Angstrom (equal to a length of 10^{-10} m)
ANOVA	Analysis of variance
ANS	Anthocyanin synthase
AQC	6-aminoquinolyl-N hydroxysuccinimidyl carbamate
ASE	Accelerated solvent extraction
BBB	Blood-brain barrier
C2H	Cinnamate 2 hydroxylase
C3'H	P-coumaroyl shikimate 3' hydroxylase
C3H	Coumarate 3-hydroxylase
C4H	Cinnamate 4-hydroxylase
CCoAOMT	Caffeoyl coA 3-O-methyltransferase
CE	Collision energies
CHI	Chalcone isomerase
CHS	Chalcone synthase
COMT	Caffeate/5-hydroxyferulate 3-O-methyltransferase
COSY	Coumarin synthase
CSE	Caffeoyl shikimate esterase
CTA	P-coumaroyltriacetic acid
CTAL	P-coumaroyltriacetic acid lactone
CTAS	P-Coumaroyltriacetic acid synthase
DFR	Dihydroflavonol 4-reductase
DHC	3,4-dihydroisocoumarins
DNA	Deoxy ribonucleic acid
DW	Dry weight
EFSA	European food safety authority
ESI	Electrospray ionization
F3'5'H	Flavonoid 3'5'-hydroxylase
F3H	Flavanone 3-hydroxylase
F5H	Ferulate 5-hydroxylase
FDR	False discovery rate
FW	Fresh weight

g	Gram
GAPDH	Glyceraldehyde-3-phosphate dehydrogenase
GO	Gene ontology
HCT	Hydroxycinnamoyl transferase
HD	Hydrangenol
hrs	Hours
IPK	Leibniz Institute of Plant Genetics and Crop Plant Research, Gatersleben
JA	Jasmonic acid
JECFA	Joint Expert Committee on Food Additives
KEGG	Kyoto Encyclopedia of Genes and Genomes
KR	Ketoreductase
LAR	Leucoanthocyanidin reductase
LC	Liquid chromatography
LOQ	Limit of Quantification
MRM	Multiple reactions monitoring
MS	Tandem mass spectrometry
MS/MS	Mass spectrometry
mΩ	Milliohm
NADH	Nicotinamide adenine dinucleotide + H
Nar	Naringenin
PAL	Phenylalanine ammonia lyase
PCA	Principal component analysis
p-CA	P-coumaric acid
PD	Phyllodulcin
Phe	Phenylalanine
PKC	Polyketide cyclase
PPP	Phenylpropanoid pathway
QIT	Quantitative ion transition
qPCR	Quantitative PCR
Res	Resveratrol
RNA	Ribonucleic acid
ROS	Reactive oxygen species
RS	Resveratrol synthase
S8H	Scopoletin 8-hydroxylase
SE	Standard error

Abbreviations

SGT	Scopoletin glucosyl transferase
SIM	Selected ion monitoring
SM	Secondary metabolites
SPE	Solid phase extraction
STCS	Stilbenecarboxylate synthase
t-CA	Trans cinnamic acid
t _R	Retention time
Umb	Umbelliferone
UPLC	Ultra-pressure reversed-phase chromatography
WGCNA	Weighted gene co-expression network analysis

10 Acknowledgement

I would like to express my deep gratitude to all those who have contributed to the completion of this PhD thesis. This journey has been long and challenging, and I could not have reached this milestone without the support and encouragement of many individuals and institutions.

First and foremost, I am profoundly grateful to my advisors, Dr. Mohammad-Reza Hajirezaei and Prof. Dr. Nicolaus von Wirén, for their unwavering guidance, patience, and mentorship throughout this research endeavor. Their expertise, insights, and dedication were instrumental in shaping the direction of this work. I am fortunate to have had the opportunity to learn from such distinguished scholars.

I am also indebted to the members of my dissertation committee for their valuable feedback and constructive criticism. Their expertise in their respective fields greatly enriched the quality of this thesis, and I am grateful for their time and commitment.

I extend my heartfelt thanks to all the members and colleagues from the Molecular Plant Nutrition group including Suresh, Undine, Geeisy, Jingyi, Bijal, Mikel, Yudelsy, Anja, Sara, Moshin, Andrea, Uwe, Alex, Melanie, Nicole, Dagmar, Babara, Christine, Heike, Ricardo, Rodolfo, Gabriel, Soumaya, Annett, Jaqueline, Elena and Elmarie. It was my pleasure to work in such an uplifting group. I would also like to especially thank Dr. Britt Leps and Bianka Jacobi in International Office at IPK who are very kind and continuously helped me during my wonderful life in Germany.

I am grateful to my friends Saravana, Surya, Anto, Pandian, Pooja and everyone else for their moral support, insights and assistance during my short stay in Germany. Their camaraderie made this academic pursuit not only intellectually rewarding but also enjoyable. I would like to acknowledge the support I received from Koetterheinrich and Ms. Frauke Engel, both financially and academically, which made this research possible. Their investment in my research and education is deeply appreciated.

Finally, I would like to express my gratitude to my family for their unwavering support, love, and understanding. Their encouragement sustained me during the most challenging moments of this journey, and I am profoundly grateful for their sacrifices.

While this thesis marks the end of one chapter, it also signifies the beginning of a new phase in my academic and professional journey. I am grateful to all those who have been a part of this process, and I look forward to continuing to contribute to the field in the years to come.

11 Curriculum Vitae

Name Goutham Padmakumar Sarala

Nationality Indian

Education:

02.2020 – 07.2023

PhD Student

1. Leibniz-Institute of Plant Genetics and Crop Plants Research (IPK)

Department of Physiology and Cell Biology Research Group: Plant Molecular Nutrition

Supervisors: Dr. Mohammad-Reza Hajirezaei and Prof. Dr. Nicolaus von Wirén

2. Martin-Luther University Halle/Wittenberg, Germany, Institute for Biology

Dissertation title: Elucidation and functional characterization of the phenylpropanoid pathway in *Hortensia* species.

11.2017 – 10.2019

University of Agricultural Sciences, Bangalore, India

Master study course: Agricultural plant biotechnology

Master thesis: Effect of phytohormones on growth, yield and quality of tomato (*Solanum lycopersicum* L.) accessions

Supervisor: Prof. Dr. S. Shyamamma

08.2013 – 07.2017

Acharya NG Ranga Agricultural University, Tirupati, India

Bachelors course: Agricultural sciences.

12 Eidesstattliche Erklärung/Declaration on oath

Hiermit versichere, dass ich die vorliegende Arbeit selbstständig verfasst habe, dass ich keine anderen Quellen und Hilfsmittel als die angegebenen benutzt habe und dass ich die Stellen der Arbeit, die ich anderen Werken – auch elektronischen Medien – dem Wortlaut oder Sinn nach entnommen habe, in jedem Fall unter Angabe der Quelle als Entlehnung kenntlich gemacht habe. Die Arbeit wurde bisher in gleicher oder ähnlicher Form keiner anderen Institution oder Prüfungsbehörde vorgelegt.

I hereby declare that I have written the submitted thesis independently and without illicit assistance of third parties. I have not used any other reference and sources than those listed in the thesis or engaged any plagiarism. All references and sources used in the presented work are properly cited and acknowledged. Further, I declare that the presented work has not been previously submitted for the purpose of academic examination, either in its original or similar form, anywhere else.

Ort/Place, Datum/Date

Unterschrift/ Signature

13 Erklärung über bestehende Vorstrafen und anhängige Ermittlungsverfahren/Declaration concerning Criminal Record and Pending Investigations

Hiermit erkläre ich, dass ich weder vorbestraft bin noch dass gegen mich Ermittlungsverfahren anhängig sind.

I hereby declare that I have no criminal record and that no preliminary investigations are pending against me.

Ort/Place, Datum/Date

Unterschrift/ Signature